Determination of the distribution of halocarbons in the tropical upper troposphere and stratosphere

Dissertation
zur Erlangung des Doktorgrades
der Naturwissenschaften

vorgelegt beim Fachbereich 14
der Johann Wolfgang Goethe – Universität
in Frankfurt am Main

vorgelegt von
Johannes Christian Laube
aus Jena

Frankfurt (2008)

vom Fachbereich 14 der

Johann Wolfgang Goethe – Universität als Dissertation angenommen.

Dekan : Prof. Dr. H. Schwalbe

Gutachter : Prof. Bernd O. Kolbesen, PD Dr. Andreas Engel

Datum der Disputation : 20.10.2008

Table of contents

0 Introduction

The production and use of many volatile halocarbons is regulated by the Montreal Protocol and its subsequent amendments (see http://ozone.unep.org/ for details), because if these substances are transported into the stratosphere, they decompose and release inorganic chlorine and/or bromine species. These inorganic chlorine/bromine species enhance the efficiency of catalytic ozone destruction cycles. This has led to two large anthropogenic effects in the stratosphere: global ozone depletion and strong loss of nearly all ozone in an altitude layer between 15 and 25 km above Antarctica during Austral spring; a phenomenon known as the ozone hole (see e.g. Solomon, 1999 for details on ozone depletion mechanisms). The stratospheric ozone layer protects the Earths surface from life-form damaging UV radiation and is also very important for the radiative balance of this planet. Therefore it is crucial to identify and quantify all substances and processes that can affect the ozone layer directly or indirectly. The tropical upper troposphere plays a key role in this context as most air enters the stratosphere via this region. But there exist only few measurements of the distribution of many halocarbons in the tropical upper troposphere and stratosphere up to now (WMO, 2007).

This thesis aims to improve the knowledge about the chemical composition of the respective atmospheric regions using measurements on whole-air samples which originated from there. For this purpose a capable analytical system for ultra trace gas analysis needed to be developed. The efforts that were undertaken to identify and quantify the targeted substances and also to assure the quality and to assess the uncertainties related to the quantification process are explained in Chapter 2 and 3.

Once in the stratosphere, the halogenated organic compounds decompose, releasing their chlorine and/or bromine atoms to initiate ozone destruction. Hence, their stratospheric distributions are influenced by local photochemical removal and also transport processes depending on the respective chemical lifetimes and transport timescales (WMO, 2007). Some substances are rather inert (e.g. most Chlorofluorocarbons) having stratospheric decomposition times in the range of years. The release rates of chlorine and bromine from those substances can be quantified with so-called “fractional release factors” (FRFs) which depend on the respective stratospheric location and residence time. The FRFs are very crucial parameters as they are used for the calculation of Ozone Depletion Potentials (ODPs) and Global Warming Potentials (GWP) and thus influence future ozone and climate predictions. The currently available FRFs are not globally integrated but originate from observations of the mid- and high-latitude lower stratosphere. Moreover, for some substances only model-derived FRFs are available (WMO, 2007). Therefore a major goal of this thesis was to derive FRFs of long-lived halocarbons from the measured data set of air samples which mainly originated from the lower and middle tropical stratosphere. The corresponding calculations, results and implications can be found in Chapter 4.

Recent research led to the finding that not only halocarbons with rather long atmospheric lifetimes such as Chlorofluorocarbons are able to reach the stratosphere but also more reactive substances which show already a substantial degradation in the troposphere (so-called very short-lived substances, VSLS). A number of chlorinated and brominated VSLS was observed inside or just below the main stratospheric entrance region, the Tropical Tropopause Layer (TTL, Schauffler et al., 1998 and 1999, Ko and Poulet et al., 2003, Law and Sturges et al., 2007). The importance of the VSLS for stratospheric ozone depletion is subject of an ongoing scientific debate. In order to bring these discussions forward whole-air samples originating from the TTL and above from the tropical stratosphere have been used to quantify all chlorinated and brominated substances that enter the stratosphere. Chapter 5 provides details on an atmospheric case study that was carried out in cooperation with the University of East Anglia. It represents the first study in which the abundances of 28 chlorinated and brominated substances in the TTL and above in the tropical stratosphere could be quantified simultaneously (Laube et al., 2008).

One result of this cooperative study was an indication for the presence of unknown halocarbons in the upper troposphere. For this reason, it was attempted to identify such substances by taking air samples at the Taunus Observatory near Frankfurt (Main), Germany. Three Chlorofluorocarbons could be first observed in the atmosphere (Laube and Engel, 2008). The corresponding investigations are summarised in closing Chapter 6.

1 Scientific background

This chapter aims to give a brief introduction to some fundamentals of atmospheric science that will be referred to in the thesis. Furthermore it provides information about air sampling techniques and gives an overview of the used analytical methods.

1.1 Halocarbons in the atmosphere

1.1.1 Atmospheric composition and quantities

The present Earth's atmosphere consists mainly of molecular Nitrogen, molecular Oxygen, Argon and a very variable amount of water vapour (up to several per cent). In addition it contains a large number of trace gases with concentrations below 0.1 volume % originating from plants, animals or human activities (source: ESPERE Climate Encyclopaedia, 2006). In contrast to their low concentrations these trace gases can have large environmental effects. Notably most halocarbons (with many of them being of anthropogenic origin) are known to be very effective in global warming. For instance, in 2005 the two halocarbons $CFCl_3$ (F11) and CF_2Cl_2 (F12) contributed about 14% of the effect of CO_2 to the anthropogenic greenhouse effect, while CO_2 is about 500,000 times more abundant (IPCC, 2007). In addition, halocarbons can enhance the destruction of ozone in the stratosphere. This occurs if chlorine or bromine is released from these molecules (see Chapter 1.1.4).

Prior to a more detailed description of the scientific background a few atmospheric quantities need to be introduced. First, to write atmospheric concentrations in mg or mol/liter is problematic because of the variable density of the atmosphere. Therefore a common trace gas unit is the volume mixing ratio (or also the dry air mole fraction) in parts per billion (ppb) or parts per trillion (ppt) which is also used in this thesis. Furthermore a number of physical quantities are used for the characterisation of air parcels. In addition to altitude in [m], pressure in [Pa] and temperature in [K] the potential temperature in [K] is an important quantity. It is a measure for the potential and thermal energy content of an air parcel. The potential temperature is defined as the temperature that an air parcel would have if it was brought to normal meteorological pressure level of p_0 = 1013 hPa by dry-adiabatical compression (Roedel, 2000). Equation (1.1) quantifies the connection between potential temperature θ, temperature T, pressure p and k – the ratio of the specific heats at constant pressure and constant volume (k-1/k = 0.286 for air).

$$\theta = T \cdot \left(\frac{p_0}{p} \right)^{\frac{k-1}{k}} \qquad (1.1)$$

For instance, fast rising air (e.g. deep convection) does not exchange much heat with its environment and thus its potential temperature can be approximated as constant in a first iteration (without considering a possible condensation of water). In combination with other quantities this can serve as a useful tool to characterise air parcels.

1.1.2 Atmospheric regions - troposphere and stratosphere

The atmosphere can be subdivided into different regions, which are partly shown in Figure 1.1.1. Whereas mean pressure and air density are decreasing monotonously with altitude the mean temperature shows some characteristic structures that are used for classification (ESPERE climate encyclopaedia, 2006). The lowest region is the troposphere where the mean temperature decreases with increasing altitude. Warm air rises, which causes strong vertical mixing in the troposphere. Its upper boundary is the tropopause, which has a variable height with time and also differs between the latitudes (Roedel, 2000). The conventional definition is the so-called thermal lapse-rate tropopause which is defined as the base of a layer above 500 hPa with a minimum thickness of 2 km in which the vertical temperature gradient is below 2 K per km (WMO, 1957). Above the tropopause the temperature starts to increase with altitude and the altitude interval with this positive temperature gradient is defined as the stratosphere.

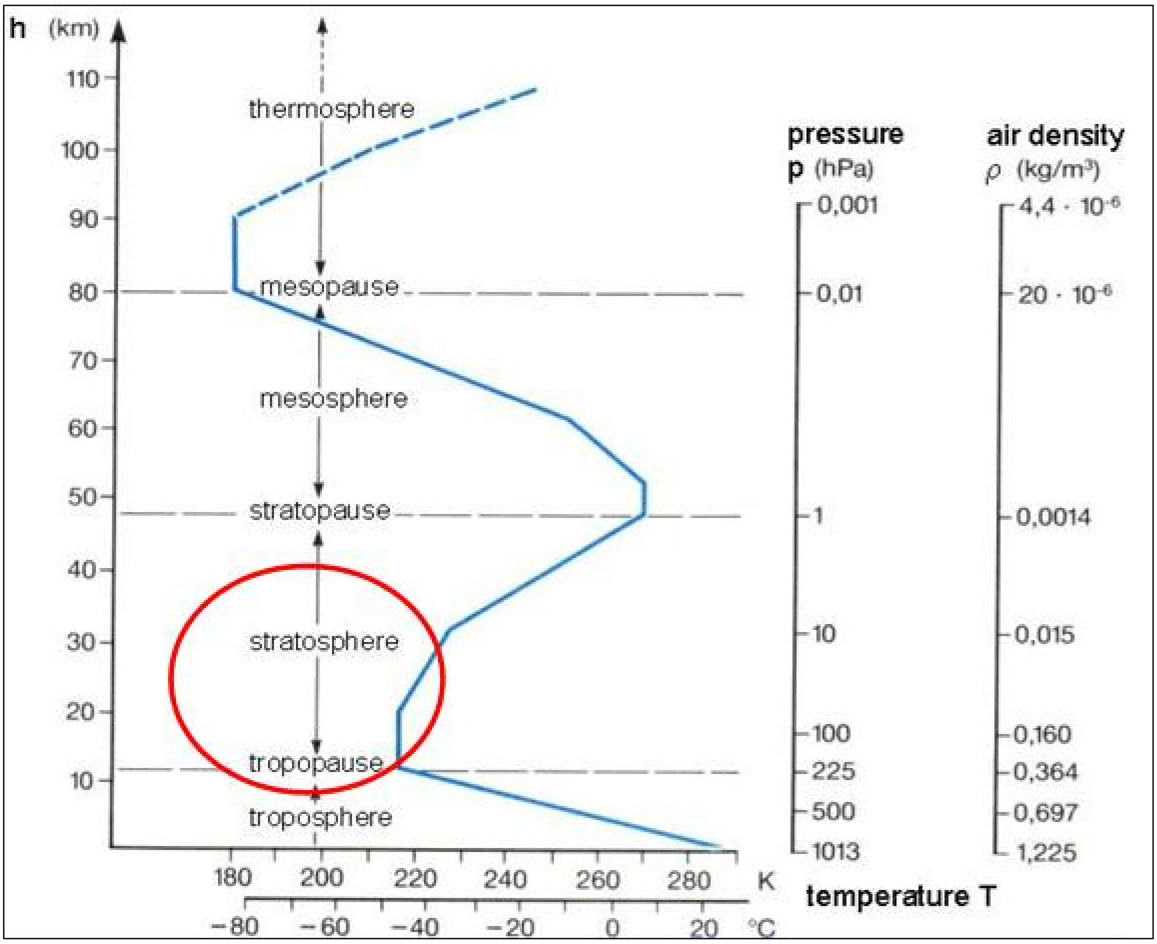

Figure 1.1.1. Classification of lower and middle atmospheric regions in combination with the behaviour of some corresponding physical quantities. The Figure was adapted from the ESPERE climate encyclopaedia (2006). In the troposphere the mean temperature decreases with increasing altitude while this trend is reversed in the stratosphere. The red circle marks the regions of interest for this thesis: the upper troposphere and lower and middle stratosphere.

The inversion is caused by the higher solar radiation in these altitudes which is generating high steady-state ozone concentrations from atmospheric oxygen via the so-called ‘‘Chapman cycle’’ reactions (Chapman, 1930). These reaction cycles also release heat. Stratospheric ozone is very important for life on earth, because it strongly absorbs light between approximately 200 and 310 nm (which also influences the temperature). Thus, solar radiation that reaches the troposphere has wavelengths longer than 290 nm which is limiting tropospheric photochemistry (Finlayson-Pitts and Pitts, 2000). A decrease in ozone would lead to health defects to humans, animals and plants due to the increased ultraviolet radiation [e.g. van der Leun et al., 1995). As the troposphere contains high amounts of water vapour, many trace gases are scavenged from the atmosphere by wet and dry deposition. In contrast, no wet or dry deposition occurs in the stratosphere. Moreover, relatively little vertical mixing occurs in this region leading to long residence and transport times in the range of years (e.g. Plumb, 2002).

A scheme of stratospheric dynamics – dominated by the so-called Brewer-Dobson circulation (Dobson et al., 1929 and Brewer, 1949) – is displayed in Figure 1.1.2. The air mainly enters the stratosphere irreversibly in the tropics and is then transported upwards to higher latitudes where it descends and re-enters the troposphere.

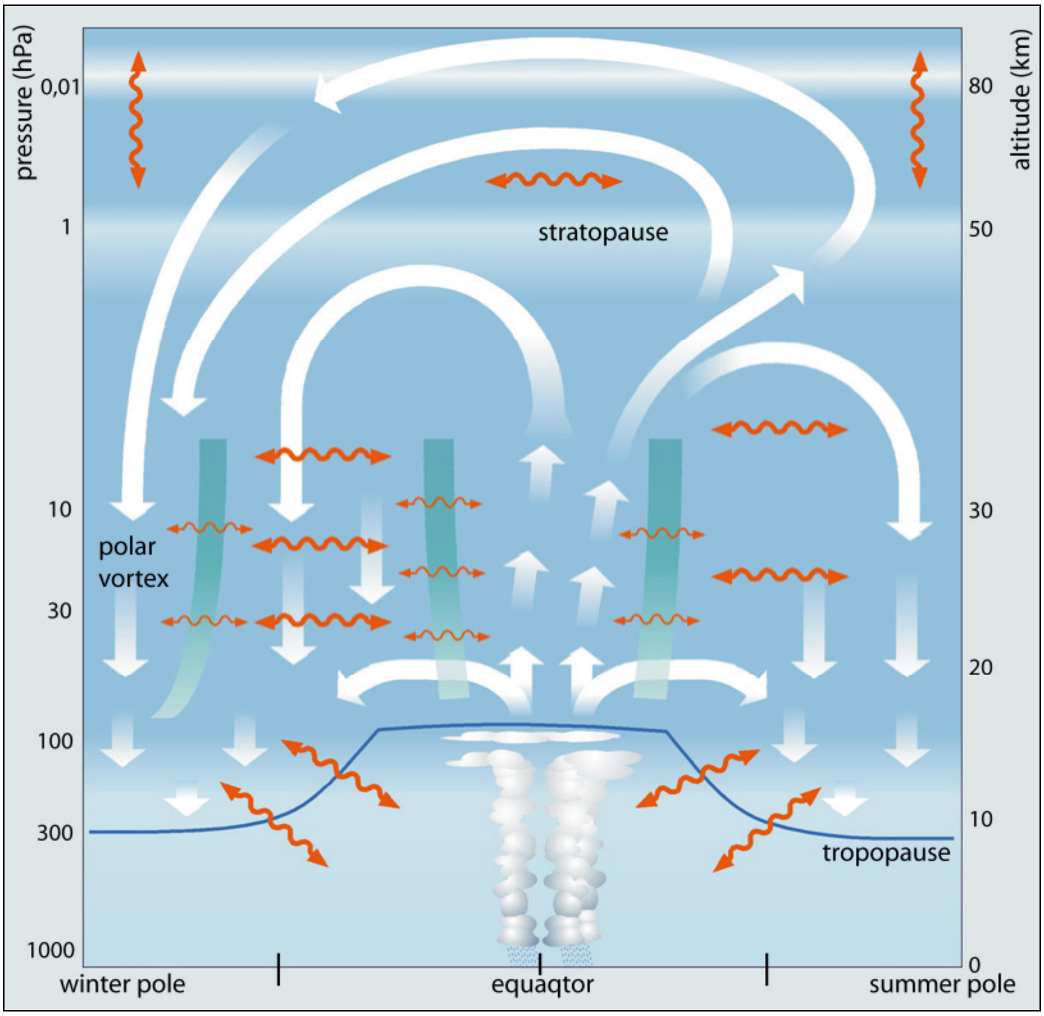

Figure 1.1.2. Scheme of stratospheric dynamics (adapted from Schmidt et al., 2001). The dominant transport pathway is the Brewer-Dobson circulation represented by the thick white arrows while the orange arrows refer to other mixing pathways. The tropopause height is variable with time and is also different in different latitudes – from around 8 km in polar regions to around 16 km in the tropics.

Other pathways (e.g. exchange across the tropopause in mid-latitudes) contribute significant amounts of air to the region called lowermost stratosphere air but little of this air does reach the middle stratosphere or the poles (see e.g. Holton et al., 1995, Plumb, 2002 or Waugh and Hall, 2002 for reviews on stratospheric dynamics). Thus, the tropical upper troposphere (between about 14 and 17 km) is considered as the main stratospheric entrance region. This important transition region is called the Tropical Tropopause Layer (TTL). A number of different definitions exist that aim to describe the extension of this region (see e.g. Highwood and Hoskins, 1998 or Gettelman and Forster, 2002). In this thesis the TTL definition given by Gettelman and Forster (2002) will be used, which defines the TTL as extending from the minimum potential temperature lapse rate to the cold point tropopause.

1.1.3 Substance classification

Halocarbons can be classified by the contained halogens and/or other functional groups. This thesis deals with the following important substance subgroups which are of anthropogenic and/or of natural (n) origin:

- Chlorofluorocarbons (CFCs, fully halogen substituted hydrocarbons, a)
- Hydrochlorofluorocarbons (HCFCs, a)
- Chlorocarbons (CCs, a, n)
- Halons (CFCs with one or more chlorine atom replaced by bromine, a)
- Bromocarbons (BCs, a, n)
- Chlorobromocarbons (CBCs, a, n)

Anthropogenic substances are e.g. used as refrigerants, (e.g. CFCs, Prinn et al., 2000), fire extinguishers (e.g. Halons, Reeves et al., 2005) or industrial solvents (e.g. Chlorocarbons such as CH_2Cl_2, Simmonds et al., 2006, or CH_3CCl_3, McCulloch and Midgley, 2001) while natural sources can originate from plant emissions (e.g. CH_3Cl, Rhew et al., 2003) or production by phytoplankton (e.g. $CHBr_3$, Quack and Wallace, 2003). Please refer to WMO (2003) and WMO (2007) for detailed overviews on sources and sinks of atmospheric halocarbons. Moreover some substances are produced from biomass burning, which is both, anthropogenic and natural (such as CH_3Cl, e.g. Andreae and Merlet, 2001).

Another widely used classification method of trace gases is due to the atmospheric lifetimes of these substances. Long-lived trace gases have long lifetimes compared to tropospheric transport time scales (>0.5 years) and show thus rather uniform distributions far from their source regions i.e. in the global background and upper troposphere. Large amounts of these substances are able to be transported intact into the stratosphere (Clerbaux and Cunnold, 2007). In contrast, very short-lived substances (VSLS) are defined as trace gases with local tropospheric lifetimes compared to tropospheric transport time scales (i.e. less than six months in practice), leading to non-uniform upper tropospheric distributions of these gases (Law and Sturges, 2007). Most anthropogenic pollutants are emitted in the mid-latitudes of the northern hemisphere and typical transport times to the tropics are in the range of months (Finlayson-Pitts and Pitts, 2000). In addition, transport into the TTL often occurs in high reaching convective systems (e.g. Gettelman et al., 2002). Thus, anthropogenic short-lived and also water soluble compounds do not reach the stratosphere in high quantities relative to the emitted quantities (e.g. Olsen et al., 2000 or Sinnhuber and Folkins, 2006). But it has been suggested, that if VSLS are emitted in the tropics significant amounts of these substances could reach the stratosphere (e.g. Yokouchi et al., 2005, Levine et al., 2007, Law and Sturges, 2007).

One major aim of this thesis was to quantify the stratospheric input of ozone-depleting substances. Thus, the target substances of this thesis were the 32 short- and long-lived chlorinated and brominated organic substances that have been observed in the upper troposphere and are thus believed to contribute to stratospheric ozone depletion (see also Tables 1-2 and 2-2 of WMO, 2007). The 22 target substances that were quantified for this work are listed in Chapter 5, Table 5.2.1 which additionally shows six target substances measured by and in cooperation with the University of East Anglia. The four missing target substances could not be quantified. These are C_2H_5Cl (chloroethane, due to air sample contaminations, see Chapter 3.1), $COCl_2$ (phosgene), CH_2ClI (chloroiodomethane) and $CHCl_2CF_3$ (HCFC-123, the latter three could not be identified with the used analytical system). As this work is interdisciplinary between Chemistry and Geosciences the target substance nomenclature will be to give both an extended totals formula and/or the most widely used name (which is usually not in agreement with the IUPAC recommendation).

1.1.4 Ozone depletion and fractional release factors

The potential of chlorinated and brominated organic substances to enhance the catalytic destruction of ozone in the stratosphere was discovered more than 30 years ago (Stolarski and Cicerone, 1974, Molina and Rowland, 1974, Wofsy et al., 1975). Once in the stratosphere, the substances are destroyed by photolysis and reactions with excited oxygen atoms (O^1D) and OH radicals. Inorganic bromine is mainly present in the form of BrO, Br, HOBr, $BrONO_2$ and

HBr. These species and the corresponding chlorine species (including BrCl and Cl_2O_2) are responsible for the catalytic destruction of ozone (e.g. Solomon, 1999). Large amounts of fluorine species are also present in the stratosphere but make only negligible contributions to ozone depletion (Finlayson-Pitts and Pitts, 2000).

Bromine has, on average and on a per atom basis, a 60 times higher efficiency to destroy ozone than chlorine (WMO, 2007). Thus, even very low mixing ratios of brominated substances of less than 0.1 ppt are of importance for stratospheric ozone depletion. Moreover, the known organic bromine compounds do not provide enough bromine to account for the observed inorganic bromine in the stratosphere (Dorf, 2005, Laube et al., 2008, Dorf et al., 2008). Chapter 5 of this thesis provides a case study which was carried out in cooperation with the University of East Anglia, UK and the Free University of Berlin, Germany and attempts to bring these discussions forward (Laube et al., 2008). Iodinated organic compounds could also affect stratospheric ozone but have not been detected in the stratosphere up to now.

The ability of a halocarbon to deplete stratospheric ozone can be characterized by an index – the Ozone Depletion Potential (ODP). The ODP is commonly derived semi-empirically (Solomon et al., 1992) and relative to that of $CFCl_3$ (F11) according to Equation 1.2 (adapted from Chapter 8.2.2 of WMO, 2007).

$$ODP_i = \frac{(\alpha \cdot n_{Br,i} + n_{Cl,i})}{n_{Cl,F11}} \cdot \frac{f_i}{f_{F11}} \cdot \frac{\tau_i}{\tau_{F11}} \cdot \frac{M_{F11}}{M_i} \qquad (1.2)$$

f - fractional halogen release factor

α - relative effectiveness of bromine compared with chlorine for ozone destruction

τ - global atmospheric lifetime

M - molecular weight

n_{Cl} (n_{Br}) - number of chlorine (bromine) atoms

Please note, that this equation can only be applied to long-lived compounds as they are well mixed throughout the troposphere and thus little influenced by the location and season of emission. The fractional release factor f_i at a given time and location is calculated from measurements of stratospheric halocarbon distributions according to Equation (1.3) which was taken from Chapter 8.2.2 of WMO (2007).

$$f_i(x,y,z,t) = \frac{\rho_{i,entry} - \rho_i(x,y,z,t)}{\rho_{i,entry}} \qquad (1.3)$$

$\rho_i(x, y, z, t)$ - mixing ratio of the halocarbon at a given stratospheric location (x,y,z) at time t

$\rho_{i,entry}$ - mixing ratio of the halocarbon in the air parcel when it entered the stratosphere

The stratospheric entry mixing ratio $\rho_{i,entry}$ can be calculated from age of air observations (see below) and the tropospheric time series of the respective substance. Only a limited range of data originating from measurements in the lower mid- and high latitude stratosphere is currently used for the calculation of fractional release factors (e.g., Schauffler et al., 2003, WMO, 2007). In chapter 4 of this thesis a new set of fractional release factors is derived for the tropical lower and middle stratosphere and compared with those of other studies.

1.1.5 Tracer-tracer-correlations and the concept of age of air

As explained above the atmospheric distribution of long-lived trace gases (so-called “tracers”) is mainly determined by transport processes and can be considered as uniform within the rather well mixed upper troposphere. In the stratosphere transport times are much longer in the range of years. Thus, if a tracer shows a concentration change with time it can be used to study stratospheric transport pathways. Moreover, the correlation between two stratospheric tracers is compact (Plumb and Ko, 1992) with different regions showing different correlation curves between tracers due to transport barriers or chemical processes. Such correlations were subject of a wide range of studies (e.g. Plumb et al., 2000, Hoor et al., 2002, Engel et al., 2002 or Werner, 2007).

Also useful for transport investigations is the “age of air” concept (Kida, 1983). Stratospheric transport times are high (on the order of years) compared with those in the troposphere. Tropospheric concentrations vary on the order of months due to different emissions of substances. For instance, a stratospheric air mass in 30 km altitude might have left the troposphere 4 years ago. To correct for this lag time the age of air concept can be used as it describes stratosphere residence times. In a first simplification step the tropical tropopause is assumed as the only place where air enters the stratosphere (Holton, 1990). Then each stratospheric air parcel is assumed to consist of a number of infinitesimally small and irreversibly mixed parcels which have experienced different transport pathways (see Figure 1.1.3). The corresponding different stratospheric residence times can be described by a distribution function (i.e. a probability distribution). This distribution function is called the “age spectrum” with the centre of this function being the “mean age of air” i.e. the mean stratospheric residence time (Hall and Plumb, 1994). Tracers with very long lifetimes (having no tropospheric or stratospheric sink in the ideal case) and appropriate tropospheric concentration trends with time (such as SF_6 or CO_2) can be used to calculate the mean age of air and the corresponding age spectrum e.g. via parameterisations of the distribution function (Hall and Plumb, 1994). The age of air has also been widely used to investigate stratospheric dynamics (e.g. Schmidt and Khedim, 1991, Volk et al., 1997, Waugh and Hall, 2002, Engel et al., 2006, Bönisch, 2006).

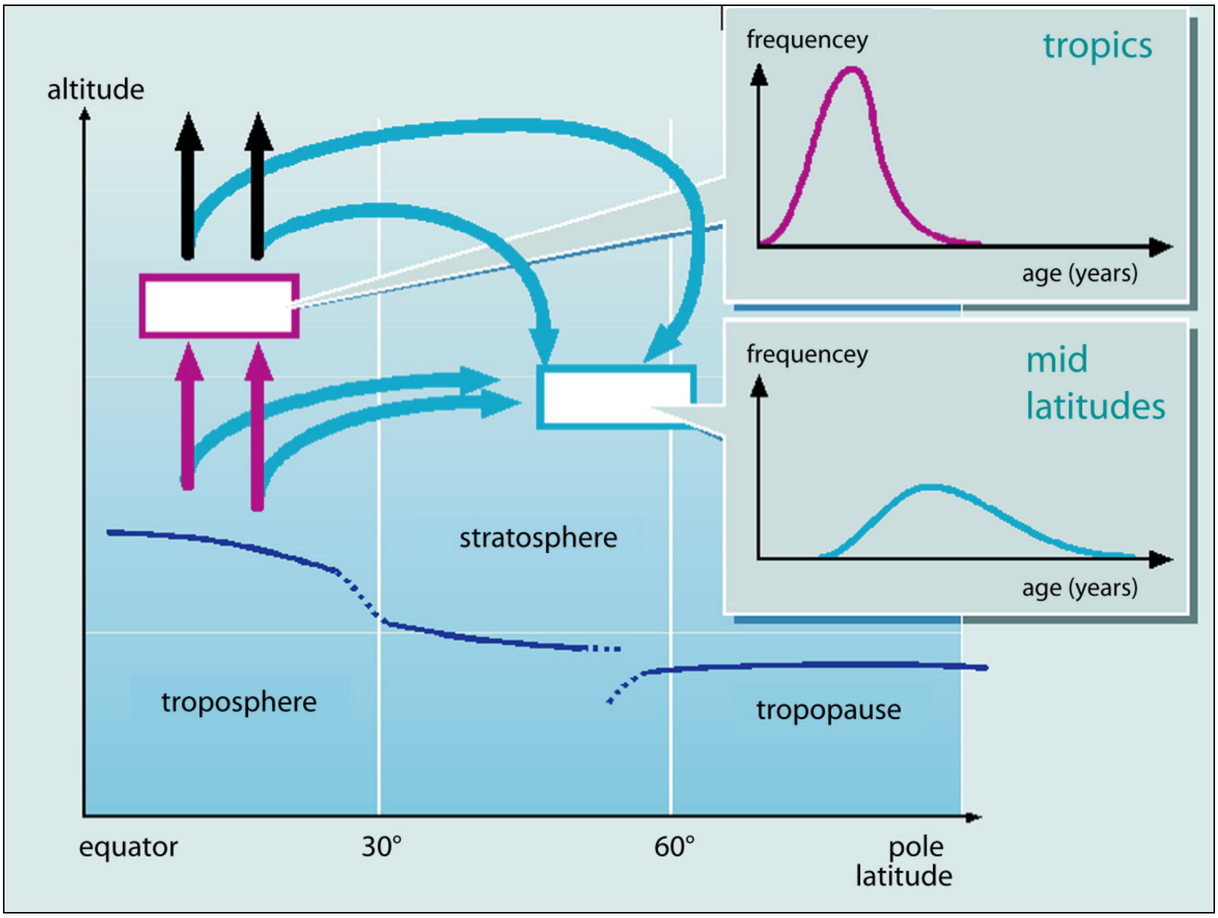

Figure 1.1.3. The concept of age of stratospheric air. A stratospheric air parcel can be described as a mixture of an ensemble of infinitesimally small and irreversibly mixed air parcels which have experienced different transport pathways. The corresponding stratospheric residence times (the "ages") can be described by a probability distribution function with the mean age being the centre of this function. The Figure was adapted from Schmidt et al. (2001).

1.2 Analytical methods

1.2.1 Air sampling techniques

A number of stratospheric and upper tropospheric air samples have been provided for this thesis. Details on how these samples were obtained will be given in the following. Three cryogenic whole-air-samplers (named BONBON-I, BONBON-II and CLAIRE) are operated by the workgroup of PD Dr. Andreas Engel at the University of Frankfurt.

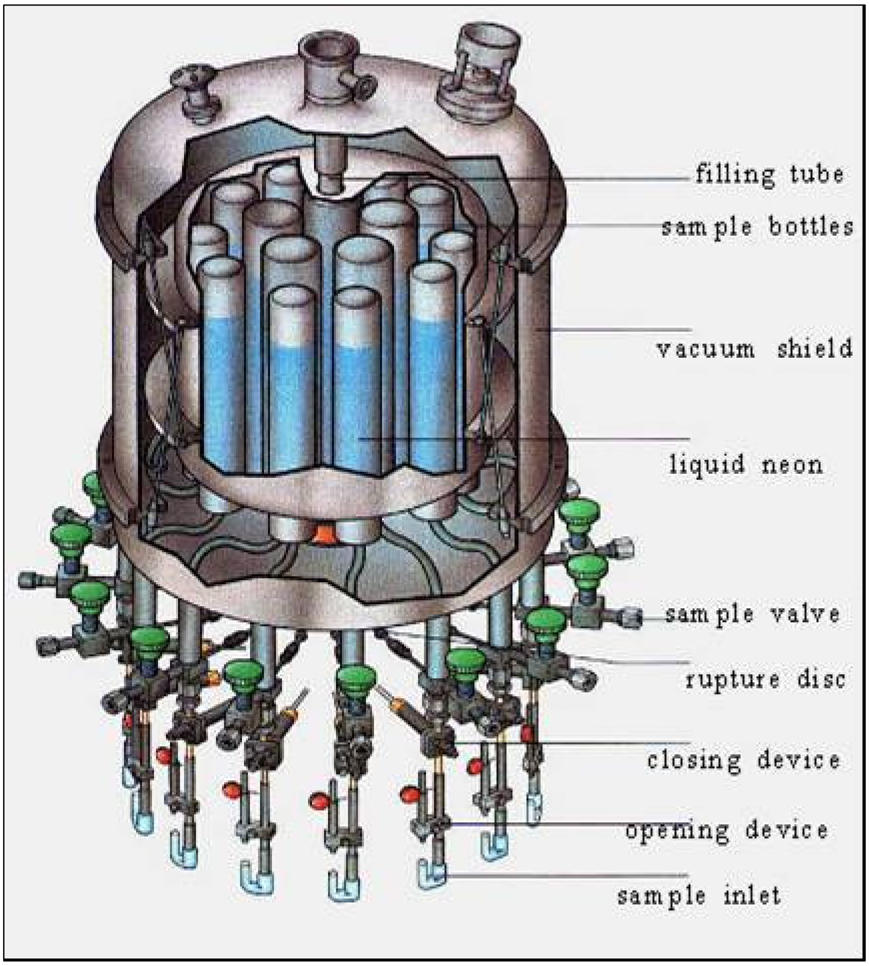

Figure 1.1.4. Lateral cut view of a BONBON whole-air-sampler. Samples are collected cryogenically as the individual containers are submersed in liquid Neon inside a Dewar. The opening device is a metal hammer which is released by smelting a wire with the discharge current of a capacitor. If released the hammer crushes a glass cap which opens a container. The closing device is a gold pipe which is cold welded using a pyrotechnical device to seal the container after collection of the air sample.

These samplers are brought into the stratosphere with large balloons launched by the French Space Agency CNES (Centre National d'Etudes Spatiales) and reach high altitudes up to 38 km. As airplanes can access only altitudes up to 21 km the balloons present a unique measurement platform for stratospheric measurements. To avoid contaminations from outgassing of the balloon or gondola parts (due to the low pressures and high radiation in the stratosphere) samples are preferentially taken during the slow descent of the balloon if the meteorological conditions permit it. The BONBON cryo-samplers consist of a Dewar which contains 15 stainless steel containers that are electropolished inside to provide a smooth and inert surface (see Figure 1.1.4). The Dewar is filled with liquid Neon before the balloon flights and cools to about 27 K. This allows sampling of large amounts of air even if at low outside pressures because the containers work as cryopumps (almost all air components are condensed inside). Each container is sealed with a glass cap which can be broken to open it. Moreover the inlets contain a gold pipe which can be cold welded using a pyrotechnical device to seal the containers once a sufficient amount of air has been condensed. These actions are performed via telecommand at those altitudes, where samples shall be collected. More technical details are given in Schmidt et al. (1987) and Engel (1993). The new cryosampler CLAIRE built in 2006 is working similar, except that it was designed to take samples during balloon ascent and can collect 26 samples.

Other air samples originated from the whole air sampler WAS of the University of Utrecht (group of Prof. T. Röckmann) operated onboard the Geophysika high altitude research aircraft. These samples were collected into evacuated two litre stainless steel containers using a trace gas free metal bellows pump (see Kaiser et al., 2006 for details).

1.2.2 Gas Chromatography with Electron Capture Detection

Gas Chromatography (GC) is a standard separation method in which the different affinities of the sample components towards a stationary and a mobile (gaseous) phase are taken advantage of (Maludzinska, 1990). Individual compounds of the analyte mixture have different physicochemical properties and are thus distributed differently between mobile and stationary phase. Further essential parts of a Gas Chromatograph are a sample injector, a separation column which is often located inside a regulatable oven to enhance separation, a detector and a data recording system (Cammann, 2001). Separation columns can be either packed (inner diameter ID between three and eight mm, length up to three meter, capable of larger analyte amounts) or capillary columns, (ID 0.1 to 0.53 mm, length up to 100 m, better separation) (Kellner et al., 2004). Micro-packed columns are a hybrid of these two column types providing a better separation than packed columns and a larger analyte capability than capillary columns.

A widely used detector – especially in environmental trace analysis – is the Electron Capture Detector (ECD). It contains an emitter of β-radiation (e.g. ^{63}Ni) which ionises the carrier gas and creates a current. This current is affected by bypassing compounds – especially those who are able to capture electrons (Kellner et al., 2004). Thus, the ECD is very sensitive towards all substances that contain electronegative substituents such as halocarbons, many sulphur containing compounds and alkyl nitrates. Its sensitivity rises with the number of halogen atoms but also with the atomic number of the contained halogen ($F < Cl < Br < I$). Disadvantages of the ECD are its limited selectivity and its response behaviour which is nonlinear and also characteristic for a compound but can not be predicted from the molecular structure (Cammann, 2001).

1.2.3 Mass Spectrometry

Another widely used option for the detection of (not only organic) compounds that were separated by GC is a Mass Spectrometer (MS). Inside a MS ions are generated from the analyte which are subsequently separated via their different mass to charge (m/z) ratios and then detected (Kellner et al., 2004). A typical method for ion generation is electron impact (EI, also called electron ionisation). Here, the analyte is bombarded with a high energy electron beam (typically ~70 eV). One or more electrons are removed from the respective molecule and the remaining excess of internal energy triggers its dissociation into characteristic fragments which are mainly cationic (Schwedt, 1996). To avoid bimolecular reactions the inside of such a MS is kept under high vacuum (typically around 10^{-3} Pa). In contrast to EI, chemical ionisation (CI) is a very soft ion generation technique and performed in a higher pressure environment (0.1 – 100 Pa). Chemical Ionisation can lead to both positive and negative ions. In the case of negative ion chemical ionisation (NICI) a reagent gas (e.g. methane) is added and acts as an energy moderator as it transfers thermal electrons with energies between 0 and 10 eV to the analyte molecule (Kellner et al., 2004, formula 1.4). The resulting molecular anions (formula 1.5) are stable in many cases – unless they contain a very electronegative substituent such as a chlorine or bromine atom. In this case the electron capture results in dissociation of the molecule and release of chlorine and/or bromine anions according to formula (1.6). These anions are then separated and detected. The NICI mode provides much lower detection limits for many halocarbons than the EI mode does (Buser, 1986) but also less selectivity and structural information.

$$CH_4 + e^-_{(70eV)} \leftrightarrow CH_4^+ + 2e^-_{(thermal)} \tag{1.4}$$

$$M + e^-_{(thermal)} + CH_4 \leftrightarrow M^- + CH_4^* \tag{1.5}$$

$$RX + e^-_{(thermal)} \leftrightarrow R^\bullet + X^- \tag{1.6}$$

The mass analyser or mass filter separates or focuses the ions. In a quadrupole filter (such as inside the Agilent 5975 MS which was used for this thesis) the ions are exposed to a high frequency electromagnetic field which can be modulated very fast to let only ions with a distinct m/z ratio pass. The ions are then detected, amplified (e.g. with an electron multiplier) and recorded as three-dimensional arrays (ion intensity, m/z ratio and time) on a computer using a data acquisition software (Kellner et al., 2004).

2 Analytical system and data analysis

2.1 Configuration of the GC-ECD-MS

In the beginning of this thesis in May 2005 the used analytical system (University of Frankfurt, Institute for Atmospheric and Environmental Sciences, workgroup of PD Dr. Andreas Engel) consisted of a pre-concentration system and a Siemens Si1 Gas Chromatograph with Electron Capture Detection. This general system has been used to analyse stratospheric air samples for more than two decades (with several slight and mostly chromatographic modifications). As mentioned in Chapter 1.2.2 the ECD is a highly sensitive detector towards halocarbons but the low concentrations of trace gases in the stratosphere necessitated a further pre-concentration. A scheme of the system is displayed in Figures 2.1.1 and 2.1.2. The additional Mass Spectrometric detection channel was attached in October 2005 (5975 inert XL mass selective detector with Performance turbo pump and High vacuum gauge controller from Agilent Technologies).

2.1.1 Pre-concentration system

The part used for pre-concentration (blue coloured in Fig. 2.1.1) was not modified. It consisted almost completely of stainless steel parts and was evacuated to about $4*10^{-2}$ mbar prior to analysis using a Leybold Trivac pump, type D4B with an activated alumina sorbent filter to prevent back streaming. The air was led towards a sample loop (1/8" stainless steel, length: ~30 cm) which was filled with porous glass beads (mesh size: 60) to provide a high surface area. This sample loop was cooled with liquid nitrogen and trace gases were condensed inside. Due to the low pressure, N_2, O_2, H_2 and the three noble gases He, Ne and Ar remained in gaseous state and passed the sample loop while the higher boiling trace gases were condensed. The uncondensed compounds reached a reference volume canister with a pressure sensor (range: 0 to 1.7 bar, full scale accuracy: 0.073 %, model 204 from SETRA Systems Inc., USA).

As these compounds represent more than 99.9 Vol.-% of dry air the pressure inside the reference volume can be used as a direct measure of the air volume that passed the sample loop. But as the pressure inside has to remain low in order to prevent condensation of major air components the amount of air which can be pre-concentrated is limited. Tests showed that the pressure inside the system has to remain below ~350 mbar to avoid a large peak from freezing of O_2. For the pre-concentration of different amounts of air it is possible to switch between three reference canisters with volumes of 0.250, 1.00 and 10.00 litres. Measurements performed for this thesis refer to the 1 litre reference canister unless stated otherwise. Due to highly variable humidity, lower tropospheric air can cause errors of up to several percent to the reference volume method. Therefore only dried calibration standards with humidity below 0.05 Vol.-% were used. To ensure a quantitative condensation the sample air flow was regulated with a needle valve to 40 ml/min at maximum during the pre-concentration process.

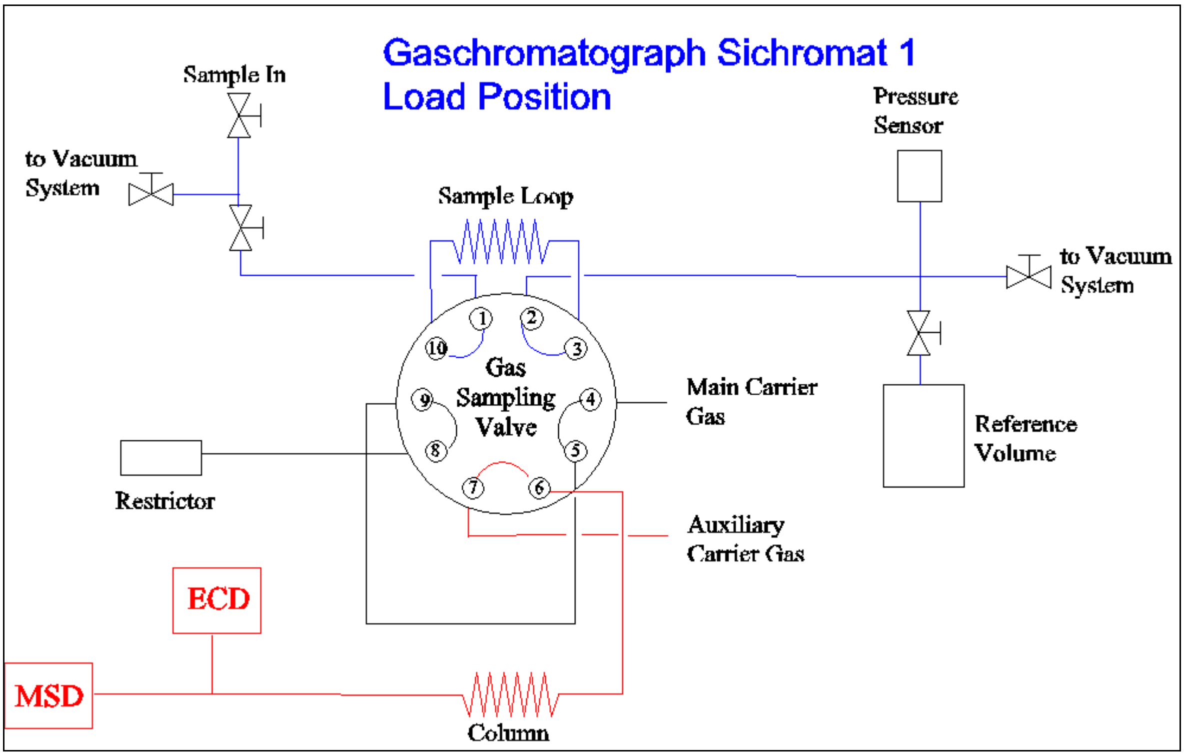

Figure 2.1.1. Scheme of the analytical setup during the preconcentration process.

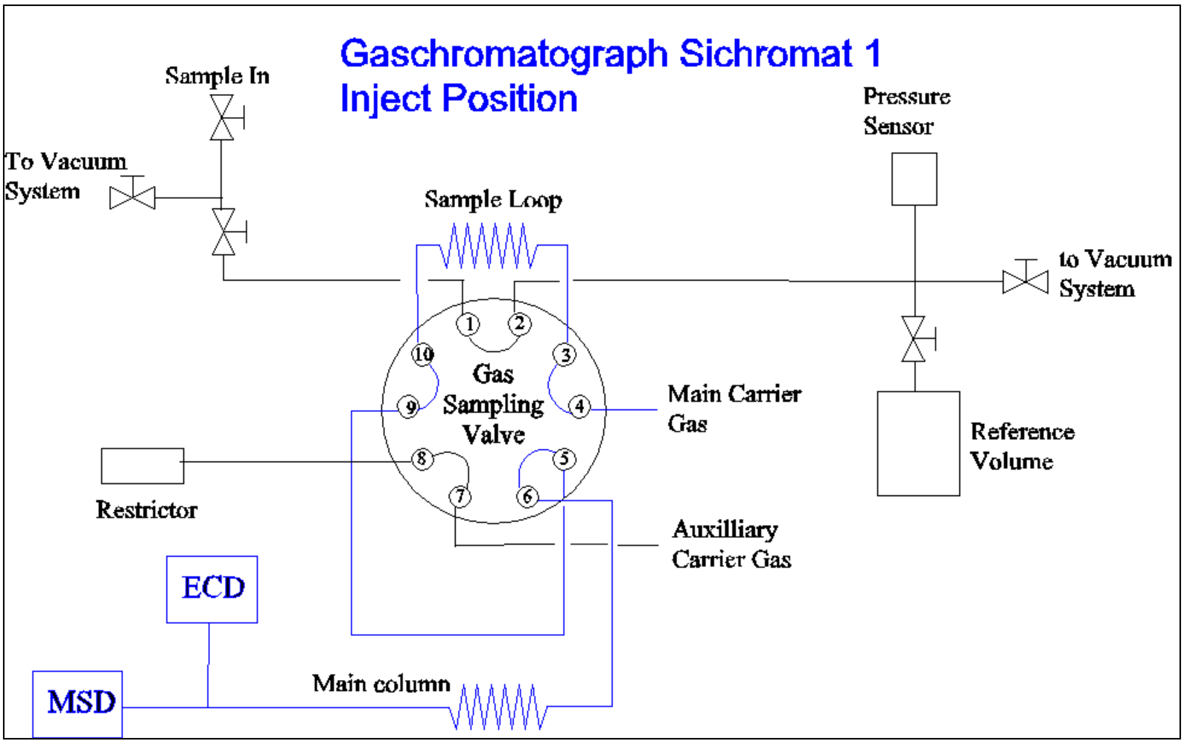

Figure 2.1.2. Scheme of the analytical setup during separation and detection.

2.1.2 Chromatography and detector details

The filled sample loop was then injected into the carrier gas flow (Figure 2.1.2) by switching the 10-port-2-position-valve (from VICI AG International) and heated to about 80 °C. Subsequent separation took place on a micro-packed Porasil C/n-octane column (1/8" stainless steel, length: ~5 meters) using a temperature program from -40 to 90 °C (to 120 °C from 2006 on; heating rates: 3 minutes at -40 °C, then with 15 °C/min to 0 °C and with 10 °C/min to end temperature). The initial carrier gas was ultra-pure Nitrogen (from Air Liquide Deutschland GmbH, purity ≥ 99.999 %-mol). Before the installation of the Mass Spectrometer it was changed to Helium (ALPHAGAZ™ 2 from Air Liquide Deutschland GmbH, purity ≥ 99.9999 %-mol) which was further purified from oxygen, hydrocarbons and moisture using a gas purification system from Chromatography Research Supplies, USA. The carrier gas flow was regulated to about 6 ml/min with a detector split of about 2.5/3.5 ml/min (MSD/ECD). This ratio was achieved by varying the length of the transfer capillaries from the splitter to the detectors (inner diameter of 0.15 mm, length to ECD: ~ 70 cm, length to MS: ~ 100 cm). The ECD detector was additional flushed with ultra-pure Nitrogen (from Air Liquide Deutschland GmbH, purity ≥ 99.999 %-mol which was further purified according to Helium, 30 ml/min) as a so-called "make-up" flow. Please note that the split ratio and also the carrier gas flow are slightly dependent on the oven temperature as the Si1 works without using electronic pressure control (EPC) valves.

2.2 Identification of substances

Before the application of the MS the GC-ECD system was able to measure SF_6, OCS and the following seven halocarbons: CF_2Cl_2 (F12), CHF_2Cl (F22), CH_3Cl, $CFCl_3$ (F11), $CF_2ClCFCl_2$ (F113), CCl_4 and CH_3CCl_3. These substances were identified by injection of static dilutions of the pure compounds and subsequent retention time comparison. The MS enabled access to a wide range of substances. The following sub-chapters describe the details of the identification process and the methods used to confirm the identity of the substances. Please note, that the substances were identified within a period of two years. Moreover, for several substances the detection limit was and/or is too high to detect atmospheric abundances with this analytical system and for others no calibration is available by now. Therefore only target substances as defined in Chapter 1.1.3 will be discussed.

2.2.1 Identification via synthetic EI-Scan

As described in Chapter 1.2.3 the Agilent 5975 is a quadrupole MS and can be operated in Electron Impact mode which provides two sub-modes. In Scan Mode a wide range of ions can be measured almost at the same time. For a scan from 15 to 300 amu carried out within 300 milliseconds the detection limit (i.e. signal/noise = 3/1) was about 1 pg for CF_2Cl_2 (F12) pre-concentrated from 300 ml of air. This corresponds to a mixing ratio detection limit of about 100 ppt. In SIM Mode a limited number of ions are measured within this period which provides much lower detection limits in the lower and sub-ppt range. As many of the target substances have atmospheric abundances in this low mixing ratio range a scan was not suitable for identification. Thus, the MS was operated in SIM mode measuring three ions at a time throughout the chromatogram and injecting the same amount (~100ml) of one air standard repeatedly. The obtained SIM chromatograms were then merged to one “synthetic scan”. But a correction was needed to take slight retention time variations between the runs into account. This could be achieved by calculating a least-square polynomial fit to the retention times of the five largest signals in the ECD chromatogram relative to the same signals of the first ECD chromatogram on that day and applying this fit to the respective MS-

SIM run (so-called retention time locking). This algorithm is part of the program gcms.pro which is written in interactive data language (IDL, version 6.2, Microsoft Windows (c) 2005, Research Systems, Inc.) and was developed in the workgroup. The complete source code can be obtained from Andreas Engel on request (gcms.5.3.pro). As examples the identifications of CH_3CCl_3 (methyl chloroform, about 40 ppt) and of CF_2BrCF_2Br (H2402, about 0.4 ppt) are shown in Figure 2.2.1 and 2.2.2.

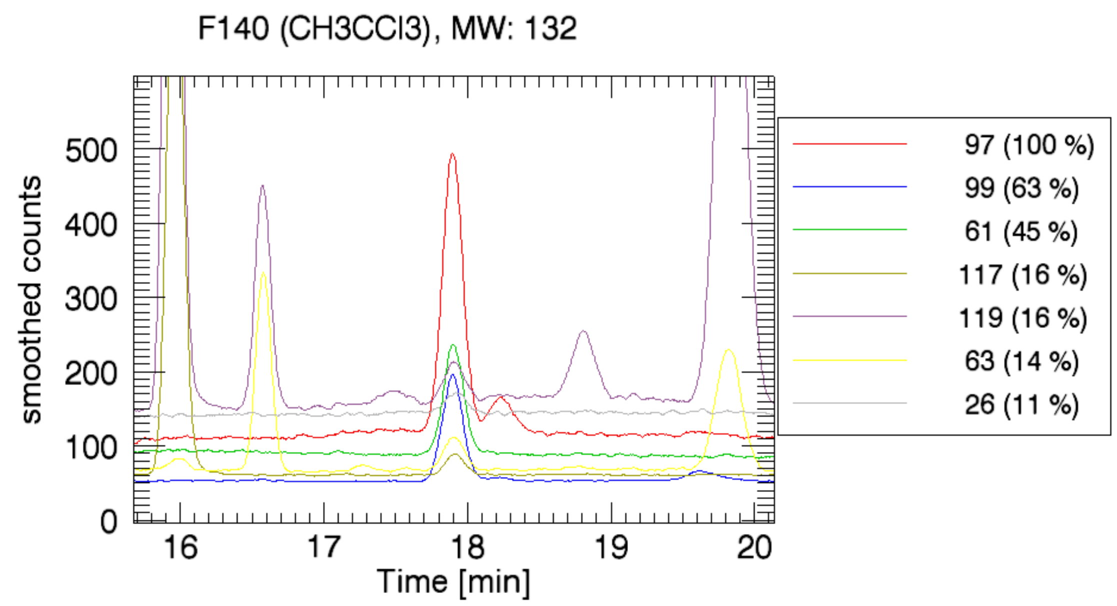

Figure 2.2.1 Identification of CH_3CCl_3 (methyl chloroform, molecular weight 132 g/mol, about 40 ppt, 100 ml of air pre-concentrated) using a "synthetic scan" generated from an overlay of GC-EI-SIM-MS chromatograms. Displayed are the abundances of the seven most abundant ions (mass/charge ratio m/z) versus retention time. In brackets one can see the expected relative abundances as listed in the NIST mass spectral library. All seven major ions occur in the expected abundance ratios.

Similar pictures for all other substances identified with this method can be found in the Appendix (Figure set A.S.1). For CH_3CCl_3 (methyl chloroform) the seven major ions could be detected in the right relative abundances as expected from the reference spectrum of the NIST mass spectral library. In contrast the spectrum of CF_2BrCF_2Br (H2402, about 0.4 ppt) illustrates the problems connected with this identification method. For substances with abundances near the detection limit not all ions could be detected especially if large signals were occurring nearby. Fortunately the signals on m/z 179 and 181 in a ratio of 1:1 are highly specific for H2402.

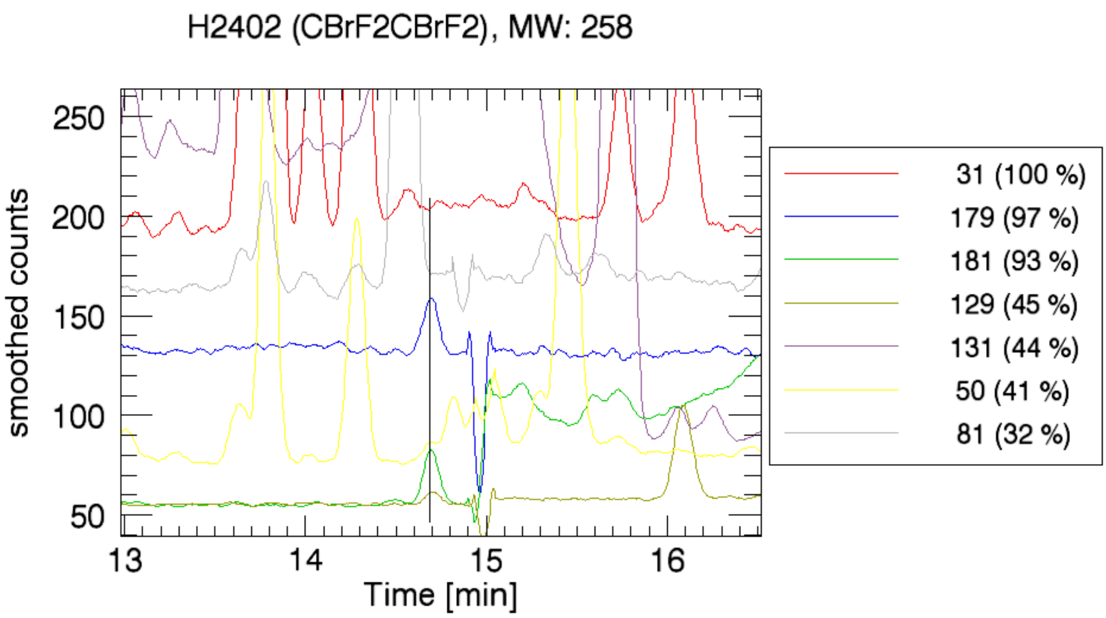

Figure 2.2.2. The same as in Figure 2.2.1 but for CF_2BrCF_2Br (H2402, molecular weight 258 g/mol , about 0.4 ppt).

But other substances with lower molar masses were affected by the limited mass resolution of the quadrupole instrument. For instance, a signal measured on ion 50 covered a mass to charge (m/z) range from 49.70 to 50.70 and all ions within that range – e.g. CF_2^+, CH_3Cl^+, $C_4H_2^+$ or $C_2F_4^{2+}$ – were assigned to this signal. In addition the number of organic substances which contain a certain fragment increases very fast with increasing number of C-Atoms. The latter is correlated with the substances boiling point and therefore with retention time. This led to the occurrence of large numbers of signals in the chromatogram at higher retention times and especially on ions having lower m/z ratios. Thus, a number of uncertain target substances remained after the synthetic scan identification process. These were substances having

a) low abundances such as CF_2BrCF_2Br (H2402) and/or

b) low molecular masses which leads to unspecific and frequently occurring fragments such as methyl chloride CH_3Cl or 1,2-dichloroethane CH_2ClCH_2Cl and/or

c) uncertainties due to coelution with one or more substances such as $CHFClCF_3$ (F124) which coeluted with $CFCl_3$ (F11), CS_2 (carbon disulfide) and i-C_5H_{12} (2-methylbutane)

2.2.2 Identification and confirmation via EI-SIM and EI-Scan

Two further EI approaches were used to identify substances and/or to confirm their identity. The above mentioned retention time correction method could not resolve low time differences. In order to assure that the 10 most abundant ions of uncertain substances occurred at exactly the same time they were measured in the same EI-SIM run while pre-concentrating trace gases from about one litre of air (using the large reference volume, for results see Appendix, Figure set A.S.4). In addition, a calibration standard that contained large amounts (around 100 ppb of 57 substances in N_2; provided by Sarah Gebhardt, MPI-CH Mainz) was measured in EI-Scan mode (see Appendix, Figure set A.S.2).

2.2.3 Confirmation via NICI

The used Agilent 5975 MS can be switched to Negative-Ion-Chemical-Ionisation (NICI) mode. In this detection mode a reactant gas (here: methane, purity: $\geq$ 99.9995 Vol.-%.) is ionised and provides thermal electrons. Chlorinated, brominated and iodinated organic substances undergo dissociative electron capture and halogen anions are formed. This is a very specific and sensitive method to detect amounts of a few parts per quadrillion (ppq) of some substances although it does not provide further structural information (see Chapter 1.2.3 for details). As another confirmation of substance identification an air standard was analysed in NICI-mode in February 2008 measuring the mass traces of the major atmospheric isotopes of chlorine (^{35}Cl and ^{37}Cl, ratio ~3:1), bromine (^{79}Br and ^{81}Br, ratio ~1:1) and iodine (^{127}I) throughout the chromatogram (see Appendix, Figure set A.S.3). Problems with this identification method are caused by coeluting substances and/or the low halogen anion formation rate of some substances (e.g. CH_3Br).

Table 2.2.1 shows the 26 target substances which could be identified including the methods and dates of identification and the ion which was used to quantify the respective substance in EI-SIM mode when measuring atmospheric samples. The latter was not always the ion with the highest abundance because of interferences with coeluting substances. If indications for a coeluting substance were found they are also mentioned in Table 2.2.1. Only targeted substances are displayed. An expanded version of this table which also includes more detailed identification information can be found in the Appendix (Figure A.1). Furthermore the identification included three Chlorofluorocarbons which have not been observed in the atmosphere before (Laube and Engel, 2008). Detailed information on that issue can be found in Chapter 6.

Table 2.2.1. Target substances which could be identified including the methods and date of identification, the quantifier ion in EI-SIM mode and indications for coeluting substances. The sorting criterion is the retention time in January 2008.

RT* [min]	Substance (name)	Identification		(Indications for) coeluting substances	Quant. ion [m/z]
		method	date		
6.1	CF_3Br (H1301)	a,c,d	Nov.2005	no	69
6.5	C_2F_5Cl (F115)	a,c,d	Nov.2005	no	85
7.9	CF_2Cl_2 (F12)	a,b,d	before 2005	dp with F1113, ion 69	**85**
9.4	CHF_2Cl (F22)	a,c,d	before 2005	ion 51 dp	67
10.3	CF_2ClBr (H1211)	a,c,d	Nov.2005	F114	129
10.4	CF_2ClCF_2Cl (F114)	a,b,d	Nov.2005	H1211, dp with F114a	**135**
10.6	CF_3CFCl_2 (F114a)	a,b,d	Nov.2005	dp with F114	**135**
11.1	CH_3Cl (methyl chloride)	a,b,d	before 2005	no	50
11.4	CH_3CF_2Cl (F142b)	a,c,d	Nov.2005	no	65
12	$CFCl_3$ (F11)	a,b,d	before 2005	CS_2, F124, i-C_5H_{12}, SO_2	103
12	$CHFClCF_3$ (F124)	a	Nov.2005	F11, CS_2, i-C_5H_{12}, SO_2	67
12.8	CH_3Br (methyl bromide)	a,b,d	Nov.2005	no	94
14.1	C_2H_5Cl (chloroethane)	a,b	Nov.2005	ions 49 and 66 dp	64
14.1	$CF_2ClCFCl_2$ (F113)	a,b,d	before 2005	F141b, a: ion 151 too high	151

Table 2.2.1 continued

RT* [min]	Substance (name)	Identification method and date		(Indications for) coeluting substances	Quant. ion [m/z]
14.4	CH_3CFCl_2 (F141b)	a,c,d	Nov.2005	F113, CH_3I, H2402	81
14.6	$CBrF_2CBrF_2$ (H2402)	a,c,d	Nov.2005	F141b, CH_3I	179
15.3	CH_2Cl_2 (dichloromethane)	a,b,d	Nov.2005	isoprene, ion 84 dp	**49**
15.8	CCl_4 (tetrachloromethane)	a,b,d	before 2005	$C_4F_6Cl_2$	117
16.7	$CHCl_3$ (chloroform)	a,b,d	Nov.2005	CH_3CHCl_2, ion 83 dp	**83**
17.1	CH_2ClBr (chlorobromomethane)	a,d	Nov.2005	CH_3CHCl_2, CH_3CCl_3	**130**
17.2	CH_3CCl_3 (methyl chloroform)	a,b,d	before 2005	CH_3CHCl_2, CH_2ClBr	117
17.4	C_2HCl_3 (trichloroethene)	a,b,d	Nov.2005	CH_3CCl_3, C_2H_5I	130
18.8	CH_2Br_2 (dibromomethane)	a,b,d	Feb.2006	C_2Cl_4, benzene	174
18.8	C_2Cl_4 (tetrachloroethene)	a,b,d	Nov.2005	CH_2Br_2, benzene	166
19.2	CH_2ClCH_2Cl (1,2-dichloroethane)	a,b,d	Nov.2005	CH_2ClI, ions 62 and 64 dp	**62**
24.3	$CHBr_3$ (bromoform)	a,b,d	Feb.2006	no	173

* – retention time in January 2008

dp – (sometimes) double peak observed

a – identified with synthetic scan from merged EI-SIM runs with pre-concentration of trace gases from about 0.1 litre of air

b – identified with high concentrated substance mixture in N_2 from MPI-CH Mainz ("Megamix")

c – identity confirmed with EI-SIM run measuring up to 10 of the most abundant ions in the same run and pre-concentrating trace gases from about 1 litre of air

d – identity confirmed with NICI-SIM due to the occurrence of chlorine, bromine and/or iodine anions in the expected isotopic ratios

bold numbers – there are indications that the signals of these ions can be influenced by coeluting substances

Only a few fluorinated and non-halogenated hydrocarbons were identified. Due to the large number of these substances present in the troposphere – the atmospheric region where all of the used calibration standards originate from – interferences with target substances can not be ruled out. Such interferences could especially have influenced those target substances which are quantified on ions with low m/z ratio and have higher retention times such as CH_3Cl, CH_2Cl_2, C_2H_5Cl and CH_2ClCH_2Cl.

To summarise, the combined identification approaches led to a very well characterised chromatographic system. The number of measurable and securely identified substances was increased from 9 to 57 of which 24 were target substances with upper tropospheric abundances above detection limits (see Table 2.2.1; CH_2ClBr and $CHBr_3$ were too low concentrated). The only target substance that was found to show a blank signal in the analytical system was CH_3Cl (methyl chloride, around 5 ppt). The chromatographic system was found to separate substances primarily via boiling point differences as is displayed in Figure 2.2.3 (corresponding data in the Appendix, Figure A.2). This correlation represents an additional confirmation of the substance identification.

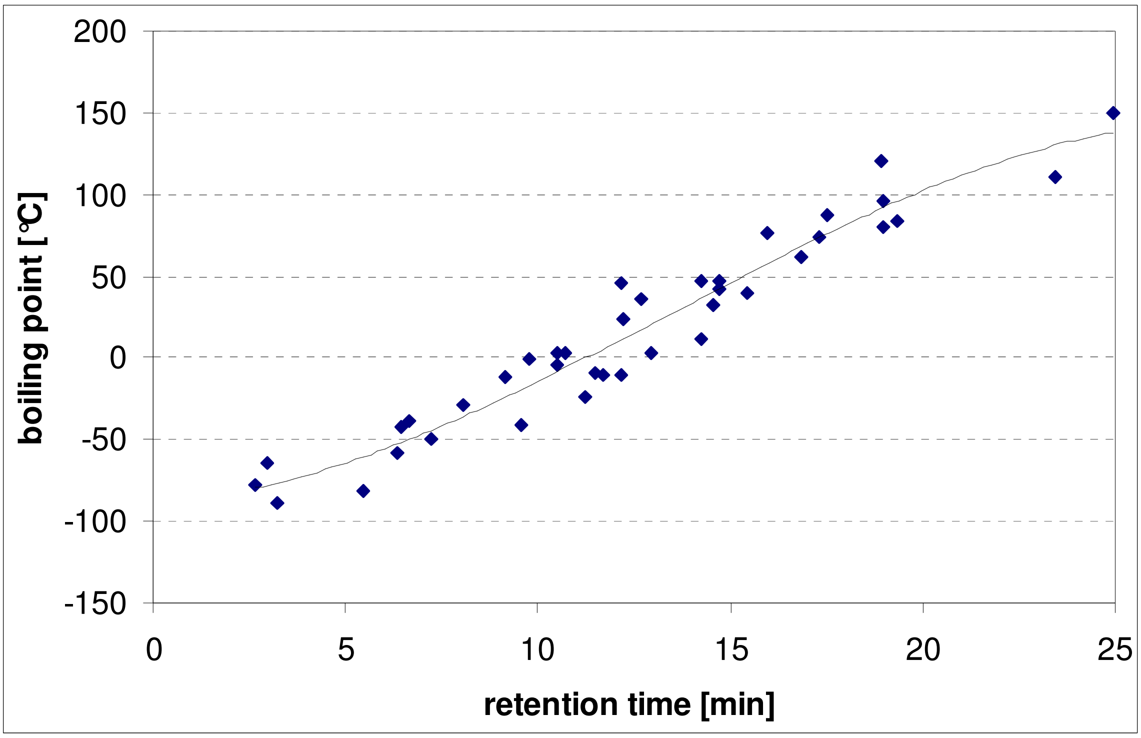

Figure 2.2.3. The chromatographic system separates compounds primarily via boiling point differences. The variations from the correlation curve (up to ± 30 °C) are mainly due to other separation criteria such as the polarity of the molecules.

2.3 Data analysis

Quantification of substances was carried out in six major steps:

1) Measurements. As the used detection methods are no absolute but relative measurement techniques the air samples were measured against a calibrated air standard. The usual sequence was starting the measuring day with a blank followed by two calibration standards, then a series of two measurements of the sample and the calibration standard again. The latter three measurements were repeated until the end of the measuring day. Usual times for one run including pre-concentration and cooling of the GC oven were between 30 and 45 minutes depending on varying record times and pre-concentrated trace gas amounts.
2) Data recording. The ECD software only recorded a two-dimensional signal – detector output voltage and time. The Software ChromPerfect Spirit from Justice Innovations was used. The MS signal was recorded using the Enhanced MSD ChemStation software, Built D.02.00.237 from Agilent Technologies. It provided the mass/charge ratio as an additional dimension and was mostly run in EI-SIM mode while measuring only between three and six ions at a time to get enhanced detection limits. Moreover, two ions of each substance were measured if possible – one for substance quantification (quantifier) and one for confirmation (qualifier). SIM methods were drawn up to record as many target substances as possible (example in the Appendix, Figure A.3). These methods contained up to 30 retention time windows switching between the ions.
3) Peak integration. ECD signals were manually integrated by determining peak start and end points and connecting these with a linear baseline. The MS signals were mainly integrated using the IDL program gcms.pro which was developed in the workgroup. Data was exported from the MSD ChemStation in comma-separated-variable (csv) format which was read in by the IDL program. The sub-chapter following this list deals with integration details.
4) Instrument drift correction. First, all signal areas and heights were corrected for the exact amount of air out of which trace gases were pre-concentrated. The resulting relative responses should be the same for all calibration standard measurements but showed a systematic drift over the measuring day for almost all substances. This drift could be caused e.g. by temperature changes in the laboratory which affect pressure sensor and vacuum pump performances. One approach to correct for it would be to use a polynomial fit function. But due to the limited number of data points (i.e. calibration standard

measurements) the drift was assumed to be linear within the short time period between two calibration standard measurements. The relative response of the calibration standard at the sample measurement time was then calculated via linear interpolation according to formula 2.3.1.

$$r_{p,n,t} = r_{p,cal1} + \frac{\left(r_{p,cal2} - r_{p,cal1}\right)\left(t_{p,n} - t_{p,cal1}\right)}{t_{p,n} - t_{p,cal2}} \tag{2.3.1}$$

$r_{p,n,t}$ – relative response (i.e. the peak parameter corrected for the exact pre-concentrated amount) at the start time t of sample run n according to peak parameter p (height or area)

$r_{p,cal1}$ and $r_{p,cal2}$ – relative responses of the surrounding calibration standard runs

$t_{p,n}$ and $t_{p,cal}$ – start times of the corresponding runs

5) Nonlinearity correction. The ECD is a nonlinear responding detector, which means that the signal areas and heights are not linear proportional to substance quantities (here: mixing ratios). Therefore nonlinearity curves were derived for each substance by measuring a calibrated dilution series. Please refer to Chapter 2.5 for further details. For the MS no correction was needed because it was working linear, which will also be shown in Chapter 2.5.
6) Mixing ratio and reproducibility calculation. The mixing ratios were derived from the calculated relative response of the calibration standard at the sample measurement time using the rule of three. Most atmospheric samples were measured only twice due to the limited amount of air available in the containers. Therefore the calibration standard measurements were used to derive reproducibilities (also called relative standard deviations, RSDs). The relative response of a calibration standard was calculated as it would have been a sample via linear interpolation from the surrounding standard measurements. This calculation was carried out for all calibration standards on the measuring day (except the first and the last one). The differences between the calculated and the measured relative responses were then used for reproducibility calculation according to Equation 2.3.2.

$$R_{p,d} = \frac{\sqrt{\frac{1}{n}\sum_{n}\left(r_{p,cal,,n,i} / r_{p,n,cal} - \frac{1}{n}\sum_{n}\left(r_{p,cal,,n,i} / r_{p,n,cal}\right)\right)^2}}{\frac{1}{n}\sum_{n}\left(r_{p,cal,,n,i} / r_{p,n,cal}\right)} \qquad (2.3.2)$$

$R_{p,d}$ – reproducibility of the calibration standard according to peak parameter p (height or area) on the measuring day d

$r_{p,cal,,n,i}$ – relative response (i.e. the peak parameter corrected for the exact pre-concentrated amount) of calibration standard cal from run n from linear interpolation of surrounding calibration standards i as calculated according to Eq. (2.3.1).

$r_{p,n,cal}$ – relative response of calibration standard cal from run n

The detection limit was determined at a signal to noise ratio of 3:1 by using the peak to peak signal/noise according Equation 2.3.3 for the calculation.

S/N = (signal height - baseline height) / (noise maximum - noise minimum) (2.3.3)

Examples of the integration result file, calculation of nonlinearity functions from dilution series and a sample retrieval can be found in the enclosed Microsoft Excel 2003 data sheets (CD: \examples\).

2.4 Peak integration

Determination of the area and height of a signal is a very sensitive parameter of the quantification process. Peak integration methods affect the calculation of the quantity as well as the precision of the obtained results. An often used method is the baseline integration (Dyson, 1998). For instance, the integrator of the commercial MSD ChemStation data analysis software from Agilent Technologies allows an automated baseline integration using initial integration events. This method works fine as long as the peak height is high relative to the noise of the signal. But as illustrated in Figure 2.4.1 for small peaks the derived peak height and area becomes highly dependent on noise maxima and minima.

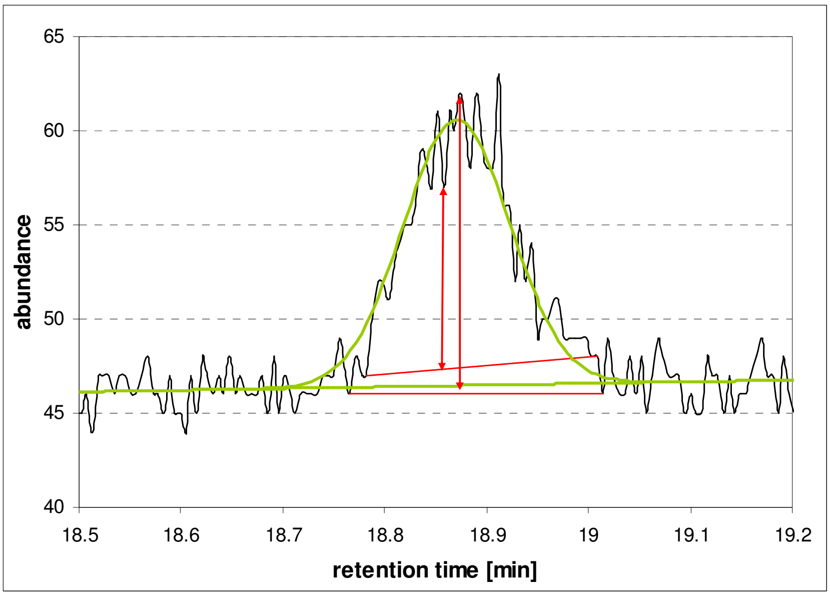

Figure 2.4.1 Comparison of different integration methods for a small peak. For the manual baseline integration peak height and also area are very sensitive to noise maxima and minima (red). This can cause bad reproducibilities as well as systematic errors in mixing ratio calculations. In contrast the Gaussian fit algorithm (green) which minimises area differences to the signal with the least sum-of-squares method gives much better reproducibilities (see also Table 2.4.1).

In order to minimise the influence of noise on peak parameters two different integration algorithms were developed in the workgroup: a smoothed-baseline algorithm and a Gaussian fit algorithm. These are included in the software above mentioned. The baseline algorithm uses an area-conserving Savitzky-Golay filter (Savitzky and Golay, 1964) to smooth the signal. The start and end of a peak is defined with adjustable threshold limits of the signals first and second order derivatives. Problems with this integration method are connected to threshold determination of small peaks because of the very low slope of the derivatives. A completely different approach is the Gaussian algorithm which uses the IDL gaussfit function to fit a Gaussian distributed peak to the signal by minimising area differences with the least sum-of-squares method. The baseline function is a direct result of this fit and can be subtracted. It is a polynomial of 1st or 2nd order (can be selected) and a quadratic baseline function was used for this thesis. In addition, a so-called “inverse” Gaussian fit algorithm was derived especially for tailing peaks. Please note, that all algorithms were designed only for well separated peaks which is why they were not used for the ECD retrievals (see Figure 3.1.1). All ECD results were derived by manual baseline integration. Table 2.4.1 shows a comparison of the MS reproducibilities of nine substances derived from eight measurements of the same amount of one air standard by using three different integration methods.

Table 2.4.1 Reproducibilities for nine substances obtained from eight measurements of the same pre-concentrated amount (~300 ml) of one air standard using different integration methods.

Substance (name)	Signal/ noise*	Reproducibility in %		
		baseline 1[a]	baseline 2[b]	Gaussian fit[c]
CF_2Cl_2 (F12)	1955	0.5	0.5	0.5
$CFCl_3$ (F11)	794	0.3	0.3	0.3
$CF_2ClCFCl_2$ (F113)	455	0.6	0.6	0.7
CH_3Cl (methyl chloride)	286	0.7	0.7	0.5
CH_2Cl_2 (dichloromethane)	98	1.9	1.4	1.0
CH_2FCl (F22)	92	0.9	1.6	1.0
$CHCl_3$ (chloroform)	53	1.8	2.3	1.2
CH_3Br (methyl bromide)	17	9.4	5.4	2.9
CF_2ClBr (H1211)	6	34	8.0	2.5

* – calculation: (signal height - baseline height) / (noise maximum - noise minimum)

a – automated baseline integration from ChemStation commercial software

b – smoothed-baseline integration from IDL program gcms.pro developed in the workgroup

c – Gaussian fit integration from IDL program gcms.pro developed in the workgroup

All methods gave comparable reproducibilities for peaks with a high signal/noise ratio. For smaller peaks the smoothed-baseline algorithm already represented an improvement but the Gaussian fit algorithm performed even better. But before choosing this algorithm for retrieval it needed to be proven that it reflects the peaks quantitatively. For this purpose different amounts of the same air standard on three different days were pre-concentrated and measured giving a total of 29 measurements with a pre-concentration range from 7 to 393 ml. These so-called pressure series were measured according to the sequence displayed in Figure 2.4.2. Figure 2.4.3 shows the means of the normalised relative detector responses as derived from the smoothed-baseline, the Gaussian fit and the inverse Gaussian fit algorithm for ten substances. The inverse Gaussian fit algorithm was only tested for tailing peaks.

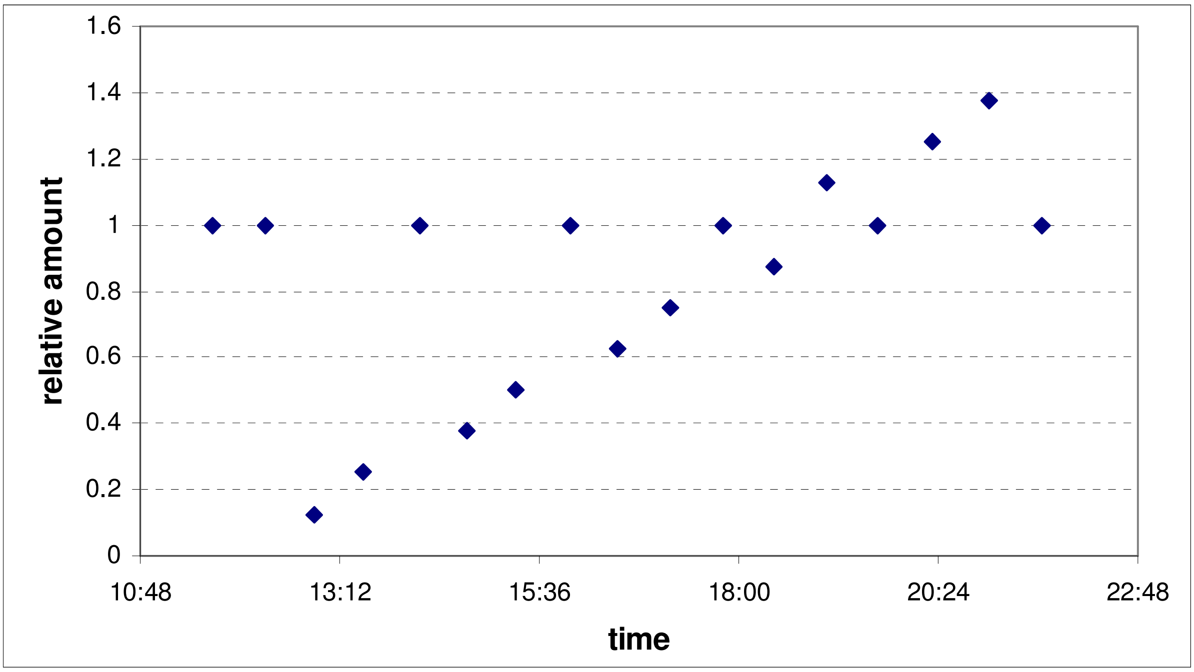

Figure 2.4.2. Illustration of a pressure series. Different amounts of the same air standard were pre-concentrated and measured with GC-EI-SIM-MS. A certain amount was pre-concentrated every third run representing a "standard" measurement. These "standard" measurements were used to correct for the instrument drift over the day.

Uncertainties in the pre-concentrated amounts arose from the limited precision of the display unit of the pressure sensor at the reference volume. This unit displayed 10 digits if about 7 ml were pre-concentrated and 550 digits for about 393 ml. Its accuracy was ± 1 digit which corresponds to uncertainties between 0.18 and 10 %. These errors rise with decreasing pre-concentration amounts and were consequently added to the 1σ measurement standard deviation error bars. Within these uncertainties the corresponding normalised relative response means as derived with the different integration methods agreed for all substances.

Additionally, as the same air standard was measured the normalised relative responses in Figure 2.4.3 should be 1.0 within the error bars. This was not true for three substances. The first was CH_3Cl (methyl chloride) because of the influence of a low blank signal which was not corrected (see also Figure 2.4.6). The deviation for CCl_4 (carbon tetrachloride) was caused by a cut-off valve in the pre-concentration system. It affected all CCl_4 measurements between October 2006 and May 2007. And the third exception was $CHCl_3$ (chloroform) which can be explained by a double peak occurrence on the quantifier ion. Nevertheless the tests proved that all compared integration methods can be considered as quantitative integration algorithms.

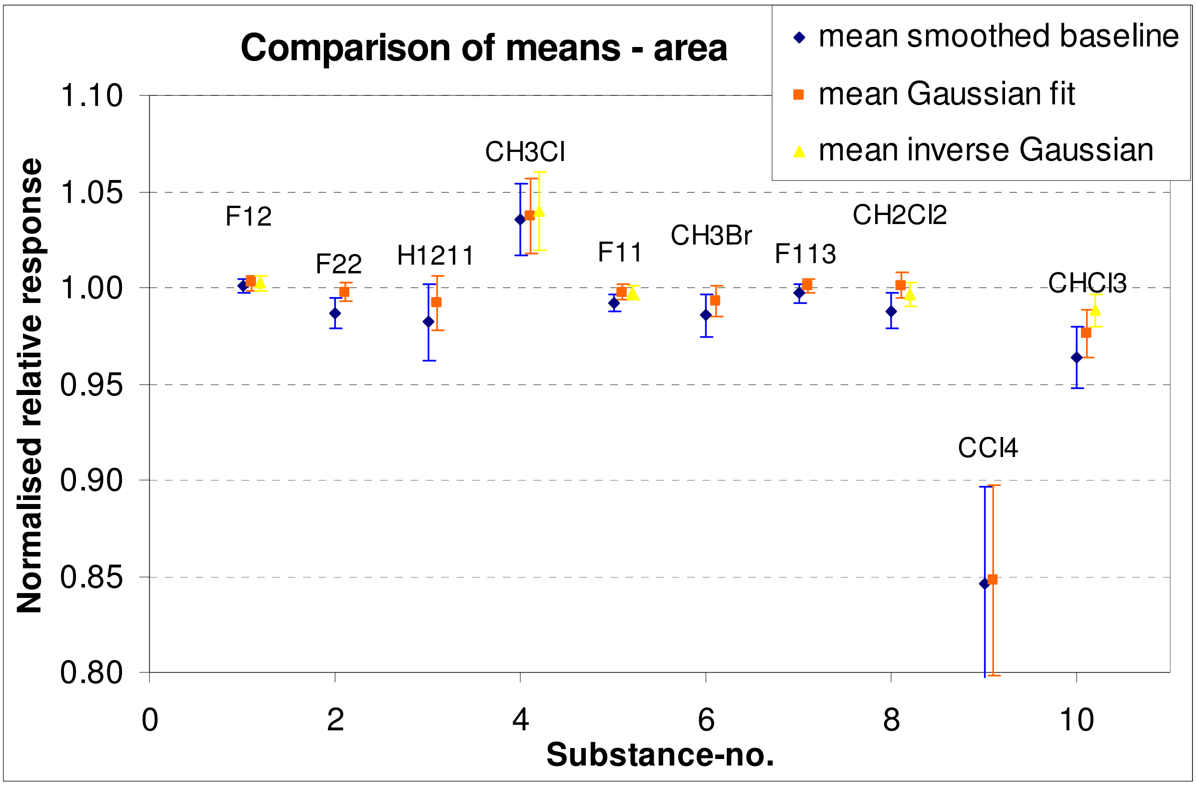

Figure 2.4.3. Integration method comparison between the smoothed-baseline (blue), the Gaussian fit (orange) and the inverse Gaussian fit (yellow) algorithms for MS peak areas of ten substances. Three pressure series were retrieved by correcting for the pre-concentrated amounts (between 7 and 393 ml). Displayed are the means of the normalised relative responses. The error bars were derived as the sum of the mean 1σ measurement standard deviation and the mean pre-concentration error divided by root of 29 (i.e. the number of measurements). For all substances the means derived with the different methods agreed within these error bars.

In Figure 2.4.4 the single data points of the normalised relative responses from the pressure series (as used to derive the mean) are displayed for the peak areas of CF_2Cl_2 (F12). The smoothed baseline and the Gaussian fit agreed for all pre-concentrated amounts. Figure 2.4.5 shows the corresponding results as retrieved from peak heights, which gave higher error bars and more often occurring deviations of the normalised relative responses from 1.0 for this substance. CF_2Cl_2 (F12) is a high peak with a pointed top. The limited data resolution at the peak top (recording frequency of 3.3 points per second) could have caused the higher error bars.

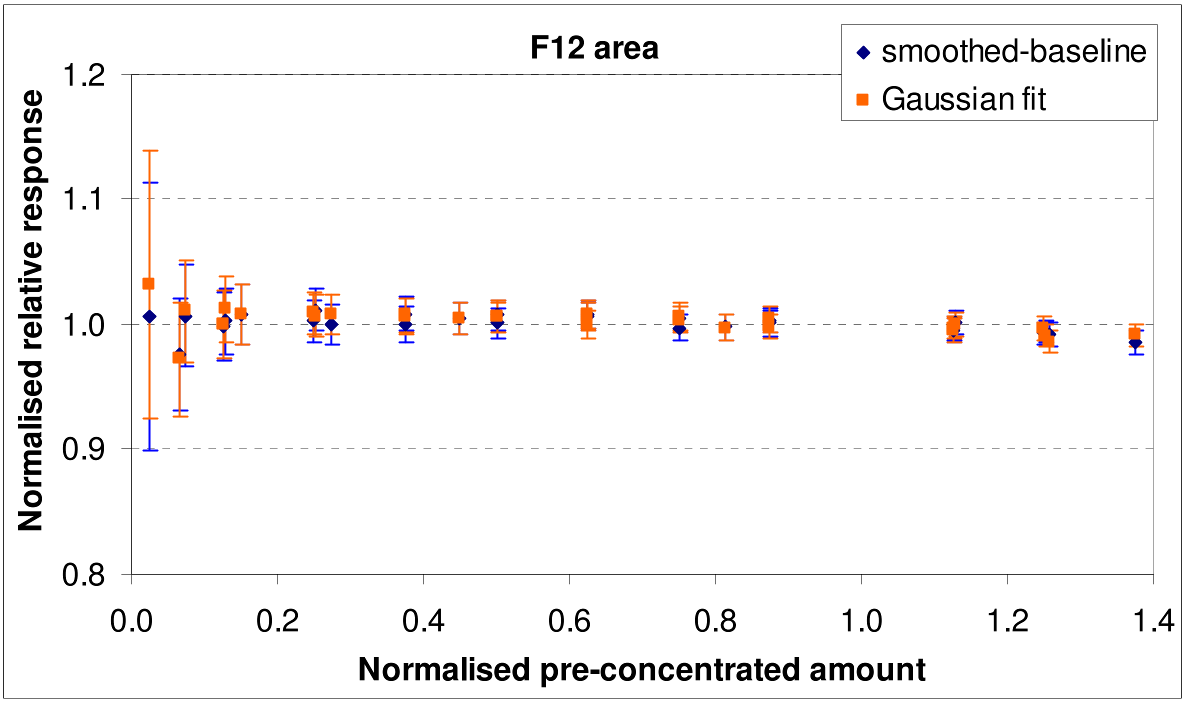

Figure 2.4.4. Integration method comparison between the smoothed-baseline and the Gaussian fit algorithm for MS peak areas of CF_2Cl_2 (F12). Displayed are the normalised relative responses as retrieved from three pressure series with different pre-concentration amounts (between 7 and 393 ml corresponding to signal/noise ratios between 50 and 2800). The integration methods agree and are also 1.0 within the error bars (the sum of the 1σ standard deviations and the pre-concentration errors).

As other substances did not show significantly better results from peak height retrievals (see Appendix, Figure set A.S.5 for integration method comparison of 12 substances) only peak areas were used for quantification. The smoothed baseline integration resulted in significant deviations of the response means from 1.0 for four additional substances compared to the Gaussian fit (Figure 2.4.3), which can be considered as a disadvantage of this method. Furthermore it is very time-consuming to adjust thresholds for a good peak match. As the inverse Gaussian fit also represents no significant improvement compared to the Gaussian fit the latter was chosen as the integration method for all further quantifications.

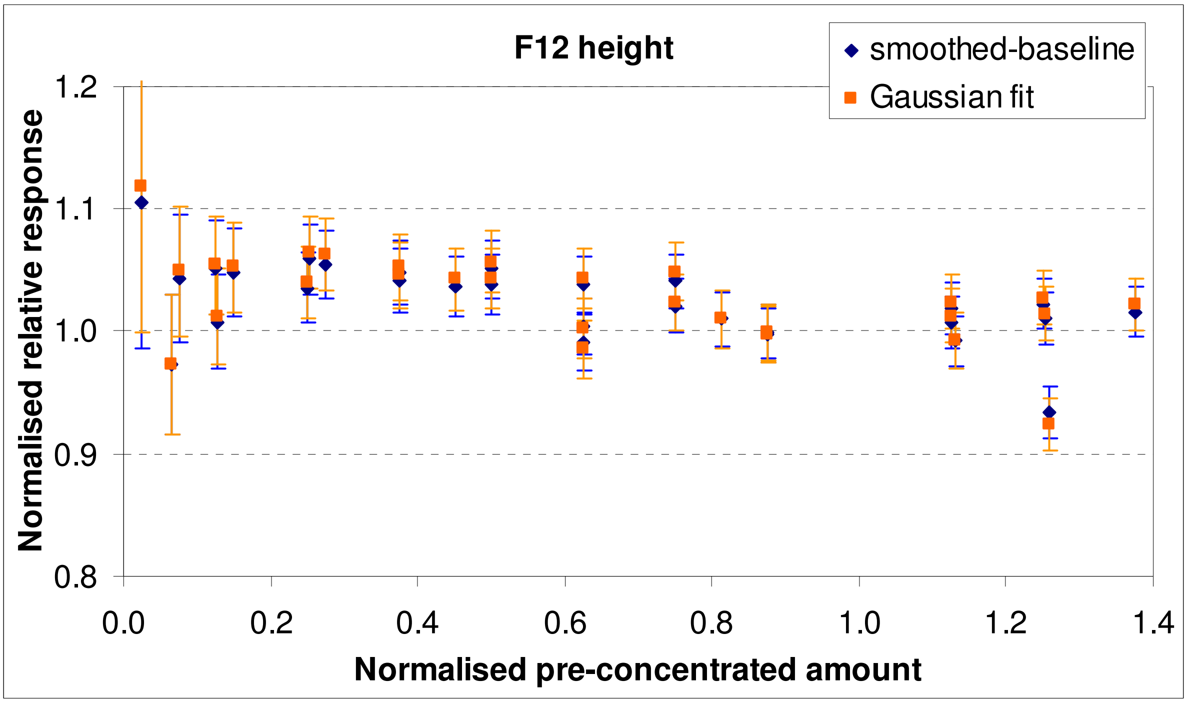

Figure 2.4.5. The same as in Figure 2.4.4 but for peak heights. For this substance retrieval using heights gives higher error bars and also more often occurring deviations of the response from 1.0 than using areas.

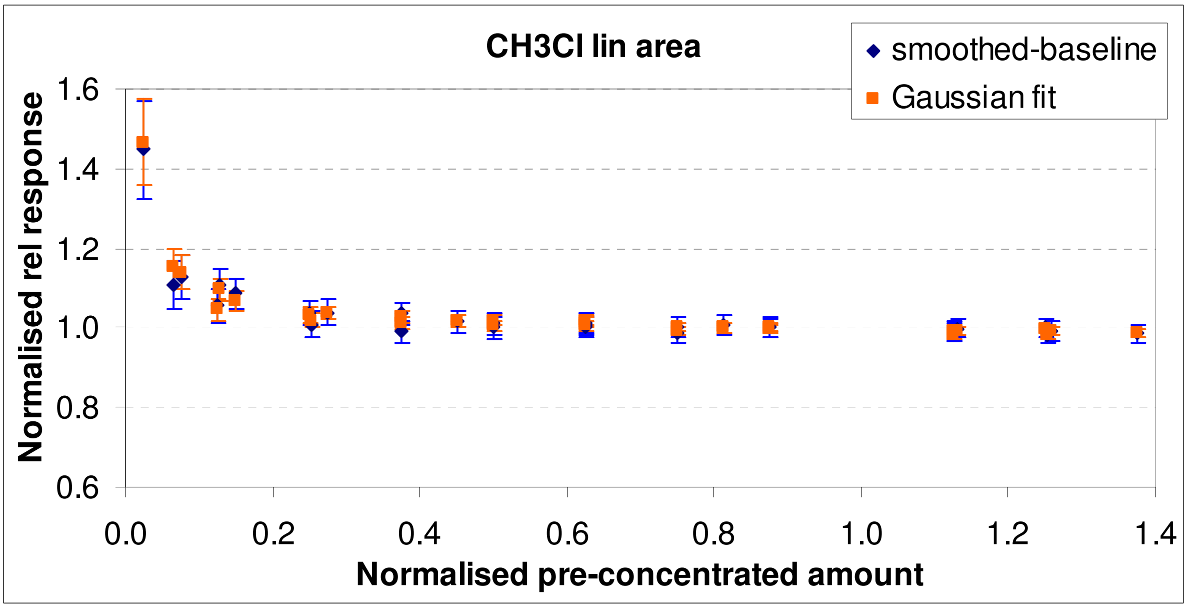

Figure 2.4.6. The same as in Figure 2.4.4 but for CH_3Cl (methyl chloride). The substance shows a small blank signal which is influencing the response calculation. This influence grows with decreasing pre-concentration amounts because of multiplication during normalisation.

2.5 Linearity of the quantification method

The measured pressure series can also be used to check the linearity of the complete MS quantification process including pre-concentration, detection, data recording, peak integration and instrument drift correction. Different data visualisation is needed for this test and Figure 2.5.1 shows an appropriate diagram for CF_2ClBr (H1211).

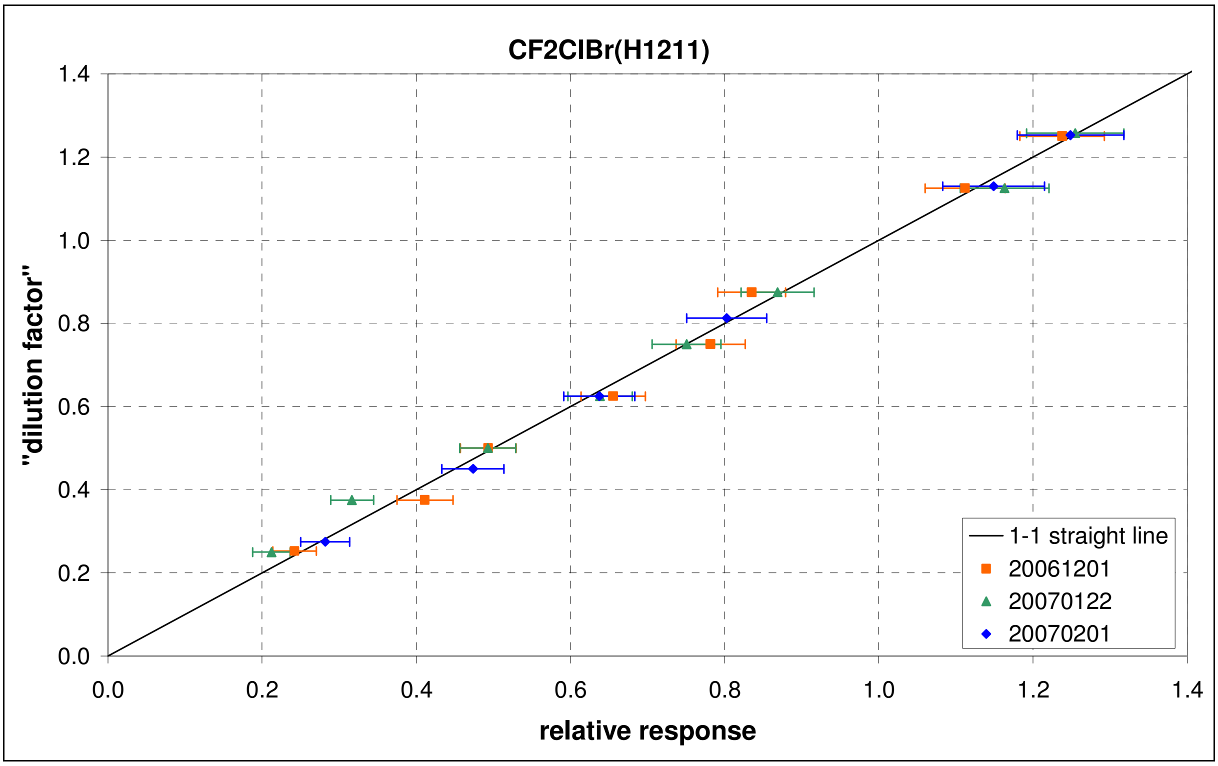

Figure 2.5.1. Linearity diagram for CF_2ClBr (H1211). Displayed are the relative responses of the MS from three pressure series versus "dilution factors" (i.e. the relative pre-concentrated amounts). The error bars are the 1σ relative measurement standard deviations plus the amount-corrected pre-concentration errors. Please note that the amount-dependency of the measurement standard deviation was not taken into account. This could have lead to an error underestimate for the signals which approached detection limit at low dilution factors. Nevertheless the complete H1211 quantification method was proven to be linear as more than 67 % of the values agreed with the 1-1 straight line within the 1σ error bars. The highest value is an outlier because O_2 is starting to condense inside the sample loop at pressures above ~350 ml which can cause peak-distortions especially for fast eluting substances.

The relative responses from the three pressure series are plotted against the relative pre-concentrated amounts. The error bars of the pressure series for the substance i (e_i) are crucial for the linearity check and were derived according Equation 2.5.1.

$$e_i = d_i * (\mathrm{e}_{\mathrm{pd,i}} + \mathrm{e}_{\mathrm{rs,i}} + \mathrm{e}_{S/N,i} - \mathrm{e}_{\mathrm{oe,i}}) \qquad (2.5.1)$$

All errors were multiplied with the corresponding “dilution factors” d_i (i.e. the relative pre-concentrated amounts). Uncertainties from the precision of the display unit of the pressure sensor at the reference volume are represented by e_{pd} (see Chapter 2.4 for details). The 1σ relative standard deviations e_{rs} were derived from calibration standard measurements only but the reproducibility is increasing with decreasing ratio of signal to noise (see Table 2.4.1). In order to simulate this dependency an additional error $\mathrm{e}_{S/N}$ was derived. For this purpose the reproducibilities (Eq. 2.3.2) and the peak-to-peak signal/noise (Eq. 2.3.3) were derived from signals of 19 substances on four measurement days and from three different calibration standards.

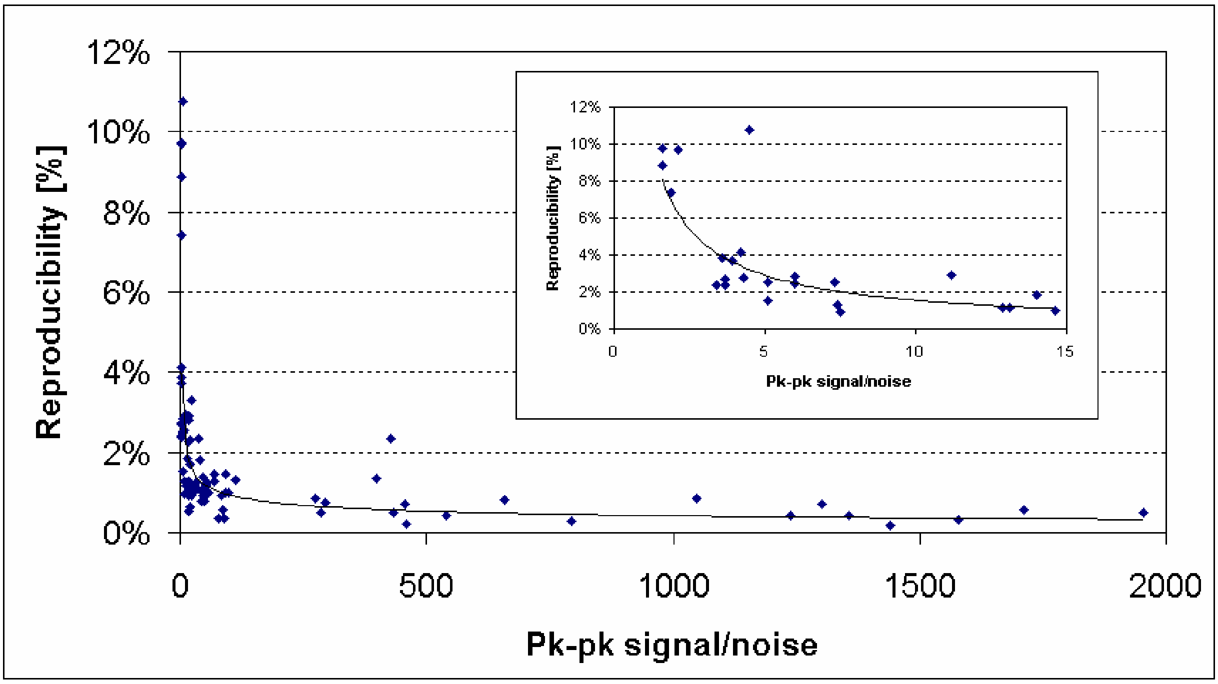

Figure 2.5.2. The reproducibilities of the quantification process plotted against the peak-to-peak signal/noise as calculated from Eq. 2.3.2 and Eq. 2.3.3. Data originates from signals of 19 substances on four measurement days in 2005, 2006 and 2007. They were derived from measurements of three different calibration standards. The mean dependency can be described by a potential function with a negligible slope between S/N 2000 and 10.

As displayed in Figure 2.5.2 these variables were found to be correlated with a potential function being the best estimate for the correlation. This function and the signal/noise ratios from the pressure series were used to assign reproducibilities $e_{S/N}$ to the different pre-concentration amounts for each substance. For a relative pre-concentration amount of 1.0 the errors e_{pd} and $e_{S/N}$ were already included in the standard deviations e_{rs} from calibration standard measurements. Thus, an addition of the three errors could have led to a slight error overestimation. But as e_{pd} and $e_{S/N}$ are independent from each other they could also have compensated. To achieve at least a partial consideration of the effect the minimum observed value of e_{rs} (0.3 %) was subtracted from all errors as a mean overestimate error e_{oe}.

The complete quantification method was found to be linear for almost all target substances as more than two-thirds of the derived relative responses agreed with the 1-1 straight line within the 1σ error bars (see Appendix, Figure set A.S.6 for all corresponding linearity diagrams). Exceptions were again CH_3Cl (methyl chloride, 54 %) and CCl_4 (carbon tetrachloride, 50%) due to the above mentioned problems.

Figure 2.5.3 shows another linearity diagram for $CFCl_3$ (F11) including additional ECD data from one of the pressure series. The comparison illustrates the different properties of MSD and ECD with the latter behaving non-linear for most substances. Therefore all ECD data needs to be corrected within the quantification process. This was done by using an existing static dilution series consisting of six flasks with dilution factors f = 1, f = 0.8528, f = 0.6902, f = 0.4970, f = 0.2519 and f = 0.000 (Strunk, 1999, Müller, 2001). This series was prepared at the institute in 1999 from dried air collected at the Taunus Observatory (at the Kleiner Feldberg near Frankfurt) which was diluted with purified synthetic air (so-called "zero air" because it contains almost no trace gases) in order to reflect the clean stratospheric air matrix. Measurements were carried out as close to sample measurements as possible (i.e. mostly within the same week) because the nonlinear response behaviour and thus the corresponding functions can change with time. Then a third order polynomial of the form $y = a + bx + cx^2 + dx^3$ was fitted to the data points (x: relative responses, y: dilution factors) using a least-sum-of-squares fit. Secondary conditions for this fit were $a = 0$ and $b + c + d = 1$ because the non-linearity function needs to run through the physically sensible points (0,0) and (1,1). For subsequent mixing ratio retrieval a dilution factor was calculated from the relative response of the calibration standard. The nonlinearity function was then adapted (stretched or compressed) to the calibration standard response again using a least-sum-of-squares fit. This correction is limited to samples having mixing ratios lower than the mother flask of the dilution series (f = 1). Furthermore the relative response of the calibration standard must be within the range of the dilution series to avoid uncertainties from extrapolation of the nonlinearity function during the fit. Problems arise e.g. for substances that continue to rise in the atmosphere and thus simply outdate the dilution series such as CHF_2Cl (F22).

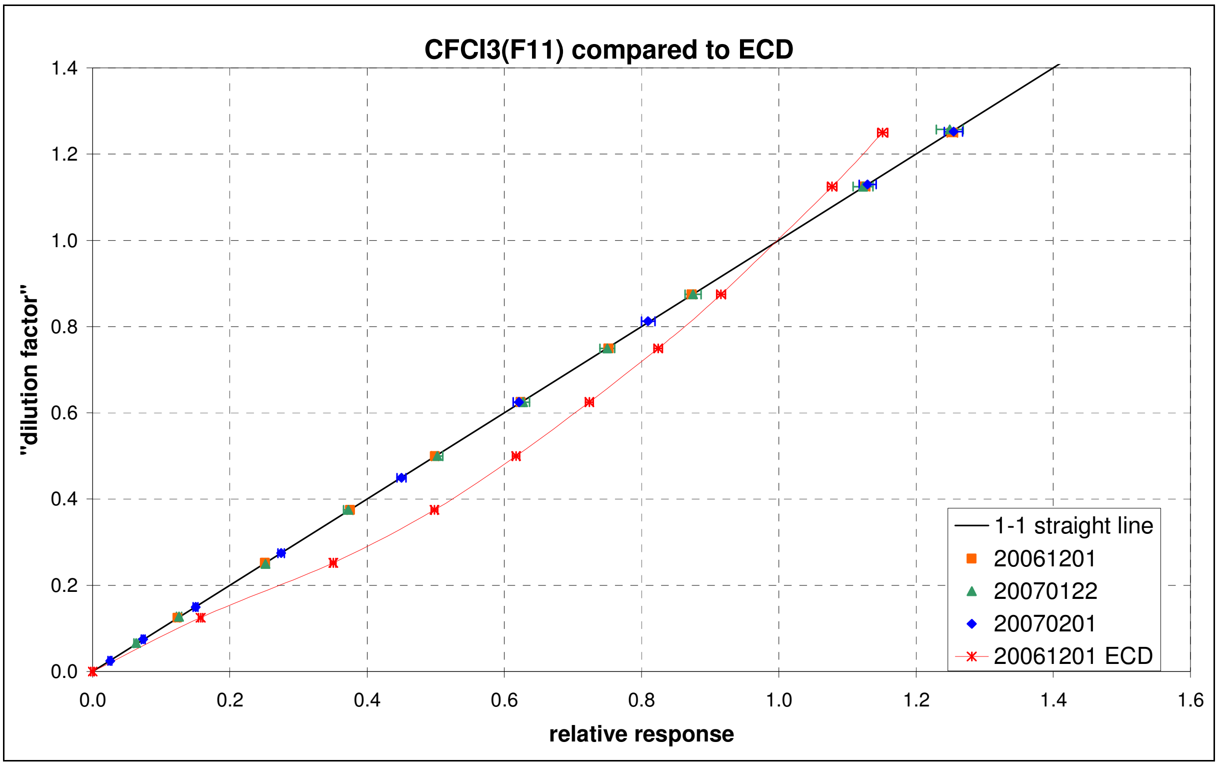

Figure 2.5.3. The same as Figure 2.5.1 but for $CFCl_3$ (F11) and with additional ECD data (red) from one pressure series. In contrast to the MS the ECD shows nonlinear response behaviour.

2.6 Conclusions

To summarise the chapter: The configuration of the analytical setup was explained as well as data analysis methods. Furthermore the chromatographic system was characterised by identifying the signals of 48 additional atmospheric trace gases with the new Mass Spectrometric detector. The total number of measurable target substances was increased from nine to 26. In addition, the integration of small peaks was enhanced by using a Gaussian fit algorithm developed in the workgroup. This algorithm compared with other integration methods and found to reflect peaks quantitatively. Finally, the linearity of the complete MS quantification process was proven.

3 Quality assurance

Table 3.1.1 shows all stratospheric and upper tropospheric air samples analysed for this thesis. Samples from three balloon flights collected with different whole-air-samplers were measured against a calibration standard named ALM-39767.

Table 3.1.1. All analysed air samples taken at altitudes above 10 km. Only uncontaminated samples were used for further retrievals i.e. 33 samples from balloon-borne whole-air-samplers and 42 samples from the WAS sampler operated on board the Geophysika high altitude research aircraft.

Flight no.	Sampler	Location	Flight date	No. of Samples*	Sample altitude range [km]
B42	BONBON II	Near Teresina, Brazil, 5°04'S, 42°52'W	08.06.2005	11/15	15 – 34
B43	BONBON I	Near Teresina, Brazil, 5°04'S, 42°52'W	25.06.2005	14/15	15 – 34
C1	CLAIRE	Air Sur l'Adour, 44°N, 0.4°E	15.10.2006	8/22**	12 – 28
R3a	WAS	Dubai – Lacarnaca, 25 – 33°N, 38 – 53°E	16.12.2005	6/9	17.2 – 17.8
R3b	WAS	Lacarnaca – Oberpfaffenhofen, 35 – 43°N, 14 – 33°E	17.12.2005	7/10	16.7 – 17.1
S3	WAS	Survey Indonesia, 8 – 12°S, 130 – 134°E	23.11.2005	13/14	15.5 – 18.3
S8	WAS	Survey South, 13 – 22°S, 131 – 134°E	06.12.2005	11/11	13.9 – 19.7
T3	WAS	Tapao – Brunei, 5 – 13°N, 101 – 115°E	11.11.2005	5/8	12.7 – 17.5

*uncontaminated high altitude samples used for final analyses/all available containers

**only 22 of 26 containers could be used for sampling as will be explained in Chapter 3.1.2

Furthermore the “TO-Tante” calibration standard was used to quantify 87 air samples collected on board the Geophysika high altitude research aircraft by the whole air sampler WAS of the University of Utrecht (see Kaiser et al., 2006 for details).

The latter were partially contaminated – most probably due to a temporal malfunction of the pump used to evacuate the containers. All samples showing contaminations in two or more target substances (which included all samples from two flights not shown in Table 3.1.1) – were not used for further retrievals. The whole-air-samplers also showed contaminations probably with balloon exhaust for a few samples and some others could not be analysed due to technical failure during sampling. The remaining data of 24 target substances (see Figure 3.1.3) was used not only for atmospheric analyses but also to evaluate the analytical system – especially the results from the two parallel detectors. Furthermore this chapter aims to assess other problems connected with the entire process of quantification such as the stability of the target substances inside the storage containers or calibration uncertainties.

3.1 Stability of substances in calibration and sample containers

It is a known problem that many organic trace gases drift in concentrations if stored in metal containers for longer time periods. These changes depend e.g. on the nature, past use, and pre-treatment of the container surface, the compound, the container pressure, the storage temperature, the ozone content and the water vapour content (Finlayson-Pitts and Pitts, 2000). They can be caused by adsorption or chemical reactions e.g. on active spots of the container walls (Pate et al., 1992, Apel et al., 1994). Surface passivations via fluorination or electro-polishing are common techniques to avoid wall reactions (Blake et al., 1994, Apel et al. 1998) but this is not sufficient in all cases. Positive changes with time have also been observed in containers. They can originate from uptake into a film of water on the container surface which can be reversed if pressure is reduced as samples are removed from the container (Finlayson-Pitts and Pitts, 2000). Moreover, rates of such concentration changes can even be similar in containers that experienced the same preparation process which can mask the drift. Thus, drift checks were performed with the different containers that were used for calibration but also for sample containers and the static dilution series used for ECD nonlinearity corrections. The results will be discussed in the following sub-chapters.

3.1.1 Calibration container evaluation

To check for concentration drifts in the calibration containers internal comparisons were carried out by measuring at least two but preferably three or more containers against each other. These experiments were performed regularly over a period of more than two years (December 2005 – January 2008) and an overview of the schedule is given in Table 3.1.2.

Table 3.1.2. Schedule of internal calibration standard comparisons carried out over a period of 25 months. The listed four calibration standards were measured against the ALM-39767 standard (inside material: acculife treated Aluminium, prepared in 1993) on the corresponding dates.

	Calibration standard name (inside material, year of preparation)			
Measuring date	TO-Mutter (passivated Aluminium, 1999)	TO-Tante (passivated Aluminium, 1999)	CO2-Mutter (passivated Aluminium, 2004)	SX-3551 (electro-polished stainless steel, 2006)
20.12.2005	X			
21.12.2005	X			
31.05.2006	X	X		
01.07.2006	X	X		
09.08.2006			X	
22.08.2006		X	X	
24.11.2006		X		
01.12.2006			X	
05.12.2006	X			
12.12.2006			X	
22.01.2007			X	
24.01.2007	X	X	X	X
31.01.2007	X	X	X	X
01.02.2007			X	
21.06.2007				X
07.08.2007				X
08.08.2007				X
15.08.2007	X	X		X
29.01.2008	X	X		X

Most samples were measured against one calibration standard named ALM-39767 (inside surface material: passivated Aluminium - “Acculife treated” from Scott Specialty Gases) which was filled in 1993. This container was checked for drifts by using the relative responses of four other containers which had different inner surface materials and are named SX-3551 (electro-polished stainless steel from Essex Cryogenics), TO-Tante, TO-Mutter and CO2-Mutter (same material for all three: passivated Aluminium from Messer-Griesheim). The corresponding results are shown in Figure 3.1.1 for CH_3Br (methyl bromide) and in Figure 3.1.2 for $CHCl_3$ (chloroform).

A linear regression was performed for the response-time-series of each standard and target substance. A significant concentration drift was assumed to be present if the regression line exceeded the 3σ error bars. The latter were calculated as will be explained in the following. The five calibration standards had very different concentrations for some substances giving different reproducibilities. Furthermore these reproducibilities varied over the comparison period. Thus, the reproducibilities were averaged from at least three measurement days for each calibration standard (except for the SX-3551 standard where only one day with more than three measurements was available). Then the error bars were derived as the mean of the reproducibilities of the two standards used to derive the corresponding relative responses. They were applied to the mean relative responses of the calibration standards and compared with the respective regression lines.

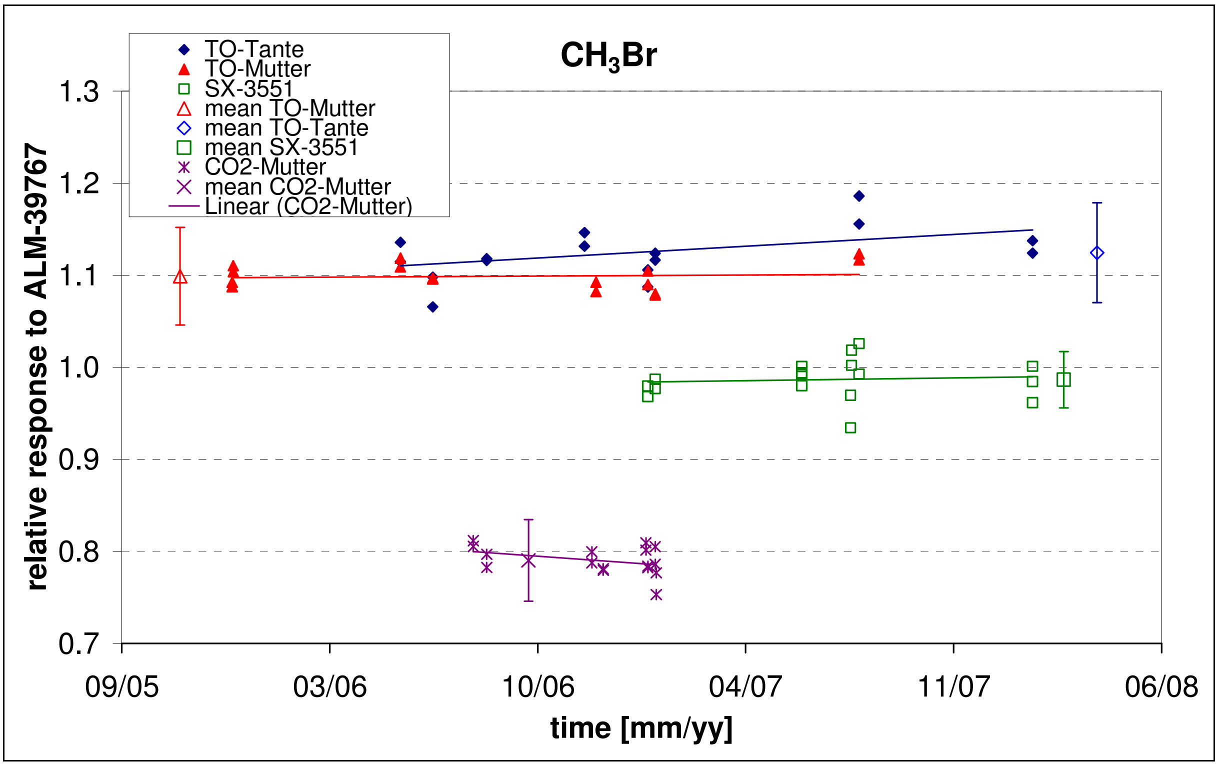

Figure 3.1.1. Relative responses of four calibration standards against the ALM-39767 standard over a period of 25 months for CH_3Br (methyl bromide). The error bars are the mean 3σ reproducibilities of the standards used to derive the relative responses. No concentration drifts outside these error bars were observed for this substance.

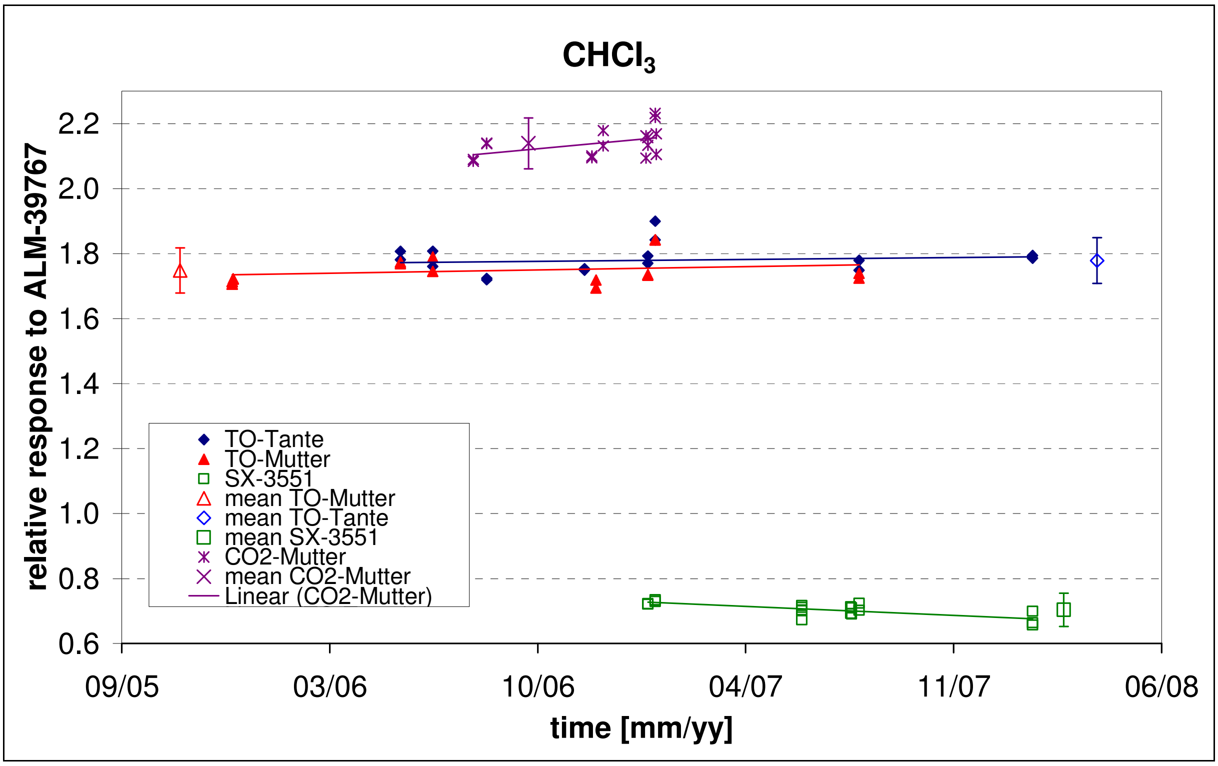

Figure 3.1.2. The same as in Figure 3.1.1 but for $CHCl_3$ (chloroform).

All target substances were found to be stable inside the mainly used calibration standard (i.e. ALM-39767). In fact the only cases, where substances failed the drift criterion were C_2Cl_4 (tetrachloroethene) which increased inside the TO-Mutter and $CHFClCF_3$ (F124) which decreased inside the TO-Mutter and TO-Tante container. These containers were excluded from quantification for the corresponding substances. It is concluded that the used five calibration containers can be used to quantify a wide range of halocarbons as they did show almost no significant concentration drifts over the periods they were measured. Nevertheless it is important to continue these internal calibration drift checks as some standards were measured only for a short time period (e.g. CO2-Mutter) but also because some substances came very close to the drift criterion such as $CHCl_3$ (chloroform) as displayed in Figure 3.1.2 (see Appendix, Figure set A.S.8 for plots of all target substances).

3.1.2 Sample container evaluation

Having assured the quality of the calibration flasks it was necessary to check the sample containers for concentration drifts, too. The following tests were carried out:

a) Nine stratospheric air samples (three from flight B42 and six from C1) were analysed again in August 2007 to check for the long term stability of target trace gases.
b) Four containers of one whole-air-sampler (CLAIRE) were filled with air before the flight (C1) – two with purified synthetic air (so-called “zero air” which contains almost no trace gases – only small amounts of two target gases: ~5 ppt of CH_3Cl which is the magnitude of the system blank signal and ~1.7 ppt of CH_3Br) and two with a calibration standard (TO-Tante). These samples experienced a stratospheric balloon flight (C1) including freezing with liquid neon and were subsequently analysed in the laboratory.
c) A similar procedure to b) was applied to another whole-air-sampler (BONBON II) but the flight conditions were only simulated by filling the Dewar of the sampler with liquid nitrogen in the laboratory.

The results of the reanalysis of three samples from flight B42 are displayed in Figure 3.1.3. This sampler was originally analysed in December 2005. Eight substances showed significant concentration changes in August 2007 compared to December 2005 in at least one of the samples: CH_3Cl (methyl chloride), CH_3Br (methyl bromide), CH_2Cl_2 (dichloromethane), $CHCl_3$ (chloroform), CCl_4 (tetrachloromethane), C_2Cl_4 (tetrachloroethene), CH_2ClCH_2Cl (1,2-dichloroethane) and C_2H_5Cl (chloroethane). If changes occurred in all containers that contained the substance they were assumed to be systematic if the mean percentage change exceeded the percentage 1σ standard deviation of the samples concentration changes. This means that the variability of the concentration changes did not exceed the changes itself. Systematic concentration changes were found for three substances: CH_3Cl, CH_2ClCH_2Cl and CCl_4. An estimate for a mixing ratio correction was derived for these substances (see Chapter 5.3.1 which provides more details). For non-systematic changes the error bars were increased accordingly except for C_2H_5Cl. This substance showed very high and variable concentration changes, which is why the corresponding data was not used for any further analysis.

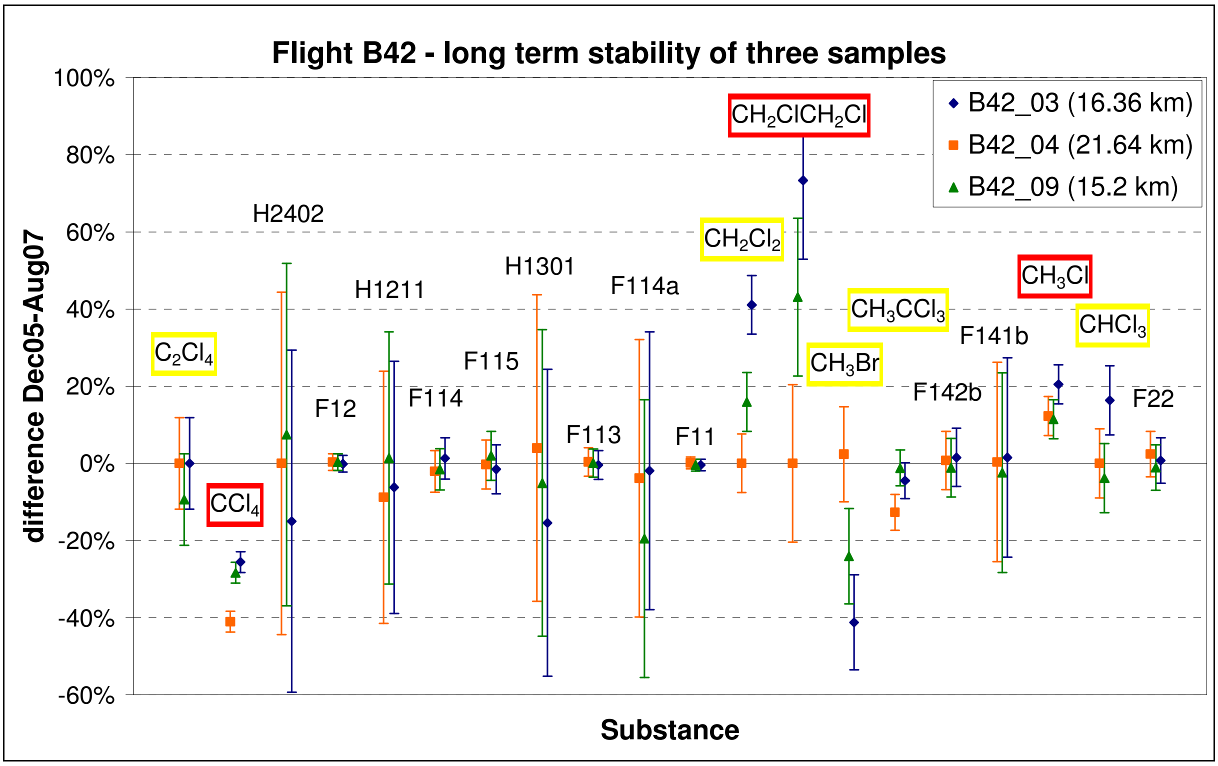

Figure 3.1.3. Long term stability of three stratospheric whole-air-samples (Flight B42 – sampler BONBON II). Displayed are the percentual changes of the 20 quantified target substances between December 2005 and August 2007 with the sum of the 3σ reproducibilities of both measuring days as error bars. Please see Chapter 5, Tables 5.4.2 and 5.4.3 for the corresponding mixing ratios. The coloured substances did change significantly in concentration (yellow: unsystematic change, red: systematic change, see text for details). Not displayed are C_2H_5Cl (chloroethane, very variable increases of several hundred percent), C_2HCl_3 and CF_3CHFCl (trichloroethene and F124, below S/N = 3 in August 2007, the latter due to slightly higher detection limits) and CH_2Br_2 (dibromomethane, identification after December 2005).

The reanalysis of flight C1 gave similar results as the same substances were affected. CCl_4 could not be assessed due to problems with a valve in the pre-concentration system which led to temporary irreproducible results for this substance. But in contrast to B42 the C1 sample concentration changes were more variable and much higher – up to several hundred percent for most substances. In addition one container was completely depleted in CH_3CCl_3 (methyl chloroform) and most containers showed high contaminations with CH_3CF_2Cl (F142b) up to several hundred ppb (probably originating from the container preparation process as this was the first flight of the CLAIRE sampler). All ten substances (i.e. the eight substances mentioned above for B42 plus CH_3CCl_3 and F142b) were excluded from further analysis for this flight.

The two containers that were filled with a calibration standard and subsequently experienced the C1 flight (see point b above) confirmed most of the above mentioned results. Nine of the ten substances (except for CH_3CCl_3) changed in concentrations. In addition CH_2Br_2 (dibromomethane) was measured and showed significant concentration changes, too. Another two containers were filled with "zero air" before the flight. Signals of CH_3Cl, $CHCl_3$, CH_2ClCH_2Cl, C_2H_5Cl and CH_3CF_2Cl (F142b) occurred afterwards.

The BONBON II sampler showed different results for the simulated flight (point c). The only substance that occurred in elevated concentrations in the "zero air" containers was C_2H_5Cl. The two containers filled with a calibration standard showed significant concentration shifts for only three substances: C_2H_5Cl (increase), CCl_4 (decrease) and C_2Cl_4 (decrease in one container).

The stratospheric air samples of the BONBON I sampler (flight B43) could not be reanalysed but the measurements in December 2005 gave altitudinal distributions for CH_3Cl, CH_3Br, CH_2Cl_2, $CHCl_3$, CCl_4, C_2H_5Cl and C_2Cl_4 which were inconsistent (highly scattered, sometimes concentration increases with altitude). This indicated instabilities in most sample containers leading to non-systematic and high concentration changes and the respective substances were excluded from further analyses for this flight. The air samples from the WAS sampler could not be reanalysed due to insufficient amount of air remaining in the containers.

To summarise, eight target substances were observed to change in concentration inside the two whole-air-samplers CLAIRE and BONBON II: CH_3Cl, CH_3Br, CH_2Cl_2, $CHCl_3$, CCl_4, C_2Cl_4, CH_2ClCH_2Cl and C_2H_5Cl. The CLAIRE sampler was found to show higher changes and to be problematic for two additional target substances: CH_3CCl_3 and CH_3CF_2Cl. An overview of the sample stability data is given in the Appendix, Figure A.4. All experiments with both whole-air-samplers showed concentration increases of C_2H_5Cl (probably originating from the container valves – several of them were observed to gas out the substance) which is why this substance was excluded from any whole-air-sampler analysis. Furthermore for many samples elevated concentrations of CH_3Cl, CH_2Cl_2 and CH_2ClCH_2Cl were observed. The only containers that did not show concentration increases of these substances were the BONBON II samples from the flight simulation. In contrast to all other containers they were analysed very quickly after filling (within two weeks). Thus it is likely that the concentration increases of these substances are due to slow processes like reactions on or desorption from the container walls. CCl_4 could be quantified in the BONBON II sampler only and decreased in concentration indicating its decomposition or deposition. This agrees with an earlier evaluation of this sampler via GC-ECD results (Engel, 1993). The flight simulation experiment showed lower but still significant concentration decreases for CCl_4. The substance is reported to react with H^+ ions on iron surfaces (Rusonik et al., 2005) to form iron (IV) chloride and CH_4. As the reaction goes stepwise intermediate products are CH_3Cl and CH_2Cl_2. In stratospheric air high concentrations of HCl occur (due to the decomposition of chlorinated halocarbons) which could trigger such reactions and explain the concentration changes of these three substances. Furthermore several substances such as C_2H_5Cl or CH_2ClCH_2Cl were measured on fragments with a low m/z ratio which are potentially influenced by coeluting substances (see Chapter 2.2, e.g. Table 2.2.1) and the corresponding concentration changes could have been those of other substances. Finally, the behaviour of the CLAIRE sampler (very high and variable concentration changes) leads to the suggestion that the passivation of the containers might have been insufficient by leaving a considerable amount of active spots on the inner container walls.

3.1.3 Dilution series evaluation

In order to check for concentration changes and also for the accuracy of the dilution factors the MS results from measurements of the two static dilution series used for ECD nonlinearity corrections (TO-DS and CO2-DS) were tested for linearity in December 2006. This was done for the nine target substances that were found to be quantifiable with the ECD (please see Chapter 3.2.1 for details). All dilution factors were considered to be correct in general because none of the containers disagreed with the 1-1 straight line for all substances. Figure 3.1.4 shows a comparison of these measurements for CH_3Cl (methyl chloride). For this substance the mixing ratios in the used calibration standards were comparable. Therefore the dilution factors and relative responses can be compared without further adjustment. The error bars were derived as the 3σ relative standard deviations according to Eq. 2.5.1. No pre-concentration error e_{pd} was included for the two dilution series as the same amount of air was pre-concentrated for these measurements. As explained in Chapter 2.5 CH_3Cl was one of two substances which did not meet the linearity criteria due to a small blank signal. For the drift check displayed in Figure 3.1.4 the 3σ error bars were used due to the limited number of dilution factors available for comparison. As expected for the pressure series agreement with the 1-1 straight line was observed for all nine relative responses measured (the two points >1 are not displayed). Both the TO- and the CO2-dilution series showed worse agreement – the error bars of only one out of four (TO-DS) and four out of five (CO2-DS) containers overlapped with the 1-1 straight line for CH_3Cl. The disagreements are most likely due to adsorption on the container walls or reactions inside the containers which led to substance decomposition or production.

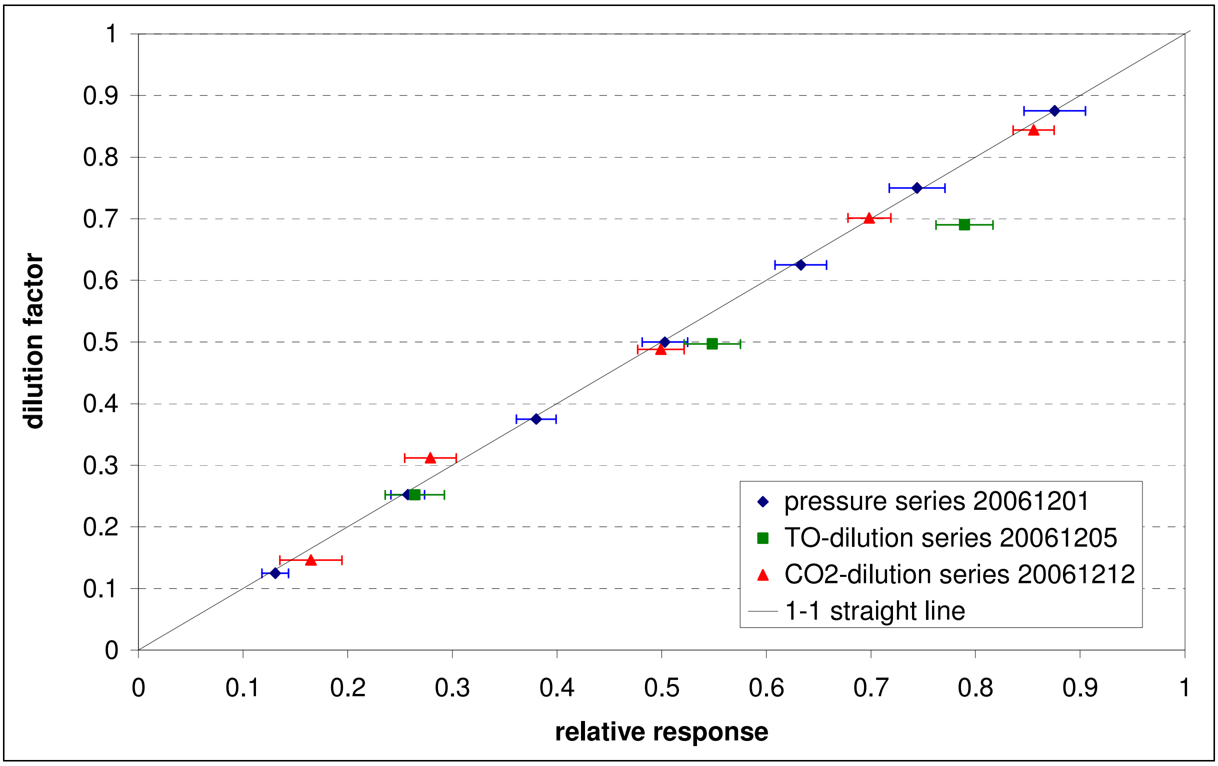

Figure 3.1.4. Comparison of the MS measurements of two dilution and one pressure series for CH_3Cl (methyl chloride). The mixing ratios in the used calibration standards were comparable which is why the data can be compared in one plot. The error bars are the 3σ relative standard deviations according to Eq. 2.5.1 but without e_{pd}. *Both dilution series showed systematic concentration changes – the TO-DS in three and the CO2-DS in one of the containers.*

Similar comparisons for the eight remaining quantifiable target substances gave the results displayed in Table 3.1.3 (see Appendix, Figure A.5 for more detailed results). Both dilution series showed complete linear MS behaviour for the four CFCs (F12, F114a, F11 and F113). For the five remaining substances not all dilution containers should be used for nonlinearity correction. The TO static dilution series has been used for more than eight years for ECD nonlinearity corrections in this workgroup. But the MS results show that earlier retrievals of CHF_2Cl (F22), CH_3Cl (methyl chloride), CCl_4 (carbon tetrachloride), $CHCl_3$ (chloroform) and

CH_3CCl_3 (methyl chloroform) are questionable and the corresponding error bars should be adapted at least.

Table 3.1.3. MS results of the concentration change check in December 2006 for the containers of two static dilution series used for ECD nonlinearity correction. The criterion for a significant concentration change is the same as in Figure 3.1.4, affected containers are displayed in bold. The four measured CFCs (F12, F114a, F11 and F113) showed no significant concentration changes in any of the containers.

Dilution container	Observed relative MS response with 3σ error bars				
	F22	CH_3Cl	CCl_4	$CHCl_3$	CH_3CCl_3
TO-DS 0.2519	**0.190 ± 0.012**	0.264 ± 0.028	**0.015 ± 0.015**(a)	**0.100 ± 0.018**	**0.116 ± 0.023**
TO-DS 0.4970	0.500 ± 0.011	**0.548 ± 0.027**	**0.298 ± 0.018**(a)	0.494 ± 0.018	0.482 ± 0.022
TO-DS 0.6902	0.683 ± 0.011	**0.789 ± 0.027**	0.659 ± 0.021(a)	0.722 ± 0.018	0.692 ± 0.023
TO-DS 0.8528	0.850 ± 0.011	**1.080 ± 0.028**	**0.690 ± 0.024**(a)	0.845 ± 0.019	0.845 ± 0.024
CO2-DS 0.14626	0.146 ± 0.014	0.165 ± 0.030	0.092 ± 0.023(b)	0.158 ± 0.018	0.131 ± 0.027
CO2-DS 0.31201	0.311 ± 0.012	**0.279 ± 0.025**	0.196 ± 0.033(b)	0.279 ± 0.016	**not detected**
CO2-DS 0.48820	0.490 ± 0.012	0.499 ± 0.022	0.559 ± 0.046(b)	0.494 ± 0.015	0.491 ± 0.030
CO2-DS 0.70129	0.700 ± 0.012	0.698 ± 0.021	0.715 ± 0.062(b)	0.676 ± 0.015	0.713 ± 0.034
CO2-DS 0.84387	0.858 ± 0.012	0.855 ± 0.020	0.941 ± 0.073(b)	0.839 ± 0.015	0.891 ± 0.037

(a) Results from measurements in July 2006

(b) CCl_4 remained uncertain because it was measured while one valve was causing irreproducible CCl_4 results.

3.2 Internal detector comparison

The GC-ECD system has been used in the workgroup for more than two decades to quantify stratospheric trace gases. This sub-chapter aims to evaluate the ECD quantification process. Three main questions will be answered:

1. The MS enabled identification of many substances. Which target substances had no or minor ECD-sensitive coeluents?

2. Two series gas containers produced via static dilution and one pressure series were used to derive different ECD nonlinearity corrections of the stratospheric mixing ratios from one flight (C1). Were the results consistent among themselves and with MS results?
3. Did the different detectors give the same results for stratospheric air sample measurements?

3.2.1 ECD evaluation regarding coeluents

As explained in Chapter 2.1 the used analytical system has two parallel detectors – an Electron Capture Detector and a Mass Spectrometer. One advantage of the ECD is its high sensitivity towards fully halogenated hydrocarbons – especially if they contain chlorine or bromine such as the CFCs and the Halons. Furthermore its sensitivity increases very fast with the number of chlorine atoms which results in high signals for $CHCl_3$ (chloroform), CCl_4 (carbon tetrachloride) and CH_3CCl_3 (methyl chloroform). But there are also disadvantages connected with this detector. The ECD is sensitive towards many substances such as most halocarbons, sulphur compounds and alkyl nitrates (Schwedt, 1996). Figure 3.2.1 shows a zoomed chromatogram of a clean air calibration standard. The large number of peaks gives an idea of the number of coeluting substances. For instance the ECD is very sensitive towards the coeluting target substance pairs of CF_3Br (H1301) & C_2F_5Cl (F115), CF_2ClBr (H1211) & CF_2ClCF_2Cl (F114) and C_2Cl_4 (tetrachloroethene) & CH_2Br_2 (dibromomethane) which makes an ECD quantification of these substances impossible. A comparison with the MS reduced the number of quantifiable target substances to nine. These are substances having no (0) or minor (1) known ECD-sensitive coeluents and in addition higher atmospheric abundances of at least several tenth ppt (2) or a high ECD sensitivity (3):

- CF_2Cl_2 (F12, 1, 2, 3)
- CHF_2Cl (F22, 0, 2)
- CF_3CFCl_2 (F114a, 0, 3)
- CH_3Cl (methyl chloride, 0, 2)
- $CFCl_3$ (F11, 1, 2, 3)
- $CF_2ClCFCl_2$ (F113, 1, 2, 3)
- CCl_4 (carbon tetrachloride, 1, 2, 3)
- $CHCl_3$ (chloroform, 1, 3)
- CH_3CCl_3 (methyl chloroform, 1, 3)

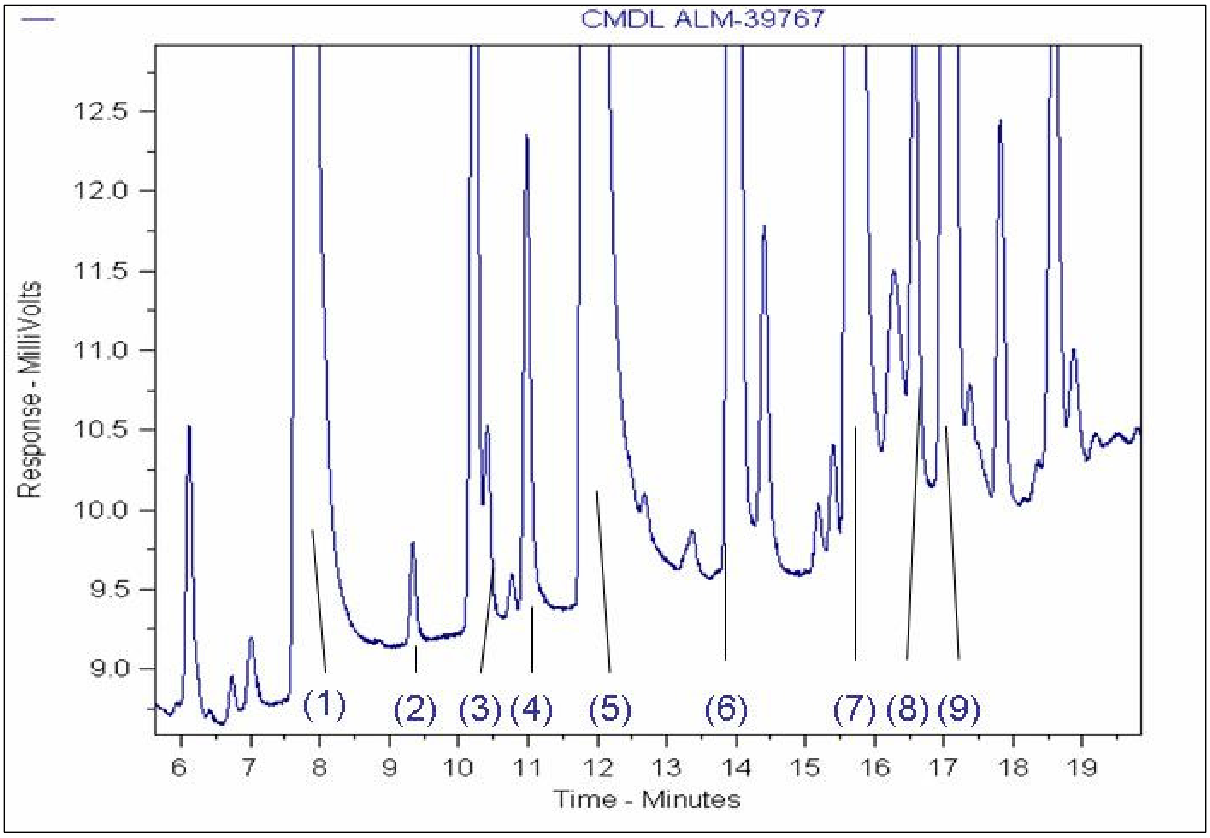

Figure 3.2.1. Zoomed ECD chromatogram of a clean air calibration standard (ALM-39767). The ECD is sensitive towards many substances which leads to a large number of peaks. By using the MS interferences from coeluting substances could be assigned. Only nine target substances were found to have no or minor ECD-sensitive coeluting substances up to now – CF_2Cl_2 *(F12, 1),* CHF_2Cl *(F22, 2),* CF_3CFCl_2 *(F114a, 3),* CH_3Cl *(methyl chloride, 4),* $CFCl_3$ *(F11, 5),* $CF_2ClCFCl_2$ *(F113, 6),* CCl_4 *(carbon tetrachloride, 7),* $CHCl_3$ *(chloroform, 8) and* CH_3CCl_3 *(methyl chloroform, 9).*

3.2.2 Comparison of different ECD nonlinearity corrections

Another problem of the ECD is its nonlinear behaviour which is different for every substance and led to high operating efforts such as regular measurements of a dilution series and additional time-consuming retrievals. Three different dilution series were used:

- the "usual" dilution series (TO-DS) prepared in 1999 as mentioned in Chapter 2.5
- a new dilution series (CO2-DS) consisting of seven flasks prepared in the workgroup in 2006
- a pressure series (PS, different pre-concentration amounts simulating a dilution, see Chapter 2.4 for details)

In contrast to the ECD the MS shows a linear relationship between analyte amount and detector response. Moreover it often allows interference-free quantification even if substances coelute (see Chapters 2.5 and 2.2). Thus, MS results were chosen as the reference to evaluate different ECD retrievals.

As the dilution series originate from the troposphere it was not clear, how well they reflect nonlinearities of a stratospheric air matrix because many substances present in the troposphere are destroyed rapidly when reaching the stratosphere or do not reach it at all. For one balloon flight (C1, 8 samples, see Table 3.1.1) the two different dilution series and one pressure series were measured near to sample measurements (which is recommended for a comparison as the ECD nonlinearity behaviour can change with time). ECD nonlinearity functions were derived for eight substances by using the different dilution series but excluding the containers that were proven to have drifted. CH_3Cl (methyl chloride) was not retrieved due to concentration changes in many containers of the dilution series and in addition its low ECD signal which led to high error bars.

Tests showed that nonlinearity retrievals did not affect the measurement error bars much. Therefore the 1σ measurement error bars (i.e. the reproducibilities of the calibration standard) were applied to all retrieved mixing ratios for comparison of the measurements. The stratospheric mixing ratios as calculated from the ECD data using different retrievals (linear and 3 x non-linear) are shown in Figure 3.2.2 for $CFCl_3$ (F11) in comparison with MS results. It is obvious that the linear retrieved ECD data can not be used here. All nonlinear retrieved ECD data agreed with the MS results for tropospheric mixing ratios around 250 ppt within the error bars. In the stratosphere, where F11 is decreasing fast with altitude none of the nonlinearity functions is able to reflect the stratospheric air matrix but the two dilution series perform better than the pressure series. Unfortunately this is not true for other substances.

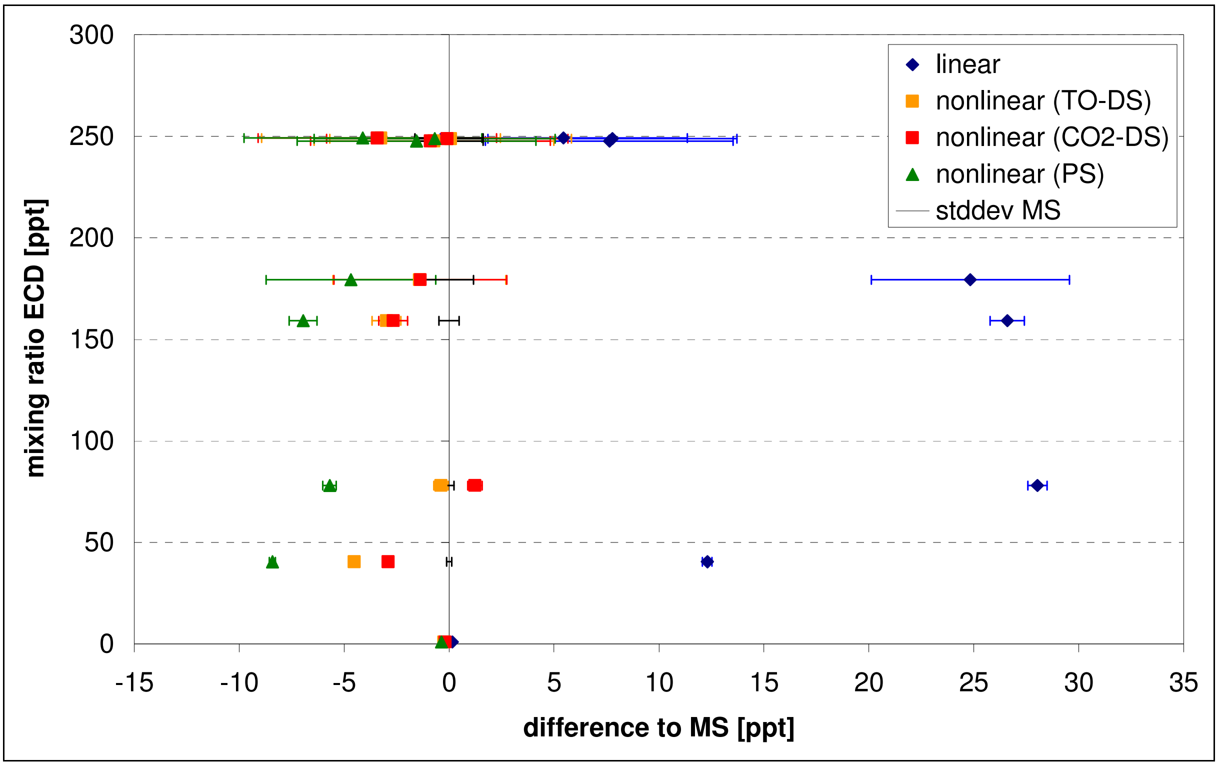

Figure 3.2.2. CFCl$_3$ *(F11) stratospheric mixing ratios for the C1 balloon flight. The ECD data as calculated linearly (blue) and via the nonlinearity functions from two dilution series (DS, red and orange) and one pressure series (green) are plotted against the mixing ratio difference to the MS (ECD minus MS). The error bars are given as the 1σ relative standard deviations (reproducibilities) of the calibration standard. No ECD data set agrees 100% with the MS.*

Figure 3.2.3 shows a similar plot for CF_2Cl_2 (F12). Here the linear ECD retrieval and the nonlinear retrieval using the CO2-dilution series come closest to MS mixing ratios. None of the dilution series was able to reflect the MS results for all eight substances. In fact the only substance where all ECD mixing ratios agreed with the MS results was CHF_2Cl (F22) as derived with the CO2-dilution series. The corresponding figures can be found in the Appendix (Figure set A.S.7).

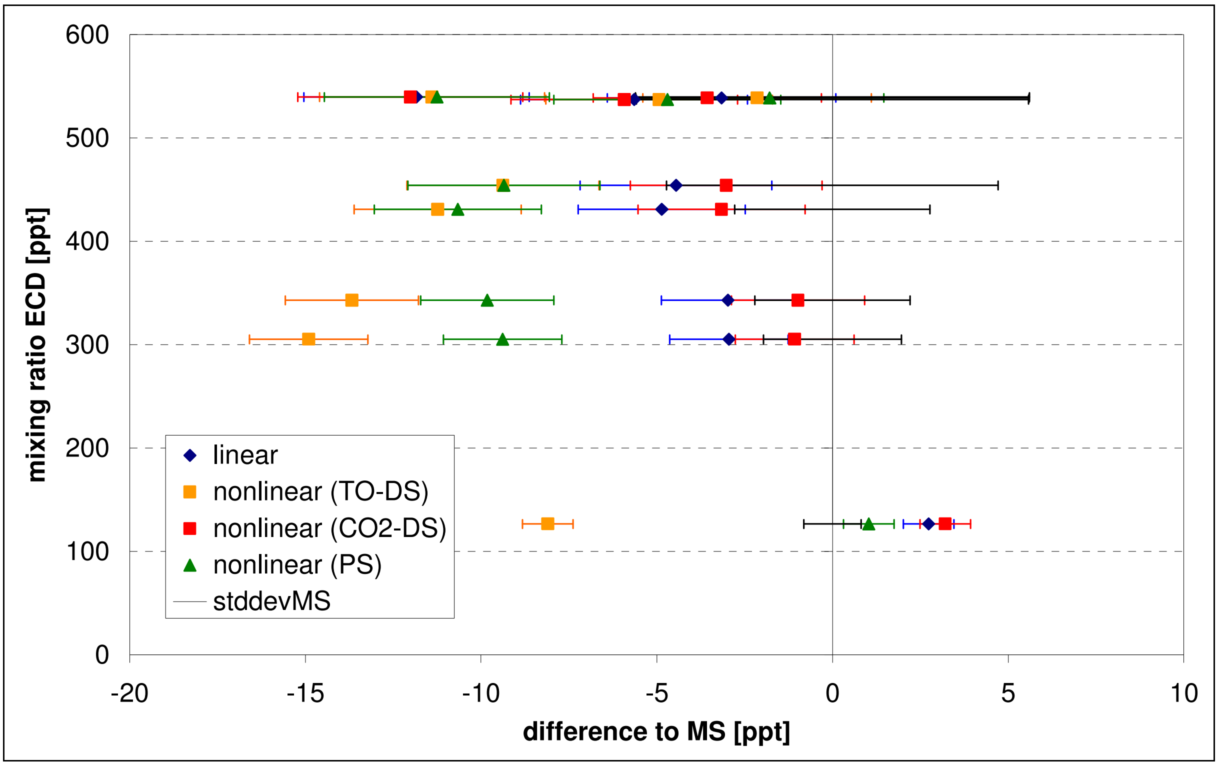

Figure 3.2.3. The same as in Figure 3.2.2 but for CF_2Cl_2 (F12).

3.2.3 Systematic comparison of stratospheric detector results

Eight samples from one flight is an insufficient amount for a systematic comparison of stratospheric ECD and MS results. The TO-dilution series was measured near to all stratospheric measurements. The results of the three whole-air-samplers (i.e. 34 samples) were checked for agreement by using the respective nonlinearity correction. The detectors were assumed to give the same results if at least two thirds of the mixing ratios agreed within their 1σ measurement error bars. This was observed for three substances: CHF_2Cl (F22, 85 %), CF_3CFCl_2 (F114a, 71 %) and $CF_2ClCFCl_2$ (F113, 68 %). F22 and F114a results even met the agreement criterion if retrieved linear. Possible explanations for the other substances' disagreements are the differences in stratospheric and tropospheric air matrices (e.g. signals from minor coeluting substances) or the low number of dilution containers available to derive nonlinearity functions. The corresponding data can be found on the enclosed CD (internal detector comparison.xls).

3.3 Calibrations and cross-comparisons

3.3.1 Calibration of substances

The attachment of the Mass Spectrometric detection channel enabled measurements of many additional target substances (see Chapter 2.2). For quantification of these substances absolute concentrations needed to be assigned to the signals. Most substances were quantified using a calibrated air standard (SX-3551) obtained in November 2006 from the Global Monitoring Division (GMD) which belongs to the Earth System Research Laboratory (ESRL) of the National Oceanic Atmospheric Administration (NOAA) in Boulder, USA. From this standard the calibration was transferred to the internal secondary standards used for stratospheric air sample measurements such as the ALM-39767 and the TO-Tante standard. This was even possible for measurements prior to November 2006 because the used calibration standards were assured not to show concentration drifts within a certain time period (see Chapter 3.1.1). Moreover, the ALM-39767 was also obtained from NOAA in 1993 with calibration values for eight target substances: CF_2Cl_2 (F12), $CFCl_3$ (F11), $CF_2ClCFCl_2$ (F113), CHF_2Cl (F22), CH_3CFCl_2 (F141b), CH_3CF_2Cl (F142b), CH_3CCl_3 (methyl chloroform) and CCl_4 (carbon tetrachloride). All mixing ratios from this initial calibration agreed with those assigned via the SX-3551 standard within their 3 σ measurement error bars. This indicates that the concentrations inside the ALM-39767 as well as the NOAA calibration scale of these substances did not significantly change in the last 15 years.

The remaining target substances were quantified via cross-comparisons with the Organic Reactive Species group at the Max-Planck-Institute for Chemistry (MPI-CH) in Mainz, GER [CH_2ClCH_2Cl (1,2-dichloroethane), C_2H_5Cl (chloroethane) and $CHFClCF_3$ (F124)] and the Atmospheric Chemistry group at the University of East Anglia (UEA) in Norwich, UK [C_2HCl_3 (trichloroethene) and C_2Cl_4 (tetrachloroethene)]. Four substances were calibrated using air samples from UEA which were measured twice at both institutes: C_2F_5Cl (F115), CF_2ClCF_2Cl (F114), CF_3CFCl_2 (F114a) and CF_2BrCF_2Br (H2402). Table 5.2.1 of Chapter 5 also provides calibration details.

Moreover the cross-comparisons provided two or three calibration values for a number of target substances. The concentrations of these substances were used to compare the different absolute calibration scales used by the three laboratories. Table 3.3.1 gives an overview of the calibration differences calculated for the SX-3551 standard. The error bars are the sum of all measurements standard deviations used to derive the mixing ratios.

3.3.2 Cross-comparison with the University of East Anglia

At the UEA the SX-3551 and ALM-39767 containers were measured three times each against the ALM-39753 calibration standard from UEA. The latter consists of the same material as the ALM-39767 and was also prepared by NOAA in 1993. The analytical system used was a GC/MS (VG/Waters "AutoSpec" EBE tri-sector instrument operated in single ion mode and using a DB5 capillary column) with a pre-concentration system which is similar to that in Frankfurt. The direct measurements of the SX-3551 showed agreement of the calibrations within the 3 σ measurement error bars except for CH_2Cl_2 (dichloromethane) and $CHCl_3$ (chloroform). The SX-3551 mixing ratios derived from the ALM-39767 measurements (calculated using the internal calibration standard comparison data set, see Chapter 3.1.1) showed additional disagreements for CH_3Br (methyl bromide) and CH_3Cl (methyl chloride). Both the SX-3551 and the ALM-39767 were assured not to drift in concentrations. Thus, the additional disagreements are most likely caused by an error underestimation due to the limited number of cross-comparison measurements. But the containers should be compared again if possible in order to confirm these speculations. The UEA group also uses the NOAA calibration scale for most of the compared substances which is one reason for the observed agreements. Furthermore the cross-comparison results show that both instruments give the same results for many substances and supports the finding of Chapter 3.1.1 that no long term concentration drifts occurred in any of the calibration standards (except for CH_2Cl_2 and $CHCl_3$ which are suspected to have drifted inside the UEA container as stated by W. T. Sturges in personal communication, 2007).

3.3.3 Cross-comparison with the Max-Planck-Institute for Chemistry

The cross-comparison with the MPI-CH was carried out using the Frankfurt analytical system. Here, the TO-Tante calibration standard was measured against the "Ruegen" standard from Mainz. The latter was calibrated by Elliot Atlas at the University of Miami, Rosenstiel School of Marine and Atmospheric Science, Miami, USA. The TO-Tante mixing ratios were used to calculate SX-3551 mixing ratios on the MPI-CH/UMiami calibration scale. $CHCl_3$ was again found to show significant calibration scale differences. In addition CF_2ClBr (H1211), CCl_4 (carbon tetra chloride), CH_3Cl (methyl chloride) and CH_3CCl_3 (methyl chloroform) differed from the NOAA scale for SX-3551. Comparison of UEA and MPI-CH mixing ratios gave disagreement for the calibrations of CH_2Cl_2, $CHCl_3$ and CH_3CCl_3. Thus, except for H1211 all substances that showed calibration scale differences were also showing concentration changes inside storage containers (see Chapters 3.1.2 and 3.1.3).

Table 3.3.1. Calibration scale comparisons of three different laboratories: Global Monitoring Division of NOAA-ESRL (Boulder, USA), the Atmospheric Chemistry group of UEA (Norwich, UK) and the Organic Reactive Species group MPI-CH (Mainz, GER, calibrated by the University of Miami, USA). All values are given in ppt and calculated for the SX-3551 calibration standard which was directly obtained from NOAA. The UEA comparison was carried out in Norwich using two different calibration standards while the MPI-CH comparison was carried out in Frankfurt. The bold numbers are significantly different to the NOAA calibration mixing ratios while the italic UEA values differ from those derived from the MPI-CH cross-comparison.

Substance	NOAA calibration		UEA (directly)		UEA via ALM-39767		MPI-CH via TO-Tante	
	Mixing ratio	3σ stddev	Mixing ratio	3σ stddev	Mixing ratio	3σ stddev	Mixing ratio	3σ stddev
C_2Cl_4	3.06*	0.18*	3.13	0.22	3.26	0.15	3.55	0.39
CCl_4	93.20	1.50	96.31	5.19	95.15	5.91	**86.13**	5.34
F12	533.9	3.30	548.5	26.86	548.5	17.13	550.0	44.88
H1211	3.19	0.03	-	-	-	-	**4.10**	0.37
F113	79.40	1.20	77.81	1.42	77.16	4.61	-	-
F11	249.8	2.40	258.0	5.77	252.2	13.42	260.3	22.72
CH_2Br_2	0.63	0.12	0.56	0.02	0.59	0.14	1.24	0.66
CH_2Cl_2	24.90	0.60	***17.16***	0.64	***19.14***	1.90	22.18	0.96
CH_3Br	9.40	0.30	10.10	1.31	**10.46**	0.72	10.26	2.58
CH_3CCl_3	15.50	0.30	*15.64*	0.58	*15.11*	1.76	**10.72**	1.14
F142b	18.70	0.30	19.59	0.89	17.95	1.01	19.07	0.99
CH_3Cl	537.7	2.70	487.7	61.95	**470.9**	18.24	**500.3**	20.52
$CHBr_3$	0.36	0.09	0.33	0.03	-	-	-	-
$CHCl_3$	7.60	0.60	***5.22***	0.21	***5.43***	1.26	**10.59**	0.71
F22	188.0	2.10	192.1	12.67	185.4	9.76	185.4	6.62

*from personal communication with Brad Hall, NOAA-ESRL, 2008

Moreover, estimates of the NOAA scale uncertainties could be obtained for a number of target substances (personal communication with Brad Hall, NOAA-ESRL, 2007). These estimates were derived based on: (1) agreement among primary standards used to define the scale and (2) estimates of the ability to monitor drift for a few compounds that can drift in containers. These estimates were given as 2 σ uncertainties and were 5 % for $CHCl_3$, 1 % for H1211, 2 % for CCl_4, 4 % for CH_3Cl and 2.5 % for CH_3CCl_3. If these estimates are added to the NOAA error bars the SX-3551 mixing ratios of CCl_4 and CH_3Cl agree with those derived via the MPI-CH/UMiami calibration scale. But the mixing ratios of $CHCl_3$, H1211 and CH_3CCl_3 are still significantly different between these two calibrations.

To summarise, the calibration scales of three laboratories were compared for 15 halocarbons. Seven substances were found to be problematic as at least two laboratories differed significantly in calibration. Such calibration differences were also observed in earlier cross-comparisons between different laboratories (e.g. Pfeilsticker et al., 2000, Butler et al., 2007). For the respective substances a conversion factor should be used when combining results from the different laboratories in one data set. The reasons for the calibration scale differences remain uncertain. But concentration drifts or shifts in the containers are a likely explanation. Also responsible could be errors during the initial gravimetric or volumetric calibration standard preparation processes as well as the presence of unknown coeluents in the different analytical systems. Moreover, some of the NOAA calibration values were derived using GC-ECD methods (F12, F11, F113, CH_3CCl_3, CCl_4, H1211 and H1301) while all others depend on GC/MS measurements. As shown in Chapters 3.1.3 and 3.2 quantification using an ECD can cause differences due to problems connected with nonlinearity corrections. In addition ECD and MSD measurements can have different sensitivities towards interferences from coeluting substances.

3.4 Conclusions

It is resumed that the efforts that were undertaken to check the quality of the trace gas measurements resulted in a number of findings. First, almost all target substances were proven to be stable in concentrations inside the air standards used for the calibration of trace gases in atmospheric samples. Many substances were also found to be stable inside the containers of two whole-air-samplers. Some substances changed in concentrations but most of them showed different behaviour in different containers, which makes a general correction very difficult (e.g. different increases or – like CH_3Br – one container from flight B42 of the

BONBON II sampler showed increases in concentration, one decreases and one showed no change at all). These changes could have been caused by slow reactions on active spots of the container walls, out gassing valves or characteristics of stratospheric air such as high ozone and hydrochloric acid concentrations or the extreme dryness. The sampling process could also be involved as the air is frozen (which results in high local concentrations) and subsequently exposed to high temperatures and pressures compared to stratospheric conditions. For future stratospheric air sampling it is suggested that each container of the BONBON whole-air-samplers should be systematically evaluated for concentration changes under varying sampling conditions (such as filling pressure, air humidity or ozone concentration) and/or that different container materials or passivation techniques should be tested. Furthermore, although the CLAIRE sampler has already been flushed with ultra-pure gases (“zero air” and N_2) for one week prior to its first flight, this procedure should be repeated to remove the contaminations with CH_3CF_2Cl (F142b).

In addition the evaluation of the static dilution series and the internal detector comparison revealed disadvantages of the ECD quantification process due to problems connected with coeluting substances and non-linearity corrections. The Mass Spectrometer was found to be the less error-prone detector in this case as it showed linear response behaviour and influences from coeluents can be identified and avoided for most substances.

Moreover, a cross-comparison of the calibration values of three different laboratories led to the finding that there are disagreements between the different scales for a number of halocarbons. A systematic and global cross-comparison of all laboratories that measure halocarbons in the atmosphere is recommended (such as the already ongoing project IHALACE – see http://www.esrl.noaa.gov/gmd/hats/ihalace for details – but for a wider range of substances). Furthermore a re-evaluation of the complete calibration scale preparation processes might be helpful in order to minimise calibration scale differences.

4 Tracer-tracer-correlations and fractional release factors of long-lived halogenated substances in the tropical stratosphere

4.1 Introduction

Very few measurements of halocarbons in the tropical stratosphere have been performed (e.g. Goldan et al., 1980, Volk et al., 1997, Schauffler et al., 1999, Laube et al., 2008). In addition, due to the elevated tropopause in the tropics (between about 15 and 18 km depending on the meteorological conditions) aircraft-based investigations such as those of Volk et al. (1997) and Schauffler et al. (1999) are only able to investigate the lower stratosphere there (up to 21 km). Other measurements are outdated as the concentrations of the analysed halocarbons have significantly changed over the past three decades. Satellite instruments provide only poor altitudinal resolutions (e.g. Moore and Remedios, 2008) and are in addition not able to quantify most halocarbons up to now. But as explained in Chapter 1 many halocarbons are strong greenhouse gases and/or able to enhance the catalytic decomposition of ozone. Moreover, the chemical composition influences the ozone distribution and the radiative balance of the stratosphere (e.g. Brasseur and Solomon, 1986). As the tropical stratosphere is very sensitive for the climate of this planet – e.g. most of the ozone is produced there (Finlayson-Pitts and Pitts, 2000) – it is important to quantify the altitudinal distributions of halocarbons in this atmospheric region.

The distributions of long-lived ozone-depleting substances (subsequently also called tracers) derived for this thesis originate from measurements on air samples collected with three balloon-borne whole-air-samplers launched in June 2005 from Brazil (5 °S) and in October 2006 from Southern France (44 °N) and also from air samples collected from a high altitude aircraft flying in tropical and mid-latitudes between 43 °N and 22 °S (see also Chapter 3, Table 3.1.1). For the first time, a set of 17 long-lived halocarbons – six CFCs, four HCFCs, three Halons and four longer-lived non-fluorinated Chloro- and Bromocarbons (as listed in Table 5.2.1 but except H1202) – was quantified in air samples originating from an altitude range between 15 and 34 km (upper troposphere and lower to middle stratosphere) in the tropics. A number of atmospheric short-lived halocarbons were also measured but will be discussed in Chapter 5.

From this data set tracer-tracer-correlation functions and fractional release factors (subsequently abbreviated as FRFs, see also Chapter 1.1.4) were calculated. The derived dependencies could help to improve future climate and ozone level predictions. FRFs are for example used for the calculation of Global Warming Potentials (e.g. Daniel et al., 1995) and the semi-empirical calculation of Ozone Depletion Potentials (ODPs, Solomon et al., 1992, Schauffler et al., 1999) which are measures for the ability of a trace gases to influence future climate and to deplete stratospheric ozone.

As examples Figure 4.1.1 shows all derived upper tropospheric and stratospheric mixing ratios (mid-latitudes and tropics) for CH_3CF_2Cl (F142b) and CF_2ClBr (H1211).

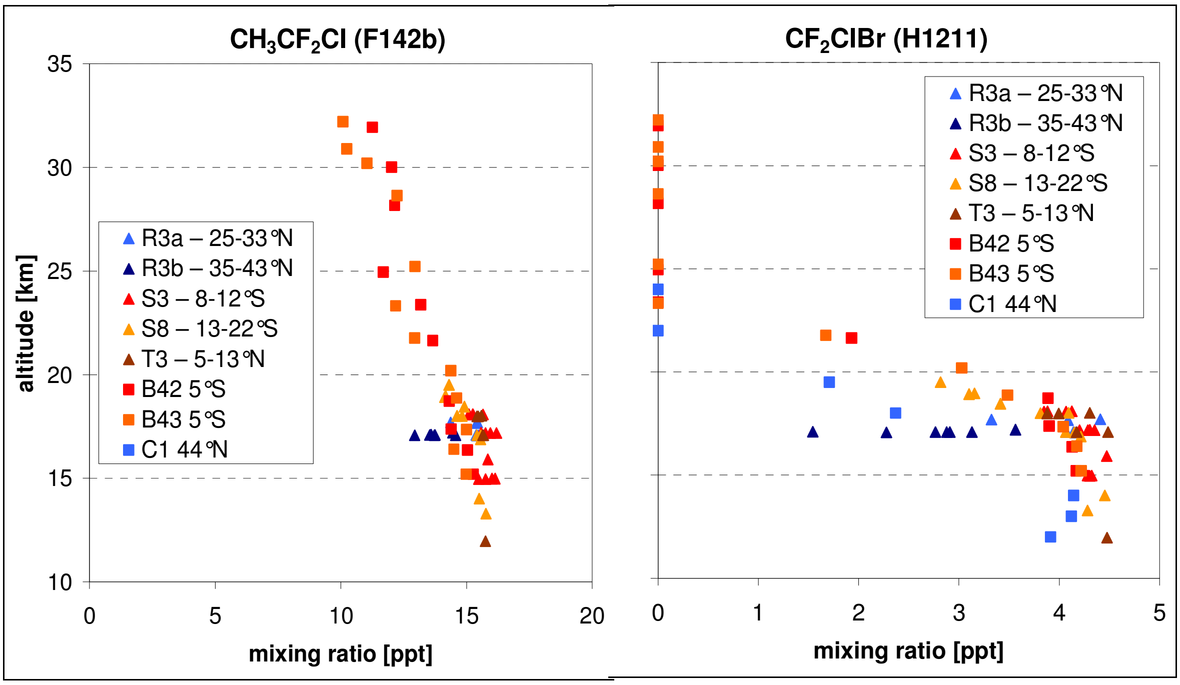

Figure 4.1.1. Mixing ratios of CH_3CF_2Cl (F142b) and CF_2ClBr (H1211) in the tropical (in orange, red and brown) and mid-latitude (in blue) upper troposphere and stratosphere. Both substances are long-lived and thus rather uniformly distributed in the upper troposphere. The tropopause was located at altitudes around 15 km in mid-latitudes and around 17 km in the tropics. In the stratosphere the mixing ratios start to decrease with increasing altitude which is mainly due to their decomposition by photolysis and reactions with excited Oxygen atoms (O^1D). H1211 decreases much faster than F142b. Moreover, for both substances higher mixing ratios are present in the tropical stratosphere than at similar altitudes in mid-latitudes. For CH_3CF_2Cl (F142b) no data of flight C1 could be used as the respective whole-air-sampler showed contaminations with this substance (see Chapter 3.1.2).

Both substances have long lifetimes compared to tropospheric transport times and thus their distributions throughout the upper troposphere (far from industrial source regions) are rather uniform. The higher radiation in the stratosphere causes their decomposition by photolysis and/or reactions with excited Oxygen atoms (O^1D) and/or OH radicals (see Chapter 1.1.4). H1211 mixing ratios decrease much faster with increasing altitude than those of F142b which is caused by the individual reactivities of the substances. Moreover, in the mid-latitude stratosphere above ~17 km lower mixing ratios are found for both substances compared to similar altitudes in the tropics. These are indications for different stratospheric regions having a characteristic chemical composition. For long-lived halocarbons which do not decompose significantly until they reach the stratosphere, tracer-tracer-correlations and FRFs can be used for investigations on these characteristics.

4.2 Tracer-tracer correlations

The correlation between the mixing ratios of two trace gases that are both long-lived (so-called tracers) is compact in the stratosphere (Plumb and Ko, 1992). But transport barriers, chemical processes and also latitudinal and seasonal variations in the vertical distributions of tracers cause different correlation curves between these substances for different stratospheric regions (e.g. Volk et al., 1997, Engel et al., 2002). Due to the major transport barriers (see Chapter 1, Figure 1.1.2) the stratosphere can be subdivided into three regions which show characteristic correlations between the tracers: tropics, mid-latitudes and the polar vortex which forms in high-latitudes at the respective winter-pole. As an example Figure 4.2.1 shows a comparison of the correlation of CF_2Cl_2 (F12) and $CFCl_3$ (F11) in the tropical and mid-latitude stratosphere. Both substances start to decrease in concentration when reaching the stratosphere. Thus, the correlations are already corrected for the tropopause height. Substantial differences between the correlations are found which confirms the dynamic isolation of the two regions and is in agreement with existing concepts of stratospheric transport (e.g. Plumb, 1996, Waugh and Hall, 2002).

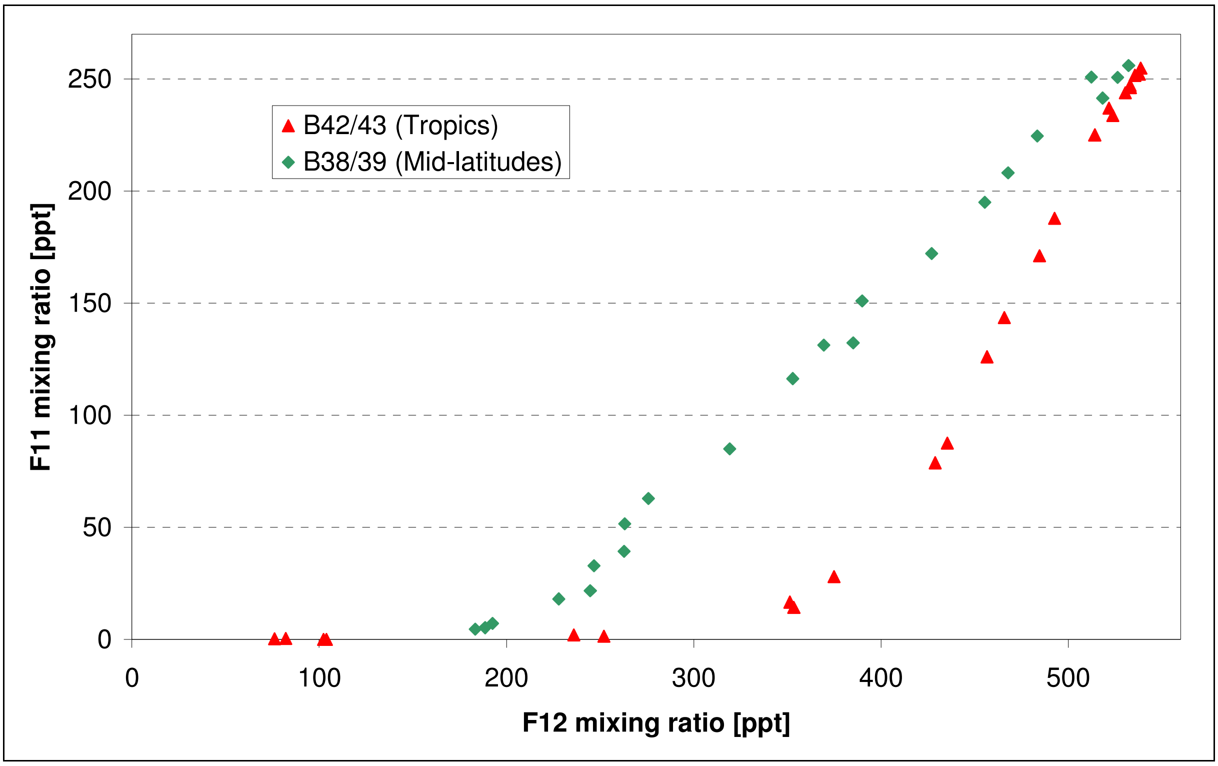

Figure 4.2.1. Correlations of the long-lived tracers CF_2Cl_2 (F12) and $CFCl_3$ (F11) in two major regions of the stratosphere: Tropics (from flights B42/43, June 2005, above Teresina, Brazil, 5 °S) and Mid-latitudes (from flights B38, October 2001 and B39, September 2002, above Air Sur l'Adour, France, 44 °N). The atmospheric regions show different correlation shapes. Lower mixing ratios correspond to higher altitudes as both substances start to decompose once they reach the stratosphere. The data originates from measurements on balloon-borne whole-air-samplers. The tropical air samples were analysed for this thesis (via GC-MS) whiles the other data was taken from Möbius (2005) (derived via GC-ECD).

The correlations in these regions are furthermore influenced by the season. For example Boering et al., 1994 performed stratospheric measurements of CO_2 (carbon dioxide) and N_2O (nitrous oxide) in northern mid-latitudes and found the correlations between these tracers to be seasonally dependent indicating that vertical transport above 20 km is slower in northern summer than in winter. Moreover, the corresponding variations are increasing with latitude. The highest variability is observed in Polar Regions where an isolated vortex forms in winter inside which characteristic correlations are found (e.g. Schmidt et al., 1991, Ivanova, 2007). In contrast, seasonal correlation changes in the tropical stratosphere are believed to be smaller

(Plumb, 2002, Plumb, 2007) which is why the analysed air samples collected in different seasons in 2005 were combined in one data set here.

For the calculation of tropical correlation functions performed for this thesis all data between 15 °S and 15 °N and above potential temperatures of 360 K were used. These criteria were chosen to include a) only tropical mixing ratios and b) the variability of the substances in the Tropical Tropopause Layer (TTL, i.e. the main stratospheric entrance region, see also Chapter 1.1.2). Due to the low number of measured samples (especially in higher altitudes) no mid-latitude correlations were calculated. Figure 4.2.2 shows the derived tropical stratospheric correlation between CF_2Cl_2 (F12) and CF_3Br (H1301).

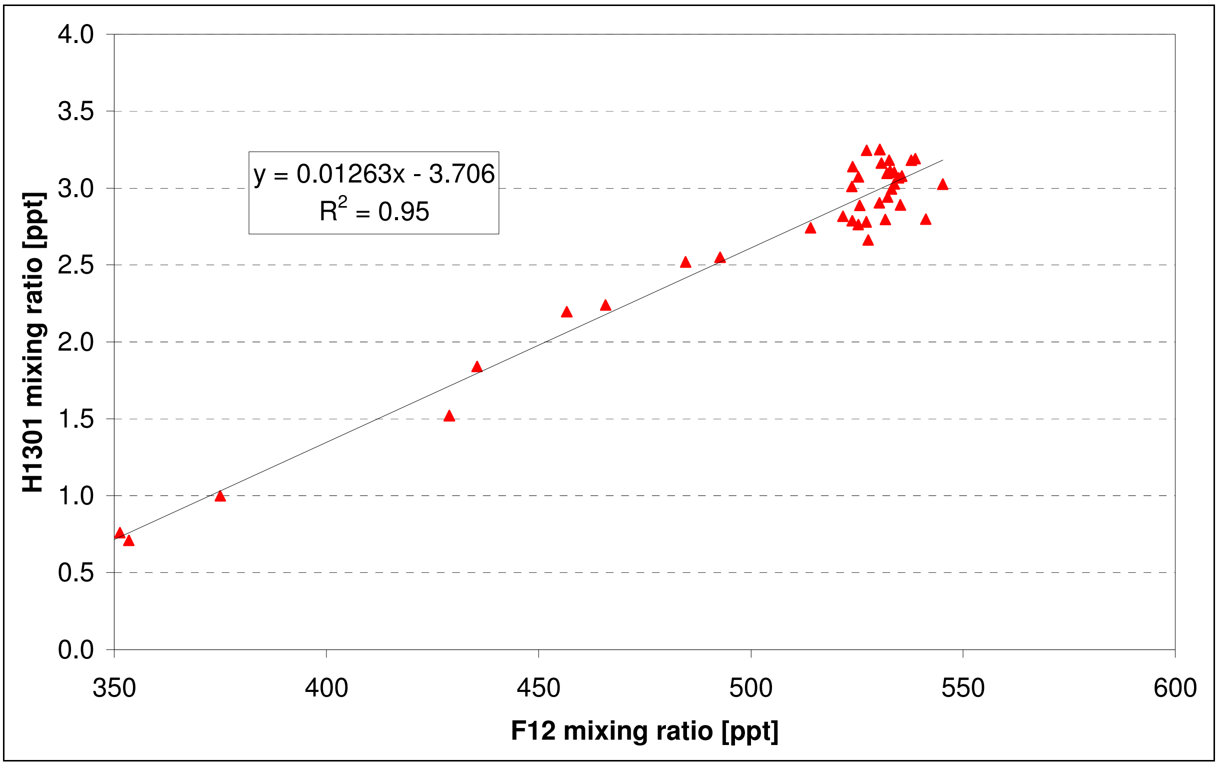

Figure 4.2.2. Tropical stratospheric correlation between CF_2Cl_2 (F12) and CF_3Br (H1301) for the year 2005 and mixing ratio ranges of 0.7 – 3.3 ppt for H1301 and 351 – 545 ppt for F12. The lower mixing ratios correspond to higher altitudes as both substances decompose due to photochemical processes. The scattering of mixing ratios is due to differences in local photochemical and mixing processes but also to the relatively high measurement uncertainties of the low concentrated H1301 (1 σ uncertainties around 4 % for tropospheric mixing ratios around 3 ppt). The observed correlation can be approximated by a linear polynomial.

The dependency of the H1301 mixing ratios to those of F12 can be described by a linear polynomial for the observed mixing ratio ranges.

Such correlation functions can be used in models (e.g. Chemical Transport Models, CTMs, see e.g. Avallone et al., 1997, McKenna et al., 2002, Grooß et al., 2002) and thus help to predict future ozone levels and climate. Many models use a steady-state atmosphere for the model initialisation in order to avoid long run times caused by equilibration processes. For this initialisation process atmospheric data is assimilated but only for a limited number of substances (such as N_2O or F12). Altitudinal distributions of other substances are then simulated via parameterisations (i.e. correlation functions). Moreover, atmospheric data originating from times after the initialisation are used to evaluate how well the models reflect atmospheric processes. The data set derived for this thesis provides access not only to current correlation functions, but also to the middle stratosphere in tropical latitudes, where few data exists for halocarbons.

Tropical correlation functions were derived for all measured long-lived target substances relative to F12. The best estimates showing the highest correlation coefficients after Pearson were polynomial fit functions in most cases. The order of the polynomial was increased stepwise. When the corresponding Pearson coefficient did not increase significantly the polynomial with the lower order was chosen. In some cases exponential fit functions were chosen as they reflected the shape of the correlation better. Table 4.2.1 shows the function parameters and the mixing ratio range which was used to derive the respective function. These functions are only valid for the given mixing ratio range and the year 2005. However, they can be shifted to other years by correcting for the time-dependence of the tropospheric release rates of each substance. Such a normalisation of correlations was described e.g. by Plumb et al., 1999. It is a complex mathematical procedure and was carried out using a two dimensional (2-D) Chemical Transport Model. This would exceed the scope of this thesis and is left to the respective user of the data. But another possibility to derive time-independent stratospheric quantities from the measurements is the calculation of fractional release factors (FRFs) which has been done and will be explained and discussed in the following sub-chapters.

Table 4.2.1. Correlation functions of long-lived halocarbons relative to CF_2Cl_2 (F12) in the TTL and tropical stratosphere (between 15 °N and 15 °S and above 360 K potential temperature). The corresponding mixing ratios can be found in the Appendix (Figure A.6) and originate from measurements of whole-air-samples collected in June, November and December 2005 (see Chapter 3, Table 3.1.1 for more details). The functions are only valid for 2005 and the given mixing ratio ranges. R^2 is the correlation coefficient after Pearson and was used to estimate the best fitting polynomial.

Substance (name)	$MR_y = f(MR_{F12}) =$	R^2	Valid for mixing ratio ranges [ppt] (substance & F12)
CF_3Br (H1301)	1.263E-02x - 3.706	0.95	0.7 – 3.3 351 – 545
C_2F_5Cl (F115)	2.419E-03x + 7.453	0.72	7.4 – 9.1 76 – 545
CHF_2Cl (F22)	$2.4584\text{E-}06x^3 - 2.058\text{E-}03x^2 + 0.589x + 65.792$	0.94	102 – 180
CF_2ClBr (H1211)	4.925E-02x - 22.032	0.86	1.6 – 4.5 485 – 545
CF_2ClCF_2Cl (F114)	7.88312E-03x + 12.374	0.92	12.8 – 17.0 76 – 545
CF_3CFCl_2 (F114a)	3.919E-03x - 0.212	0.90	0.7 – 2.1 236 – 545
CH_3Cl (methyl chloride)[a]	$3.6956\text{E-}03x^2 - 1.521x + 229.950$	0.76	80 – 500 200 - 530
CH_3CF_2Cl (F142b)	$1.9710\text{E-}07x^3 - 1.5681\text{E-}04x^2 + 4.248\text{E-}02x + 7.513$	0.93	9.7 – 16.2 76 – 545
high mixing ratios of $CFCl_3$ (F11)	$-1.0457\text{E-}02x^2 + 11.899x - 3121.811$	0.90	150 – 258 465 – 545
low mixing ratios of $CFCl_3$ (F11)	1.5495E-02exp(0.019642x)	0.99	2 – 150 236 – 465
$CHFClCF_3$ (F124)[b]	$4.3473\text{E-}08x^3 - 3.3411\text{E-}05x^2 + 8.512\text{E-}03x - 0.132$	0.96	0.3 – 1.6 76 – 545

Table 4.2.1 continued

Substance (name)	$MR_y = f(MR_{F12}) =$	R^2	Valid for mixing ratio ranges [ppt] (substance & F12)
CH_3Br (methyl bromide)[a]	$9.8157E\text{-}04x^2 - 0.898x + 205.430$	0.99	1.1 – 6.7 493 – 545
$CF_2ClCFCl_2$ (F113)	$1.4883E\text{-}04x^2 + 7.192E\text{-}02x - 0.902$	0.98	5.5 – 82 76 – 545
CH_3CFCl_2 (F141b)[d]	$7.6232E\text{-}05x^2 - 9.614E\text{-}03x + 1.063$	0.88	0.6 – 20.6 76 – 545
$CBrF_2CBrF_2$ (H2402)[b]	$6.041E\text{-}03x - 2.822$	0.68	0.3 – 0.46 514 – 538
CCl_4 (tetrachloro-methane)[c]	$y = 0.600x - 235.677$	0.90	2 – 96.7 396 – 545
CH_3CCl_3 (methyl chloroform)	$y = 0.132x - 53.626$	0.87	4 – 19.5 435 – 545

"exp(x)" stands for potentiation of x with the Euler number as the basis

"E-02" stands for an exponent of -2 to the basis 10

a - only data of flight B42 used due to indications for concentration shifts or contaminations in other containers

b - only data of flights B42 and B43 was used for the same reason

c - only data of flights B42 and S3/S8/T3 was used for the same reason

d - F141b was not measured on S8 and T3 samples

4.3 Calculation of fractional release factors

As explained in Chapter 1.1.4 a fractional release factor (FRF) is a relative quantity. It can be described as the inorganic halogen fraction released from a halocarbon at a given location and time in the stratosphere. For a FRF calculation according to Eq. (1.3) (taken from WMO, 2007) two quantities must be known: the mixing ratio of a substance at a given altitude and the corresponding mixing ratio of the substance when it entered the stratosphere. The former was measured and the latter can be calculated from the mean age of the air (i.e. the mean stratospheric residence time, see Chapter 1.1.5) and tropospheric concentration-time series for long-lived substances. A calculation is also possible for very short lived substances (VSLS), but the corresponding FRFs are highly variable and depend on the season and location of the respective emissions in the troposphere (Ko and Poulet, 2003). For that reasons no FRFs were calculated for VSLS.

$$f_i(x,y,z,t) = \frac{\rho_{i,entry} - \rho_i(x,y,z,t)}{\rho_{i,entry}} \tag{1.3}$$

$\rho_i(x,y,z,t)$ - mixing ratio of the halocarbon at a given stratospheric location (x,y,z) at time t

$\rho_{i,entry}$ - mixing ratio of the halocarbon in the air parcel when it entered the stratosphere

A number of different methods to derive fractional release factors of halocarbons have been described in the literature. The quantity itself was first defined by Solomon and Albritton (1992) according to Eq. (1.3). As few stratospheric measurements of halocarbons were available at this time Solomon et al. (1992) used models and a semi-empirical analysis of measured stratospheric profiles for methane and other gases to estimate FRFs. Daniel et al. (1995) combined measurements of air samples originating from the arctic stratosphere and model calculations to derive FRFs relative to $CFCl_3$ (F11) by assuming that most halocarbons show linear correlations with this substance. Schauffler et al. (2003) and Newman et al. (2006) improved this calculation by deriving the FRFs as a function of mean age of air from aircraft-based observations in the lower stratosphere in middle and high latitudes. Moreover they included the effect of an age spectrum in their calculations which will be explained in the following.

Each stratospheric air parcel can be assumed to consist of a large number of infinitesimally small parcels which have experienced different transport pathways since crossing the tropical tropopause (see Chapter 1.1.5). Thus, a probability distribution function of residence times can be assigned to the air parcel which is the so-called age spectrum (see also Figure 1.1.3). It describes how the composition of an air parcel is altered by mixing processes with older and newer air parcels. Schauffler et al. (2003) and Newman et al. (2006) used the estimated age spectra to calculate the amount of a halocarbon for a given mean age that would be present without decomposition of the substance in the stratosphere. This amount represents the stratospheric entry mixing ratio $\rho_{i,entry}$ of the substance corrected for concentration changes caused by mixing processes in the stratosphere.

To calculate it, the past tropospheric distributions of the respective trace gas must be known. A number of longer-lived halocarbons are continuously measured in the frame of a global ground-based network (see http://www.esrl.noaa.gov/gmd/). These stations are located far from industrial source regions. As long-lived halocarbons do not significantly decompose in the troposphere they are rather uniformly distributed throughout the well-mixed background and upper troposphere (see also Chapter 1.1.3). Thus, globally averaged tropospheric time series can be derived for these substances on a monthly basis. These data are publicly accessible under the above mentioned internet address. Schauffler et al. (2003) and Newman et al. (2006) used such time trends and an age spectra method described by Waugh and Hall (2002) to simulate stratospheric mixing.

The calculation of FRFs in this thesis was performed using a procedure which is similar to those of Schauffler et al. (2003) and Newman et al. (2006). The applied method was described by Engel et al. (2002) and includes effects from an age spectrum as well as global tropospheric time trends. First for every sample the mean age of air (i.e. the centre of the age spectrum) was derived from mixing ratios of SF_6 (sulphur hexafluoride) which were measured within the workgroup for flight B42 (T. Möbius, personal communication, 2006) and by the University of Heidelberg (I. Levin, personal communication, 2006) for flights B43 and C1, both using GC-ECD techniques (in two samples of C1 remained insufficient amounts of air for these measurements). SF_6 is a very inert substance which is not decomposing in the troposphere or the lower and middle stratosphere. Moreover, its concentrations continue to increase considerably in the troposphere (e.g. Stiller et al., 2008). Thus, SF_6 mixing ratios can be directly used to calculate a mean stratospheric residence time by assigning the mixing ratio observed in the stratosphere to a certain time of the past tropospheric SF_6 trend (e.g. Strunk et al., 2000, Bönisch, 2006). As the corresponding age spectra can not be measured directly they were derived from the mean ages via a parameterisation (according to Engel et al., 2002 which based their calculations on Hall and Plumb, 1994). It was assumed that the ratio of the squared width of the spectrum Δ^2 to the mean age Γ is constant throughout the stratosphere (Eq. 4.1).

$$\frac{\Delta^2}{\Gamma} = const. \tag{4.1}$$

A constant ratio of 0.7 was used here. Subsequently the corrected stratospheric entry mixing ratio was calculated for each substance and sample by assigning mixing ratio distributions to the age spectra via the above mentioned tropospheric time series (according to the calculation of total chlorine in Engel et al., 2002).

For five substances no monthly tropospheric trend data was available from NOAA-ESRL: C_2F_5Cl (F115), CF_2ClCF_2Cl (F114), CF_3CFCl_2 (F114a), CF_2BrCF_2Br (H2402) and $CHFClCF_3$ (F124). Thus, a linear time trend was derived from the annually averaged mixing ratios back to 1998 which were taken from Table 1-1 of WMO (2003) and Table 1-2 of WMO (2007) (AGAGE, in situ data was used except for H2402: UEA, flasks). However, the mixing ratios for 2005 derived from these trend functions did not match with the measured mixing ratios originating from air samples collected in the TTL in 2005. This is likely to be caused by differences in absolute calibration scales (see also Chapter 3.3). But the FRFs are only fractions i.e. relative values to the entrance mixing ratios. Thus, the trend functions were shifted to the mixing ratios observed in the TTL using a conversion factor. These factors, the corresponding tropospheric time series and also the source codes of the program used for this thesis' calculations can be found on the enclosed CD (\troptrends\).

No SF_6 data was available for the samples collected at the high altitude aircraft (Flights R3, S3, S8 and T3). To assign a mean age of air to these samples a correlation of mean age of air and a tracer was derived for the tropical stratosphere.

$$\Gamma = 28.71 - 0.19 \cdot MR_{F12} + 5.08 \cdot 10^{-5} \cdot (MR_{F12})^2 - 4.55 \cdot 10^{-7} \cdot (MR_{F12})^3 \tag{4.2}$$

A polynomial of the form of Equation (4.2) gave a well reflection of the correlation of mean ages Γ and CF_2Cl_2 (F12) mixing ratios (MR_{F12}) of the lower stratospheric data resulting from the balloon flights B42 and B43 (SF_6 measurements were performed within the workgroup for B42 and by the University of Heidelberg for B43, personal communication with T. Möbius and I. Levin, 2006). Please note, that this function is only valid for the tropical stratosphere in 2005 at mean ages below 3.5 years and a F12 mixing ratio range from 545 to 350 ppt. The

FRFs were then calculated according to those of the other flights but using the “F12 mean age”.

4.4 Results and comparisons of fractional release factors

As explained in the previous sub-chapter the correlations between two long-lived halocarbons are characteristic for different stratospheric regions in which the air masses have experienced similar transport pathways. This can also be observed if FRFs are plotted against the corresponding mean ages of air as shown in Figure 4.4.1 for $CFCl_3$ (F11). In the tropics F11 decreases much faster with increasing mean age than in mid-latitudes. The highest FRF differences are observed for mean ages of air between two and four years. Also displayed in Figure 4.4.1 is the mid-/high-latitude correlation derived by Newman et al. (2006) which consists of two functions: a quadratic polynomial to calculate FRFs for low ages of air up to 1.5 years and a cubic polynomial for higher ages. The derived mid-latitudinal and subtropical FRFs are comparable with the fit functions of Newman et al. (2006) but the tropical FRFs are higher for higher ages of air (flights B42 and B43). The faster decomposition of F11 in the tropical stratosphere is most likely caused by the higher radiation relative to regions at higher latitudes. Model studies predict loss rates of F11 that are higher by an order of magnitude in the tropics compared to mid-latitudes (e.g. Lee, 1994).

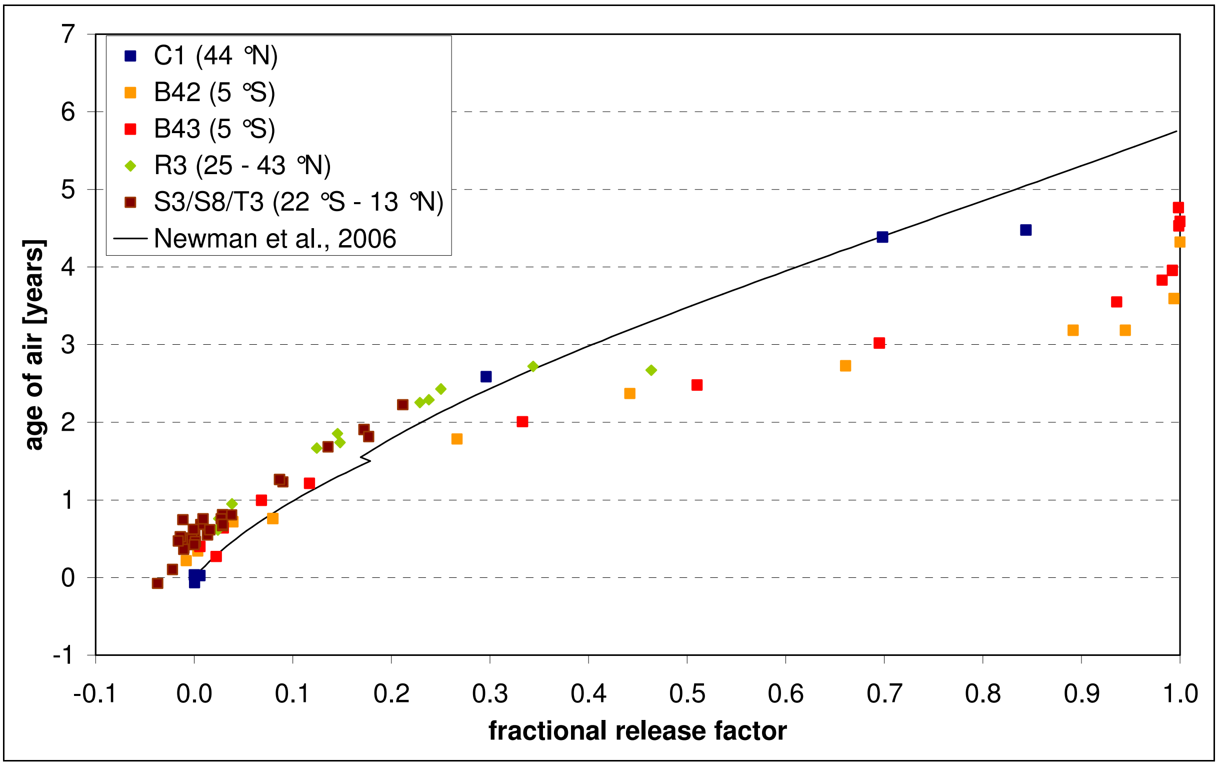

Figure 4.4.1. Fractional release factors (FRFs) and mean ages of air for $CFCl_3$ (F11). The mean age is plotted on the y-axis because it increases with altitude. The cold colours (blue and green) represent data of mid-latitudinal origin while the warm colours (orange, red and brown) represent tropical and subtropical data. Small negative values occur for low ages and FRFs caused by atmospheric variability and measurement uncertainties. The black curve is the correlation derived by Newman et al. (2006) using data from lower stratospheric aircraft observations in middle and high latitudes. This correlation consists of two functions: a quadratic polynomial for low ages of air up to 1.5 years and a cubic polynomial for higher ages. The derived mid-latitudinal and subtropical FRFs are comparable to the fit functions of Newman et al. (2006) but the tropical FRFs differ for higher ages.

Not all long-lived halocarbons show such a characteristic behaviour in different stratospheric regions. In Figure 4.4.2 the FRFs of CHF_2Cl (F22) are depicted. F22 decomposes very slowly compared to F11 and its FRF-mean-age correlation is not characteristic for different stratospheric regions. In logical consistency the corresponding correlation functions derived by Newman et al. (2006) are comparable with this thesis' data set. Similar plots and the corresponding FRF values for all halocarbons listed in Table 4.4.1 can be found in the Appendix (Figure set A.S.9 and Figure A.7).

In general, good agreement with the correlation functions derived by Newman et al. (2006) was found for low ages of air (up to 0.5 – 2 years depending on the individual substance). For higher ages most target substances were found to decompose faster in the tropics than in higher latitudes. The only exceptions were halocarbons with low stratospheric decomposition rates which showed comparable or slightly lower FRFs: CHF_2Cl (F22), CH_3CF_2Cl (F142b), C_2F_5Cl (F115) and CF_2ClCF_2Cl (F114).

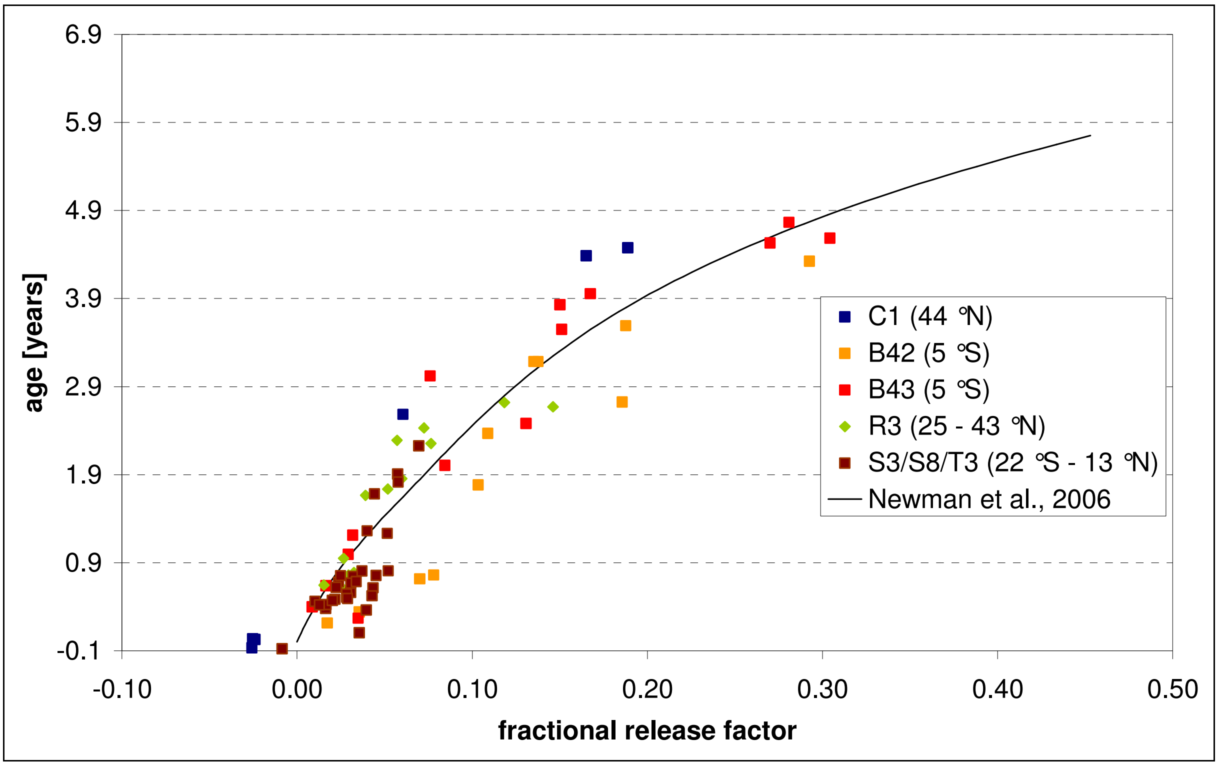

Figure 4.4.2. The same as in Figure 4.4.1 but for CHF_2Cl (F22). F22 is decomposing very slowly in the stratosphere. Thus, its FRF-mean-age correlation is less influenced by different transport pathways or radiation and shows no characteristic behaviour for stratospheric regions which are separated by transport barriers.

Two substances – CF_3CFCl_2 (F114a) and $CHFClCF_3$ (F124) – could not be compared as no FRF-mean-age functions of these substances were derived by Newman et al. (2006). In order to quantify the observed regional differences polynomial fit functions were derived which allow the calculation of tropical FRFs from the mean age of air (see Table 4.4.1). FRFs can be assumed to be constant in time for a given mean age-of-air (e.g. Newman et al., 2007) but depend in addition on the respective stratospheric region due to this thesis' findings.

Therefore the derived tropical correlation functions can be used for a wider time range than the correlation functions and are valid as long as there are no major changes to general stratospheric circulation and composition.

Table 4.4.1. Correlation functions to derive FRFs of long-lived halocarbons from the mean age of air in the lower and middle tropical stratosphere. The measurement data and correlation criteria used for the calculations are the same as in Table 4.2.1. The functions are only valid for the given FRF and mean age ranges. R^2 is the correlation coefficient after Pearson.

Substance (name)	Correlation function (y = tropical FRF and x = mean age [years])	R^2	Validity ranges (FRF & mean age in years)
CF_3Br (H1301)	$y = 3.9733E\text{-}02x^3 – 9.9256E\text{-}02x^2 + 0.103x$	0.96	0.0 – 1.0 0.0 – 3.6
C_2F_5Cl (F115)	$y = 1.1828E\text{-}02x^2 – 3.335E\text{-}02x$	0.84	0.0 – 0.12 0.0 – 4.8
CF_2Cl_2 (F12)	$y = 8.1036E\text{-}03x^3 – 2.3322E\text{-}03x^2 + 2.285E\text{-}02x – 7.79E\text{-}03$	0.98	0.00 – 0.86 0.4 – 4.8
CHF_2Cl (F22)	$y = 4.2606E\text{-}03x^3 – 2.0133E\text{-}02x^2 + 6.373E\text{-}02x$	0.91	0.0 – 0.30 0.0 – 4.8
CF_2ClBr (H1211)	$y = 0.27463x^3 - 0.95103x^2 + 1.253x - 0.470$	0.76	0.0 – 1.0 0.6 – 2.4
CF_2ClCF_2Cl (F114)	$y = 0.01642x^3 - 0.14042x^2 + 0.434x - 0.415$	0.90	0.0 – 0.23 1.8 – 4.8
CF_3CFCl_2 (F114a)	$y = 8.2770E\text{-}02x^2 - 0.166x + 9.217E\text{-}02$	0.86	0.0 – 1 0.7 – 4.3
CH_3Cl (methyl chloride)	$y = 4.2029E\text{-}02x^3 - 0.33389x^2 + 0.913x - 0.216$	0.97	0.0 – 0.9 0.2 – 4.3
CH_3CF_2Cl (F142b)	$y = 2.6102E\text{-}03x^2 + 1.566E\text{-}02x$	0.59	0.0 – 0.19 0.0 – 4.8
$CFCl_3$ (F11)	$y = -4.93799E\text{-}02x^4 + 0.3862x^3 - 0.9261x^2 + 1.008x - 0.351$	0.98	0.0 – 1.0 0.7 – 3.6

Table 4.4.1 continued

Substance (name)	Correlation function (y = tropical FRF and x = mean age [years])	R^2	Validity ranges (FRF & mean age in years)
$CHFClCF_3$ (F124)	$y = 0.165x - 0.113$	0.91	0.0 – 0.7 0.7 – 4.8
CH_3Br (methyl bromide)	$y = 1.5358x^2 + 1.212x$	0.94	0.0 – 1.0 0.0 – 2.8
$CF_2ClCFCl_2$ (F113)	$y = 6.3908E\text{-}04x^3 + 4.2781E\text{-}02x^2 - 7.891E\text{-}03x$	0.97	0.0 – 1.0 0.0 – 4.8
CH_3CFCl_2 (F141b)	$y = -2.1026E\text{-}03x^3 + 6.6695E\text{-}02x^2 - 5.382E\text{-}02x$	0.95	0.0 – 1.0 0.0 – 4.7
$CBrF_2CBrF_2$ (H2402)	$y = 0.4102x^2 - 0.190x$	0.90	0.0 – 1 0.0 – 2
CCl_4 (tetrachloro-methane)	$y = 7.3196E\text{-}02x^3 - 0.2971x^2 + 0.527x$	0.87	0.0 – 1.0 0.0 – 3.1
CH_3CCl_3 (methyl chloroform)	$y = -1.1677E\text{-}02x^3 + 0.1151x^2 + 6.521E\text{-}02x$	0.82	0.0 – 1.0 0.0 – 3.2

For the semi-empirical calculation of ODPs averaged FRF values are used (WMO, 2007). Moreover, these values are calculated relative to the averaged FRF of $CFCl_3$ (F11). Table 4.4.2 shows a comparison of these WMO values (which are mainly those derived by Daniel et al., 1995) with the averaged relative tropical FRFs of this thesis. The latter were derived according to the method of Schauffler et al. (2003) and are thus comparable. The error bars represent the variability of the relative FRFs over the averaged mean age range. Most of the substances were observed to decompose relatively fast with increasing mean age in the tropics which leads to relatively high variabilities if the FRFs are averaged over a wide mean age range. Consistently most of the relative FRF means agree with those of the WMO within this uncertainty criterion.

Table 4.4.2. Comparison of averaged FRFs relative to an averaged FRF of $CFCl_3$ (F11) in the tropics with current WMO values which originate from observations in mid- and high-latitudes (see Table 8-1 of WMO, 2007). The given error bars do not include measurement or calculation uncertainties but represent only the 1σ variability of the FRF within the mean age range used for averaging. The bold numbers are significantly different from those used in WMO (2007).

Substance (name)	tropical mean FRF relative to F11*	mean FRF relative to F11 (from WMO, 2007)
$CFCl_3$ (F11)**	0.74 ± 0.28	0.55
CF_2Cl_2 (F12)	0.56 ± 0.38	0.60
$CF_2ClCFCl_2$ (F113)	0.72 ± 0.39	0.75
CF_2ClCF_2Cl (F114)	**0.14 ± 0.09**	0.28 ± 0.02
CF_3CFCl_2 (F114a)	0.69 ± 0.51	n. a.
C_2F_5Cl (F115)	0.05 ± 0.06	n. a.
CHF_2Cl (F22)	**0.23 ± 0.11**	0.35
CH_3CFCl_2 (F141b)	0.76 ± 0.41	0.72
CH_3CF_2Cl (F142b)	**0.12 ± 0.07**	0.36
$CHFClCF_3$ (F124)	0.64 ± 0.20	0.52
CH_3CCl_3 (methyl chloroform)	1.21 ± 0.25	1.08
CCl_4 (tetrachloromethane)	1.14 ± 0.31	1.06
CH_3Cl (methyl chloride)	0.93 ± 0.15	0.80
CH_3Br (methyl bromide)	1.14 ± 0.55	1.12
CF_2ClBr (H1211)	1.26 ± 0.28	1.18
CF_3Br (H1301)	0.90 ± 0.49	0.62
$CBrF_2CBrF_2$ (H2402)	**1.36 ± 0.00**	1.22

*averaged for mean ages between 2.0 to 4.5 years;

**F11: absolute averaged FRF is given

n. a.: not available, model derived values were used for ODP calculations

However, four substances were found to have significantly different relative mean FRFs in the tropics. CF_2BrCF_2Br (H2402) showed a higher relative mean FRF which is caused by its rapid decomposition – the substance is already depleted to values below detection limits at mean ages of two years. CF_2ClCF_2Cl (F114), CHF_2Cl (F22) and CH_3CF_2Cl (F142b) showed lower relative mean FRFs in the tropics. This is surprising because in this thesis no evidence was found for a slower decomposition of halocarbons in the tropical stratosphere compared to mid-latitudes (see respective FRFs in the Appendix, Figure A.7 or Figure set A.S.9). But as the derived tropical values of CHF_2Cl (F22) and CH_3CF_2Cl (F142b) agree with those of Schauffler et al. (2003) derived from mid- and high-latitudes (0.29 ± 0.02 for F22 and 0.08 ± 0.04 for F142b) the values used in WMO (2007) are to be questioned.

For the other non-agreeing substance (i.e. F114) the WMO uses the averaged relative FRF of Schauffler et al. (2003) (0.28 ± 0.02) but this thesis' calculations resulted in a tropical value which is lower by a factor of two (0.14 ± 0.09). These discrepancies can not be explained with current understanding of atmospheric processes and remain an unresolved issue. It is recommended to reassess the fractional release of F114, F22 and F142b in the non-tropical stratosphere where most ozone loss occurs. Moreover, Daniel et al. (1995) assumed for simplification, that all tracer-tracer-correlation functions relative to F11 are linear and thus the FRF relative to F11 are valid throughout the stratosphere. But this simplification is not applicable to the tropical stratosphere (see Figure 4.2.1) and accordingly calculated averaged FRFs relative to F11 are highly imprecise and thus questionable. For improved ODP calculations the FRF correlations with mean age as derived by Schauffler et al. (2003), Newman et al. (2006) and in this thesis should be used.

4.5 Conclusions

The measured set of air samples originating from the lower and middle tropical stratosphere was used to characterise the altitudinal distribution of 17 long-lived halocarbons in this region of the atmosphere. On the example of CF_2Cl_2 (F12) and $CFCl_3$ (F11) it was shown that tracer-tracer-correlations of long-lived halocarbons in the tropical stratosphere are different from those in mid- and high-latitudes. This characteristic behaviour agrees with findings of earlier studies which used distributions of other long-lived compounds such as CO_2 (carbon dioxide), CH_4 (methane) or N_2O (nitrous oxide) to investigate stratospheric transport (see e.g. Boering et al., 1994 or the review of Plumb et al., 2007). It is likely to be caused by the higher radiation levels in the tropical stratosphere and its isolation from other atmospheric regions due to existing transport barriers (see Chapter 1.1.2). A unique set of fit functions relative to CF_2Cl_2 (F12) was derived to approximate the observed correlations. As very few measurements of long-lived halocarbons exist in this atmospheric region the fit functions could serve as a useful tool for the parameterisation and evaluation of models.

Furthermore fractional release factors (FRFs) were derived from the observed mixing ratios and related to the mean age of air. The tropical FRFs were internally and externally compared with mid- and high-latitude FRFs. Characteristic differences were found for air masses which entered the stratosphere more than 0.5 to 2.5 years prior to sample collection (depending on the individual substance). The mid-latitude FRFs where found to increase significantly slower with mean age than tropical FRFs for 11 out of 15 long-lived halocarbons (F114a and F124 could not be compared). Moreover, FRFs averaged over an age-range were calculated relative to an average FRF of $CFCl_3$ (F11). They were compared with similarly averaged values originating from observations in the mid- and high-latitude stratospheric which are currently used by the World Meteorological Organization for the semi-empirical calculation of Ozone Depletion Potentials (ODPs). The values were in agreement though highly variable in the tropics for most substances. Therefore the ODPs calculated by the WMO can be considered as globally integrated, except for CF_2ClCF_2Cl (F114), CHF_2Cl (F22) and CH_3CF_2Cl (F142b) which should be reassessed and also for C_2F_5Cl (F115) for which no FRF is given by the WMO and CF_3CFCl_2 (F114a) which is not mentioned at all in the respective literature (Chapter 8 of WMO, 2007).

For the first time correlations of the FRFs of a set of 17 halocarbons were calculated as functions of the mean age of air for the lower and middle tropical stratosphere. These correlations can be considered as time-independent and are highly recommended for the parameterisation of models in order to reassess the chemical composition and the radiative balance in this region. Changes to these quantities could influence the Radiative Forcings and thus the Global Warming Potentials (GWPs) which are currently assigned to the corresponding halocarbons. As some of these substances significantly contribute to the anthropogenic greenhouse effect future climate predictions might also be affected.

5 Contribution of very short-lived organic substances to stratospheric chlorine and bromine in the tropics – a case study

5.1 Introduction and air sample origin

This chapter addresses one major aim of this thesis i.e. to quantify the amount of chlorine and bromine that reaches the stratosphere in its main entrance region: the Tropical Tropopause Layer (TTL). Due to the much higher ozone destruction efficiency of bromine compared to chlorine even very low mixing ratios of brominated substances of less than 0.1 part per trillion (ppt) are of importance for stratospheric ozone depletion (see Chapter 1.1.3). Especially the brominated very short-lived substances (VSLS) are suspected "to make a significant contribution to total stratospheric bromine and its effect on stratospheric ozone" (Law and Sturges, 2007).

The uncertainties in the amounts of VSLS reaching the stratosphere are due to the short atmospheric lifetimes of these substances (less than half a year) compared to tropospheric transport times which leads to a highly variable tropospheric distribution in time and space (Law and Sturges, 2007). Additionally there have been very few measurements in the TTL or above in the tropical lower stratosphere. Published observations of VSLS in the inner tropics above 15 km are presented in Schauffler et al. (1998 and 1999), Sinnhuber and Folkins (2006) and Law and Sturges (2007). Schauffler et al. (1998) performed measurements of nine brominated substances up to about 21 km while Sinnhuber and Folkins (2006) only used $CHBr_3$ (bromoform) data from three campaigns in 1996, 1999 and 2004 for comparison with models. Law and Sturges (2007) combined data at altitudes between 10 and 17.5 km originating from six measurement campaigns that were carried out within a period of eight years (1996 - 2004) to estimate the amount of chlorine and bromine from VSLS that is present in the tropical upper troposphere. Also several model studies were performed to quantify in particular the influence of brominated VSLS to ozone depletion (Dvortsov et al., 1999; Nielsen et al., 2001; Levine et al., 2007). Current estimates of the World Meteorological Organisation for the upper tropical troposphere range from 52 to 60 ppt for chlorine and 3.1 to

4.0 ppt for bromine from VSLS, but measurements show a much higher variability and uncertainty (see e.g. the data set presented in Law and Sturges, 2007).
The samples analysed for this chapter originated from flight B42 of the BONBON II whole-air-sampler launched with a balloon near Teresina, Brazil (5°04'S, 42°52'W) on 08 June 2005 (see Table 3.1.1). This flight was part of a campaign for the validation of the ENVISAT satellite. Between 15.2 and 34 km altitude 15 samples were collected by pumping air cryogenically into electropolished stainless steel cylinders (for details see Chapter 1.2.1 or Schmidt et al., 1987 and Engel et al., 1997). Three samples could not be analysed due to technical failure during sampling and one sample showed contamination from the balloon exhaust. No samples were available below 15 km for technical reasons. The results from this flight were chosen for a case study because the respective whole-air-sampler behaved best and could be characterised best with regard to the stability of long-lived and very short-lived halocarbon concentrations inside the sample containers (see Chapter 3.1.2).

5.2 Analytical procedure

The whole air samples were analysed in December 2005 using Gas Chromatography with Electron Impact Mass Spectrometric detection (GC-EI-MS; Siemens Si1 GC with Agilent 5975 MS) at the University of Frankfurt. Some substances were quantified by Dave R. Worton and William T. Sturges at and in cooperation with the University of East Anglia (UEA). The corresponding measurements were carried out in February 2006 using GC-Negative Ion Chemical Ionisation-MS (GC-NICI-MS; Agilent 6890/5973). Trace gases in the air samples were pre-concentrated on two bed adsorbent trap containing Carbograph-TD and Carboxen-1000 at -10 °C using a Peltier cooler and using about 2 litres of air. Separation took place on a Restek 502.2 capillary column. The MS was operated in NICI-SIM (Selected Ion Monitoring) mode monitoring ions with m/z 35, 37, 79 and 81 throughout the chromatogram. The Frankfurt analytical system provides high precisions and detection limits in the lower and sub-ppt range (see Chapter 2.1 for a detailed description). In EI mode the substances are broken into characteristic cations using a high energy electron beam. This often allows quantification even if several substances elute at the same time. The UEA system uses NICI - a very sensitive and substance-specific method to detect amounts of a few parts per quadrillion (ppq) of especially brominated organic substances (Buser, 1986). Bromine anions are formed via dissociative electron capture from thermal electrons provided by an ionised reactant gas (here: methane). The masses 79 and 81 in a ratio of 1:1 are typical for bromine in the atmosphere, consisting of a nearly 50:50 mixture of these two isotopes. Chlorine can also be detected in a similar way by measuring on the relevant chlorine masses. However, if substances coelute no quantification is possible with this method. The NICI detection also allows no certain identification of the detected compounds in the chromatogram and is based on the compounds retention times which must be known. A list of the quantified compounds including measurement places, source of calibration and detection limits can be found in Table 5.2.1.

Table 5.2.1. Measured compounds grouped by substance classes with source of calibration and detection limits.

Substance group	Formula (name)	Calibration source	Detection limit [ppt]
CFCs	CF_2ClCF_3 (F115)	UEA	0.4
	CF_2Cl_2 (F12)	NOAA-2001	0.3
	CF_2ClCF_2Cl (F114)	UEA	0.2
	$CFCl_2CF_3$ (F114a)	UEA	0.1
	$CFCl_3$ (F11)	NOAA-1993	0.1
	$CFCl_2CF_2Cl$ (F113)	NOAA-2002	0.1
Halons	CF_3Br (H1301)	NOAA-2006	0.4
	CF_2ClBr (H1211)	NOAA-2006	0.6
	CF_2BrCF_2Br (H2402)	UEA	0.2
	CF_2Br_2 (H1202)*	UEA	0.001
HCFCs	CHF_2Cl (F22)	NOAA-2006	0.5
	$CHFClCF_3$ (F124)	U. Miami	0.4
	CH_3CF_2Cl (F142b)	NOAA-1994	0.3
	CH_3CFCl_2 (F141b)	NOAA-1994	0.3
Longer-lived non-fluorinated chloro- and	CH_3Cl (methyl chloride)	NOAA-2003	19
	CCl_4 (carbon tetrachloride)	NOAA-2002	0.2
	CH_3CCl_3 (methyl chloroform)	NOAA-2003	0.3

Table 5.2.1 continued

Substance group	Formula (name)	Calibration source	Detection limit [ppt]
bromocarbons	CH_3Br (methyl bromide)	NOAA-2003	0.4
VSLS	CH_2Cl_2 (dichloromethane)	NOAA-1992	0.8
	$CHCl_3$ (chloroform)	NOAA-1992	0.4
	CH_2ClCH_2Cl (1,2-dichloroethane)	U. Miami	0.1
	C_2HCl_3 (trichloroethene)[b]	UEA	1.8
	C_2Cl_4 (tetrachloroethene)	UEA	0.7
	CH_2BrCl (chlorobromomethane)[*,b]	UEA	0.01
	$CHBrCl_2$ (dichlorobromomethane)[*,b]	UEA	0.006
	$CHBr_2Cl$ (chlorodibromomethane) [*,b]	UEA	0.003
	CH_2Br_2 (dibromomethane)[*,a]	UEA	0.004
	$CHBr_3$ (bromoform)[*,a,b]	UEA	0.007

*measured by D. R. Worton and W. T. Sturges at the University of East Anglia
a – identified after Dec 2005 on the Frankfurt analytical system
b – detection limits of the Frankfurt GC-EI-SIM-MS were below upper tropospheric abundances

5.3 Corrections, comparisons and air mass origin

5.3.1 Concentration drift correction

To assure the quality of the data, three cylinders were measured again in August 2007 at the University of Frankfurt (see also Chapter 3.1.2). The Chlorofluorocarbons (CFCs), Hydrochlorofluorocarbons (HCFCs) and Halons proved to be stable, whereas the CH_3Cl (methyl chloride), CH_2ClCH_2Cl (1,2-dichloroethane) and CCl_4 (tetrachloromethane) mixing ratios had changed systematically in the cylinders. A wall reaction follows the first-order rate law and, if it is slow, can be approximated as a linear process with respect to time. Assuming that such a process is responsible for the observed drift an increase of 0.73 % per month for CH_3Cl, of 2.90 % for CH_2ClCH_2Cl and a decrease of 1.57 % per month for CCl_4 was calculated relative to their initially measured values. The mixing ratios of both substances in the air samples were corrected by linear extrapolation of the calculated trends to the flight date. Four other substances – CH_2Cl_2 (dichloromethane), $CHCl_3$ (chloroform), C_2Cl_4 (tetrachloroethene) and CH_3Br (methyl bromide) – also showed concentration changes but these were non-systematic and/or did not occur in all reanalysed samples. For these substances the maximum extrapolated difference (at most ± 0.6 % per month) was added to the error bars as a systematic error. The substances measured at the UEA could not be rechecked except for the CH_2Br_2 (dibromomethane) content of one sample which was the same within the 1σ measurement uncertainties.

5.3.2 Intercomparison with ground-based observations

Most of the longer-lived compounds are measured regularly at remote sampling locations by the Global Monitoring Division (GMD) which belongs to the Earth System Research Laboratory (ESRL) of the National Oceanic Atmospheric Administration (NOAA), USA. Longer-lived trace gases show rather uniform concentrations in the global background and upper troposphere because their atmospheric lifetimes are high compared with the corresponding transport times. In order to check the quality of the measurements the mixing ratios in the sample collected at 15.2 km were compared with the globally averaged mixing ratios derived from NOAA-ESRL ground-based observations in June 2005 (these mixing ratios can be accessed under http://www.esrl.noaa.gov/gmd/). The measurements of CF_2Cl_2 (F12), $CFCl_3$ (F11), $CF_2ClCFCl_2$ (F113), CHF_2Cl (F22), CH_3CF_2Cl (F142b, CH_3CFCl_2 (F141b, CCl_4 (carbon tetrachloride), CH_3CCl_3 (methyl chloroform) and CF_2ClBr (H1211) agreed within 3 %. In combination with the observed VSLS mixing ratios (which were also not super-elevated, see below) this indicates that a well mixed air mass with little influence from local deep convection was sampled.

However, three of the longer-lived substances showed higher differences. The first is CF_3Br (H1301) which was found to be 8.8 % higher than the NOAA-ESRL reference but still within the 2σ measurement uncertainties. The second is CH_3Br (methyl bromide) which was 14.7 %

(1.14 ppt) lower than the NOAA-ESRL reference. This discrepancy could be caused by a decrease of mixing ratio with altitude in the troposphere as reported by Blake et al. (1997) but also by a decrease due to instability within this particular sample cylinder. The third substance showing a difference to NOAA-ESRL values was CH_3Cl (methyl chloride). 601 ppt of CH_3Cl were found at 15 km while the globally averaged mixing ratio from remote ground stations in June 2005 was 538 ppt. One possible explanation could be that the correction of the drift in the cylinders was insufficient. However, the South American tropical rainforest is reported to be a source region of CH_3Cl. Gebhardt et al. (2008) found levels around 600 ppt for CH_3Cl in air samples taken at altitudes around 10 km above Surinam in October 2005. As CH_3Cl is longer-lived in the atmosphere the observed elevated mixing ratio could originate from the rainforest without being influenced from local deep convection.

5.3.3 Air mass origin

Trajectories were calculated by Katja Grunow of the Free University Berlin (FUB) using a model (Langematz et al. 1987, Reimer and Kaupp, 1997) with a resolution of 1.25° x 1.25° and 59 potential temperature levels and operational ECMWF fields as meteorological input. In Figure 5.3.1 ten-day backward trajectories are shown.

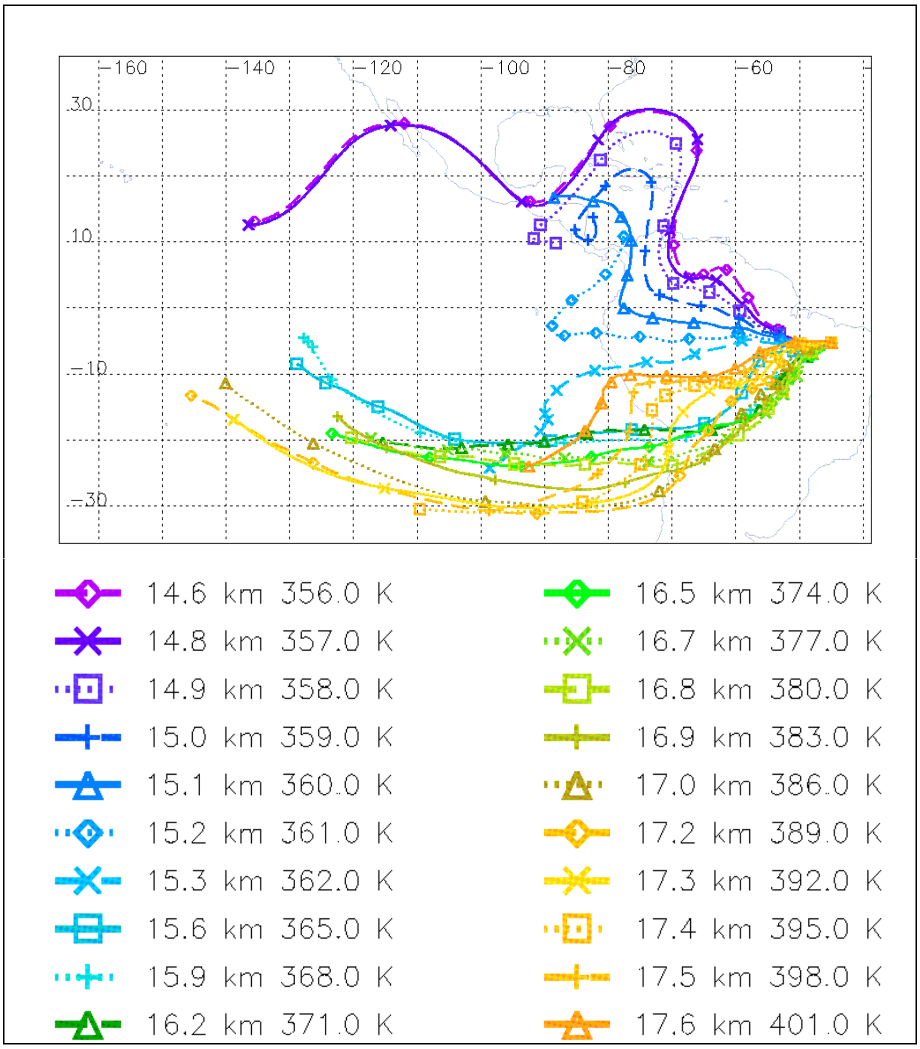

Figure 5.3.1. Ten-day backward trajectories as calculated by K. Grunow at the Free University of Berlin using a model with a resolution of 1.25° x 1.25° on 59 potential temperature levels. They were initialised at 5.28 °S and 44.99 °W within the TTL on 08 June 2005. The trajectories show, that the air around 15 km was coming from North-West while the air around 16.5 km was coming from South-West both travelling over the South American continent.

They were initialised at 5.28 °S and 44.99 °W which is the mean geographical location of the samples taken at 15.2 and 16.4 km altitude. The trajectories show, that the air around 15 km was most probably coming from North-West while the air around 16.5 km travelled over South-West South America. Other backward trajectories were initialised 2.5° north, east, south and west from this place and showed similar results. It is concluded that the air sampled in the TTL has most probably been influenced from air masses travelling over the South American continent which originated from both hemispheres.

5.4 Organic chlorine and bromine

During the balloon flight the cold-point tropopause was located at 16.8 km (385 K potential temperature). The two lowest samples were collected at 15.2 km (359 K) and 16.36 km (371 K) within the TTL. For all further discussions, the TTL definition given by Gettelman and Forster (2002) will be used. According to this definition the TTL extends from the minimum potential temperature lapse rate to the cold point. Air parcels reaching the level of zero radiative heating, which is located at 15 ± 0.5 km and 360 K, are expected to be transported to the stratosphere (Gettelman et al., 2004). Thus, it will be assumed that the signatures of both samples originating from the TTL are very likely to be injected into the stratosphere. However, since many processes influence the composition of the tropical region around 15 km (see e. g. Tuck et al., 2004) no global significance is claimed for the lowest altitude sample. On the other hand the air sampled at 16.4 km was located very close to the upper limit of the TTL and thus its chemical composition should be more representative for the inner tropics (Gettelman and Forster, 2002). The total halogen mixing ratios and the contribution of the source gas subgroups at the different altitudes are shown in Figure 5.4.1 for chlorine and 5.4.2 for bromine.

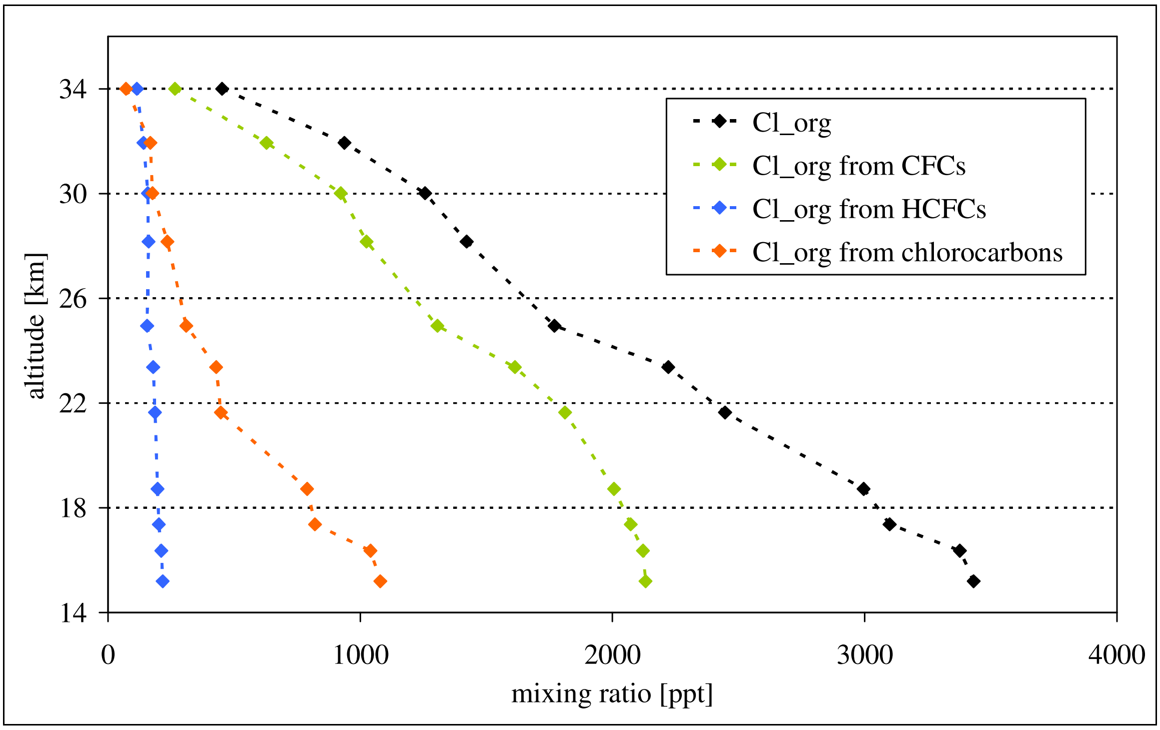

Figure 5.4.1. Total mixing ratios of chlorine from organic source gases (Cl_{org}) and contributions of substance subgroups to that total in the different altitudes. The data for chlorocarbons include VSLS and non-fluorinated longer-lived chlorocarbons (see Tables). Chlorine from H1211 is only included in the Cl_{org} values. The error bars are less than the size of the symbols and include the 1σ uncertainties of the measurements and the sample instability errors if observed.

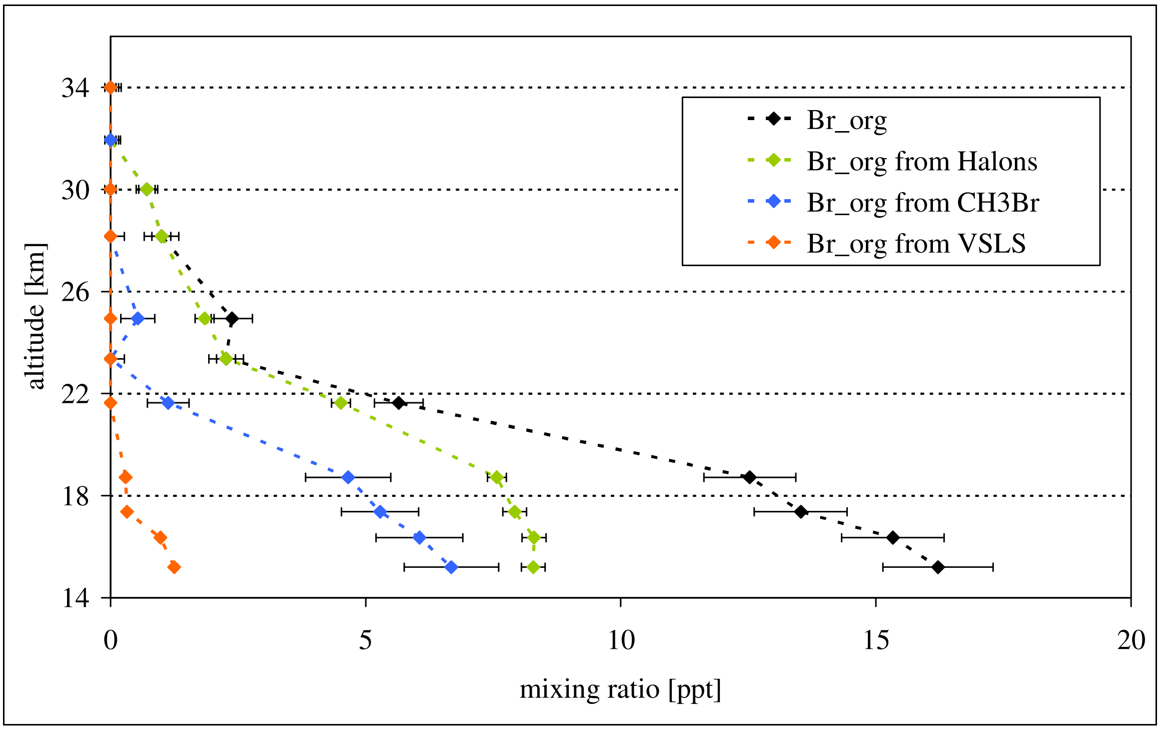

Figure 5.4.2. The same as Figure 5.4.1 but for bromine.

The error bars χ_{org} include the 1σ measurement uncertainties and the sample instability errors as calculated using equation (5.1) and weighting with the number of chlorine or bromine atoms contained in the respective substance.

$$\chi_{org} = \pm \left[\sum_i e_{si,i} + \sqrt{\sum_i (\sigma_{sm,i}^2 + \sigma_{ct,i}^2)} \right] \tag{5.1}$$

The sample instability errors e_{si} (if observed) are systematic errors. For that reason they were summed up separately. Due to the limited amount the samples where measured only twice. Thus σ_{sm} is the standard deviation of the calibration standard on the measuring day. As an internal secondary standard was used for the measurements σ_{ct} is the standard deviation from the calibration of that standard. As σ_{sm} and σ_{ct} are statistic errors the square root of the sum of the squares can be taken. Calibration uncertainties are not included in the error bars. Please note, that the samples at 28 and 32 km altitude could not be measured at the UEA due to insufficient amount of air remaining in the containers. Thus, the values for total organic bromine and chlorine in these samples do not include the mixing ratios of CF_2Br_2 (H1202),

CH_2BrCl (chlorobromomethane), $CHBrCl_2$ (dichlorobromomethane), CH_2Br_2 (dibromomethane), $CHBr_2Cl$ (chlorodibromomethane) and $CHBr_3$ (bromoform). Table 5.4.1 shows the total halogen mixing ratios corresponding to the values shown in Figure 5.4.1 and 5.4.2 and the altitude range, over which the air has been sampled during the slow descent of the balloon.

Table 5.4.1. The measured total organic halogen mixing ratios with 1σ measurement and sample instability uncertainties in ppt. All samples where collected during balloon descent and represent altitude ranges, while Θ is the potential temperature. Also shown are the derived inorganic mixing ratios in ppt (see next sub-chapter). Their errors include the measurement uncertainties as well as the uncertainties from NOAA-ESRL ground-based measurements.

Altitude [km]	Range [km]	Θ [K]	Cl_{org}	Cl_{org} error	Br_{org}	Br_{org} error	Cl_y	Cl_y error	Br_y	Br_y error
34.00	1.5	1036.7	452	10	0.0	0.2	3062	11	17.5	0.4
31.94*	1.1	907.8	937	12	0.0	0.2	2558	13	17.5	0.4
30.01	0.7	819.7	1257	12	0.7	0.2	2228	13	16.7	0.4
28.17*	0.5	751.1	1422	12	1.0	0.3	2063	14	16.4	0.5
24.95	0.7	636.5	1771	14	2.4	0.4	1703	15	15.0	0.6
23.37	0.9	577.8	2221	16	2.3	0.3	1244	18	15.0	0.5
21.64	0.6	521.2	2447	18	5.7	0.5	1008	19	11.6	0.6
18.72	0.4	437.7	2996	24	12.5	0.9	444	26	4.6	1.1
17.37	0.3	402.5	3099	22	13.5	0.9	340	24	3.6	1.1
16.36	0.6	371.1	3377	29	15.3	1.0	55.7	30	1.8	1.2
15.20	0.5	359.2	3431	30	16.2	1.1	-0.1	31	0.9	1.2

*Not measured at the University of East Anglia - several substances are not included (see Table 5.2.1).

Longer-lived halocarbon data from the flight are shown in Table 5.4.2 while in Table 5.4.3 the mixing ratios of the VSLS for the four lowest altitude samples can be found. C_2Cl_4 (tetrachloroethene, 1.02 ppt) and $CHBr_3$ (bromoform, 0.016 ppt) could only be detected in the sample collected at 15.2 km and are therefore not listed. $CHClBr_2$ (chlorodibromomethane) and C_2HCl_3 (trichloroethene) were below detection limit (see Table 5.2.1) for all samples. Also not shown are low mixing ratios of up to 2.7 ppt of CH_2Cl_2 (dichloromethane) which were detected in some samples collected at higher altitudes. As CH_2Cl_2 should be completely depleted at these altitudes non-systematic processes in the canisters are suggested as an explanation and these systematic blank values were included in the error calculation. For the other VSLS rather uniform canister and system blanks were found. These blanks were below 0.02 ppt for all species and the mixing ratios were corrected for them.

Table 5.4.2. Observed mixing ratios of CFCs, HCFCs and longer-lived non-fluorinated chloro- and bromocarbons in ppt (n. d. – not detected; n. m. – not measured). The mixing ratios of CH_3Cl *(methyl chloride) and* CCl_4 *(tetrachloromethane) were corrected for concentration changes in the sample canisters.* CF_2Br_2 *(H1202) was measured by D. R. Worton and W. T. Sturges at the University of East Anglia.*

	Altitude [km] / Mixing ratio [ppt]										
Substance	15.20	16.36	17.37	18.72	21.64	23.37	24.95	28.17	30.01	31.94	34.00
F12	538.7	537.8	530.4	523.8	492.8	465.8	435.5	375.0	353.4	252.1	103.9
F11	254.8	252.1	243.9	233.7	187.9	143.6	87.54	28.04	14.32	1.55	n. d.
F113	80.90	80.89	78.05	70.76	72.49	68.90	43.57	49.87	43.85	27.21	7.84
F114	16.65	16.66	16.58	16.36	16.39	16.12	15.06	15.5	15.35	14.92	13.28
F115	8.82	8.97	8.76	8.94	8.73	8.48	8.48	8.38	8.29	8.14	7.82
F114a	2.05	2.01	1.94	1.69	1.70	1.58	1.48	1.25	1.19	n. d.	n. d.
F22	164.0	160.3	152.6	151.1	142.2	138.6	125.1	130.5	130.8	121.2	102.9
F141b	18.05	17.35	16.65	15.01	14.62	13.17	8.76	8.73	7.45	3.98	0.87
F142b	15.27	15.04	14.39	14.31	13.66	13.18	11.69	12.14	12.02	11.26	9.65
F124	1.61	1.56	1.48	1.33	1.32	1.08	0.66	0.69	0.66	0.69	0.41
CH_3Cl	600.9	570.8	459.8	427.3	182.9	254.6	241.4	224.0	171.0	164.8	71.84
CCl_4	93.50	93.70	75.52	77.47	58.54	37.58	12.51	1.63	n. d.	n. d.	n. d.
CH_3CCl_3	19.22	19.50	18.08	16.11	9.96	7.98	4.82	n. d.	0.61	n. d.	n. d.
CH_3Br	6.68	6.05	5.28	4.66	1.13	n. d.	0.54	n. d.	n. d.	n. d.	n. d.
H1211	4.17	4.13	3.9	3.89	1.93	n. d.	n. d.	n. d.	n. d.	n. d.	n. d.
H1301	3.19	3.18	3.25	3.01	2.55	2.24	1.84	1.00	0.71	n. d.	n. d.
H2402	0.43	0.46	0.35	0.30	n. d.	n. d.	n. d.	n. d.	n. d.	n. d.	n. d.
H1202	0.034	0.035	0.029	0.031	0.018	0.010	0.002	n. m.	n. d.	n. m.	n. d.

Table 5.4.3. Observed mixing ratios of VSLS in ppt. C_2Cl_4 (tetrachloroethene, 1.0 ppt) and $CHBr_3$ (bromoform, 0.016 ppt) were only detected at 15.2 km and are not listed. $CHClBr_2$ (chlorodibromethane) and C_2HCl_3 (trichloroethene) were below detection limit (n. d. - not detected). The mixing ratios of CH_2ClCH_2Cl (1,2-dichloroethane) were corrected for concentration changes in the sample canisters. Five substances were measured by D. R. Worton and W. T. Sturges at the University of East Anglia ($CHBr_3$, $CHClBr_2$, CH_2BrCl, $CHBrCl_2$ and CH_2Br_2).

Altitude [km]	CH_2Cl_2 [ppt]	$CHCl_3$ [ppt]	CH_2ClCH_2Cl [ppt]	CH_2BrCl [ppt]	$CHBrCl_2$ [ppt]	CH_2Br_2 [ppt]
18.72	1.9	n. d.	n. d.	0.020	n. d.	0.139
17.37	2.3	n. d.	n. d.	0.030	n. d.	0.147
16.36	9.8	1.9	5.6	0.090	0.010	0.439
15.20	11.2	2.7	6.2	0.087	0.017	0.549

In the TTL at 15.2 km 3431 ± 30 ppt of chlorine from organic substances were found. About 62.1 % of the chlorine was present in the form of CFCs, while HCFCs contributed 6.3 %, longer-lived non-fluorinated chlorocarbons 30.1 % and CF_2ClBr (H1211) 0.1 %. Only 1.4 % (47.1 ± 5.7 ppt) of chlorine came from VSLS, whereby the main contribution was from CH_2Cl_2 (22.4 ± 1.8 ppt). The estimated tropical upper tropospheric mixing ratio in Table 2-2 of Law and Sturges (2007) is 55 ppt (range: 52 – 60 ppt) for total chlorine from VSLS including 1.5 ppt from C_2H_5Cl (chloroethane) which is the only source gas estimated by Law and Sturges (2007) that was not quantified in this thesis (see also Chapter 3.1.2). Taking this into account, Law and Sturges (2007) derived an average of 53.5 ppt (range: ~51 – 58 ppt) for the remaining chlorinated VSLS in the tropical upper troposphere. This agrees with the findings of this chapter within the given error bars. At 16.4 km 3377 ± 30 ppt of organic chlorine were found with 1.1 % (36.6 ± 5.1 ppt) from VSLS. As described above the air mass sampled is very likely to have been transported into the stratosphere because of its location above the level of zero radiative heating. Above the tropopause the total organic chlorine decreases with altitude due to conversion into inorganic species. At the highest flight altitude

(34 km) all short lived source gases were depleted to values below detection limits and the remaining organic chlorine was 452 ± 10 ppt. This corresponds to about 13% of the amount observed in the TTL.

Organic bromine at 15.2 km was 16.2 ± 1.1 ppt with 51 % present in the form of Halons, 41 % in the form of CH_3Br (methyl bromide) and 8 % (1.25 ± 0.08 ppt) originating from the five brominated VSLS listed in Table 5.4.3. In 16.4 km a fraction of bromine from VSLS of about 6 % (0.98 ± 0.08 ppt) was found. Both VSLS contributions are substantially lower than the global tropical upper tropospheric mixing ratio of 3.5 ppt (range: 3.1 – 4.0 ppt) estimated by Law and Sturges (2007). In particular CH_2Br_2 (dibromomethane) was found to be the dominant very short-lived brominated source gas at 15.2 km with a mixing ratio of 0.55 ± 0.001 ppt while the $CHBr_3$ (bromoform) mixing ratio was very low (0.016 ± 0.005 ppt) in this sample. Sinnhuber and Folkins (2006) presented higher $CHBr_3$ mixing ratios of up to about 0.2 ppt above 15 km in the tropics. This is not in contrast with the findings of this thesis as the VSLS have a high atmospheric variability. Moreover the mixing ratios agree with previous observations of Schauffler et al. (1998), who found about 0.5 ppt of CH_2Br_2 in the inner tropics at 15 km altitude while $CHBr_3$ was near or below detection limit. Also in agreement with Schauffler et al. (1998) CH_2Br_2 was observed up to 18.7 km. In common with chlorine, the organic bromine mixing ratio decreased with altitude in the stratosphere, but in contrast to chlorine no brominated organic substances were detected in both samples collected above 30 km.

5.5 Inorganic chlorine and bromine

Inorganic chlorine (Cl_y) and bromine (Br_y) are the sum of all inorganic chlorine and/or bromine containing substances in the stratosphere. These substances are directly involved in ozone depletion processes and mainly originate from the decomposition of the organic chlorinated and brominated compounds. Cl_y and Br_y can be calculated as the difference between the total amount of halogen which initially entered the stratosphere and the total measured halogen amount from organic substances. The stratospheric entry mixing ratio for each substance must be known for this calculation. As the air is ascending very slowly in the

TTL and above the entry mixing ratio needs to be corrected for tropospheric time trends and how the air masses are mixed on their transport upwards.

Here, a procedure for the calculation of the mean stratospheric entry mixing ratios described by Engel et al. (2002) is used. First for every sample the mean age of air was derived from mixing ratios of SF_6 which were measured by means of GC-ECD within the workgroup (T. Möbius, personal communication, 2006). The mean age of air is a measure of the stratospheric residence time of an air parcel. According to Hall and Plumb (1994) every stratospheric air parcel consists of a large number of irreversibly mixed parcels and its age can be described with a distribution function. The mean age of air is the centre of this function. As only the mean age can be calculated from SF_6 measurements a width parameterisation according to Engel et al. (2002) was used to derive the distribution function. Using this function and global tropospheric time trends the amount of trace gas that would be present without chemical degradation (i.e. the mean entrance mixing ratio) was calculated (similar to calculations in Chapter 4.3). Global tropospheric trend data was again taken from NOAA-ESRL (anonymous FTP data from http://www.esrl.noaa.gov/gmd/).

For substances without these trend functions available a simplified procedure was applied. First it was assumed that the sample from 15.2 km is reflecting the mean stratospheric entrance mixing ratio. For CH_3Cl (methyl chloride), CF_2BrCF_2Br (H2402) and the VSLS, which show no systematic or significant global trend, the observed mixing ratio in that sample was assumed as the stratospheric entry mixing ratio for all other samples.

The same assumption was made for C_2F_5Cl (F115), CF_2ClCF_2Cl (F114), CF_3CFCl_2 (F114a), CF_3CHFCl (F124) and CF_2Br_2 (H1202) but the mixing ratios of these substances were additionally corrected for their tropospheric trend to reconstruct the tropospheric time series backwards (extrapolated linear trend between 2003 and 2004 as reported in Table 1-2 of Clerbaux and Cunnold, 2007; AGAGE, in situ data was used except for H2402: UEA, flasks). The derived Cl_y and Br_y and the corresponding total chlorine and bromine from the entrance mixing ratios are depicted in Figure 5.5.1. Please note, that the contribution from a product gas injection as derived by Law and Sturges, 2007 (i.e. inorganic and/or organic decomposition products entering the stratosphere, 40 – 50 ppt of chlorine estimated) was not considered in the Cl_y calculation. For comparison with the measurements Cl_y and Br_y are also shown in Table 5.4.1.

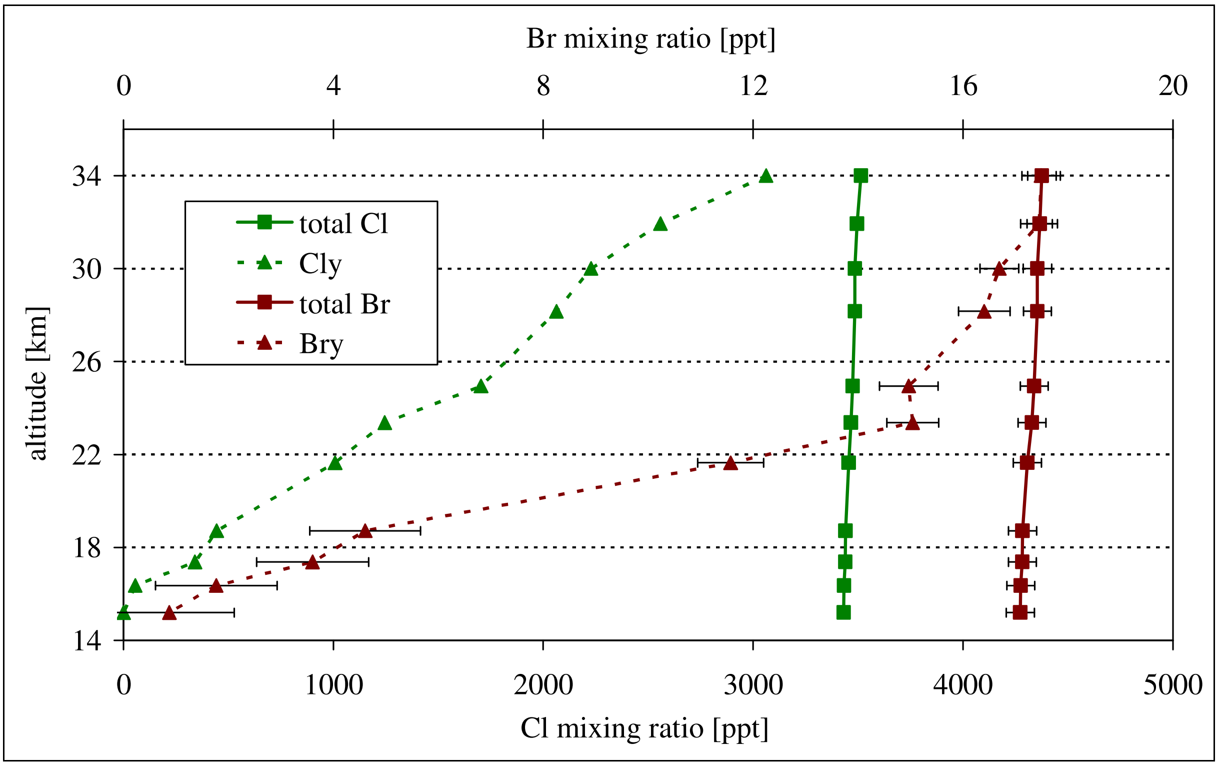

Figure 5.5.1. The derived inorganic chlorine (Cl_y) and bromine (Br_y) and the corresponding total Cl and Br for the different altitudes. The error bars are the same as in Table 5.4.1 and less than the size of the symbols for chlorine.

The error of the total chlorine/bromine χ_{total} was derived as the sum of the measurement uncertainties of CH_3Cl, F115, F114, F114a, F124, H1202, H2402 and the VSLS according to Eq. (5.1) and χ_{NOAA} – the standard deviations of the global mixing ratios for all other substances averaged over 2001 (the earliest year of mean stratospheric air entry) as provided by NOAA-ESRL. Both errors were calculated with respect to the number of chlorine/bromine atoms. The error of the inorganic chlorine/bromine χ_y is the sum of χ_{org} and χ_{NOAA}. Please note that the influence of the measurements on Cl_y, Br_y and the corresponding error bars decreases with altitude. Changes in Cl_y/Br_y due to mean age of air calculations carried out with SF_6 mixing ratios ± 2σ of the measured values were also calculated and ranged from -6 to +2 ppt for Cl_y and from -0.03 to +0.03 ppt for Br_y. In addition, changes of Cl_y/Br_y originating from different width parameterisations of the age distribution function were estimated. The respective Cl_y changes ranged from -8 to +7 ppt while Br_y varied between -0.04 and +0.12 ppt. It is concluded that both uncertainties have little influence on the derived Cl_y/Br_y.

The derived Cl_y at 15.2 km is zero within the error bars (-0.1 ± 31 ppt) and proves the good agreement with most global tropospheric mixing ratio observations by NOAA-ESRL. Notable is the sharp increase to 340 ± 24 ppt just above the tropopause, which is mostly caused by the rapid decomposition of the non-fluorinated chlorocarbons.

For Br_y low mixing ratios of 1.8 ± 1.2 ppt at 16.4 km and 3.6 ± 1.1 ppt at 17.4 km were inferred. At 34 km, where all organic bromine is destroyed 17.5 ± 0.4 ppt of Br_y were derived based on the organic bromine from ground-based NOAA observations and measurements on the air sample collected in the TTL. During another balloon flight on the 17 June 2005 BrO (i.e. the major inorganic bromine gas in the stratosphere during daylight, see e.g. Lary, 1996) was measured by the University of Heidelberg using Differential Optical Absorption Spectroscopy (DOAS). By using a photochemical model and correcting for the BrO/Br_y ratio they derived 21.5 ± 2.5 ppt of Br_y at 33 km (Dorf, 2005, Dorf et al., 2008). Thus, both calculations differ by 4.0 ppt but the significant uncertainty range of that difference (± 2.9 ppt) should be noted. Such differences were also found in earlier studies (e. g. Salawitch et al., 2005; Feng et al., 2006, Law and Sturges, 2007) and a number of causes could account for it. The observations and calculations presented here are mainly based on the NOAA calibration scale. For instance, the other large global monitoring network AGAGE found 0.72 ppt higher bromine from H1211 and H1301 in 2004 (see Table 1-2 in Clerbaux and Cunnold, 2007) probably reflecting differences in absolute calibration scales (see also Chapter 3.3). This could explain a part of the difference in the derived Br_y values. Another possibility is that the observed TTL region did not represent global VSLS mean entrance mixing ratios to the stratosphere. An injection of higher amounts of source gases at different seasons, latitudes or longitudes due to the local influence of convection might have lead to higher Br_y (see e. g. Levine et al., 2007). Especially bromoform was found to be higher in other studies (Sinnhuber and Folkins, 2006; Law and Sturges, 2007). One could assume that the 3.5 ppt of bromine from VSLS in the upper tropical troposphere as estimated by Law and Sturges (2007) are more representative for air entering the stratosphere. Using this VSLS amount the calculated Br_y would be 19.75 ppt which agrees with the 21.5 ± 2.5 ppt derived from BrO (Dorf, 2005, Dorf et al., 2008) even without deriving error bars.

A direct product gas injection as proposed by Ko et al. (1997) could also cause the difference in Br_y by bringing inorganic bromine species contained in the upper tropospheric aerosol (Murphy and Thompson, 2000) or in gaseous form into the stratosphere. Another option is the presence of additional brominated organic substances. As shown in Figure 5.5.2 the UEA has found substances showing signals at ions with m/z 79 and 81 (the two stable isotopes of bromine) in the NICI chromatogram of the sample taken at 15.2 km altitude.

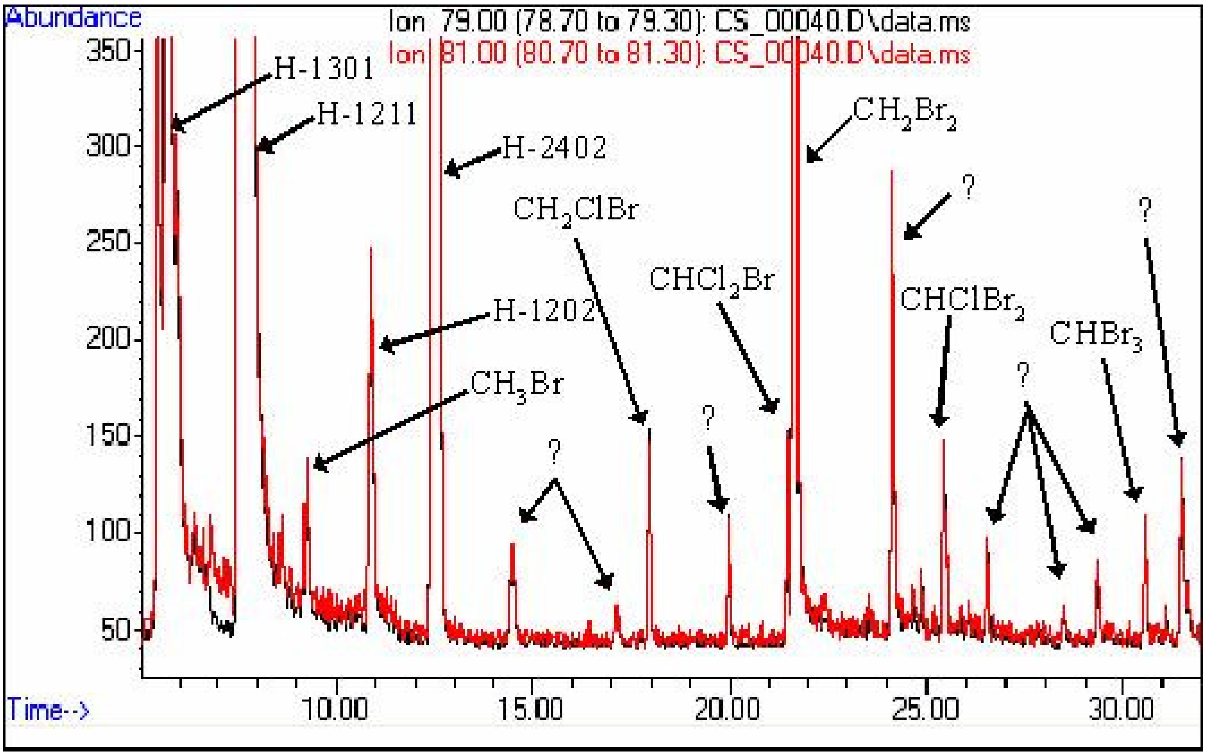

Figure 5.5.2. The chromatogram of the air sample collected at 15.2 km altitude as analysed with GC-NICI-MS by D. R. Worton and W. T. Sturges at the University of East Anglia (taken from Laube et al., 2008). The displayed ions with a mass/charge ratio of 79 and 81 in a ratio of 1:1 are specific for bromine containing species which indicates that at least eight additional brominated substances are present in the tropical tropopause region. The peaks at about 14.5, 17, 20 and 26.5 minutes retention time are suggested to belong to C_2H_5Br (bromoethane), $CF_3CHClBr$ (halothane), C_3H_7Br (n-propyl bromide) and CH_2BrCH_2Br (1,2-dibromoethane) but at least four further unidentified brominated compounds remain.

They suggest four of these signals to belong to C_2H_5Br (bromoethane), $CF_3CHClBr$ (halothane), C_3H_7Br (n-propyl bromide) and CH_2BrCH_2Br (1,2-dibromoethane) but at least four further unidentified signals remain. Please note, that in NICI mode the size of a peak is not indicative for its concentration. For instance, in Figure 5.5.2 CH_3Br (methyl bromide) appears as a small peak, but is more abundant than CF_2ClBr (H1211). Some of the peaks were also present in samples taken at higher altitudes. These are strong indications for a further contribution from organic source gases to stratospheric bromine.

5.6 Conclusions

This study adds to the very few available measurement-based data on VSLS in the tropical upper troposphere and lower stratosphere. From measurements of 28 chloro- and bromocarbons including ten very short-lived substances a VSLS contribution of 6 – 8 % (0.98 – 1.25 ppt) to total organic bromine and 1.1 – 1.4 % (36.6 – 47.1 ppt) to total organic chlorine entering the stratosphere above Brazil in June 2005 was derived in cooperation with the University of East Anglia (UEA). In addition the UEA found strong indications for the presence of additional bromine source gases in this region. Identification and quantification of these substances is crucial for future estimates of stratospheric bromine. Cl_y and Br_y values based on ground-based observations from NOAA-ESRL and the Frankfurt/UEA measurements were derived. Br_y was calculated to be 17.5 ± 0.4 ppt in 34 km altitude which is in disagreement with Br_y derived from quasi-simultaneous observations of BrO (Dorf, 2005, Dorf et al., 2008). An additional source of stratospheric bromine is a likely explanation in order to reconcile Br_y derived from organic substances with Br_y derived from the measurements of BrO. However, if calibration uncertainties and the atmospheric variability of VSLS are taken into account the derived Br_y values could agree within their error bars. Further studies with higher spatial and temporal coverage and also a wider range of substances are needed to quantify the global influence of very short-lived brominated and chlorinated organic substances on stratospheric ozone. Differences in absolute calibration scales need to be resolved.

6 First atmospheric observations of three chlorofluorocarbons

6.1 Introduction

Due to the finding of the UEA, that unknown brominated organic substances are present in the global background atmosphere (see previous chapter, e.g. Figure 5.5.2) an attempt was made to identify such substances in tropospheric air. For this purpose air samples were taken at the Institute's observatory in the Taunus Mountains near Frankfurt (Main) and checked for unknown brominated organic compounds. No such substances could be detected but one air sample contained high amounts of Chlorofluorocarbons that were previously unknown in the atmosphere. The subsequent investigations are discussed in this chapter.

Only seven Chlorofluorocarbons (CFCs) had been observed in the atmosphere before (e.g. Clerbaux and Cunnold, 2007). These CFCs have rather long atmospheric lifetimes of more than 40 years. Five of them – CF_2Cl_2 (F12), $CFCl_3$ (F11), CF_2ClCF_2Cl (F114), CF_3CFCl_2 (F114a) and $CF_2ClCFCl_2$ (F113) – are decreasing in the global background atmosphere due to their regulation under the Montreal Protocol on Substances that Deplete the Ozone Layer (see Table 1.2 of Clerbaux and Cunnold, 2007 for details). The only exception is C_2F_5Cl (F115) which was recently reported to have stabilised in concentration (Reimann et al., 2007). For CF_3Cl (CFC-13) there is no up-to-date trend data available. This is due to its very long atmospheric lifetime. Here, the first atmospheric observations of three CFCs are reported. The newly observed substances contain a double bond and are thus expected to have short atmospheric lifetimes relative to tropospheric transport times (i.e. below half a year). Considerable amounts of such short-lived substances are able to reach the stratosphere. Law and Sturges (2007) estimated about 55 ppt (range: 52 – 60 ppt) of chlorine from ten short-lived substances to be present in the main stratospheric entrance region, the tropical upper troposphere. Thus, although their ozone depletion potential might be small, the newly observed short-lived CFCs are potential contributors to stratospheric chlorine. But none of them is covered by the Montreal Protocol.

6.2 Analytical procedure

Air samples were taken at the Taunus Observatory at the Kleiner Feldberg (50°13'29.6" N, 8°26'28.7" E) near Frankfurt (Main), Germany between October and December 2007. Stainless steel and also silanized stainless steel canisters were used for sampling. The canisters were tested prior to use and none of them showed a blank signal in any CFC. The canisters were evacuated using a turbo pump which was also checked to be free of CFCs. They were filled by simply opening them in order to avoid effects from a compressor or a drying agent. A CFC-free and preconditioned stainless steel sampling line was used to avoid breath contaminations. Samples were not dried before measuring and no pressure regulator was used. The calibration standard was measured with and without attached pressure regulator. No significant concentration difference in any CFC was observed proving that the pressure regulator did not gas out these substances. For analysis trace gases out of 500 - 1000 ml of air were pre-concentrated (using the 10 litre reference container) and the MS was run in electron impact selected ion monitoring (EI-SIM) or EI-Scan mode. As shown in Chapter 2 (Figure 2.2.3) the chromatographic system separates substances primary via boiling points covering a range from -90 to 150 °C. MS detection limits were below 1 ppt for almost every halocarbon and below 0.3 ppt for the six measurable CFCs (except F13; ECD detection limits of the six CFCs were below 0.1 ppt). Different blanks were carried out by injecting vacuum or pre-concentrating carrier and make-up gas but none of the detectors showed a blank signal in any CFC.

6.3 Identification of the substances in a plume

On the 02 October 2007 an air sample was taken at the Taunus Observatory. During analysis using the system described above the ECD showed a number of additional signals with a high abundance. Figure 6.3.1 shows the zoom of the ECD chromatogram in comparison with an unpolluted air sample. Several large signals occurred in addition to the known peaks belonging to CF_2Cl_2 [F12, (1)], CF_2ClBr/CF_2ClCF_2Cl [H1211/F114, coeluting, (2)], $CFCl_3$

[F11, (3)], $CF_2ClCFCl_2$ [F113, (4)] and CCl_4 (5). This was a strong indication towards halocarbons as the ECD is very sensitive towards these substances. The MS was first operated in EI-SIM mode measuring only a few ions at a time to achieve enhanced detection limits.

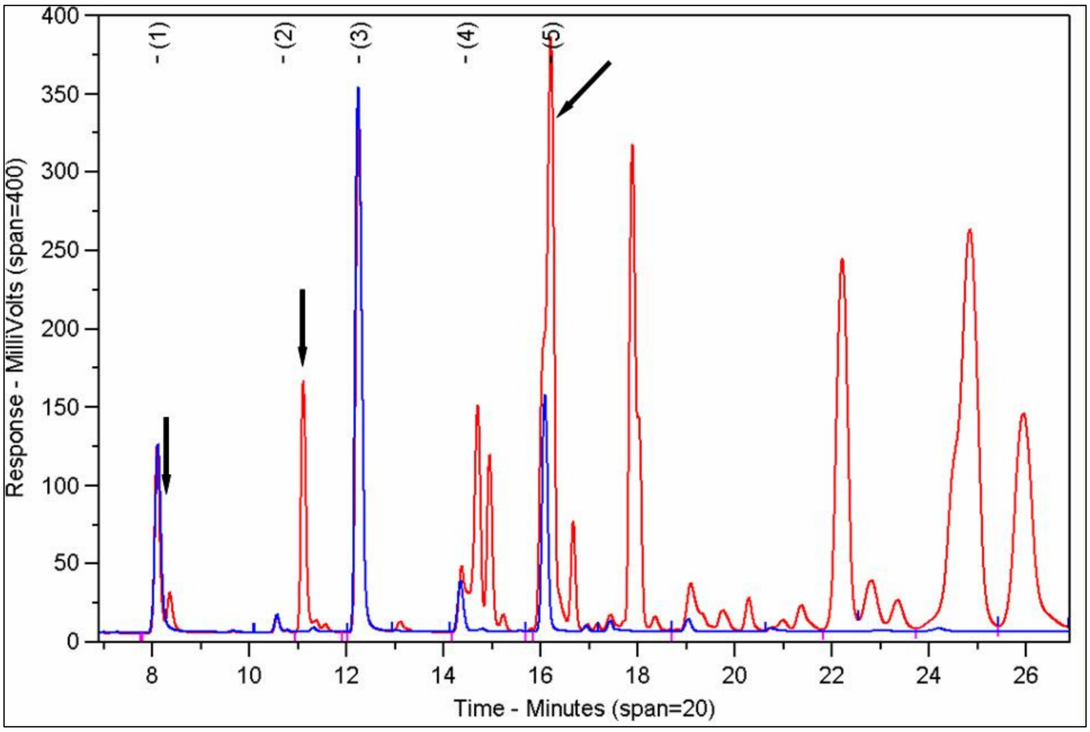

Figure 6.3.1. Comparison of the chromatograms from two air samples taken at the Taunus Observatory operated by the University of Frankfurt. Trace gases were concentrated cryogenically from one litre of air and detected using an ECD. The blue line represents unpolluted air while the red line is the plume sample taken on the 02 October 2007 which showed a number of unidentified large signals. The known large peaks are CF_2Cl_2 *[F12, (1)],* CF_2ClBr/CF_2ClCF_2Cl *[H1211/F114, coeluting, (2)],* $CFCl_3$ *[F11, (3)],* $CF_2ClCFCl_2$ *[F113, (4)] and* CCl_4 *(5). Three of the unknown substances could be identified by now and are labelled with black arrows: trifluorochloroethene at 8.4 minutes, 3-chloropentafluoropropene at 11.1 minutes and 4,4-dichlorohexafluoro-1-butene at 16.2 minutes.*

To identify the unknown signals the sample was measured again, this time pre-concentrating about one litre of air and operating the MS in EI-Scan mode scanning all mass fragments from 15 to 300 atomic mass units (amu). Figure 6.3.2 shows the mass spectrum at 8.4 minutes retention time.

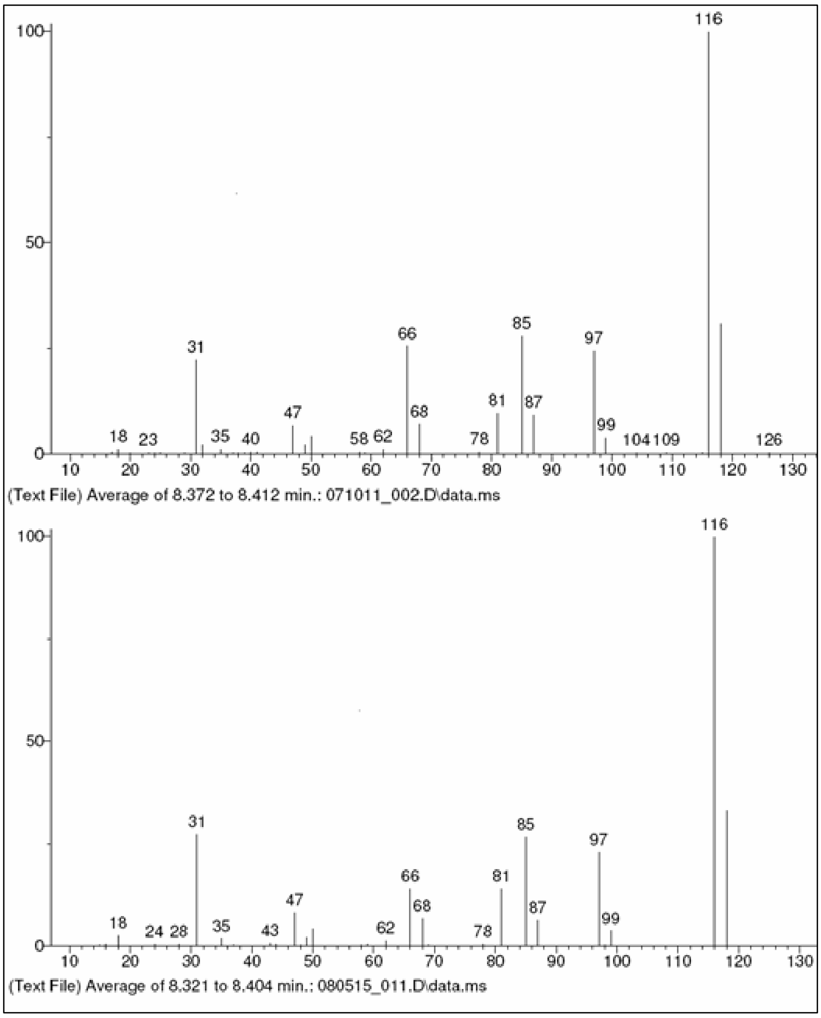

Figure 6.3.2. The upper mass spectrum belongs to a chromatogram of an air sample taken at the Taunus Observatory near Frankfurt. The background spectrum was subtracted in order to remove peaks originating from air entering the system through small leaks and from the decaying signals of CO_2 which elutes at about 4 minutes. Trace gases were concentrated cryogenically from 1 litre of air and measured by means of GC-MS (EI-Scan mode).The averaged spectrum at about 8.4 minutes retention time belongs to a substance eluting near CF_2Cl_2 (F12) and gave a 97 % probability match with that of chlorotrifluoroethene (C_2F_3Cl) as listed in the NIST mass spectral library. Expected relative abundances for C_2F_3Cl were 100 % for mass/charge ratio (m/z) 116, 87 % for m/z 31, 38 % for m/z 66, 33 % for m/z 85, 33 % for m/z 118, 31 % for m/z 97, 26 % for m/z 47, 17 % for m/z 81, 13 % for m/z 68 and 11 % for m/z 87. The lower mass spectrum is that of C_2F_3Cl (purity: 98 %) as obtained from Sigma-Aldrich Corporation which was subsequently diluted to ppb levels with ultra-pure Nitrogen (from Air Liquide Deutschland GmbH, purity ≥ 99.999 %-mol) and measured on the same instrument under similar conditions.

The background was subtracted in order to remove peaks originating from air entering the system through small leaks (within the operating parameters recommended by Agilent Technologies) but also from CO_2 which elutes at about 4 minutes and still showed significantly larger signals on its main fragment (m/z 44) at 8 minutes than all other present ions. The result of a search in the NIST mass spectral library (see reference) gave a 97 % probability match with C_2F_3Cl (chlorotrifluoroethene). In addition, the second best matching substance had a probability of less than 1 %. All important mass fragments were found to be present. The expected relative abundances differed slightly in some cases, which could be caused by the above mentioned interferences from the atmospheric matrix of the air sample but also by the limited mass resolution of the MS and its reduced sensitivity in the lower m/z range. The substance eluted just after F12 which had a retention time of 8.1 minutes. As the chromatographic system separates primary via boiling points this substance should have a boiling point of about -20 °C. C_2F_3Cl boils at -28.4°C. Moreover the pure compound could be obtained from Sigma-Aldrich Corporation (purity: 98%) in 2008. It was statically diluted to ppb levels with ultra-pure Nitrogen (from Air Liquide Deutschland GmbH, purity $\geq$ 99.999 %-mol). The subsequent MS-Scan measurements confirmed the identity of the substance by giving a similar mass spectrum at the same retention time which is also shown in Figure 6.3.2. These measurements also confirmed the above mentioned reduced sensitivity of the MS for ions with lower m/z ratio.

The mass spectra at 11.1 and 16.2 minutes retention time gave 99 % probability matches with the NIST library spectra of CF_2CFCF_2Cl (3-chloropentafluoropropene) and $CF_2CFCF_2CFCl_2$ (4,4-dichlorohexafluoro-1-butene) and the comparisons of spectra are depicted in Figures 6.3.3 and 6.3.4. The respective second best matches were both below 1 % probability. Both substances boiling points also fitted very well with their retention times. 3-chloropentafluoropropene boils at 8°C and eluted 0.45 minutes after CF_3CFCl_2 (F114a) which boils at 3 °C. For 4,4-dichlorohexafluoro-1-butene boiling points between 67 and 71 °C have been reported (source: Beilstein Crossfire database) and it coeluted with CCl_4 which boils at 77 °C. CF_2CFCF_2Cl and $CF_2CFCF_2CFCl_2$ could not be obtained as pure compounds by now. But taking into account the agreement between boiling points and mass spectra the identification of the substances is considered as certain.

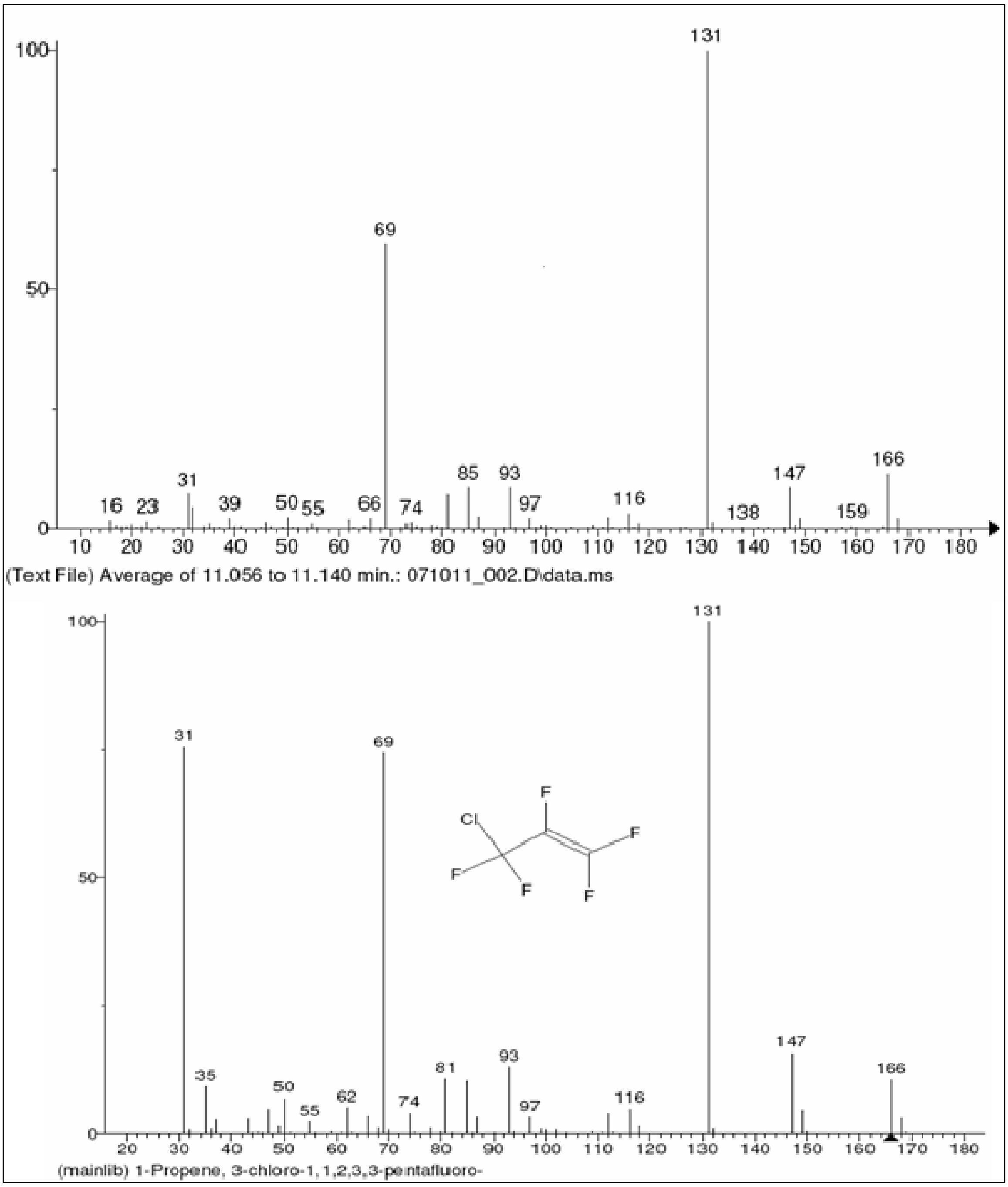

Figure 6.3.3. The same as in Figure 6.3.2 but for CF_2CFCF_2Cl *(3-chloropentafluoropropene) at 11.1 minutes retention time and the lower spectrum belonging to the NIST library spectra. No pure compound could be obtained in this case but the match probability given by NIST was 99 % and the boiling point (8°C) fits well because the substance eluted 0.45 minutes after* CF_3CFCl_2 *(F114a) which boils at 3 °C.*

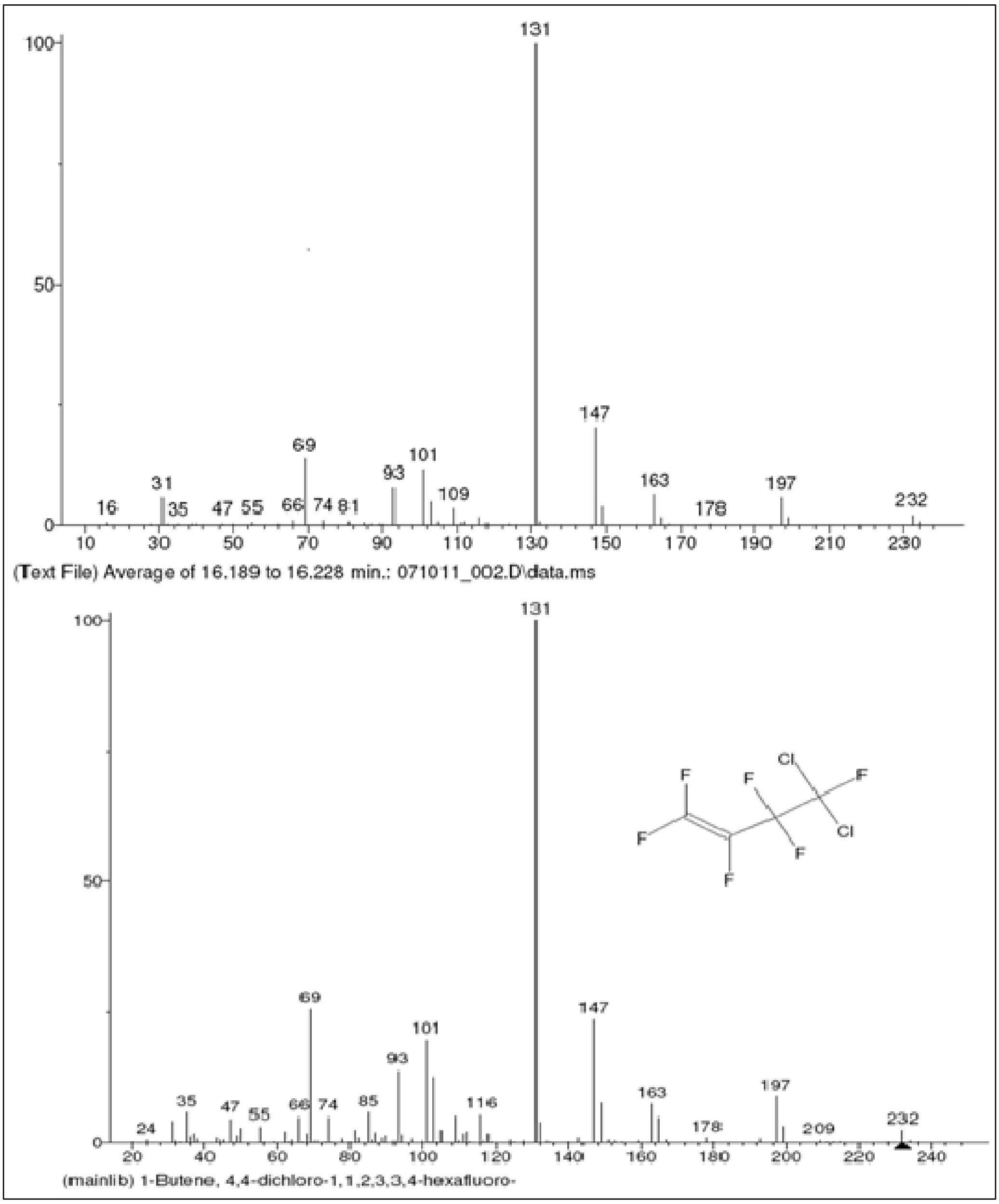

Figure 6.3.4. The same as in Figure 6.3.2 but for $CF_2CFCF_2CFCl_2$ (4,4-dichlorohexafluoro-1-butene) at 16.2 minutes retention time and the lower spectrum belonging to the NIST library spectra. No pure compound could be obtained in this case but the match probability given by NIST was 99 % and the reported boiling points (67 and 71 °C) fit well because the substance coeluted with CCl_4 which boils at 77 °C.

None of the three substances has been reported in the atmosphere before. All other unknown signals are likely to be caused by halocarbons, too (see below). However, they could not be identified yet due to the fact that comparison with the library gave no exact match. Possible explanations are the coelution of two or more substances or simply missing reference mass spectra.

6.4 Mixing ratio estimates, calibration and air mass origin

As in 2007 no calibration was available for the identified substances a method for a minimum and maximum concentration estimate was derived. Laube and Engel (2008) inferred the sensitivity relative to F12 for six different halocarbons: $CFCl_3$ (F11) on m/z 103, $CF_2ClCFCl_2$ (F113) on m/z 151, CHF_2Cl (F22) on m/z 67, CF_2ClBr (H1211) on m/z 129, CH_3Br on m/z 94 and $CHCl_3$ on m/z 83. This method was improved by using an expanded data set from measurements of four different calibration standards on 20 measuring days over a period of two years in order to achieve a better reflection of the MS sensitivity range. Moreover, C_2Cl_4 (on m/z 166) data was included as a seventh substance, because it is chemically very similar to the new substances (fully halogenated and double bond contained). The MS sensitivities to the substances (s_i) were calculated according to equation (6.1).

$$s_i = h_i / (a * \rho_i) \tag{6.1}$$

$$S_i = s_i / s_{F12} \tag{6.2}$$

The signal height h of the substance i is divided by the sample amount a and the substance mixing ratio ρ_i. The relative sensitivity S_i is then given by division of s_i with s_{F12} (Eq. 6.2). Values of S_i were between 0.04 and 1.20. To consider the fact that only one mass fragment was used for the quantification of a substance a fragmentation correction factor according to equation (6.3) was introduced.

$$f_i = r_q / \sum_{j=1}^{j=10} r_j \tag{6.3}$$

$$C_i = S_i / f_i \tag{6.4}$$

This factor f_i is given by r_q - the relative abundance of the mass fragment used to quantify the substance - divided by the sum of the relative abundances r_j of all major mass fragments.

Only fragments with an abundance of more than 10% relative to the main fragment were used and 10 fragments included at most. The corrected relative sensitivity C_i is then given by the relative sensitivity S_i divided by the fragmentation factor f_i (Eq. 6.4). Derived values for C_i ranged from 0.20 to 3.41. Subsequently minimum and maximum mixing ratios for the newly observed CFCs via the F12 mixing ratio of the sample were calculated. The derived mixing ratio ranges were 1.1 – 18.4 ppb for C_2F_3Cl, 0.5 – 8.8 ppb for CF_2CFCF_2Cl and 0.6 – 9.2 ppb for $CF_2CFCF_2CFCl_2$ in the plume observed on 02 October 2007. As mentioned above C_2F_3Cl could be obtained later and was diluted to ppb levels (lowest dilution: 4.5 ppb) in order to calibrate the measurements. The calculated plume sample mixing ratio was 9.8 ppb which is in agreement with the estimate above.

Trichlorofluoroethene is also known as R-1113 and is toxic. Cook and Pierce (1973) reported an LC_{50} (i.e. the concentration which kills 50% of a sample population) of 1000 ppm and its ERPG-3 (i.e. the maximum airborne concentration below which individuals could be exposed for up to 1 hour without life-threatening health effects) is 300 ppm (source: http://cameochemicals.noaa.gov). Like most fluoroalkenes 3-chloropentafluoropropene and an isomer of dichlorohexafluorobutene are also reported to be highly toxic (Thun and Kimbrough, 1981, Clayton, 1977). Considering the fact that C_2F_3Cl carries a double bound and is highly flammable its atmospheric lifetime is expected to be very short. Similar halocarbons which contain a double bond such as C_2Cl_4 (tetrachloroethene) or C_2HCl_3 (trichloroethene) have lifetimes in the range of days to months (Keene et al., 1999, Ko and Poulet et al., 2003). Thus it is suggested that the observed plume originated from a local source which is supported by the low wind speed (~ 1m/s) on the sampling day. However, concentrations close to the source could have been much higher – especially if that source was located indoors. Other large unknown signals were observed, which are likely to be chlorofluoroalkenes due the occurrence of characteristic fragments like m/z 147 and 149 or m/z 197 and 199. Both pairs showed an abundance ratio of 3:1 which is – in combination with the high ECD sensitivity – an indication towards the $C_2F_4Cl^+$ and the $C_3F_6Cl^+$ fragments. Thus it can not be ruled out that the sum of the chlorofluoroalkenes could have reached concentrations which affect human health. On the Kleiner Feldberg six days backward trajectories on different pressure levels are calculated regularly by the German Weather Service (DWD), Offenbach, Germany with the DWD-GME model. They showed that air masses had been advected from the southwest sector with rather low wind speed probably originating from the densely populated Rhein-Main area.

6.5 Subsequent observations

Six more air samples were collected at the Taunus Observatory and one at the High Altitude Research Station Jungfraujoch (Switzerland) and subsequently measured by running the MS in SIM mode while monitoring C_2F_3Cl on m/z 116 for quantification and 118 for confirmation, CF_2CFCF_2Cl on m/z 131 (q) and 166 (c) and $CF_2CFCF_2CFCl_2$ on m/z 147 (q) and 131 (c). The substances were present all the time except for the sample taken directly (but still using the sampling line) at the exhaust of the observatories air conditioning system which was free of short-lived CFCs. An indoor sample taken at the institute contained no C_2F_3Cl and no CF_2CFCF_2Cl but a very small amount of $CF_2CFCF_2CFCl_2$. The estimated mixing ratios for the six outdoor samples were in the lower ppt range and can be found in Table 6.5.1.

Table 6.5.1. Wind data and mixing ratio estimates of the novel detected CFCs for different air samples taken at the Taunus Observatory. In case of C_2F_3Cl the pure compound could be obtained and thus a calibration was possible. The corresponding error bars are an estimate of the sum of all errors from preparation of the calibration standards but also include the measurement standard deviations. All derived C_2F_3Cl mixing ratios did agree with the estimated range from the relative sensitivity method.

Date 2007	Wind speed 1h mean [m/s]	Wind Direction	Mixing ratio C_2F_3Cl [ppt]	Estimated mixing ratio range [ppt]		
				C_2F_3Cl	C_3F_5Cl	$C_4F_6Cl_2$
02 Oct	1	NW	9800 ± 1800	1100 – 18400	530 – 8800	550 – 9200
06 Nov	6	NW	0.34 ± 0.09	0.2 – 3.3	0.2 – 3.0	0.1 – 1.2
21 Nov	4	S	0.41 ± 0.10	0.2 – 3.6	0.1 – 1.4	0.1 – 1.1
05 Dec	5	SW	0.93 ± 0.23	0.4 – 7.1	0.4 – 6.7	0.1 – 2.3
12 Dec*	~10	NE	0.11 ± 0.03	0.1 – 1.5	0.2 – 1.2	0.1 – 1.0
21 Dec	5	SE	0.23 ± 0.06	0.1 – 2.0	0.1 – 1.7	0.1 – 1.2

*sample taken at the Jungfraujoch High Altitude Research Station (Switzerland)

The estimated mixing ratios for the six outdoor samples were in the lower and sub-ppt range and can be found in Table 6.5.1. The corresponding MS signals were reintegrated compared to Laube and Engel (2008) by using an improved version of the integration software. These samples were also used to evaluate the relative sensitivity method. Mixing ratio ranges were predicted for five calibrated compounds. The calibration-derived mixing ratios of CF_2ClCF_2Cl (F114) on m/z 135, C_2F_5Cl (F115) on m/z 85, CCl_4 on m/z 117 and CH_3Cl on m/z 50 were found to agree with the estimated ranges from the relative sensitivity method for all seven air samples. In case of C_2F_3Cl a subsequent calibration was carried out and all calculated mixing ratios also agreed with the estimated ranges, which is shown in Table 6.5.1. Thus, the relative sensitivity method can be considered as a useful tool to provide first indications of halocarbon mixing ratios in air samples.

Due to the few data no correlation with wind speed or wind direction could be observed. All three short-lived CFCs were also present at the Jungfraujoch though it can not be ruled out that they were emitted from the station itself. Several calibration standards were also checked for the presence of these substances. All of them contained low amounts of the CFCs and two even showed contaminations with C_2F_3Cl probably originating from the pressure regulator or the cylinder valve. The properties of C_2F_3Cl are very similar to those of F12 (boiling points and several main fragments such as m/z 31, 35, 50, 66, 85 and 87). Thus, coelution is very likely to occur in other chromatographic systems. Contaminations could cause falsified calculations of F12 mixing ratios if an ECD or MS is used for detection.

The observed substances are very likely connected with chlorofluoro(co)polymers – particularly polychlorotrifluoroethene (PCTFE, tradenames are Kel-F, Neoflon or Aclar). PCTFE was first commercialized in 1934 by Hoechst (Utracki, 1995) and is still widely used in equipment manufacturing because of its excellent thermoplastic properties, chemical resistance and good impermeability to gases and vapours (Abusleme and Manzoni, 2004). The main precursor for PCTFE production is chlorotrifluoroethene. Birnbaum et al. (1968) studied the toxicity of the pyrolysis of PCTFE and found it to increase rapidly with rising temperature. The thermal degradation of PCTFE and copolymers of it were studied by Zulfiqar et al. (1994) who found the monomer (i.e. chlorotrifluoroethene) to be the major product and amongst others chloropentafluoropropene in traces. Long et al. (1984) carried out infrared multiphoton dissociation experiments and found the toxic substances COF_2, COFCl, and CF_2ClCOF to be the exclusive products in the presence of oxygen. The MS scan chromatogram of the plume sample was checked but none of these product gases could be detected. The microbial biodegradation of $CF_2ClCFCl_2$ (F113) and $CHClFCClF_2$ (F123a) are also possible sources of chlorotrifluoroethene. A detailed overview on that topic was given by Field and Sierra-Alvarez in 2004. But as 3-chloropentafluoropropene and dichlorohexafluorobutenes are also used for the production of copolymers (e.g. Robb et al., 1962, Lo et al., 1959) it is suggested, that the observed high abundances were generated by the thermal degradation of a fluoropolymer blend.

6.6 Conclusions

It was shown that chlorotrifluoroethene, 3-chloropentafluoropropene and 4,4-dichlorohexafluoro-1-butene are present in the atmosphere. The substances were identified through comparison of their mass spectra with the NIST library and their retention times were in agreement with the expectation based on the boiling point. Moreover, other substances were observed which are suspected to be chlorofluoroalkenes, too. But these compounds could not be identified up to now. The identified CFCs showed high mixing ratios in the lower ppb range in a plume but the substances were also observed to be present in background ambient air with mixing ratios in the lower and sub-ppt range. These CFCs are not listed in the Scientific Assessment of Ozone Depletion 2006 of the World Meteorological Organisation/United Nations Environment Programme (WMO/UNEP) (see Table 1-4 of Clerbaux and Cunnold, 2007) or the Montreal Protocol and its subsequent amendments. The substances are most probable of anthropogenic origin. But although their contribution to ozone depletion can be expected to be rather small it is important to find out more about their sinks and sources and their ability to reach the stratosphere. Furthermore all known CFCs are strong greenhouse gases. Thus it is suggested to establish continuous measurements of these substances and to investigate their atmospheric lifetimes in order to assess their possible influence on the global background atmosphere. Considering human health it is also important to find out if plumes containing high amounts of the CFCs can occur again – outdoor as well as indoor.

7 Summary and outlook

The aim of this thesis was to investigate distributions of 32 volatile chlorinated and/or brominated halocarbons that are currently believed to be present in the tropical upper troposphere and stratosphere and to contribute to stratospheric ozone depletion and also to global warming. For this purpose an analytical system was established, which is capable to measure ultra-low concentrated atmospheric trace gases. A quadrupole Mass Spectrometric (MS) Detector was attached to an existing Gas Chromatograph with pre-concentration system and Electron Capture Detector (ECD). The characterisation of the chromatographic system was significantly enhanced by the subsequent identification of 48 additional volatile organic compounds. Furthermore a Gaussian fit algorithm, which was developed in the workgroup, was applied to the chromatographic signals. This algorithm was proven to reflect peaks quantitatively and to enhance the performance of the integration process – especially the reproducibilities for peaks with a low signal to noise ratio. As it is known that the Electron Capture Detector responds nonlinear the new MS detector was checked for such behaviour and found to respond linear. In logical consistency the complete quantification process including e.g. pre-concentration of trace gases and signal integration can be considered as linear responding within the investigated parameter ranges.

Moreover, the long term stability of the targeted halocarbons was proven inside the calibration standard containers over a period of 25 months. Many substances were also found to be stable inside the containers used for storage of air samples but a number of substances showed significant concentration changes. These were mainly CH_3Cl (methyl chloride), CH_3Br (methyl bromide), CH_2Cl_2 (dichloromethane), $CHCl_3$ (chloroform), CCl_4 (tetrachloromethane), C_2Cl_4 (tetrachloroethene), CH_3CCl_3 (methyl chloroform), CH_2ClCH_2Cl (1,2-dichloroethane) und C_2H_5Cl (chloroethane). But the number of affected substances and also the corresponding concentration changes varied between the individual containers. A systematic investigation of the influence of possible causes (e.g. air sampling methods, container materials) is recommended. Results from both internal detectors were compared and revealed biases and disadvantages of the ECD caused by its lower selectivity and its non-linear response behaviour. Consequently the MS detector was chosen for the quantification of atmospheric trace gases.

The quantification process was performed relative to externally calibrated air standards. To assess the uncertainties connected with different absolute calibration scales cross-comparisons between calibration standards of three different laboratories were carried out. Most substances' calibrations agreed within the measurement uncertainties but significant differences were observed for CF_2ClBr (H1211), CH_3Cl (methyl chloride), CH_2Cl_2 (dichloromethane), $CHCl_3$ (chloroform), CCl_4 (tetrachloromethane) and CH_3CCl_3 (methyl chloroform). As five of these substances were also observed to show concentration changes inside sample containers it is likely, that such changes are responsible for calibration differences.

In addition to the detailed assessment of uncertainties connected with the analytical quantification process a set of air samples was available for measurements. These samples mainly originated from the upper troposphere and lower and middle stratosphere in the tropics and the determined halocarbon quantities were used to investigate their distributions in the respective atmospheric regions.

In detail, the altitudinal distributions and interrelations of 17 long-lived halocarbons in the tropical stratosphere were determined and compared with those of other stratospheric regions. Tracer-tracer-correlations of these substances in the tropical stratosphere were found to differ from those in mid- and high-latitudes. Characteristic fit functions relative to CF_2Cl_2 (F12) which are valid for the tropical stratosphere in 2005 were derived as well as time-independent fit functions of fractional release factors (FRFs) relative to the mean age of air. Both sets of correlations could be used for the parameterisation and evaluation of models and also to reassess the Global Warming Potentials (GWPs) of the corresponding halocarbons which might affect future climate predictions. However, the data set on halocarbons in the tropical stratosphere is still insufficient to investigate the variability of tracer-tracer-correlations and FRFs caused by dynamical and photochemical processes. Therefore it is important for future research to perform additional measurements there and – if possible – to extend the measurements to the upper tropical stratosphere in order to characterise the sink of those halocarbons that are still present in these altitudes.

In addition, the amount of chlorine and bromine present in the form of organic compounds inside and above the main stratospheric entrance region (the Tropical Tropopause Layer, TTL) was quantified in the frame of a case study. This was possible because of a cooperation with scientists from the University of East Anglia which carried out measurements of six additional halocarbons leading to a total of 28 quantified target substances. Ten of these substances have short atmospheric lifetimes compared with the mean transport times of tropospheric air to the stratosphere (i.e. lifetimes below 0.5 years) and show non-uniform distributions in the upper troposphere. The contribution of these substances to stratospheric ozone depletion is subject of an ongoing scientific debate. In the performed case study a fraction range of short-lived halocarbons of 6 – 8 % (0.98 – 1.25 ppt) relative to the sum of bromine from organic substances and of 1.1 – 1.4 % (36.6 – 47.1 ppt) for the corresponding sum of chlorine was calculated to enter the stratosphere above Brazil in June 2005. Moreover by combining the data with tropospheric reference data and age of air observations the abundances of inorganic chlorine and bromine (Cl_y and Br_y) were derived. At an altitude of 34 km an amount of 3062 ppt of Cl_y and 17.5 ppt of Br_y from organic source gases was calculated. The latter is significantly lower than Br_y mixing ratios inferred from quasi-simultaneous BrO measurements at 33 km altitude above Brazil (Dorf, 2005, Dorf et al., 2008). But at the University of East Anglia indications for the presence of unknown brominated organic substances in the TTL were found which might cause this difference.

Finally, a major result of this thesis adds to the knowledge of the composition of the troposphere as three Chlorofluorocarbons (CFCs) were first observed. Trifluorochloroethene, 3-chloropentafluoropropene and 4,4-dichlorohexafluoro-1-butene were found in air samples collected at the Taunus Observatory near Frankfurt (Main) and the Jungfraujoch High Altitude Research Station in Switzerland (Laube and Engel, 2008). Identification was possible because of an air plume containing high concentrations of these substances. It is suggested that the abundances found on this occasion originated from a local source. The atmospheric lifetimes of these substances are expected to be rather short as they contain a double bond. A quantitative calibration could only be derived for trifluorochloroethene but not for the other species by now. Thus, a relative sensitivity method was derived to get a first indication of the observed atmospheric abundances. All three CFCs could also be detected in air masses representative of background conditions, though with much lower concentrations.

These species and some of their degradation products are toxic and could also be relevant for stratospheric and tropospheric ozone depletion. It is important to find out more about their atmospheric distributions, lifetimes, sinks and sources and their ability to reach the stratosphere to assess their possible influence on the global atmosphere. This will be done in the frame of the project “CLEARFOGG – Checking Layers of the Earths AtmospheRe For halogenated Ozone-depleting and Greenhouse Gases". This research project aims to perform a systematic scan of the atmosphere because there are indications for the presence of a number of halogenated organic compounds which are unknown by now. It was recently decided to be funded by the British National Environmental Research Council and will be carried out at the University of East Anglia mainly by the author of this thesis.

Publications

Papers

Laube, J. C., Braß, M., Röckmann, T., Worton, D. R., Sturges, W. T., Levin, I., Bönisch, H., Möbius, T. and Engel, A., Fractional release factors of long-lived halogenated substances in the tropical stratosphere, ***manuscript in preparation***

Laube, J. C., Engel, A., Bönisch, H., Möbius, T., Worton, D. R., Sturges, W. T., Grunow, K. and Schmidt, U., Contribution of very short-lived organic substances to stratospheric chlorine and bromine in the tropics – a case study, Atmos. Chem. Phys. Discuss., 8, 8491–8515, 2008 www.atmos-chem-phys-discuss.net/8/8491/2008/

Laube, J. C. and Engel, A., First atmospheric observations of three chlorofluorocarbons, Atmos. Chem. Phys., 8, 5143–5149, 2008, www.atmos-chem-phys.net/8/5143/2008/

Conference talks

Laube, J. C., Werner, A. and Engel, A., First atmospheric observations of C_2F_3Cl and C_3F_5Cl by means of GC/ECD/MS, DPG conference, Darmstadt, Germany, 10 – 14 March 2008

Laube, J. C., Engel, A., Boenisch, H., Möbius, T., Dorf, M., Pfeilsticker, K., Worton, D. R., Sturges, W. T., and Schmidt, U., Comparison of the stratospheric chlorine and bromine loading in tropic and mid-latitudes derived from balloon-borne observations, EGU General Assembly, Vienna, Austria, April 2007

Conference posters

Laube, J. C., Engel, A., Bönisch, H., Möbius, T., Worton, D. R. and Sturges, W. T., The impact of very short-lived organic substances on stratospheric ozone depletion - A case study, SPARC General Assembly, Bologna, August 31-September 5, 2008

References

Abusleme, J. A. and Manzoni, C., Synthesis of thermoplastic perhalogenated (co)polymers of chlorotrifluoroethylene, European Patent, EP1067146, 2004

Andreae, M.O., and Merlet, P., Emission of trace gases and aerosols from biomass burning, Global Biogeochem. Cycles, 15 (4), 955-966, 2001

Apel, E. C., Calvert, J. G. and Fehsenfeld, F. C., The Nonmethane Hydrocarbon Intercomparison Experiment (NOMHICE): Tasks 1 and 2, J. Geophys. Res., 99, 16651-16664, 1994

Apel, E. C., Calvert, J. G., Greenberg, J. P., Riemer, D., Zika, R., Kleindienst, T. E., Lonneman, B. A., Fung, K. and Fujita, E., Generation and validation of oxygenated volatile organic carbon standards for the 1995 Southern Oxidants Study Nashville Intensive, J. Geophys. Res., 103, 22,281-22,294, 1998

Avallone, L. M., and Prather, M. J., Tracer-tracer correlations: Three-dimensional model simulations and comparisons to observations, J. Geophys. Res., 102, 19,233-19,246, 1997

Birnbaum, H. A., Scheel, L. D., and Coleman, W. E., The toxicology of the pyrolysis products of polychlorotrifluoroethylene, Am. Ind. Hyg. Assoc. J., 29, 61-65, 1968

Blake, D. R., Smith, Jr., T. W., Chen, T.-Y., Whipple, W. J. and Rowland, F. S., Effects of Biomass Burning on Summertime Nonmethane Hydrocarbon Concentrations in the Canadian Wetlands, J. Geophys. Res., 99, 1699-1719, 1994

Blake, N. J., Blake, D. R., Chen, T. Y., Collins, J. E., Sachse, G. W., Anderson, B. E. and Rowland, F. S., Distribution and seasonality of selected hydrocarbons and halocarbons over the Western Pacific basin during PEM-West A and PEM-West B, J. Geophys. Res., 102, 28315-28331, 1997

Bönisch, H., Untersuchung des Transports in der untersten Stratosphäre anhand von in-situ Messungen langlebiger Spurengase, Dissertation, Johann Wolfgang Goethe-Universität Frankfurt, 2006

Boering, K. A., Daube Jr., B.C., Wofsy, S.C., Loewenstein, M., Podolske, J. R. and Keim, E.R., Tracer-tracer relationships and lower stratospheric dynamics: CO_2 and N_2O correlations during SPADE, Geophys. Res. Lett., 21, 2567-2570, 1994.

Brasseur, G. and Solomon, S., Aeronomy of the middle atmosphere, 2nd edition, Kluwer Academic Publishers Group, Dordrecht, Holland, 1986

Brewer, A. W., Evidence for a world circulation provided by the measurements of helium and water vapour distribution in the stratosphere, Q. J. R. Meteorol. Soc., 75, 351-363, 1949

Buser, H. R., Selective detection of brominated aromatic compounds using Gas Chromatography/Negative Chemical Ionization Mass Spectrometry, Anal. Chem., 58, 2913, 1986

Butler, J. H., Wallace, D. W. R., Carpenter, L. J., Hall, B., Montzka, S. A., Quack, B., Atlas, E., Smythe-Wright, D. and Yvon-Lewis, S., A need for intercalibration of atmospheric and oceanic measurements of short-lived halocarbons, Poster, EGU General Assembly 2007, Vienna, Austria, 2007

Cammann, K., Instrumentelle Analytische Chemie: Verfahren, Anwendungen und Qualitätssicherung, Heidelberg; Berlin: Spektrum, Akad. Verl., 2001

Chapman, S., On ozone and atomic oxygen in the upper atmosphere, Philos. Mag., 10, 369–383, 1930

Clayton, J. W., Toxicology of the fluoroalkenes: review and research needs, Environ. Health Persp., 21, 255-267, 1977

Clerbaux, C. and Cunnold, D. M., et al., Halogenated Long-lived Compounds, Scientific assessment of ozone depletion: 2006, Global Ozone Research and Monitoring Project – Report No. 50, Chapter 1, World Meteorological Organization, Geneva, 2007

Cook, E. W. and Pierce, J. S., Toxicology of fluoro-olefins, Nature, 242, 337-338, doi:10.1038/242337a0, 1973

Daniel, J.S., Solomon, S. and Albritton, D.L., On the evaluation of halocarbon radiative forcing and global warming potentials, J. Geophys. Res., 100, 1271-1285, 1995

Dobson, G. M. B., Harrison, D. and Lawrences, J., Measurements of the amount of ozone in the earth's atmosphere and its relation to other geophysical conditions, Proc. Roy. Soc. London, A, 456-486, 1929

Dorf, M., Investigation of inorganic stratospheric bromine using balloon-borne DOAS measurements and model simulations, Dissertation, University of Heidelberg, Germany, 2005

Dorf, M. Butz, A., Camy-Peyret, C. Chipperfield, M. P., Kritten, L. and Pfeilsticker, K., Bromine in the tropical troposphere and stratosphere as derived from balloon-borne BrO observations, Atmos. Chem. Phys. Discuss., 8, 12999–13015, 2008, www.atmos-chem-phys-discuss.net/8/12999/2008/

Dvortsov, V. L., Geller, M. A., Solomon, S., Schauffler, S. M., Atlas, E. L. and Blake, D. R., Rethinking reactive halogen budgets in the midlatitude lower stratosphere, Geophys. Res. Lett., 26(12), 1699-1702, 1999

Dyson, N. A., Chromatographic Integration Methods, 2nd edition, Royal Society of Chemistry, ISBN:0854045104, 1998

Engel, A., Untersuchungen zur Vertikalverteilung von Carbonylsulfid (COS) in der Stratosphäre, Dissertation, Rheinisch-Westfälische Technische Hochschule Aachen, 1993

Engel, A., Schmidt, U. and Stachnik, R. A., Partitioning between chlorine reservoir species deduced from observations in the Arctic winter stratosphere, J. Atm. Chem, 27, 107-126, 1997

Engel A., Strunk, M., Müller, M., Haase, H.-P., Poss, C., Levin, I. and Schmidt, U., Temporal development of total chlorine in the high-latitude stratosphere based on reference distributions of mean age derived from CO2 and SF6, J. Geophys. Res., 107(D12), 4136, doi:10.1029/2001JD000584, 2002

Engel, A., Bönisch, H., Brunner, D., Fischer, H., Franke, H., Günther, G., Gurk, C., Hegglin, M., Hoor, P., Königstedt, R., Krebsbach, M., Maser, R., Parchatka, U., Peter, T., Schell, D., Schiller, C., Schmidt, U., Spelten, N., Szabo, T., Weers, U., Wernli, H., Wetter, T. and Wirth, V., Highly resolved observations of trace gases in the lowermost stratosphere und upper troposphere from the Spurt project: an overview, Atmos. Chem. Phys, 283-301, 2006

ESPERE Climate Encyclopaedia – English full version 2004 – 2006, URL of all PDF versions: http://espere.mpch-mainz.mpg.de/documents/pdf/, English offline version supported by the International Max Planck Research School on Atmospheric Chemistry and Physics

Feng, W., Chipperfield, M. P., Dorf, M., Pfeilsticker, K. and Ricaud, P., Mid-latitude ozone changes: studies with a 3-D CTM forced by ERA-40 analyses, Atmos. Chem. Phys., 7, 2357-2369, 2007

Field, J. A. and Sierra-Alvarez, R., Biodegradability of chlorinated solvents and related chlorinated aliphatic compounds, Reviews in Environmental Science & Bio/Technology, 3, 185–254, doi:10.1007/s11157-004-4733-8, 2004

Finlayson-Pitts, B. J. and Pitts, J. N. Jr., Chemistry of the Upper and Lower Atmosphere – Theory, Experiments and Applications; Academic Press, San Diego, CA, USA and London, United Kingdom, 2000

Gebhardt, S., Colomb, A., Hofmann, R., Williams, J. and Lelieveld, J., Halogenated organic species over the tropical rainforest, Atmos. Chem. Phys. Discuss., 8, 1159–1190, 2008 http://www.atmos-chem-phys-discuss.net/8/1159/2008/

Gettelman, A. and de F. Forster, P. M., A climatology of the tropical tropopause layer, J. Meteorol. Soc. Jpn., 80(4B), 911– 924, 2002

Gettelman, A., de F. Forster, P. M., Fujiwara, M., Fu, Q., Voemel, H., Gohar, L. K., Johanson, C. and Ammerman, M., Radiation balance of the tropical tropopause layer, J. Geophys. Res., 109, D07103, doi:10.1029/2003JD004190, 2004

Goldan, P. D., Kuster, W. C., Albritton, D. L. and Schmeltkopf, A. L., Stratospheric $CFCl_3$, CF_2Cl_2, and N_2O height profile measurements at several latitudes, J. Geophys. Res., 85, 413–423, 1980

Grooß, J.-U., et al., Simulation of ozone depletion in spring 2000 with the Chemical Lagrangian Model of the Stratosphere (CLaMS), J. Geophys. Res., 107(D20), 8295, doi:10.1029/2001JD000456, 2002

Hall, T. M. and Plumb, R. A., Age as a diagnostic of stratospheric transport, J. Geophys. Res., 99, 1059–1070, 1994

Highwood, E. J. and Hoskins, B. J., The tropical tropopause, Q. J. R. Meteorol. Soc., 124(549), 1579– 1604, 1998

Holton, J. R., On the global exchange of mass between the stratosphere and the troposphere, J. Atmos. Sci., 47, 392-395, 1990

Holton, J. R., Haynes, P. H., McIntyre, M. E., Douglass, A. R., Rood, R. B. and Pfister, L., Stratosphere-troposphere exchange, Rev. Geophys., 33, 403–439, 1995

Hoor, P., Fischer, H., Lange, L., Lelieveld, J. and Brunner, D., Seasonal Variations of a mixing layer in the lowermost stratosphere as identified by the CO-O_3 correlation from in-situ measurements, J. Geophys. Res., 107, 2002

IPCC, 2007: Forster, P., V. Ramaswamy, P. Artaxo, T. Berntsen, R. Betts, D.W. Fahey, J. Haywood, J. Lean, D.C. Lowe, G. Myhre, J. Nganga, R. Prinn, G. Raga, M. Schulz and R. Van Dorland: Changes in Atmospheric Constituents and in Radiative Forcing. In: Climate Change 2007: The Physical Science Basis. Contribution of Working Group I to the Fourth Assessment Report of the Intergovernmental Panel on Climate Change, Cambridge University Press, Cambridge, United Kingdom and New York, NY, USA, 2007

Ivanova, E., Evaluation of transport and ozone loss in the Antarctic polar vortex by using tracer-based coordinates, PhD thesis, Johann Wolfgang Goethe Universitaet, Frankfurt am Main, 2007

Kaiser, J., Engel, A., Borchers, R. and Röckmann, T., Probing stratospheric transport and chemistry with new balloon and aircraft observations of the meridional and vertical N2O isotope distribution, Atmos. Chem. Phys., 6, 3535–3556, 2006

Keene, W.C., Khalil, M.A.K., Erickson, D.J. III, McCulloch, A., Graedel, T.E., Lobert, J.M., Aucott, M.L., Gong, S.L., Harper, D.B., Kleiman, G., Midgley, P., Moore, R.M., Seuzaret, C., Sturges, W.T., Benkovitz, C.M., Koropalov, V., Barrie, L.A. and Li, Y.F., Composite global emissions of reactive chlorine from anthropogenic and natural sources: Reactive Chlorine Emissions Inventory, J. Geophys. Res., 104 (D7), 8429-8440, 1999

Kellner, R. A., Mermet, J.-M., Otto, M., Valcarcel, M. and Widmer, H. M., Analytical Chemistry – A Modern Approach to Analytical Science, Second Edition, WILEY-VCH, Weinheim, 2004

Kida, H., General Circulation of Air Parcels and Transport Characteristics Derived from a Hemispheric GCM, Part 2, Very Long-Term Motions of Air Parcels in the Troposphere and Stratosphere, J. Meteorol. Soc. Jpn., 61, 510-522, 1983.

Ko, M. K. W., Sze, N. D., Scott, C. J. and Weisenstein, D. K., On the relation between stratospheric chlorine/bromine loading and short-lived tropospheric source gases, J. Geopyhs. Res. 102(D21), 25,507–25,518, 1997

Ko, M. K. W., and Poulet, G., et al., Very short-lived halogen and sulphur substances, Chapter 2 in Scientific Assessment of Ozone Depletion: 2002, Global Ozone Research and Monitoring Project–Report No. 47, World Meteorological Organization, Geneva, Switzerland, 2003

Langematz, U., Labitzke, K. and Reimer, E., Synoptic analysis and trajectories during the MAP/GLOBUS campaign 1983, Planetary and Space Science, 35(5), 525-538, doi:10.1016/0032-0633(87)90120-6, 1987

Lary, D. J., Gas phase atmospheric bromine chemistry, J. Geophys. Res., Vol. 101, 1505–1516, 1996

Laube, J. C. and Engel, A., First atmospheric observations of three chlorofluorocarbons, Atmos. Chem. Phys. Discuss., 8, 6683–6695, 2008

Laube, J. C., Engel, A., Bönisch, H., Möbius, T., Worton, D. R., Sturges, W. T., Grunow, K. and Schmidt, U., Contribution of very short-lived organic substances to stratospheric chlorine and bromine in the tropics – a case study, Atmos. Chem. Phys. Discuss., 8, 8491–8515, 2008

Law, K. S. and Sturges, W. T., et al., Halogenated very short-lived substances, Scientific assessment of ozone depletion: 2006, Global Ozone Research and Monitoring Project – Report No. 50, Chapter 2, World Meteorological Organization, Geneva, 2007

Lee, J. M., Determination of stratospheric lifetimes of HCFCs and other halogenated hydrocarbons from balloon-borne profile measurements, PhD thesis, University of East Anglia, Norwich, United Kingdom, 1994

Levine, J. G., Braesicke, P., Harris, N. R. P., Savage, N. H. and Pyle, J. A., Pathways and timescales for troposphere-to-stratosphere transport via the tropical tropopause layer and their relevance for very short lived substances, J. Geophys. Res., 112, D04308, doi:10.1029/2005JD006940, 2007

Lo, E. S., Elizabeth, N. J., Copolymers of dichlorohexafluorobutene, US-Patent, 2914514, 1959

Long, G. R., Prentice, L. D., and Bialkowski, S. E., Chemical reactions following the IRMPD of C2F3Cl, Appl. Phys. B, 34, 97-106, doi:10.1007/BF00697955, 1984

Maludzinska, G., Dictionary of Analytical Chemistry, Amsterdam: Elsevier Science Publishers, 1990

McCulloch, A., and Midgley, P. M., The history of methyl chloroform emissions: 1951-2000, Atmos. Environ.,35 (31), 5311-5319, 2001

McKenna, D. S., Grooß, J.-U., Günther, G., Konopka, P., Müller, R. and Carver, G., A new Chemical Lagrangian Model of the Stratosphere (CLaMS), 2, Formulation of chemistry scheme and initialization, J. Geophys. Res., 107, 4256, doi:10.1029/2000JD000113, 2002

Möbius, T., Untersuchungen zu Unterschieden in Tracer-Tracer-Korrelationen innerhalb und außerhalb des arktischen Polarwirbels, Diploma thesis, Johann Wolfgang Goethe Universität, Frankfurt am Main, 2005

Molina, M. J., and Rowland, F. S., Stratospheric sink for chlorofluoromethanes: Chlorine atom catalyzed destruction of ozone, Nature, 249, 820–812, 1974

Montzka, S. A. and Fraser, P. J., et al., Controlled substances and other source gases, Scientific assessment of ozone depletion: 2002, Global Ozone Research and Monitoring Project – Report No. 47, Chapter 1, World Meteorological Organization, Geneva, 2003

Moore, D. P. and Remedios, J. J., Growth rates of stratospheric HCFC-22, Atmos. Chem. Phys., 8, 73–82, 2008, www.atmos-chem-phys.net/8/73/2008/

Müller, M., Untersuchungen stratosphärischer Transportprozesse mittels der Verteilung langlebiger Spurengase, Dissertation, Johann Wolfgang Goethe Universität Frankfurt, 2001

Murphy, D. M., and Thompson, D. S., Halogen ions and NO+ in the mass spectra of aerosols in the upper troposphere and lower stratosphere, Geophys. Res. Lett., 27, 3217-3220, 2000

Newman, P. A., Nash, E. R., Kawa, S. R., Montzka, S. A. and Schauffler, S. M., When will the Antarctic ozone hole recover?, Geophys. Res. Lett., 33, L12814, doi:10.1029/2005GL025232, 2006

Newman, P. A., Daniel, J. S., Waugh, D. W. and Nash, E. R., A new formulation of equivalent effective stratospheric chlorine (EESC), Atmos. Chem. Phys., 7, 4537–4552, 2007

Nielsen, J. E. and Douglass, A. R., A simulation of bromoform's contribution to stratospheric bromine, J. Geophys. Res., 106(D8), 8089-8100, 2001

NIST Mass Spectral Search Program for the NIST/EPA/NIH Mass Spectral Library, Version 2.0 d, Build Apr 26, 2005, Distributed by the Standard Reference Data Program of the National Institute of Standards and Technology, Copyright © 1987-2005 by the U.S. secretary of Commerce on behalf of the United Stated of America. All rights reserved.

Olsen, S. C., Hannegan, B. J., Zhu, X. and Prather, M. J., Evaluating ozone depletion from very short-lived halocarbons, Geophys. Res. Lett., 27, 10, 1475-1478, 2000

Pate, B., Jayanty, R. K. M., Peterson, M. R. and Evans, G. F., Temporal Stability of Polar Organic Compounds in Stainless Steel Canisters, J. Air Waste Manage. Assoc., 42, 460-462, 1992

Pfeilsticker, K., Sturges, W.T., Bösch, H., Camy-Peyret, C., Chipperfield, M.P., Engel, A., Fitzenberger, R., Müller, M., Payan, S. and Sinnhuber, B.-M., Lower stratospheric organic and inorganic bromine budget for the Arctic winter 1998/99, Geophys. Res. Lett., 27 (20), 3305-3308, 2000

Plumb, R. A. and Ko, M. K. W., Interrelationships between mixing ratios of long-lived stratospheric constituents, J. Geophys. Res., 97, 10,145–10,156, 1992

Plumb, R. A., A “tropical pipe” model of stratospheric transport, J. Geophys. Res., 101, 3957–3972, 1996

Plumb, I. C., Vohralik, P. F. and Ryan, K. R., Normalization of correlations for atmospheric species with chemical loss, J. Geophys. Res., 104, 11,723–11,732, 1999

Plumb, R. A., Waugh, D. W. and Chipperfield, M. P., The effect of mixing on tracer relationships in the polar vortices, J. Geophys. Res., 105, 10 047-10 062, 2000

Plumb, R. A., Stratospheric transport, J. Meteorol. Soc. Jpn., 80, 793–809, 2002

Plumb, R. A., Tracer interrelationships in the stratosphere, Rev. Geophys., 45, RG4005, doi:10.1029/2005RG000179, 2007

Prinn, R.G., Weiss, R.F., Fraser, P.J., Simmonds, P.G., Cunnold, D.M., Alyea, F.N., O’Doherty, S., Salameh, P., Miller, B.R., Huang, J., Wang, R. H. J., Hartley, D.E., Harth, C., Steele, L.P., Sturrock, G., Midgley, P.M. and McCulloch, A., A history of chemically and radiatively important gases in air deduced from ALE/GAGE/-AGAGE, J. Geophys. Res., 105, 17751-17792, 2000

Quack, B. and Wallace, D.W.R., Air-sea flux of bromoform: Controls, rates, and implications, Global Biogeochem. Cycles, 17 (1), 1023, 2003

Reeves, C.E., Sturges, W. T., Sturrock, G.A., Preston, K., Oram, D.E., Schwander, J., Mulvaney, R., Barnola, J.-M. and Chappellaz, J., Trends of halon gases in polar firn air: implications for their emission distributions, Atmos. Chem. Phys., 5, 2055-2064, 2005

Reimann, S., Vollmer, M. K., Folini, D., Steinbacher, M., Hill, M., Buchmann, B., Zander, R. and Mahieu, E., Observations of Long-Lived Anthropogenic Halocarbons at the High-Alpine site of Jungfraujoch (Switzerland) for Assessment of Trends and European Sources, Sci. Total Environ., 391 (2-3), 224-231, 2008

Reimer, E. and Kaupp, H., Source indentification of odour compounds using trajectories, Proc. ECOINFORMA 97, Eco-Informa Press, Bayreuth, 572-577, 1997

Rhew, R.C., Ostergaard, L., Saltzman, E.S. and Yanofsky, M.F., Genetic control of methyl halide production in Arabidopsis, Curr. Biol., 13 (20), 1809-1813, 2003

Robb, L. E., Westfield, N. J., Polyblends of a thermoplastic tetra-fluoroethylene polymer, US-Patent 3019206, 1962

Roedel, W., Physik unserer Umwelt: die Atmosphaere, 3rd Edition, Berlin; Heidelberg; New York; Barcelona; Hongkong; London; Mailand; Paris; Singapur; Tokio: Springer, 2000

Rusonik, I., Cohen, H. and Meyerstein, D., Reduction of CCl4 by Iron Powder in Aqueous Solution, Eur. J. Inorg. Chem., 1227–1229, doi: 10.1002/ejic.200400979, 2005

Salawitch, R. J., Weisenstein, D. K., Kovalenko, L. J., Sioris, C. E., Wennberg, P. O., Chance, K., Ko, M. K. W., and McLinden, C. A., Sensitivity of ozone to bromine in the lower stratosphere, Geophys. Res. Lett., 32, 5811, doi:10.1029/2004GL021504, 2005

Savitzky, A. and Golay, M.J.E., Smoothing and Differentiation of Data by Simplified Least Squares Procedures, Anal. Chem., 36(8),1627-1639, 1964

Schauffler, S. M., Atlas, E. L., Flocke, F., Lueb, R. A., Stroud, V. and Travnicek, W., Measurements of bromine containing organic compounds at the tropical tropopause, Geophys. Res. Lett., 25(3), 317-320, 1998

Schauffler, S. M., Atlas, E. L., Blake, D. R., Flocke, F., Lueb, R. A., Lee-Taylor, J. M., Stroud, V. and Travnicek, W., Distributions of brominated organic compounds in the troposphere and lower stratosphere, J. Geophys. Res., 104(D17), 21513-21535, 1999

Schmidt, U., Kulessa, G., Klein, E., Röth, E.-P., Fabian, P. and Borchers, R., Intercomparison of balloon borne cryogenic whole air samplers, Planet. Space Sci., 35, 647-656, doi:10.1016/0032-0633(87)90131-0, 1987

Schmidt, U. and Khedim, A., In Situ Measurements of Carbon Dioxide in the Winter Arctic Vortex and at Midlatitudes: An Indicator of the 'Age' of Stratospheric Air, Geophys. Res. Lett., 18, 763-766, 1991

Schmidt, U., Bauer, R., Khedim, A., Klein, E., Kulessa, G. and Schiller, C., Profile observation of long-lived trace gases in the Arctic vortex, Geophys. Res. Lett. 18, 767-770, 1991

Schmidt, U., A. Engel & C. M. Volk, Ist der Ozonabbau gestoppt? Forschung Frankfurt, 11-19, 2001

Schwedt, G., Taschenatlas der Analytik, 2. Auflage, Stuttgart, New York: Thieme, 1996

Simmonds, P.G., Manning, A.J., Cunnold, D.M., McCulloch, A., O’Doherty, S., Derwent, R.G., Krummel, P.B., Fraser, P.J., Dunse, B., Porter, L.W., Wang, R.H.J., Greally, B.R., Miller, B.R., Salameh, P., Weiss, R.F. and Prinn, R.G., Global trends, seasonal cycles, and European emissions of dichloromethane, trichloroethene, and tetrachloroethene from the AGAGE observations at Mace Head, Ireland, and Cape Grim, Tasmania, J. Geophys. Res., 111, D18304, doi: 10.1029/2006JD007082, 2006

Sinnhuber, B.-M., and Folkins, I., Estimating the contribution of bromoform to stratospheric bromine and its relation to dehydration in the tropical tropopause layer, Atmos. Chem. Phys., 6, 4755-4761, 2006

Solomon, S. and Albritton, D., Time-dependent ozone depletion potentials for short- and long-term forecasts, Nature, 357, 33–37, doi:10.1038/357033a0, 1992

Solomon, S., Tuck, A. F., Mills, M., Heidt, L. E. and Pollock, W. H., On the evaluation of ozone depletion potentials, J. Geophys. Res., 97, 825-842, 1992

Solomon, S., Stratospheric ozone depletion: a review of concepts and history. Reviews of Geophysics, 37, 275-316, 1999

Stiller, G. P. von Clarmann, T., Höpfner, M., Glatthor, N., Grabowski, U., Kellmann, S., Kleinert, A., Linden, A., Milz, M., Reddmann, T., Steck, T., Fischer, H., Funke, B., Lopez-Puertas, M. and Engel, A., Global distribution of mean age of stratospheric air from MIPAS SF_6 measurements, Atmos. Chem. Phys., 8, 677–695, 2008, www.atmos-chem-phys.net/8/677/2008/

Stolarski, R. S., and Cicerone, R. J., Stratospheric chlorine: A possible sink for ozone, Can. J. Chem., 52, 1610–1615, 1974

Strunk, M., An experimental study on the mean age of stratospheric air, Dissertation, Johann Wolfgang Goethe Universität, Frankfurt, 1999

Strunk, M., Engel, A. Schmidt, U. Wetter, T. Levin, I. and Glatzel-Mattheier, H., CO_2 and SF_6 as stratospheric age tracers: Consistency and the effect of mesospheric SF_6-loss, Geophys. Res. Lett., 27, 341-344, 2000

Thun, M. and Kimbrough, R. D., Fatal chemical pneumonia from 1,1,2,3,3-pentafluoro-3-chloropropene in an unmarked gas tank, Clin. Toxicol., 18, 481-7, 1981

Tuck, A. F., Hovde, S. J., Kelly, K. K., Reid, S. J., Richard, E. C., Atlas, E. L. Donnelly, S. G., Stroud, V. R., Cziczo, D. J., Murphy, D. M., Thomson, D. S., Elkins, J. W., Moore, F. L. Ray, E. A., Mahoney, M. J. and Friedl, R. R., Horizontal variability 1 - 2 km below the tropical tropopause, J. Geophys. Res., 109, D05310, doi:10.1029/2003JD003942, 2004

Utracki, L. A., History of commercial polymer alloys and blends (from a perspective of the patent literature), Polym. Eng. Sci, 35, 2-17, doi:10.1002/pen.760350103, 1995

Van der Leun, J., Tang, X., and Tevini, M., Environmental effects of ozone depletion: 1994 assessment, Ambio, 14, 138, 1995

Volk, C.M., Elkins, J.W., Fahey, D.W., Sutton, G.S., Gilligan, J.M., Loewenstein, M., Podolske, J.R., Chan, K.R. and Gunson, M.R., Evaluation of source gas lifetimes from stratospheric observations, J. Geophys. Res., 102 (D21), 25543-25564, 1997

Waugh, D. W., and Hall, T. M., Age of stratospheric air: Theory, observations, and models, Rev. Geophys., 40(4), 1010, doi:10.1029/2000RG000101, 2002

Werner, A. S., Quantifying transport into the lowermost stratosphere, PhD thesis, Johann Wolfgang Goethe Universitaet, Frankfurt am Main, 2007

WMO, 1957: WMO-Bulletin, Volume 6, 136, World Meteorological Organization, Geneva, Switzerland, 1957

WMO 2003: World Meteorological Organization/United Nations Environment Programme, Scientific Assessment of Ozone Depletion: 2002. Global Ozone Research and Monitoring Project–Report No. 47, Geneva, Switzerland, 2003

WMO 2007: World Meteorological Organization/United Nations Environment Programme, Scientific Assessment of Ozone Depletion: 2006. Global Ozone Research and Monitoring Project–Report No. 50, Geneva, Switzerland, 2007

Wofsy, S. C., McElroy, M. B., and Yung, Y. L., The chemistry of atmospheric bromine, Geophys. Res. Lett., 2, 215–218, 1975

Yokouchi, Y., Hasebe, F., Fujiwara, M., Takashima, H., Shiotani, M., Nishi, N., Kanaya, Y., Hashimoto, S., Fraser, P., Toom-Sauntry, D., Mukai, H. and Nojiri, Y., Correlations and emission ratios among bromoform, dibromochloromethane, and dibromomethane in the atmosphere, J. Geophys. Res., 110, D23309, doi: 10.1029/2005JD006303, 2005

Zulfiqar, S., Zulfiqar, M., Masroor Rizvi, Arshad Munir and McNeill, I. C., Study of the thermal degradation of polychlorotrifluoroethylene, poly(vinylidene fluoride) and copolymers of chlorotrifluoroethylene and vinylidene fluoride, Polym. Degrad. Stabil., 43, 423-430, 1994

List of Figures

List of Tables

Acknowledgements

I would like to express my gratitude to the following people for their support and assistance:

- Prof. Dr. Bernd O. Kolbesen for supervising this work and making it possible for me to do a doctorate in Chemistry but also for constructive scientific as well as exciting non-scientific discussions.

- PD Dr. Andreas Engel who is by far the best boss I have had up to now. Thanks for giving me the chance to jump from polymer synthesis to analytical air chemistry, for scientific guidance, for teaching me a great deal of scientific knowledge and a unique way of how to work effectively while maintaining an excellent balance between a liberal scientific atmosphere and constructive pressure.

- Prof. Dr. Ulrich Schmidt and Prof. Dr. Andreas Terfort for agreeing to take part in the assessment of this work and Prof. Dr. Joachim Curtius for discussions, hints and a student-friendly lift in his car.

- Again Prof. Dr. U. Schmidt as well as Prof. Dr. Klaus Pfeilsticker and Dr. Jonathan Williams for valuable discussions and suggestions not only in the frame of the PhD Advisory Committee.

- All my colleagues from the Physics of the Atmosphere group for their company and support during the last years. Special thanks to Harald Bönisch for proof-reading my thesis, his never-ending readiness for discussions on all issues and his ability to question every detail before drawing a final conclusion. I would like to emphasize my thanks to Anja Werner, Tanja Möbius and Anna Christian Kuhn for help and discussions which were exciting and also essential for understanding experimental atmospheric science, as for example error bars (especially Anja), analytical techniques (especially Tanja) or the tropical UT/LS (especially Anna Christina). To all colleagues: Many thanks for your teamwork, your willingness to share experience and knowledge and the very cooperative atmosphere! I also wish Andrea Heil and Stefan Sala good luck for their scientific and/or non-scientific future!

- All technical and administrative supporters, especially Robert Sitals for various improvisations and for letting me off from repaying welcome money, but also Werner Haunold, Robert Röder, Christine Lidzba and Mrs. Igelbrink for always being more than ready to help!

- Prof. William T. Sturges and Dave Worton from the University of East Anglia for an excellent cooperation. Bill: I am sure it will be a pleasure to work with you!

- Marc Brass and Prof. Dr. Thomas Roeckmann from the University of Utrecht and the teams from M55 Geophysica and CNES France, without who no atmospheric samples would have been there to analyse.

- Dr. I. Levin of the University of Heidelberg for providing SF_6 data and Katja Grunow of the Free University of Berlin for her meteorological support.

- The colleagues from the Global Monitoring Division of NOAA-ESRL for making their measurements and results publicly available (special thanks to Steve Montzka for the permission to use them).

- All other national and international supporters, especially Sarah Gebhardt and Tineke Lelieveld from the IMPRS in Mainz, Marcel Dorf from the University of Heidelberg, Martin Steinbacher from EMPA Switzerland, Brad Hall from NOAA-ESRL and Elliot Atlas from the University of Miami.

- My wife and children for giving me incredible amounts of support, fun, help, energy and love and a life perspective which is amazingly still improving.

- All my family and friends for their support and company during this chapter of my life.

Moreover I thank the High Altitude Research Station Jungfraujoch, the Hessisches Landesamt für Umwelt und Geologie and the German Weather Service. This work was possible because

of funding from the European Space Agency, the Deutsches Zentrum fuer Luft- und Raumfahrt (project 50EE0016), the European Union (SCOUT-O3 project GOCE-CT-2003-505390) as well as the Deutsche Forschungsgesellschaft (CAWSES project EN 367/4).

Zusammenfassung und Ausblick

Das Ziel dieser Arbeit war die Untersuchung der Verteilung von 32 flüchtigen halogenierten Kohlenwasserstoffen in der oberen Troposphäre sowie unteren und mittleren Stratosphäre in den Tropen. Die Zielsubstanzen waren 32 chlorierte und/oder bromierte Kohlenwasserstoffe, die bereits in der oberen tropischen Troposphäre (der stratosphärischen Haupteintragsregion) nachgewiesen worden sind und somit nicht nur nicht nur zur globalen Erwärmung sondern auch zum stratosphärischen Ozonabbau beitragen können (WMO, 2007, IPCC, 2007). Es existieren bisher nur sehr wenige Beobachtungen von Halogenkohlenwasserstoffen in der tropischen Stratosphäre. Diese sind zum Teil veraltet (z. B. Goldan et al., 1980) oder beschränken sich auf die untere Stratosphäre (z. B. Volk et al., 1997, Schauffler et al., 1999). Die chemische Zusammensetzung der tropischen Stratosphäre beeinflusst jedoch den dortigen Strahlungshaushalt und somit das Klima dieses Planeten. Deswegen war es äußerst wichtig, die Höhenverteilungen von Halogenkohlenwasserstoffen in dieser atmosphärischen Region zu charakterisieren.

Für die Untersuchung der Verteilungen wurde zunächst ein analytisches System zur Messung von äußerst gering konzentrierten atmosphärischen Spurengasen aufgebaut. Ein existierendes Gas-Chromatographie-System (GC) mit kryogener Anreicherungseinheit und einem Elektronen-Einfang-Detektor (ECD) wurde um ein Quadrupol-Massenspektrometer (MS) als zusätzlichen parallelen Detektor erweitert. Dies ermöglichte die signifikante Verbesserung der Charakterisierung des chromatographischen Systems, da 48 weitere flüchtige organische Verbindungen identifiziert werden konnten. Die Nachweisgrenzen des neuen GC-MS-Systems liegen im Bereich von 10^{-12} bis 10^{-13} mol/mol Luft für die Zielsubstanzen.

Für die Integration der chromatographischen Signale wurde ein in der Arbeitsgruppe entwickelter Gaußscher Fit-Algorithmus evaluiert. Die Vorteile dieses Algorithmus' liegen in der Verbesserung der Reproduzierbarkeiten bei der Integration von chromatographischen Signalen mit niedrigem Verhältnis von Signal zu Rauschen (mittlere Reproduzierbarkeiten um 3 % bei einem Verhältnis von Signal zu Rauschen von 4:1) sowie in Zeit-Ersparnissen bei der Auswertung durch eine partielle Automatisierung. Mithilfe von Vergleichen von Testreihen wurde nachgewiesen, dass der Algorithmus chromatographische Signale quantitativ widerspiegelt.

Da der ECD bekanntermaßen nichtlineare Abhängigkeiten des Detektorsignals von der Analytkonzentration zeigt, erfolgte eine entsprechende Überprüfung des neuen massenspektrometrischen Detektors. Es konnte nachgewiesen werden, dass dieser über einen weiten Bereich linear arbeitet. Folglich kann der komplette Quantifizierungsprozess – inklusive kryogener Anreicherung von Spurengasen sowie Integration und Auswertung der Signale – als linear innerhalb der untersuchten Parameterbereiche angenommen werden.

Weitere Untersuchungen betrafen die Langzeitstabilität der Zielsubstanzen. Es konnte nachgewiesen werden, dass fast alle Zielsubstanzen in den zur Kalibrierung genutzten Gasflaschen keine Konzentrationsänderungen außerhalb der Fehlergrenzen über einen Beobachtungszeitraum von 25 Monaten zeigten. Viele Zielsubstanzen waren auch in den untersuchten Probenbehältern von zwei ballongetragenen Luftprobensammlern langzeitstabil. Es wurden jedoch für einige Substanzen signifikante Konzentrationsänderungen festgestellt. Dies betraf hauptsächlich CH_3Cl (Methylchlorid), CH_3Br (Methylbromid), CH_2Cl_2 (Methylenchorid), $CHCl_3$ (Chloroform), CCl_4 (Tetrachlormethan), C_2Cl_4 (Tetrachlorethen), CH_3CCl_3 (Methylchloroform), CH_2ClCH_2Cl (1,2-Dichlorethan) und C_2H_5Cl (Chlorethan). Hier variierten sowohl die Anzahl der betroffenen Substanzen als auch die jeweiligen Konzentrationsänderungen stark von Behälter zu Behälter. Deshalb ist es empfehlenswert, dass weitere systematische Untersuchungen im Hinblick auf z. B. verschiedene Sammeltechniken oder Behältermaterialien durchgeführt werden um die Effekte und deren Ursachen besser zu charakterisieren.

Zudem erfolgte ein Vergleich der Ergebnisse der beiden internen Detektoren. Der ECD ist – bedingt durch seine geringere Selektivität und sein nichtlineares Verhalten – in diesem Fall der deutlich fehleranfälligere Detektor. Aus diesem Grund wurden ausschließlich MS-Ergebnisse für die Quantifizierung von atmosphärischen Spurengasen herangezogen.

Die Quantifizierung der Zielsubstanzen erfolgte als relative Methode mithilfe von extern kalibrierten Luft-Standards. Eine Einschätzung der Unsicherheiten die mit international verschiedenen absoluten Eichskalen verbunden sind, konnte durch Quervergleiche von kalibrierten Luftstandards aus drei verschiedenen Labors erzielt werden. Die Kalibrierwerte der meisten Substanzen stimmten innerhalb der Messungenauigkeiten überein. Sechs Substanzen zeigten jedoch signifikante Unterschiede: CF_2ClBr (H1211), CH_3Cl (Methylchlorid), CH_2Cl_2 (Methylenchlorid), $CHCl_3$ (Chloroform), CCl_4 (Tetrachlormethan) und CH_3CCl_3 (Methylchloroform). Für fünf dieser Substanzen wurden auch

Konzentrationsänderungen innerhalb der Probenbehälter beobachtet (siehe oben). Somit stellen diese Änderungen eine der wahrscheinlichen Ursachen für die beobachteten Eichskalenunterschiede dar.

Zusätzlich zu der detaillierten Untersuchung der mit dem Quantifizierungsprozess verknüpften Unsicherheiten stand eine Reihe von Luftproben für Messungen zur Verfügung. Diese Luftproben stammten hautsächlich aus der oberen Troposphäre und der unteren und mittleren Stratosphäre in den Tropen. Ein Teil dieser Proben wurde mithilfe von ballongetragenen kryogenen Luftprobensammlern von Forschern der Universität Frankfurt gewonnen, ein anderer Teil von Forschern der Universität Utrecht (Niederlande) von einem hochfliegenden Forschungsflugzeug aus gesammelt. Die bestimmten Gehalte an halogenierten Kohlenwasserstoffen wurden benutzt, um die Verteilungen der Substanzen in diesen atmosphärischen Regionen zu untersuchen.

Im Einzelnen konnten die Korrelationen und Höhenverteilungen von 17 halogenierten Kohlenwasserstoffen mit langen atmosphärischen Lebenszeiten von mehr als einem halben Jahr (so genannte Tracer) in der tropischen unteren und mittleren Stratosphäre bestimmt werden. Diese wurden mit den Verteilungen in anderen stratosphärischen Regionen verglichen. Die gefundenen Tracer-Tracer-Korrelationen unterscheiden sich von denen in mittleren und hohen Breiten. Die sich aus den Verteilungen ergebenden Korrelations-Funktionen relativ zu CF_2Cl_2 (F12) sind gültig für die tropische Stratosphäre im Jahr 2005. Zudem wurden zeitunabhängige partielle Freisetzungsfaktoren und zugehörige Abhängigkeiten dieser Faktoren von der mittleren stratosphärischen Aufenthaltszeit der Luft (dem so genannten mittleren Alter) berechnet. Beide Sets an Korrelationsfunktionen könnten und sollten benutzt werden, um Modelle (z. B. Chemische Transportmodelle) zu parameterisieren und zu evaluieren, um Vorhersagen für die Entwicklung der Ozonschicht zu verbessern. Auch sollte eine Neubewertung der Global Warming Potentials (GWPs) der untersuchten Substanzen unter Einbeziehung der zusätzlichen tropischen Daten erfolgen, was sich auf Vorhersagen zur Entwicklung des Klimas auswirken könnte. Jedoch ist der zur Verfügung stehende Datensatz von halogenierten Kohlenwasserstoffen in der tropischen Stratosphäre unzureichend für Untersuchungen der durch dynamische und photochemische Prozesse verursachten Variabilität der Tracer-Tracer-Korrelationen und partiellen Freisetzungsfaktoren. Deshalb ist von großer Wichtigkeit, dass weitere Messungen in dieser Region der Atmosphäre durchgeführt werden. Wenn möglich, sollten diese Messungen auf die obere tropische Stratosphäre ausgedehnt werden, um z. B. die atmosphärische Senke der besonders langlebigen halogenierten Kohlenwasserstoffe besser zu charakterisieren.

Des Weiteren konnte im Rahmen einer Fallstudie die Menge an Chlor und Brom, die die Stratosphäre über deren Haupteintragsregion (die Tropische Tropopausenschicht) erreicht, ermittelt werden (Laube et al., 2008). Dies wurde durch eine Kooperation mit der University of East Anglia ermöglicht. Dort konnten sechs Substanzen zusätzlich zu den 22 in Frankfurt am oben beschriebenen System gemessenen Zielsubstanzen quantifiziert werden. Zehn der 28 quantifizierten Zielsubstanzen haben kurze atmosphärische Lebenszeiten im Vergleich zu den mittleren Transportzeiten von troposphärischer Luft zur Stratosphäre (Lebenszeiten unter einem halben Jahr). Deswegen zeigen diese Substanzen sehr uneinheitliche Verteilungen in der oberen Troposphäre. Der Beitrag dieser Verbindungen zur stratosphärischen Ozonzerstörung ist Gegenstand einer anhaltenden wissenschaftlichen Diskussion. In der durchgeführten Fallstudie konnte der Anteil dieser Verbindungen an der Summe der organischen Halogenverbindungen zu 6 – 8 % (Mischungsverhältnisse von 0.98 – 1.25 parts per trillion, ppt) für Brom und zu 1.1 – 1.4 % (36.6 – 47.1 ppt) für Chlor bestimmt werden. Diese Werte gelten jedoch nur für die Luftmassen, die die Stratosphäre im Juni 2005 über Teresina, Brasilien erreichten. Im Vergleich mit aktuellen Schätzungen der World Meteorological Organization und des United Nations Environmental Program (WMO/UNEP, siehe WMO, 2007) für die obere tropische Troposphäre ergab sich eine gute Übereinstimmung bei den Einträgen an kurzlebigen chlorierten Verbindungen. Für die bromierten kurzlebigen Substanzen schätzt die WMO/UNEP jedoch – wohlgemerkt global – einen signifikant höheren Eintrag in den Tropen.

Darüber hinaus konnte in der Fallstudie die Summe der anorganischen Chlor- und Bromspezies (Cl_y und Br_y), welche direkt verantwortlich für den katalytischen Ozonabbau sind, bestimmt werden. Dies war möglich durch Berechnungen auf der Grundlage des mittleren Alters der gesammelten Luftmassen sowie der zugehörigen troposphärischen Referenzdaten der einzelnen Substanzen. In einer Höhe von 34 km wurden Cl_y zu 3062 ppt und Br_y zu 17.5 ppt bestimmt. Dieses Mischungsverhältnis für Br_y ist signifikant niedriger als ein mithilfe von spektroskopischen Beobachtungen einer wichtigen anorganischen Bromspezies (BrO) bestimmter Wert (BrO-Messungen in zeitlicher und örtlicher Nähe durchgeführt, siehe Dorf, 2005 sowie Dorf et al., 2008). Eine mögliche Erklärung für diese Differenz wäre der Eintrag von zusätzlichen organischen Bromverbindungen in die

Stratosphäre. Tatsächlich wurden an der University of East Anglia im Rahmen der Kooperation Hinweise auf die Anwesenheit solcher Verbindungen in der stratosphärischen Haupteintragsregion gefunden.

Ein weiteres Ergebnis dieser Arbeit stellt schließlich eine Erweiterung des Wissens über die chemische Zusammensetzung der Troposphäre dar. Es konnten drei Fluorchlorkohlenwasserstoffe (FCKWs) erstmalig in der Atmosphäre beobachtet werden. C_2F_3Cl (Trifluorchlorethen), CF_2CFCF_2Cl (3-Chlorpentafluorpropen) sowie $CF_2CFCF_2CFCl_2$ (4,4-Dichlorhexafluor-1-buten) konnten in Luftproben nachgewiesen werden, welche in Deutschland am Taunus-Observatorium nahe Frankfurt (Main) sowie in der Schweiz an der hochalpinen Forschungsstation Jungfraujoch gesammelt wurden (Laube and Engel, 2008). Die Identifikation war möglich aufgrund einer Abluftfahne die hohe Konzentrationen dieser Substanzen enthielt. Es wird angenommen, dass diese Konzentrationen von einer lokalen Quelle stammten. Die atmosphärischen Lebenszeiten dieser Substanzen werden als relativ kurz eingeschätzt (d. h. unter einem halben Jahr), da sie eine Doppelbindung enthalten. Eine Quantifizierung über die Herstellung von statischen Verdünnungen war bisher nur für Trifluorchlorethen möglich. Deswegen wurde eine relative Sensitivitätsmethode für eine erste Abschätzung der beobachteten Konzentrationen der anderen beiden FCKWs entwickelt. In der Abluftfahne lagen die sowohl die bestimmten als auch die abgeschätzten Konzentrationen im Bereich von einigen ppb (parts per billion).

Alle drei Substanzen konnten auch in saubereren Luftmassen (so genannte atmosphärische Hintergrundluft, z. B. vom Jungfraujoch) nachgewiesen werden, die auftretenden und abgeschätzten Konzentrationen waren jedoch deutlich geringer (unterer sowie sub-ppt-Bereich). Diese Verbindungen und einige ihrer Abbauprodukte sind toxisch und könnten zudem relevant für stratosphärische und troposphärische Ozonzerstörungsprozesse sein. Für eine Einschätzung ihres Einflusses auf die globale Atmosphäre ist es empfehlenswert, die entsprechenden atmosphärischen Verteilungen, Lebenszeiten, Senken und Quellen und auch die Fähigkeit der Substanzen, die Stratosphäre zu erreichen, weiter zu untersuchen.

Das Forschungsprojekt "CLEARFOGG – Checking Layers of the Earths AtmospheRe For halogenated Ozone-depleting and Greenhouse Gases" beinhaltet die Durchführung solcher Untersuchungen. Die Atmosphäre soll systematisch nach unbekannten halogenierten Kohlenwasserstoffen abgesucht werden, da es zahlreiche Indikationen für das Vorhandensein solcher Substanzen gibt. Der britische National Environmental Research Council entschied vor kurzem, dieses Projekt zu fördern. Es wird an University of East Anglia hauptsächlich vom Autor dieser Arbeit durchgeführt werden.

Curriculum vitae

Name:	Johannes Christian Laube
Date of birth:	19.12.1977
Place of birth:	Jena, Germany
Nationality:	German

May 2005 – Oct 2008

PhD student, Institute for Atmosphere and Environment and Institute for Inorganic and Analytical Chemistry at the Johann Wolfgang Goethe University Frankfurt, Germany, Supervisors: PD Dr. Andreas Engel and Prof. Dr. Bernd O. Kolbesen.

Participation in a Graduate School, the International Max Planck Research School for Atmospheric Chemistry and Physics.

Feb 2004 – Mar 2005

Employee, Centre of Excellence for Polysaccharide Research at the Friedrich Schiller University Jena, Germany, Research group of Prof. Dr. Thomas Heinze.

Jan 2004

Diploma (Degree: Diploma Chemist), Master thesis performed in the research group of Prof. Thomas Heinze at the Centre of Excellence for Polysaccharide Research, Friedrich Schiller University Jena, Germany, Title: Polykationen auf der Basis von Stärke: Synthese, Struktur und Eigenschaften (Polycations on the basis of starch: synthesis, structure and properties).

Oct 1997 – Jan 2004

Student of Chemistry, Friedrich Schiller University Jena, Germany, Study of chemistry with focus on organic and bioorganic chemistry.

1996

Certificate: general qualification for university entrance, Johann Wolfgang von Goethe grammar school Ilmenau, Germany.

retention time Jan 2008 [min]	substance (name)	identification method	identification date	(indications for) coeluting substances	identified on ions (max 5 listed):					🟩 Quantifier
2.2	C2F6 (perfluoroethane)	a	Nov.2005	no	🟩 69	🟧 119				🟧 Qualifier
2.4	SF6 (sulfur hexafluoride)	a,c	before 2005	Xe, CO2	🟧 127	🟩 89	108			
~3	C2H6 (ethane)	a	Nov.2005	CO2	27	26	29	30		
5.2	C3F8 (perfluoropropane)	a,c	Nov.2005	CHF3	🟧 69	31	🟩 169	50		
5.2	CHF3 (HFC23)	a,c	Nov.2005	C3F8, ion 51 dp	🟧 69	🟩 51	31	50		
6.1	CF3Br (H1301)	a,c,d	Nov.2005	no	🟩 69	🟧 129	131	148	150	
~6.5	C3H8 (propane)	a	Nov.2005	no	29	27	43			
6.5	C2F5Cl (F115)	a,c,d	Nov.2005	no	🟩 85	119	🟧 69	31	87	
7	OCS (carbonyl sulfide)	a,c	before 2005	no	🟩 60	🟧 62				
7.9	CF2Cl2 (F12)	a,b,d	before 2005	dp with F1113, ion 69	🟩 85	87	🟧 50	101	35	
8.1	C2F3Cl (F1113)	e	Oct.2007	dp with F12	🟩 116	118	85	97	66	
8.5	CHF2CF3 (HFC125)	a,c	Feb.2006	no	🟩 51	101	🟧 69	31	50	
~9	i-C4H10 (i-butane)	a	Nov.2005	no	43	27				
9.4	CHF2Cl (F22)	a,c,d	before 2005	ion 51 dp	🟧 51	31	🟩 67	35		
~10	n-C4H10 (n-butane)	a	Nov.2005	no	43	29	27			
10.3	CH2FCF3 (HFC134a)	a,c	Feb.2006	a: ion 33 too low	🟧 33	69	🟧 83	31	51	
10.3	CF2ClBr (H1211)	a,c,d	Nov.2005	F114	85	87	🟩 129	🟧 131	31	
10.4	CF2ClCF2Cl (F114)	a,b,d	Nov.2005	H1211, dp with F114a	85	🟩 135	87	🟧 101	31	
10.6	CF3CFCl2 (F114a)	a,b,d	Nov.2005	dp with F114	🟩 135	85	87	66		
10.8	C3F5Cl (3-chloropentafluoropropene)	e	Oct.2007	large signal on ion 69	🟩 131	69	🟧 166	147	93	
11.1	CH3Cl (methyl chloride)	a,b,d	before 2005	no	🟩 50	15	🟧 52	49		
11.4	CH3CF2Cl (F142b)	a,c,d	Nov.2005	no	🟩 65	🟧 45	85	31	64	
11.6	CHF2CF2Cl (F124a)	a,c	Nov.2005	no	🟩 101	51	85	67	69	
12.1	CS2 (carbon disulfide)	a,c	Nov.2005	F11, F124, i-C5H12, SO2	🟩 76	🟧 78	38			
12	CFCl3 (F11)	a,b,d	before 2005	CS2, F124, i-C5H12, SO2	🟧 101	🟩 103	66	35	47	
12	CHFClCF3 (F124)	a,c	Nov.2005	F11, CS2, i-C5H12, SO2	🟩 67	51	31	101	🟧 69	
~12	i-C5H12 (2-methylbutane)	a	Nov.2005	F11, CS2, F124, SO2	43	41	57	27	29	
~12.5	CH2CHCHCH2 (1,3-butadiene)	b	Aug.2007	n-C5H12	43	41	27	29	39	
~12.5	n-C5H12 (n-pentane)	a	Nov.2005	1,3-butadiene	39	54	53	27	50	
12.8	CH3Br (methyl bromide)	a,b,d	Nov.2005	no	🟩 94	🟧 96	93	95		
14.1	C2H5Cl (chloroethane)	a,b	Nov.2005	ions 49 and 66 dp	🟩 64	🟧 29	27	66	49	
14.1	CF2ClCFCl2 (F113)	a,b,d	before 2005	F141b, a: ion 151 too high	101	🟩 151	103	🟧 153		
14.4	CH3CFCl2 (F141b)	a,c,d	Nov.2005	F113, CH3I, H2402	🟩 81	45	61	26	35	
14.6	CH3I (methyl iodide)	a,b,d	Nov.2005	F141b, H2402	🟩 142	127				
14.6	CBrF2CBrF2 (H2402)	a,c,d	Nov.2005	F141b, CH3I	🟩 179	🟧 181	129	50		
15.3	CH2Cl2 (dichloromethane)	a,b,d	Nov.2005	isoprene, ion 84 dp	🟩 49	🟧 84	86	51	47	
~15.5	CH2C(CH3)CHCH2 (isoprene)	b	Aug.2007	CH2Cl2	67	68	53	39	40	
15.7	C2H5Br (bromoethane)	b	Aug.2007	no	29	27	🟩 108	110		
15.8	CCl4 (tetrachloromethane)	a,b,d	before 2005	C4F6Cl2	🟩 117	🟧 119	121	82	47	
15.8	C4F6Cl2 (4,4-dichlorohexafluoro-1-butene)	e	Oct.2007	CCl4, ion 147 dp	131	69	🟩 147	101	93	
16.7	CHCl3 (chloroform)	a,b,d	Nov.2005	CH3CHCl2	🟩 83	🟧 85	47	87	48	
~17	CH3CHCl2 (1,1-dichloroethane)	b	Aug.2007	CHCl3, CH2ClBr	63	65	27	83	61	
17.1	CH2ClBr (chlorobromomethane)	a,d	Nov.2005	CH3CHCl2, CH3CCl3	49	🟩 130	128	51		
17.2	CH3CCl3 (methyl chloroform)	a,b,d	before 2005	CH3CHCl2, CH2ClBr	🟧 97	99	61	🟩 117	119	
17.2	C2H5I (iodoethane)	b,d	Aug.2007	CH3CCl3, CH3CHCl2, CH2ClBr	🟩 156	127		🟩		🟧 Qualifier
17.4	C2HCl3 (trichloroethene)	a,b,d	Nov.2005	CH3CCl3, C2H5I	95	🟩 130	132	🟧 97	60	
18.8	CH2Br2 (dibromomethane)	a,b,d	Feb.2006	C2Cl4, C6H6	🟩 174	93	95	172	🟧 176	
18.8	C2Cl4 (tetrachloroethene)	a,b,d	Nov.2005	CH2Br2, C6H6	🟩 166	🟧 164	131	129	47	
~19	C6H6 (benzene)	a,b	Feb.2006	CH2Br2, C2Cl4	78	77	51	50	52	
19.2	CH2ClCH2Cl (1,2-dichloroethane)	a,b,d	Nov.2005	CH2ClI, ions 62 and 64 dp	🟩 62	🟧 64	27	49	61	
19.4	CH2ClI (chloroiodomethane)	b,d	Aug.2007	CH2ClCH2Cl	🟩 176	🟧 178	49	141	127	
~23	C6H5CH3 (toluene)	a,b	Feb.2006	no	91	92	39	65	63	
23.6	CH2BrCH2Br (1,2-dibromoethane)	b	Aug.2007	C6H5Cl	🟩 107	🟧 109				
23.6	C6H5Cl (chlorobenzene)	b	Aug.2007	CH2BrCH2Br	🟩 112	🟧 77	114			
24.3	CHBr3 (bromoform)	a,b,d	Feb.2006	no	🟩 173	🟧 171	175	91	93	
~27.5	CH2I2 (diiodomethane)	b	Aug.2007	no	268	141	127			
~32	CHCl2CHCl2 (1,1,2,2-tetrachloroethane)	b	Aug.2007	no	83	85	95	87	131	

dp - (sometimes) double peak occuring
a - identified with synthetic scan from merged EI-SIM runs with pre-concentration of trace gases from about 0.1 litre of air
b - identified with high concentrated mixture from MPI-CH Mainz ("Megamix")
c - confirmed with EI-SIM run measuring up to 10 of the most abundant ions in the same run and pre-concentrating trace gases from about 1 litre of air
d - confirmed with NICI-SIM due to the occurrence of chlorine, bromine and/or iodine anions in the expected isotopic ratios
e - identified with a sample taken at the Taunus Observatory, see Chapter 4 for details
red writing - there are indications that the signals of these ions can be influenced by coeluting substances and should be avoided for quantification if possible
🟩 green coloured - ions wer regularly used to quantify the substance
🟧 orange coloured - ions wer regularly used to qualify the substance

Figure A.1. Extended identification overview.

substance name	formula	M (g/mol)	boiling point (°C)	bp source	retention time on 15.08.2007 [min]
perfluoroethane	C2F6	138	-78.0	www.airliquidewelding.pl/airliquide.de	2.66
sulfur hexafluoride	SF6	146	-63.9	www.airliquidewelding.pl/airliquide.de	2.95
ethane	CH3CH3	30	-88.6	wikipedia.de on 10.09.2007	3.24
trifluormethane (HFC23)	CHF3	70	-82.0	www.airliquidewelding.pl/airliquide.de	5.47
H1301	CBrF3	148	-58.0	wikipedia.de on 10.09.2007	6.32
propane	CH3CH2CH3	44	-42.0	wikipedia.de on 10.09.2007	6.44
F115	CClF2CF3	154	-39.1	www.airliquidewelding.pl/airliquide.de	6.64
carbonyl sulfide	COS	60	-50.0	wikipedia.de on 10.09.2007	7.25
F12	CF2Cl2	120	-29.2	wikipedia.de on 10.09.2007	8.05
isobutane	CH3CH(CH3)CH3	58	-11.7	wikipedia.de on 10.09.2007	9.14
F22	CHClF2	86	-40.8	Arbeitsrichtlinie Schutz der Ozonschicht	9.58
n-butane	CH3CH2CH2CH3	58	-0.5	wikipedia.de on 10.09.2007	9.76
H1211	CBrClF2	164	-4.0	wikipedia.de on 10.09.2007	10.49
F114	CClF2CClF2	170	3.5	wikipedia.de on 10.09.2007	10.5
F114a	CCl2FCF3	170	3.0	www.patentstorm.us/patents/6077819-description.html	10.69
methyl chloride	CH3Cl	50	-24.2	wikipedia.de on 10.09.2007	11.25
F142b	CH3CClF2	100	-9.2	Arbeitsrichtlinie Schutz der Ozonschicht	11.49
F124a	CHF2CF2Cl	136	-10.8	www.airliquidewelding.pl/airliquide.de	11.71
carbon disulfide	CS2	76	46.3	wikipedia.de on 10.09.2007	12.17
F124	CHClFCF3	136	-11.0	www.ghc.de	12.17
F11	CFCl3	136	23.7	wikipedia.de on 10.09.2007	12.2
n-pentane	CH3(CH2)3CH3	72	36.0	wikipedia.de on 10.09.2007	12.67
methyl bromide	CH3Br	94	3.6	wikipedia.de on 10.09.2007	12.96
chloroethane	C2H5Cl	64	12.0	Merck (http://www.chemdat.info)	14.22
F113	CCl2FCClF2	186	47.6	Merck (http://www.chemdat.info)	14.25
F141b	CH3CCl2F	116	32.0	www.gischem.de	14.56
methyl iodide	CH3I	142	42.0	wikipedia.de on 10.09.2007	14.69
H2402	CBrF2CBrF2	258	47.5	Arbeitsrichtlinie Schutz der Ozonschicht	14.7
dichloromethane	CH2Cl2	84	39.8	wikipedia.de on 10.09.2007	15.45
tetrachloromethane	CCl4	152	76.7	wikipedia.de on 10.09.2007	15.98
chloroform	CHCl3	118	61.2	wikipedia.de on 10.09.2007	16.83
methyl chloroform (F140)	CH3CCl3	132	74.0	wikipedia.de on 10.09.2007	17.33
trichloroethene	C2HCl3	130	87.0	wikipedia.de on 10.09.2007	17.49
tetrachloroethene	C2Cl4	164	121.0	wikipedia.de on 10.09.2007	18.92
dibromomethane	CH2Br2	172	96.0	Merck (http://www.chemdat.info)	18.97
benzene	C6H6	78	80.1	wikipedia.de on 10.09.2007	18.99
1,2-dichloroethane	C2H4Cl2	98	83.8	wikipedia.de on 10.09.2007	19.32
toluene	C7H8	92	110.6	wikipedia.de on 10.09.2007	23.42
bromoform	CHBr3	250	149.5	wikipedia.de on 10.09.2007	24.96
perfluoropropane	C3F8	188	-36.7	www.airliquidewelding.pl/airliquide.de	no signal
HFC125	CHF2CF3	120	-48.5	www.airliquidewelding.pl/airliquide.de	no signal
HFC134a	CH2FCF3	102	-26.0	wikipedia.de on 10.09.2007	no signal

Figure A.2. Boiling points and molar masses.

Retention time	Substance (name)	required retention time window		Priority	Identified on ions:				
2.22	C2F6	2	2.4	1	69	119			
2.37	SF6	2	3	3	127	89	108		
5.18	C3F8	4.8	5.7	1	69	31	169	50	
5.19	CHF3 (HFC23)	4.8	5.7	3	69	51	31	50	
6.13	CF3Br (H1301)	5.6	6.5	1	69	129	131	148	150
6.45	CF3CF2Cl (F115)	6	6.9	1	85	119	69	31	87
7.02	COS	6.6	8	3	60	62			
7.86	CF2Cl2 (F12)	7.4	8.8	1	85	87	50	101	35
8.14	C2F3Cl (F1113)	7.8	8.6	2	116	118	85	97	66
8.52	CHF2CF3 (HFC125)	8.1	8.8	3	51	101	69	31	50
9.44	CHF2Cl (F22)	9.05	9.8	1	51	31	67	35	
10.28	CH2FCF3 (HFC134a)	9.9	10.5	3	33	69	83	31	51
10.3	CF2ClBr (H1211)	10	10.7	1	85	87	129	131	31
10.36	CF2ClCF2Cl (F114)	10	10.8	1	85	135	87	101	31
10.56	CF3CFCl2 (F114a)	10.3	11	1	135	85	87	66	
10.8	CF2CFCF2Cl	10.5	11.1	2	131	69	166	147	93
11.12	CH3Cl	10.8	11.7	1	50	15	52	49	
11.4	CH3CF2Cl (F142b)	11	11.7	1	65	45	85	31	64
11.6	CHF2CF2Cl (F124a)	11.3	11.9	2	101	51	85	67	69
12.1	CS2	11.8	12.6	3	76	78	38		
12.02	CFCl3 (F11)	11.6	12.6	1	101	103	66	35	47
12.02	CHFClCF3 (F124)	11.6	12.4	1	67	51	31	101	69
12.8	CH3Br	12.4	13.4	1	94	96	93	95	
14.05	C2H5Cl	13.7	14.35	1	64	29	27	66	49
14.12	CF2ClCFCl2 (F113)	13.7	14.5	1	101	151	103	153	
14.4	CH3CFCl2 (F141b)	14	14.55	1	81	45	61	26	35
14.56	CH3I	14.25	14.8	2	142	127			
14.62	CBrF2CBrF2 (H2402)	14.3	14.85	1	179	181	129	50	
15.3	CH2Cl2	15	15.6	1	49	84	86	51	47
15.65	C2H5Br	15.3	16	2	29	27	108	110	
15.84	CCl4	15.55	16.25	1	117	119	121	82	47
15.8	CF2CFCF2CFCl2	15.45	16.15	2	131	69	147	101	93
16.7	CHCl3	16.45	17.15	1	83	85	47	87	48
17.1	CH2ClBr	16.8	17.5	1	49	130	128	51	
17.19	CH3CCl3 (F140)	16.85	17.65	1	97	99	61	117	119
17.2	C2H5I	16.85	17.65	2	156	127			
17.35	C2HCl3	17.05	17.75	1	95	130	132	97	60
18.8	CH2Br2	18.5	19.1	1	174	93	95	172	176
18.75	C2Cl4	18.55	19.2	1	166	164	131	129	47
19.15	CH2ClCH2Cl	18.65	19.6	1	62	64	27	49	61
19.35	CH2ClI	19	19.8	2	176	178	49	141	127
23.6	CH2BrCH2Br	23.4	24.3	2	107	109			
23.6	C6H5Cl	23.4	24.3	2	112	77	114		
24.27	CHBr3	24.2	25	1	173	171	175	91	93

Quantifier
Qualifier

SIM method from 18.01.2008

time (min)	SIM group	ions	time (min)	SIM group	ions
2.00	1 (4*50ms)	69, 89, 119, 127	13.60	14	29, 64, 45, 81, 151, 153
4.00	2 (4*50ms)	51, 69, 129, 169	14.25	15	64, 81, 142, 151, 179, 181
5.70	3 (4*50ms)	60, 69, 85, 129	15.00	16	49, 84, 108, 117, 119, 147
6.80	4 (4*50ms)	60, 62, 69, 85	16.45	17	83, 85, 97, 117, 130, 156
7.40	5 (4*50ms)	50, 60, 85, 116	18.40	18	62, 64, 127, 166, 174, 176
8.10	6 (4*50ms)	51, 69, 85, 116	19.00	19	62, 64, 166, 174, 176, 178
9.00	7 (4*50ms)	51, 67, 85, 116	22.20	20	97, 99, 107, 112, 171, 173
9.80	8 (6*50ms ab hier)	33, 83, 101, 129, 131, 135	23.40	21	77, 107, 109, 112, 171, 173
10.55	9	50, 101, 129, 131, 135, 166			
10.80	10	50, 52, 65, 131, 135, 166			
11.20	11	45, 50, 52, 65, 101, 103			
11.80	12	67, 69, 70, 76, 101, 103			
12.40	13	64, 67, 94, 96, 101, 103			

injection valve switchback after 17.8 minutes
end after 25 minutes
red written: ion potentially influenced by other substances
🟥 red coloured: below detection limit

Figure A.3. Example of an EI-SIM-MS method.

	B42 reanalysis: concentration changes between Dec, 2005 and Aug, 2007				BONBONII sampler check filled and flight simulated			C1 reanalysis: concentration changes between November 2006 and August 2007							CLAIRE sampler check filled before flight				
Substance	B42 error bars*	B42_03	B42_04	B42_09	B42_02 (TO-Tante)	B42_05 (TO-Tante)	B42_01 (zero air, ppt)	B42_15 (zero air, ppt)	C1 error bars*	C1_15	C1_18	C1_20	C1_07	C1_19	C1_14	C1_ 25 (TO-Tante)	C1_ 26 (TO-Tante)	C1_ 23 (zero air, ppt)	C1_ 24 (zero air, ppt)
C2Cl4	11.8%	n. d.	n. d.	-9.4%	-13.0%	-10.1%	n. d.	n. d.	12.7%	n. d.	-7.0%	3.7%	n. d.	n. d.	75.8%	4.6%	4.7%	n. d.	n. d.
C2H5Cl	11.0%	292.0%	79.7%	223.8%	29.1%	16.1%	0.2	0.5	8.0%	334.1%	495.6%	447.0%	450.9%	811.2%	871.5%	2237.6%	2558.7%	49.1	44.3
C2HCl3	n. d.	n. d.	n. d.	n. d.	0.2%	-2.9%	n. d.	n. d.	41.6%	n. d.	n. d.	n. d.	n. d.	n. d.	n. d.	0.8%	3.3%	n. d.	n. d.
CCl4	2.7%	-25.6%	-41.0%	-28.4%	-5.6%	-10.6%	n. d.	n. d.	40.6%	-3.3%	-2.6%	-4.8%	8.5%	-3.2%	-24.8%	-1.4%	-6.8%	n. d.	n. d.
H2402	44.4%	-15.0%	n. d.	7.4%	16.8%	11.0%	n. d.	n. d.	28.2%	13.9%	-4.9%	-1.9%	n. d.	n. d.	28.4%	-7.3%	3.3%	n. d.	n. d.
F12	2.2%	-0.1%	0.3%	0.3%	0.0%	0.0%	n. d.	n. d.	4.9%	0.2%	0.2%	0.0%	1.0%	0.6%	0.4%	-1.0%	0.0%	n. d.	n. d.
H1211	32.7%	-6.2%	-8.8%	1.3%	-9.0%	7.7%	n. d.	n. d.	22.9%	-2.7%	-4.3%	-5.8%	n. d.	n. d.	5.9%	-9.3%	-4.0%	n. d.	n. d.
F114	5.3%	1.3%	-2.1%	-1.5%	3.2%	3.7%	n. d.	n. d.	7.8%	-0.1%	1.9%	-0.7%	1.4%	-3.9%	-5.1%	0.1%	0.3%	n. d.	n. d.
F115	6.3%	-1.6%	-0.3%	2.0%	2.6%	-0.4%	n. d.	n. d.	12.1%	-0.5%	4.5%	1.2%	0.9%	0.6%	2.7%	1.3%	0.1%	n. d.	n. d.
H1301	39.7%	-15.4%	4.0%	-5.1%	-1.6%	-5.6%	n. d.	n. d.	50.3%	2.1%	0.4%	-1.4%	-6.3%	-9.8%	-20.6%	-2.7%	-3.0%	n. d.	n. d.
F113	3.7%	-0.4%	0.4%	0.0%	0.3%	-0.2%	n. d.	n. d.	4.4%	0.1%	0.5%	0.1%	0.6%	3.7%	1.4%	-0.5%	0.6%	n. d.	n. d.
F114a	36.0%	-2.0%	-3.9%	-19.5%	3.2%	3.7%	n. d.	n. d.	32.3%	-11.4%	5.9%	-4.0%	-12.1%	-19.7%	-6.7%	4.2%	-10.0%	n. d.	n. d.
F11	1.5%	-0.4%	0.1%	-0.5%	0.2%	0.1%	n. d.	n. d.	2.8%	0.5%	-0.2%	-0.3%	2.5%	1.2%	-0.7%	-0.5%	0.3%	n. d.	n. d.
CH2Br2	32.3%	n. m.	n. m.	n. m.	n. d.	n. d.	n. d.	n. d.	32.2%	n. d.	n. d.	n. d.	n. d.	n. d.	n. d.	17.8%	20.3%	n. d.	n. d.
CH2Cl2	7.6%	41.1%	n. d.	15.9%	0.0%	-0.5%	n. d.	n. d.	4.9%	370.6%	139.9%	187.0%	1004.5%	1086.0%	365.3%	11.9%	10.3%	n. d.	n. d.
CH2ClCH2Cl	20.4%	73.3%	n. d.	43.1%	1.5%	1.3%	n. d.	n. d.	8.9%	304.4%	125.1%	165.6%	488.6%	890.0%	339.7%	49.3%	54.1%	3.4	2.7
CH3Br	12.3%	-41.2%	2.3%	-24.1%	3.4%	1.2%	1.2	1.1	15.5%	24.4%	38.2%	34.3%	352.8%	542.8%	115.5%	4.5%	8.8%	n. d.	n. d.
CH3CCl3	13.8%	-4.5%	-12.7%	-1.2%	-0.7%	-0.2%	n. d.	n. d.	13.8%	8.6%	5.9%	12.2%	n. d.	-100.0%	4.2%	-0.8%	1.1%	n. d.	n. d.
F142b	7.5%	1.5%	0.7%	-1.1%	-1.4%	-1.0%	n. d.	n. d.	10.5%	-18.1%	-22.7%	-2.8%	3101.6%	3.4%	38304.1%	5962.5%	20.0%	393.2	0.9
F141b	25.8%	1.5%	0.3%	-2.4%	-2.3%	-3.5%	n. d.	n. d.	18.9%	1.8%	5.2%	-0.7%	-0.2%	2.6%	5.0%	-7.6%	-7.7%	n. d.	n. d.
CH3Cl	5.1%	20.5%	12.2%	11.4%	1.4%	0.9%	5.6	9.4	4.0%	165.1%	103.9%	125.3%	374.2%	652.3%	182.8%	45.4%	52.6%	103.6	116.9
CHCl3	9.0%	16.3%	n. d.	-3.8%	1.9%	0.1%	n. d.	n. d.	7.0%	-100%	-100%	-100%	n. d.	n. d.	-100.0%	3.9%	5.5%	0.8	0.7
F124	26.8%	n. d.	n. d.	n. d.	14.2%	8.2%	n. d.	n. d.	19.4%	n. d.	n. d.	n. d.	n. d.	n. d.	n. d.	0.1%	1.3%	n. d.	n. d.
F22	5.9%	0.7%	2.4%	-1.1%	2.1%	-0.7%	n. d.	n. d.	6.3%	-1.0%	-0.4%	-0.5%	0.2%	-2.8%	1.0%	2.1%	-10.3%	n. d.	n. d.

*error bars are the sum of the 3sigma reproducibilities of two measurement days

🟥 red: significant concentration shifts detected

🟨 yellow: substance contained in zero air or system blank

red writing: contamination with this substance

n.d. - not detected

n.m. - not measured

Figure A.4. Data overview of trace gas stability experiments with two whole-air-samplers.

Comparison CH3Cl on m/z 50 Si1-MS different dilution series								**CH3Cl**	0	0		**CF2ClCFCl2 (F113) on m/z 151**								**CF2ClCFCl2 (F113) on m/z 151**			
				confirmed with TO-dilution series 20060701					1.4	1.4		pressure series 20061201				TO-dilution series 20061205				CO2-dilution series 20061212			
pressure series 20061201				TO-dilution series 20061205				CO2-dilution series 20061212						**reproducibility of the work**		**0.49%**				**0.42%**			
		reproducibility of the working std:		**0.66%**				**0.34%**				dilution factor	rel_resp_area	error	linear?	dilution factor	rel_resp_area	error	linear?	dilution factor	rel_resp_area	error	linear?
dilution factor	rel_resp_area	3 sigma error	linear?	dilution factor	rel_resp_area	3 sigma error	3sigma linear?	dilution factor	rel_resp_area	3 sigma error	linear?	0.125	0.12568931	0.00430787	yes	0.2519	0.25196565	0.00951719	yes	0.14626	0.14803147	0.01061098	yes
0.125	0.130671201	0.012746811	yes	0.2519	0.264011457	0.028301021	yes	0.14626	0.164779246	0.02967817	yes	0.2525	0.25532168	0.00571229	yes	0.497	0.50021946	0.00851491	yes	0.31201	0.30562958	0.00894434	yes
0.2525	0.257424104	0.015959374	yes	0.497	0.548426962	0.026810106	no	0.31201	0.278980318	0.02458399	no	0.375	0.37689173	0.00688298	yes	0.6902	0.6897031	0.00826628	yes	0.4882	0.48990904	0.00822834	yes
0.375	0.380191647	0.01891013	yes	0.6902	0.789387081	0.027166319	no	0.4882	0.499194584	0.02215482	yes	0.5	0.5006886	0.00801782	yes	0.8528	0.84787047	0.00820839	yes	0.70129	0.70173963	0.00782078	yes
0.5	0.503118216	0.02165444	yes	0.8528	1.08038934	0.027894248	no	0.70129	0.698413511	0.02051344	yes	0.625	0.62368529	0.00910046	yes					0.84387	0.85503012	0.00768193	yes
0.625	0.633055428	0.024568465	yes					0.84387	0.855477132	0.01979381	yes	0.75	0.75123077	0.0102151	yes								
0.75	0.744049856	0.026678551	yes									0.875	0.87405792	0.01123794	yes								
0.875	0.875653887	0.029471139	yes									1.125	1.12393447	0.01327769	yes								
1.125	1.117991476	0.034165264	yes									1.25	1.25505304	0.01434264	yes								
1.25	1.245323105	0.036632654	yes									**CCl4 on m/z 117**								**CCl4 on m/z 117**			
CF2Cl2 (F12) on m/z 85								**CF2Cl2 (F12) on m/z 85**				pressure series 20061201				TO-dilution series 20060701				CO2-dilution series 20061212			
pressure series 20061201				TO-dilution series 20061205				CO2-dilution series 20061212						**reproducibility of the work**		**2.31%**				**8.05%**			
		reproducibility of the working std:		**0.45%**				**0.47%**				dilution factor	rel_resp_area	error	linear?	dilution factor	rel_resp_area	error	linear?	dilution factor	rel_resp_area	error	linear?
dilution factor	rel_resp_area	error	linear?	dilution factor	rel_resp_area	error	linear?	dilution factor	rel_resp_area	error	linear?	0.125	0.11653891	0.01452068	yes	0.2519	0.01458369	0.01482206	no	0.14626	0.09190701	0.02258656	yes
0.125	0.125062902	0.003591311	yes	0.2519	0.252043189	0.006293869	yes	0.14626	0.146653159	0.00707417	yes	0.2525	0.23949755	0.02695936	yes	0.497	0.29831684	0.01817246	no	0.31201	0.19554016	0.03341202	no
0.2525	0.254229621	0.004447273	yes	0.497	0.499841741	0.005705083	yes	0.31201	0.30796129	0.00613531	yes	0.375	0.36534978	0.03960089	yes	0.6902	0.65893539	0.02139752	yes	0.4882	0.55851247	0.04605816	yes
0.375	0.37746388	0.005175932	yes	0.6902	0.68937472	0.005595116	yes	0.4882	0.494938021	0.00582781	yes	0.5	0.48198073	0.05113825	yes	0.8528	0.69007985	0.02427506	no	0.70129	0.71475284	0.06184734	yes
0.5	0.503217045	0.005878883	yes	0.8528	0.849445563	0.005601574	yes	0.70129	0.699862157	0.00575572	yes	0.625	0.47203973	0.0493976	no					0.84387	0.94091087	0.0725564	yes
0.625	0.624925723	0.006511297	yes					0.84387	0.852216957	0.00579505	yes	0.75	0.77590985	0.08040719	yes								
0.75	0.754889194	0.007208238	yes									0.875	0.78208971	0.08045323	yes								
0.875	0.87366759	0.007782308	yes									1.125	1.1874554	0.12087823	yes								
1.125	1.122140194	0.008997111	yes									1.25	1.41524162	0.14350321	yes								
1.25	1.246161554	0.009587537	yes									**CHCl3 on m/z 83**				confirmed with TO-dilution series 20060701				**CHCl3 on m/z 83**			
CHF2Cl (F22) on m/z 67				confirmed with TO-dilution series 20060701				**CHF2Cl (F22) on m/z 67**				pressure series 20061201				TO-dilution series 20061205				CO2-dilution series 20061212			
pressure series 20061201				TO-dilution series 20061205				CO2-dilution series 20061212						**reproducibility of the work**		**1.27%**				**0.74%**			
		reproducibility of the working std:		**0.57%**				**0.71%**				dilution factor	rel_resp_area	error	linear?	dilution factor	rel_resp_area	error	linear?	dilution factor	rel_resp_area	error	linear?
dilution factor	rel_resp_area	error	linear?	dilution factor	rel_resp_area	error	linear?	dilution factor	rel_resp_area	error	linear?	0.125	0.12063589	0.00566633	yes	0.2519	0.09960804	0.01763283	no	0.14626	0.15807671	0.0181582	yes
0.125	0.125832294	0.005237735	yes	0.2519	0.189815064	0.012401445	no	0.14626	0.146408819	0.01411243	yes	0.2525	0.24946122	0.00839353	yes	0.497	0.49378578	0.01755249	yes	0.31201	0.2787794	0.01573943	yes
0.2525	0.253273766	0.007366697	yes	0.497	0.499819248	0.011175651	yes	0.31201	0.310762582	0.01237151	yes	0.375	0.36260116	0.01051564	yes	0.6902	0.72187517	0.01839855	yes	0.4882	0.49390295	0.01494135	yes
0.375	0.372440139	0.009186378	yes	0.6902	0.683262786	0.010910689	yes	0.4882	0.489910557	0.01188823	yes	0.5	0.49359196	0.01302871	yes	0.8528	0.84545744	0.01936484	yes	0.70129	0.67615335	0.01474603	yes
0.5	0.507313814	0.011267655	yes	0.8528	0.849510519	0.010883744	yes	0.70129	0.700144559	0.01189744	yes	0.625	0.62517414	0.01545147	yes					0.84387	0.83886158	0.01484018	yes
0.625	0.628008779	0.012961389	yes					0.84387	0.857544781	0.01207699	yes	0.75	0.7490502	0.01761913	yes								
0.75	0.753886757	0.01472306	yes									0.875	0.87620402	0.01981945	yes								
0.875	0.864137136	0.016155335	yes									1.125	1.1180936	0.02384468	yes								
1.125	1.120609607	0.019618594	yes									1.25	1.2485436	0.0260204	yes								
1.25	1.242671093	0.021204394	yes									**CH3CCl3 on m/z 117**				confirmed with TO-dilution series 20060701				**CH3CCl3 on m/z 117**			
CF3CFCl2 (F114a) on m/z 135								**CF3CFCl2 (F114a) on m/z 135**				pressure series 20061201				TO-dilution series 20061205				CO2-dilution series 20061212			
pressure series 20061201				TO-dilution series 20061205				CO2-dilution series 20061212						**reproducibility of the work**		**1.37%**				**2.98%**			
		reproducibility of the working std:		**3.85%**				**3.53%**				dilution factor	rel_resp_area	error	linear?	dilution factor	rel_resp_area	error	linear?	dilution factor	rel_resp_area	error	linear?
dilution factor	rel_resp_area	error	linear?	dilution factor	rel_resp_area	error	linear?	dilution factor	rel_resp_area	error	linear?	0.125	0.12773964	0.0189733	yes	0.2519	0.11609507	0.0228803	no	0.14626	0.13142158	0.0272059	yes
0.125	0.112168278	0.016074544	yes	0.2519	0.277827183	0.030070212	yes	0.14626	0.13687554	0.02909238	yes	0.2525	0.24718168	0.02200478	yes	0.497	0.48195566	0.0222195	yes	0.31201	FALSCH	0.02745423	no
0.2525	0.243174372	0.024270809	yes	0.497	0.480044994	0.035342296	yes	0.31201	0.296429074	0.03006047	yes	0.375	0.35245256	0.02431832	yes	0.6902	0.69150704	0.02290799	yes	0.4882	0.49117398	0.03007614	yes
0.375	0.420561388	0.03584169	yes	0.6902	0.641779713	0.040763463	yes	0.4882	0.475578192	0.03355682	yes	0.5	0.49259123	0.0287491	yes	0.8528	0.84530418	0.02382554	yes	0.70129	0.71290921	0.03427105	yes
0.5	0.53697305	0.041612549	yes	0.8528	0.92193594	0.045679775	yes	0.70129	0.733202895	0.03885678	yes	0.625	0.62182334	0.0322337	yes					0.84387	0.8914093	0.0373769	yes
0.625	0.591018463	0.043002162	yes					0.84387	0.863746371	0.04271589	yes	0.75	0.76747905	0.0363852	yes								
0.75	0.769755934	0.054970838	yes									0.875	0.89772758	0.03967794	yes								
0.875	0.817861044	0.057489591	yes									1.125	1.14451646	0.04742168	yes								
1.125	1.177731012	0.080864783	yes									1.25	1.2951196	0.05279501	yes								
1.25	1.163043896	0.079134543	yes																				
CFCl3 (F11) on m/z 103								**CFCl3 (F11) on m/z 103**															
pressure series 20061201				TO-dilution series 20061205				CO2-dilution series 20061212															
		reproducibility of the working std:		**0.52%**				**0.30%**															
dilution factor	rel_resp_area	error	linear?	dilution factor	rel_resp_area	error	linear?	dilution factor	rel_resp_area	error	linear?												
0.125	0.123634469	0.003385265	yes	0.2519	0.248699782	0.007335082	yes	0.14626	0.147068177	0.00781375	yes												
0.2525	0.25119012	0.00403026	yes	0.497	0.499323174	0.006791226	yes	0.31201	0.307118364	0.00642135	yes												
0.375	0.375261719	0.004581438	yes	0.6902	0.68986233	0.006767754	yes	0.4882	0.491575056	0.00573132	yes												
0.5	0.498976714	0.005060686	yes	0.8528	0.852154254	0.006861287	yes	0.70129	0.702120852	0.00523985	yes												
0.625	0.623931826	0.005523177	yes					0.84387	0.851672533	0.00501119	yes												
0.75	0.751833154	0.005985352	yes																				
0.875	0.87309991	0.006376444	yes																				
1.125	1.125566492	0.007189697	yes																				
1.25	1.25302929	0.007584782	yes																				

Figure A.5. Results of the MS retrieval of two dilution series used for ECD nonlinearity correction.

final UCSE data			**GPS**	**data from Marc Braß, University of Utrecht**																				
pot. Temp. [K]	**longitude**	**latitude**	**altitude**	**mean longitude**	**mean latitude**	**mean altitude**	**sample**	H1301	F115	F12	F22	H1211	F114	F114a	CH3Cl	F142b	F11	CH3Br	F113	F141b	H2402	CCl4	F140	F124
						S3 – 8-12°S	**Survey Indonesia 23.11.05**																	
361.703	132.023	**-10.971**	14.961	132.024	-10.970	15536.00	S3/02	2.90	8.63	530.28	168.94	4.31	16.42	1.83		15.76	249.83		80.37	19.98		88.31	16.95	
361.722	132.610	**-10.231**	14.965	132.609	-10.232	15550.00	S3/03	2.89	8.19	525.63	167.61	4.28	16.73	1.89		15.48	253.26		79.93	19.66		86.59	16.77	
360.273	133.158	**-9.493**	14.980	133.158	-9.493	15553.50	S3/04	2.80	8.84	541.20	170.92	4.29	16.80	1.78		16.13	254.40		80.57	20.61		96.40	17.52	
359.396	133.618	**-8.904**	14.981	133.736	-8.907	16117.50	S3/05	2.80	8.77	531.67	169.66	4.32	16.69	1.89		16.02	251.19		79.87	20.21		87.73	16.89	
406.389	133.243	**-9.600**	18.082	133.246	-9.599	18259.50	S3/06	2.79	8.23	523.90	163.74	4.07	16.55	1.94		15.66	243.32		78.36	19.34		79.72	17.07	
408.863	132.548	**-10.398**	18.079	132.552	-10.396	18309.00	S3/07	2.76	8.47	525.29	165.24	3.85	16.72	1.84		15.26	243.55		79.80	16.83		72.45	16.03	
411.089	131.835	**-11.229**	18.083	131.835	-11.229	18307.00	S3/08	3.16	9.08	530.74	169.45	4.13	16.57	1.87		15.25	246.54		78.79	16.39		78.85	16.94	
411.808	131.129	**-12.052**	18.086	131.128	-12.053	18267.00	S3/09	3.14	9.04	523.98	166.35	3.88	16.53	1.82		15.10	240.98		78.75	17.11		72.35	17.02	
385.858	131.034	**-11.812**	17.184	131.034	-11.811	17545.00	S3/10	3.07	8.66	534.77	172.56	4.20	16.55	1.75		15.94	252.14		80.00	18.55		83.17	17.35	
383.912	132.379	**-10.272**	17.193	132.378	-10.273	17515.00	S3/12	3.24	8.65	527.25	169.40	4.31	16.53	1.78		15.58	248.59		79.40			73.03	17.01	
388.167	133.020	**-9.509**	17.186	133.021	-9.508	17523.50	S3/13	3.10	8.79	533.74	172.24	4.29	16.53	1.77		15.75	251.64		80.70	18.93		81.29	16.85	
384.743	133.621	**-8.785**	17.184	133.628	-8.787	17425.50	S3/14	3.03	9.10	545.20	179.95	4.35	16.85	1.80		16.19	257.75		82.48	19.58		96.66	19.04	
365.712	133.617	**-9.080**	15.914	133.616	-9.082	16401.00	S3/15	2.94	8.67	532.27	170.98	4.47	16.71	1.91		15.85	252.83		80.76	17.99		93.86	17.03	
367.272	133.082	**-9.730**	15.922	133.084	-9.728	16404.50	S3/20		8.10	479.44	155.72		14.90	1.81		14.34	227.25		73.02			55.63		
						S8 – 13-22°S	**Survey South 06.12.05**																	
374.836	131.547	**-14.483**	16.873	131.546	-14.480	17202.50	S8/01	3.10	8.59	532.05	169.66	4.22	16.48	1.81		15.56	250.39		79.38			91.40	16.73	
358.801	131.157	**-13.653**	13.291	131.170	-13.655	13943.00	S8/12	2.89	8.67	535.20	168.59	4.28	16.66	1.98		15.78	252.19		81.27			92.73	16.65	
						T3 – 5-13°N	**Tapao – Brunei 11.11.05**																	
380.875	103.457	**12.077**	17.078	103.451	12.077	17502.00	T3/12	3.11	8.75	532.82	173.12	4.49	16.63	1.95		15.67	249.42		79.14			92.17	15.70	
385.018	105.816	**11.164**	17.076	105.812	11.165	17471.00	T3/13	3.03	8.70	533.81	172.93	4.17	16.79	1.84		15.64	249.65		79.31			69.72	16.73	
405.320	108.048	**9.752**	17.980	108.043	9.754	18284.50	T3/14	2.66	8.45	527.63	168.28	3.99	16.51	1.82		15.42	243.01		76.35			80.60	15.34	
409.235	110.206	**8.224**	17.980	110.207	8.222	18285.50	T3/15	2.78	8.34	527.17	167.65	3.88	16.68	1.88		15.46	243.00		77.57			69.23	15.99	
417.842	112.225	**6.835**	18.018	112.227	6.834	12734.50	T3/17	3.07	8.80	525.35	168.77	4.31	17.01	2.02		15.59	248.18		78.64			76.90	16.53	
350.090	114.440	**5.526**	11.963	114.423	5.525	818.00	T3/18	3.18	8.76	532.56	171.30	4.48	16.67	1.84		15.76	253.79		81.81			81.00	18.51	
mean pot. T. [K]			**mean alt [m]**			**B42 5°S**	**Teresina**																	
1036.7			34000						7.82	103.85	102.85		13.28		71.84	9.65			7.84	0.87				0.41
907.8			31940						8.14	252.13	121.17		14.92		164.74	11.26	1.55		27.21	3.98				0.69
819.7			30010					0.71	8.29	353.42	130.82		15.35	1.19	170.94	12.02	14.32		43.85	7.45				0.66
751.1			28170					1.00	8.38	374.96	130.46		15.50	1.25	223.95	12.14	28.04		49.87	8.73		1.63		0.69
636.5			24950					1.84	8.48	435.46	125.12		15.06	1.48	241.37	11.69	87.54	0.54	43.57	8.76		12.51	4.82	0.66
577.8			23370					2.24	8.48	465.78	138.57		16.12	1.58	254.59	13.18	143.57		68.90	13.17		37.58	7.98	1.08
521.2			21640					2.55	8.73	492.75	142.15	1.93	16.39	1.70	182.89	13.66	187.86	1.13	72.49	14.62		58.54	9.96	1.32
437.7			18720					3.01	8.94	523.78	151.11	3.89	16.36	1.69	427.33	14.31	233.70	4.66	70.76	15.01	0.30	77.47	16.11	1.33
402.5			17370					3.25	8.76	530.37	152.64	3.90	16.58	1.94	459.82	14.39	243.90	5.28	78.05	16.65	0.35	75.52	18.08	1.48
371.1			16360					3.18	8.97	537.81	160.25	4.13	16.66	2.01	570.83	15.04	252.12	6.05	80.89	17.35	0.46	93.70	19.50	1.56
359.2			15200					3.19	8.82	538.73	163.96	4.17	16.65	2.05	600.92	15.27	254.80	6.68	80.89	18.05	0.43	93.45	19.22	1.61
						B43 5°S	**Teresina**																	
961.1			33160						7.67	102.35	99.74		13.34			10.90			7.73	0.85				0.32
912.3			32210						7.43	76.27	105.30		12.76			10.09	0.34		5.47	0.62				0.39
858.5			30900						7.68	82.16	106.08		12.89			10.24	0.40		5.91	0.59				0.43
832.5			30200						8.10	235.98	123.36		14.36	0.72		11.04	2.02		24.83	3.47				0.54
765.9			28630					0.76	8.40	351.31	127.01		15.18	1.15		12.24	16.69		44.39	7.10				0.61
652.1			25220					1.52	8.64	428.92	140.79		15.69	1.39		12.95	78.87		60.27	11.89			4.15	0.74
578.9			23320					2.20	8.61	456.62	134.89		15.06	1.49		12.18	126.11		59.81	12.18			5.67	0.89
524.2			21770					2.52	8.85	484.61	144.33	1.67	15.81	1.83		12.94	171.12		66.42	13.74			9.85	1.02
461.9			20190					2.74	8.91	514.08	156.61	3.03	16.64	1.82		14.38	225.04		77.21	16.58	0.31		15.35	1.37
431.6			18870					2.82	8.75	521.69	158.16	3.48	16.87	1.85		14.61	237.00		78.71	16.46	0.34		9.47	1.53
414.2			17350					2.99	8.99	533.13	162.08	4.04	16.53	1.83		15.00	246.11		80.13	17.75	0.45		15.69	1.40
380.4			16400					3.10	8.87	532.95	160.98	4.18	16.37	1.98		14.50	247.09		76.26	6.37	0.35			1.42
360.8			15200					3.08	8.90	535.52	164.66	4.22	16.59	1.78		14.99	251.59		80.61	18.31	0.41		13.67	1.48

Figure A.6. Mixing ratios [ppt] of long-lived halocarbons in the TTL and tropical stratosphere.

pot. Temp. [K]	altitude [km]	SF6 mean age [years]	fractional release factors																
			H1301	F115	F12	F22	H1211	F114	F114a	CH3Cl	F142b	F11	CH3Br	F113	F141b	H2402	CCl4	CH3CCl3	F124
B42 (June 2005, Teresina, 5 °S)																			
1036.7	34.00	4.32	1.0	0.08	0.81	0.29	1.0	0.19	1.0	0.88	0.19	1.00	1.00	0.91	0.93	1.0	1.00	1.00	0.63
907.8	31.94	3.59	1.0	0.05	0.53	0.19	1.0	0.10	1.0	0.73	0.11	0.99	1.00	0.67	0.72	1.0	1.00	1.00	0.42
819.7	30.01	3.18	0.75	0.03	0.34	0.14	1.0	0.07	0.37	0.72	0.07	0.94	1.00	0.47	0.49	1.0	1.00	0.98	0.46
751.1	28.17	3.18	0.65	0.02	0.30	0.14	1.0	0.06	0.34	0.63	0.06	0.89	1.00	0.40	0.40	1.0	0.98	1.00	0.43
636.5	24.95	2.73	0.35	0.02	0.19	0.19	1.0	0.09	0.22	0.60	0.12	0.66	0.94	0.47	0.42	1.0	0.87	0.85	0.48
577.8	23.37	2.37	0.22	0.02	0.13	0.11	1.0	0.03	0.17	0.58	0.03	0.44	1.00	0.16	0.16	1.0	0.61	0.74	0.17
521.2	21.64	1.78	0.11	0.00	0.08	0.10	0.53	0.01	0.11	0.70	0.03	0.27	0.86	0.11	0.10	1.0	0.39	0.63	0.03
437.7	18.72	0.76	-0.03	-0.02	0.02	0.08	0.06	0.01	0.12	0.29	0.03	0.08	0.41	0.13	0.13	0.27	0.20	0.27	0.09
402.5	17.37	0.72	-0.11	0.00	0.01	0.07	0.06	0.00	-0.01	0.23	0.02	0.04	0.33	0.04	0.03	0.15	0.22	0.17	-0.01
371.1	16.36	0.34	-0.09	-0.02	-0.01	0.04	0.01	0.00	-0.05	0.05	-0.01	0.00	0.23	0.00	0.01	-0.11	0.03	0.04	-0.04
359.2	15.20	0.22	-0.09	0.00	-0.01	0.02	0.00	0.00	-0.07	0.00	-0.02	-0.01	0.15	0.00	-0.03	-0.02	0.03	0.03	-0.06
B43 (June 2005, Teresina, 5 °S)																			
978.6	33.62	4.53	1.0	0.12	0.86	0.27	1.0	0.23	1.0		0.14	1.00	-0.57	0.93	0.95	1.0		1.00	0.52
961.1	33.16	4.76	1.0	0.10	0.85	0.28	1.0	0.22	1.0		0.17	1.00	0.76	0.93	0.96	1.0		1.00	0.72
912.3	32.21	4.59	1.0	0.09	0.81	0.30	1.0	0.19	1.0		0.06	1.00	1.00	0.91	0.93	1.0		1.00	0.63
858.5	30.90	3.96	1.0	0.05	0.56	0.17	1.0	0.13	0.62		0.11	0.99	1.00	0.70	0.75	1.0		1.00	0.63
832.5	30.20	3.83	1.0	0.02	0.42	0.15	1.0	0.08	0.54		0.03	0.98	1.00	0.58	0.60	1.0		1.00	0.50
765.9	28.63	3.55	0.73	0.02	0.34	0.15	1.0	0.08	0.40		0.03	0.94	1.00	0.46	0.50	1.0		1.00	0.49
652.1	25.22	3.02	0.46	-0.01	0.20	0.08	1.0	0.05	0.27		0.01	0.69	0.66	0.27	0.20	1.0		0.88	0.40
578.9	23.32	2.48	0.23	0.00	0.15	0.13	1.0	0.09	0.22		0.10	0.51	0.87	0.27	0.22	1.0		0.82	0.31
524.2	21.77	2.01	0.12	-0.02	0.09	0.08	0.59	0.05	0.04		0.07	0.33	1.00	0.19	0.14	1.0		0.65	0.24
461.9	20.19	1.21	0.05	-0.02	0.04	0.03	0.27	0.00	0.05		0.00	0.12	0.40	0.05	0.02	0.25		0.36	0.04
431.6	18.87	0.99	0.03	0.00	0.02	0.03	0.16	-0.02	0.03		0.00	0.07	1.00	0.03	0.03	0.19		0.59	-0.06
414.2	17.35	0.64	-0.03	-0.02	0.00	0.02	0.03	0.00	0.04		-0.01	0.03	0.73	0.01	-0.03	-0.08		0.26	0.05
380.4	16.40	0.27	-0.06	0.00	0.00	0.03	0.00	0.01	-0.03		0.04	0.02	1.00	0.06	0.64	0.15		1.00	0.06
360.8	15.20	0.40	-0.05	-0.01	0.00	0.01	-0.02	0.00	0.07		0.00	0.01	1.00	0.00	-0.05	0.02		0.33	0.02
C1 (October 2006, Air Sur l'Adour, 44 °N)																			
	24.00	4.48	0.68		0.43	0.19	1.0					0.84		0.52	0.49	1.0	0.93	1.00	
	22.00	4.39	0.53		0.36	0.17	1.0					0.70		0.44	0.39	1.0	0.80	0.88	
	18.00	2.58	0.17		0.15	0.06	0.43					0.30		0.19	0.15	0.45	0.32	0.56	
	14.01	0.03	-0.06		-0.01	-0.02	0.01					0.01		0.01	-0.03	0.03	0.08	0.02	
	13.00	-0.07	-0.07		-0.01	-0.03	0.02					0.00		0.01	-0.02	0.07	0.10	0.04	
	12.00	0.03	-0.11		-0.02	-0.03	0.07					0.00		0.01	-0.03	0.07	0.08	0.03	
R3a (16.12.05, Dubai – Lacarnaca, 25-33°N, mean age from B42/B43 correlation with F12)																			
403.6	17.27	0.74	-0.07			0.03	0.00				0.02	0.02		0.03			0.10	0.05	
406.8	17.27	0.59	-0.20			0.03	0.02				0.03	0.02		0.02			0.06	0.00	
409.7	17.24	0.93	0.03			0.03	0.01				0.01	0.04		0.04			0.18	0.07	
422.0	17.78	0.62	-0.01			0.02	-0.06				0.02	0.02		0.03			0.14	0.00	
432.7	17.73	0.77	0.00			0.03	0.02				0.02	0.03		0.04			0.17	0.07	
432.6	17.71	1.83	0.03			0.06	0.20				0.04	0.15		0.10			0.22	0.29	
R3b (17.12.05, Lacarnaca – Oberpfaffenhofen, 35-43°N, mean age from B42/B43 correlation with F12)																			
429.5	17.08	1.65	0.15			0.04	0.14				0.04	0.12		0.09			0.24	0.28	
425.6	16.95	3.11	0.32			0.13	0.62				0.04	0.47		0.32			0.54	0.65	
431.4	16.86	2.41	0.11			0.07	0.30				0.07	0.25		0.19			0.44	0.47	
423.6	16.82	2.27	0.15			0.06	0.30				0.07	0.24		0.16			0.40	0.41	
429.7	16.81	1.71	0.10			0.05	0.25				0.03	0.15		0.11			0.32	0.32	
426.6	16.76	2.23	0.12			0.08	0.33				0.07	0.23		0.16			0.35	0.45	
420.7	16.70	2.79	0.23			0.12	0.45				0.10	0.34		0.23			0.44	0.55	
S3 (23.11.05, Survey Indonesia, 8-12°S, mean age from B42/B43 correlation with F12)																			
361.7	15.54	0.53	0.03	0.00	0.00	0.03	-0.03	0.00	0.02		0.01	0.00		0.00	-0.12		0.15	-0.04	
361.7	15.55	0.71	0.03	0.05	0.01	0.03	-0.03	-0.02	-0.01		0.02	-0.01		0.00	-0.11		0.16	0.01	
360.3	15.55	0.07	0.07	-0.02	-0.02	0.04	-0.03	-0.02	0.05		0.00	-0.02		-0.01	-0.15		0.09	-0.18	
359.4	16.12	0.48	0.07	-0.02	0.00	0.03	-0.04	-0.02	-0.01		-0.01	-0.01		0.00	-0.13		0.16	-0.05	
406.4	18.26	0.78	0.06	0.04	0.02	0.05	0.02	-0.01	-0.04		0.00	0.03		0.02	-0.09		0.23	0.00	
408.9	18.31	0.73	0.07	0.01	0.01	0.05	0.08	-0.02	0.02		0.03	0.03		0.00	0.05		0.30	0.05	
411.1	18.31	0.51	-0.06	-0.06	0.00	0.03	0.01	-0.01	0.00		0.04	0.01		0.02	0.08		0.24	-0.04	
411.8	18.27	0.78	-0.05	-0.05	0.02	0.04	0.07	-0.01	0.03		0.04	0.04		0.02	0.04		0.30	0.00	
385.9	17.55	0.35	-0.02	-0.01	-0.01	0.02	-0.01	-0.01	0.06		0.00	-0.01		0.00	-0.04		0.21	-0.10	
383.9	17.52	0.65	-0.09	-0.01	0.01	0.02	-0.03	-0.01	0.05		0.01	0.01		0.01			0.30	-0.02	
388.2	17.52	0.39	-0.04	-0.02	0.00	0.02	-0.03	-0.01	0.06		0.01	-0.01		-0.01	-0.06		0.22	-0.06	
384.7	17.43	-0.11	0.00	-0.05	-0.03	-0.01	-0.04	-0.02	0.04		0.01	-0.04		-0.04	-0.09		0.10	-0.33	
365.7	16.40	0.45	0.02	-0.01	0.00	0.02	-0.07	-0.02	-0.02		0.00	-0.01		-0.01	-0.01		0.10	-0.06	
S8 (06.12.05, Survey South, 13-22°S, mean age from tropical correlation with F12)																			
374.8	17.20	0.46	-0.03	0.00	0.00	0.03	-0.01	0.00	0.03		0.02	0.00		0.01			0.13	-0.04	
383.9	17.39	0.59	0.02	0.01	0.01	0.02	0.00	-0.01	-0.07		0.02	0.00		0.02			0.19	-0.02	
387.3	17.41	0.59	0.02	0.02	0.01	0.04	0.02	-0.01	-0.02		0.03	0.02		0.02			0.27	0.05	
411.0	18.22	1.21	0.11	0.02	0.04	0.05	0.08	-0.02	-0.02		0.04	0.09		0.06			0.31	0.16	
407.2	18.24	1.24	0.05	0.05	0.04	0.04	0.02	-0.01	0.07		0.05	0.09		0.06			0.43	0.18	
358.8	15.15	0.49	0.00	-0.02	0.00	0.04	-0.07	-0.02	0.01		0.02	-0.01		-0.04			0.36	-0.09	
435.6	18.61	1.66	0.08	0.00	0.07	0.04	0.18	-0.01	0.09		0.01	0.14		0.09			0.41	0.23	
441.3	19.09	2.21	0.09	-0.01	0.12	0.07	0.25	0.00	0.12		0.04	0.21		0.13			0.44	0.36	
434.0	19.26	1.89	0.06	0.01	0.09	0.06	0.24	0.00	0.07		0.05	0.17		0.10			0.22	0.28	
450.4	19.64	1.80	0.12	0.01	0.08	0.06	0.32	0.00	0.08		0.05	0.18		0.09			0.45	0.24	
358.8	13.94	0.33	0.04	-0.01	-0.01	0.04	-0.03	-0.01	-0.06		0.01	-0.01		-0.02			0.12	-0.06	
T3 (11.11.05, Tapao – Brunei, 5-13°N, mean age from tropical correlation with F12)																			
380.9	17.50	0.43	-0.04	-0.02	0.00	0.01	-0.08	-0.01	-0.04		0.02	0.00		0.01			0.12	0.02	
385.0	17.47	0.39	-0.01	-0.01	0.00	0.01	0.00	-0.02	0.02		0.02	0.00		0.01			0.33	-0.06	
405.3	18.28	0.64	0.11	0.02	0.01	0.03	0.04	0.00	0.02		0.02	0.03		0.05			0.22	0.08	
409.2	18.29	0.66	0.07	0.03	0.01	0.03	0.07	-0.02	0.00		0.02	0.03		0.03			0.33	0.04	
417.8	12.73	0.73	-0.03	-0.03	0.01	0.02	-0.03	-0.04	-0.08		0.01	0.01		0.02			0.26	0.02	

Figure A.7. Fractional release factors of long-lived halocarbons in the lower and middle mid-latitude and tropical stratosphere.

Figure set A.S.1. Identification: EI-SIM-MS.

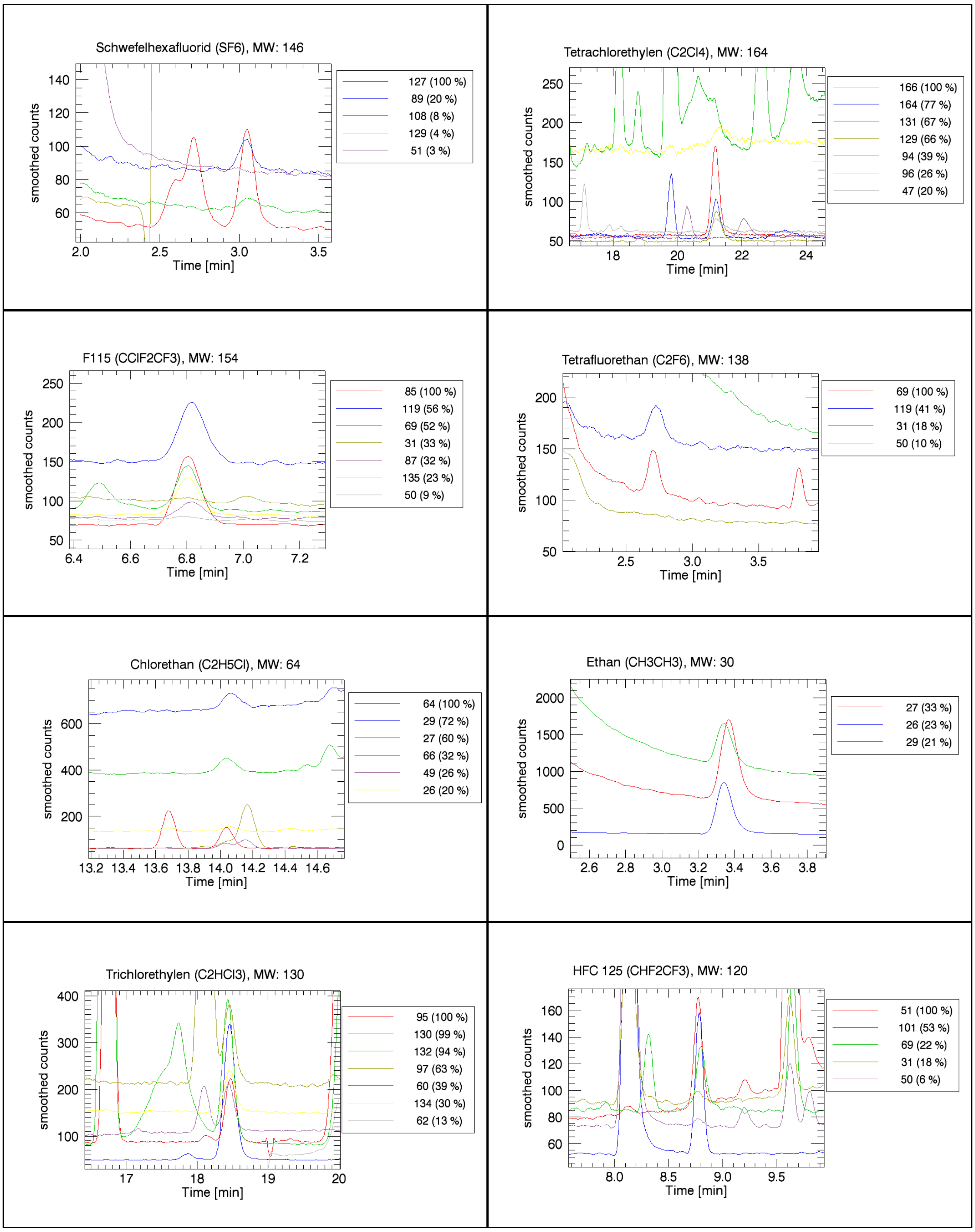

Tetrafluorpopan (C3F8), MW: 188

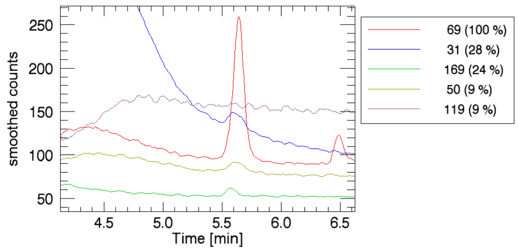

Propan (CH3CH2CH3), MW: 44

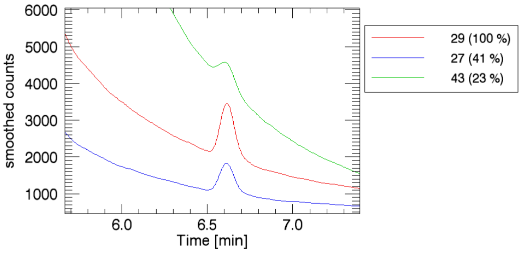

Tetrachlormethan (CCl4), MW: 152

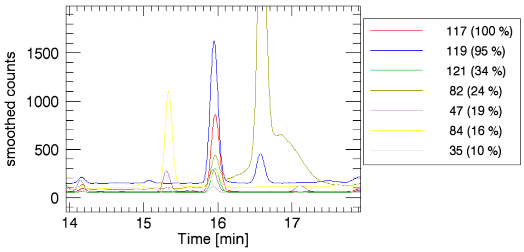

H2402 (CBrF2CBrF2), MW: 258

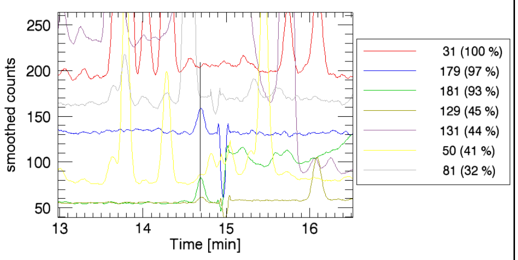

F12 (CF2Cl2), MW: 120

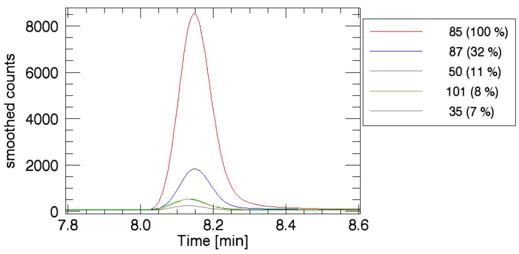

H1211 (CBrClF2), MW: 164

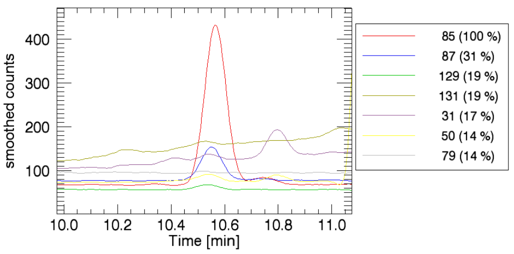

F114 (CClF2CClF2), MW: 170

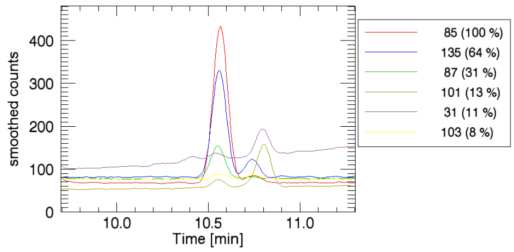

F113 (CCl2FCClF2), MW: 186

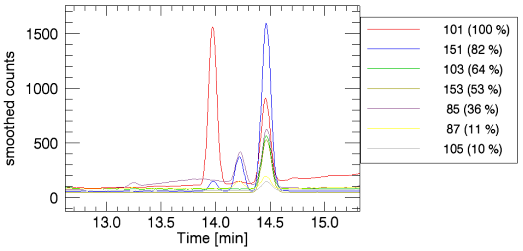

H1301 (CBrF3), MW: 148

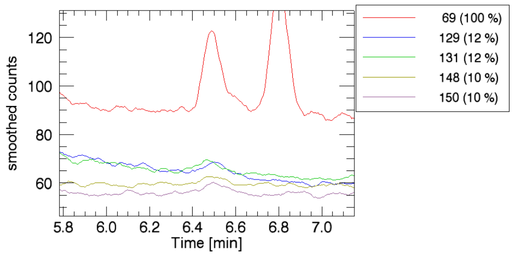

F114a (CCl2FCF3), MW: 170

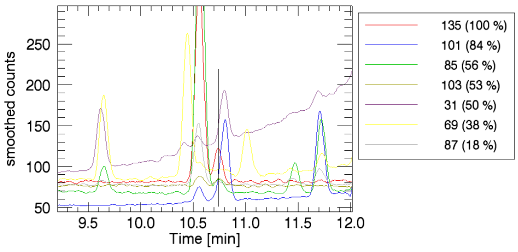

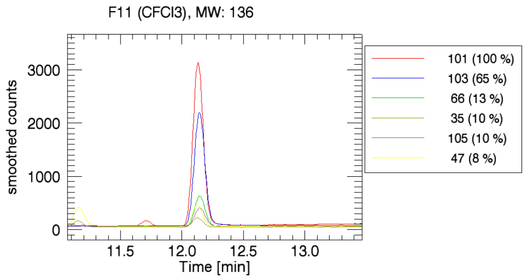
F11 (CFCl3), MW: 136
smoothed counts
3000
2000
1000
0
11.5
12.0
12.5
13.0
Time [min]
101 (100 %)
103 (65 %)
66 (13 %)
35 (10 %)
105 (10 %)
47 (8 %)

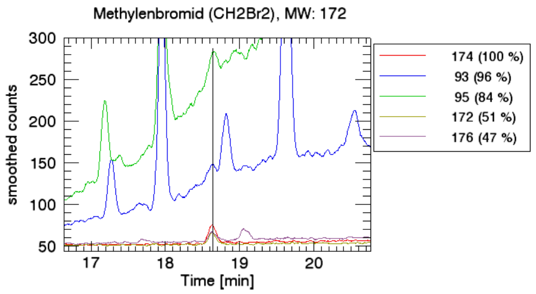
Methylenbromid (CH2Br2), MW: 172
smoothed counts
300
250
200
150
100
50
17
18
19
20
Time [min]
174 (100 %)
93 (96 %)
95 (84 %)
172 (51 %)
176 (47 %)

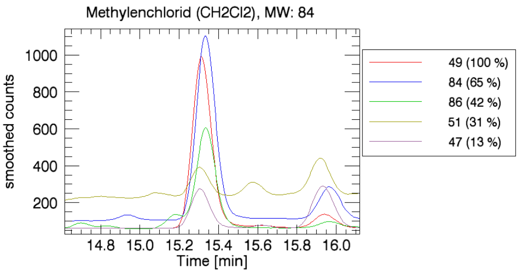
Methylenchlorid (CH2Cl2), MW: 84
smoothed counts
1000
800
600
400
200
14.8
15.0
15.2
15.4
15.6
15.8
16.0
Time [min]
49 (100 %)
84 (65 %)
86 (42 %)
51 (31 %)
47 (13 %)

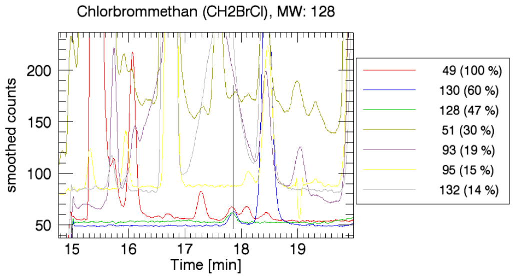
Chlorbrommethan (CH2BrCl), MW: 128
smoothed counts
200
150
100
50
15
16
17
18
19
Time [min]
49 (100 %)
130 (60 %)
128 (47 %)
51 (30 %)
93 (19 %)
95 (15 %)
132 (14 %)

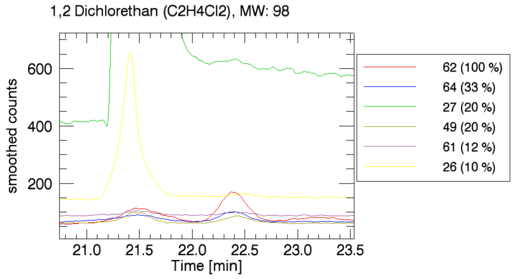
1,2 Dichlorethan (C2H4Cl2), MW: 98
smoothed counts
600
400
200
21.0
21.5
22.0
22.5
23.0
23.5
Time [min]
62 (100 %)
64 (33 %)
27 (20 %)
49 (20 %)
61 (12 %)
26 (10 %)

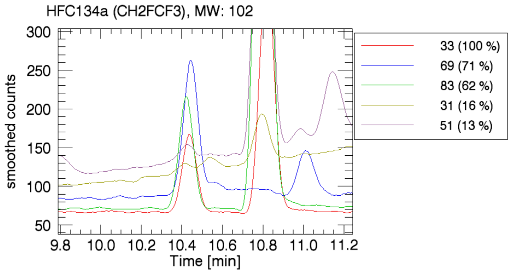
HFC134a (CH2FCF3), MW: 102
smoothed counts
300
250
200
150
100
50
9.8
10.0
10.2
10.4
10.6
10.8
11.0
11.2
Time [min]
33 (100 %)
69 (71 %)
83 (62 %)
31 (16 %)
51 (13 %)

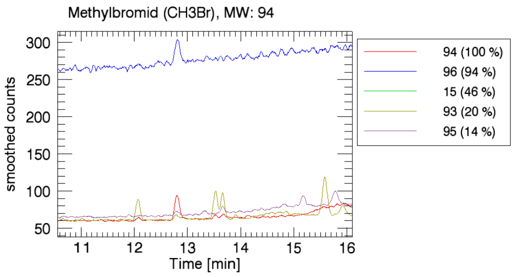
Methylbromid (CH3Br), MW: 94
smoothed counts
300
250
200
150
100
50
11
12
13
14
15
16
Time [min]
94 (100 %)
96 (94 %)
15 (46 %)
93 (20 %)
95 (14 %)

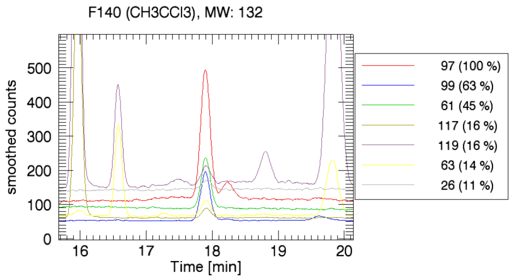
F140 (CH3CCl3), MW: 132
smoothed counts
500
400
300
200
100
0
16
17
18
19
20
Time [min]
97 (100 %)
99 (63 %)
61 (45 %)
117 (16 %)
119 (16 %)
63 (14 %)
26 (11 %)

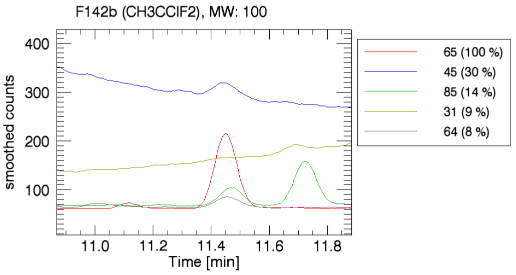
F142b (CH3CClF2), MW: 100
smoothed counts
400
300
200
100
11.0
11.2
11.4
11.6
11.8
Time [min]
65 (100 %)
45 (30 %)
85 (14 %)
31 (9 %)
64 (8 %)

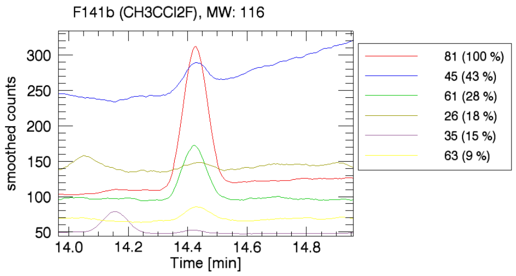
F141b (CH3CCl2F), MW: 116
smoothed counts
300
250
200
150
100
50
14.0
14.2
14.4
14.6
14.8
Time [min]
81 (100 %)
45 (43 %)
61 (28 %)
26 (18 %)
35 (15 %)
63 (9 %)

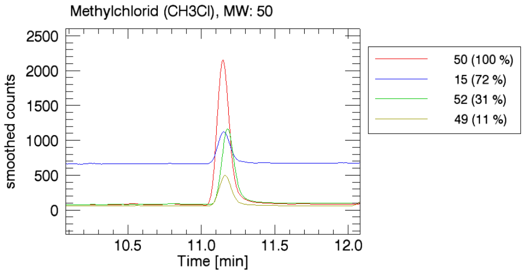
Methylchlorid (CH3Cl), MW: 50

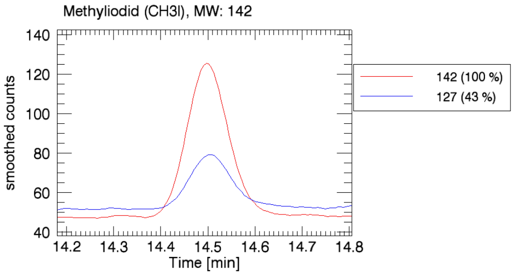
Methyliodid (CH3I), MW: 142

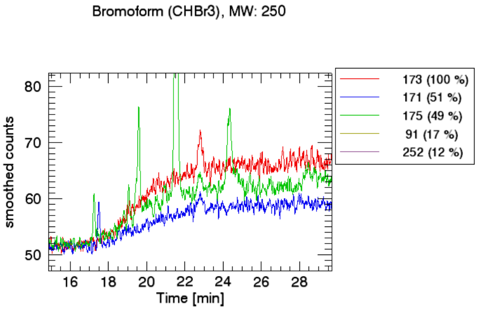
Bromoform (CHBr3), MW: 250

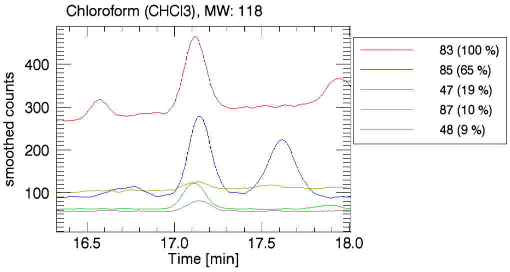
Chloroform (CHCl3), MW: 118

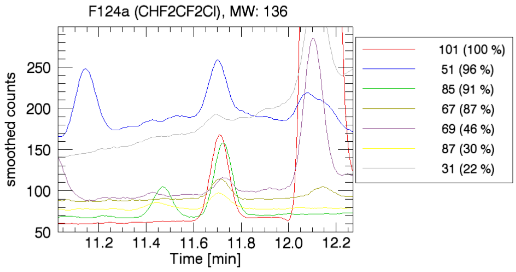
F124a (CHF2CF2Cl), MW: 136

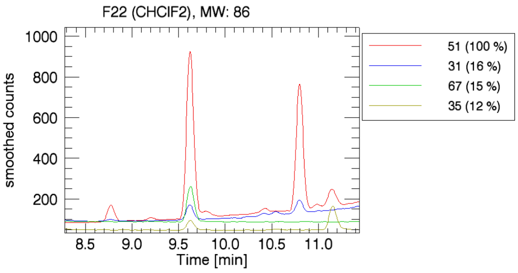
F22 (CHClF2), MW: 86

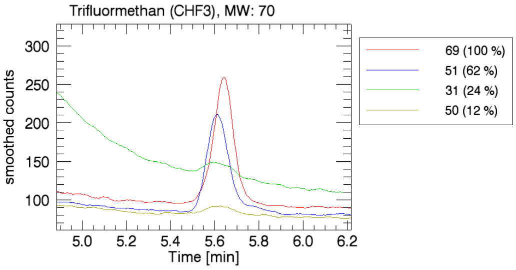
Trifluormethan (CHF3), MW: 70

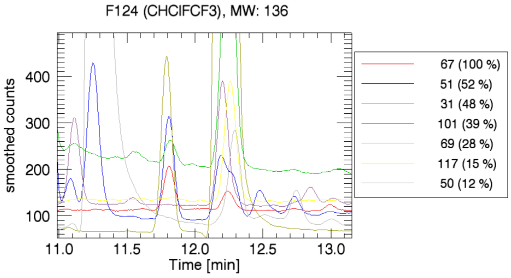
F124 (CHClFCF3), MW: 136

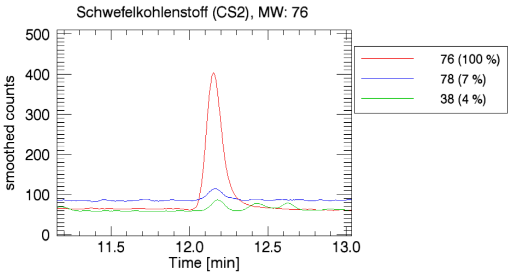
Schwefelkohlenstoff (CS2), MW: 76

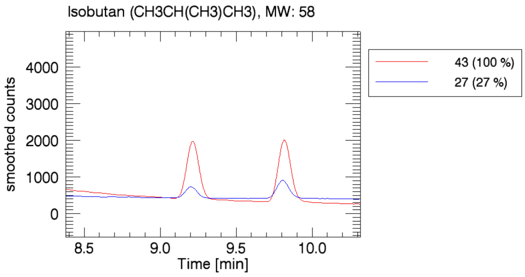
Isobutan (CH3CH(CH3)CH3), MW: 58

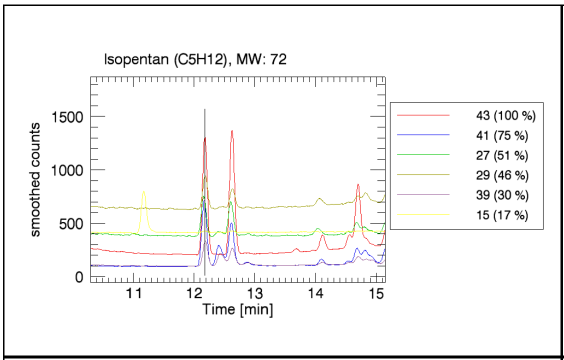

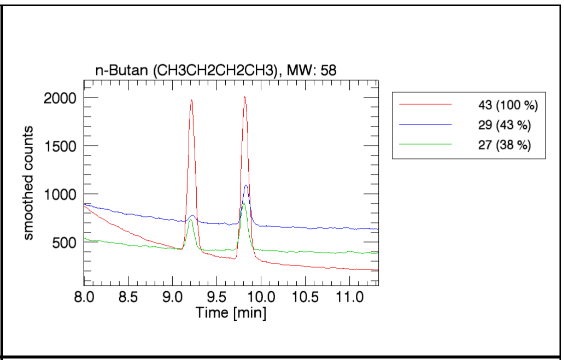

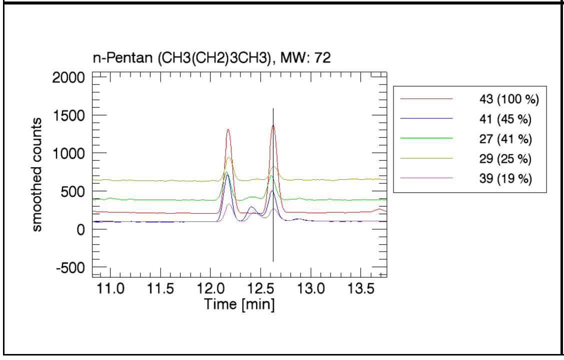

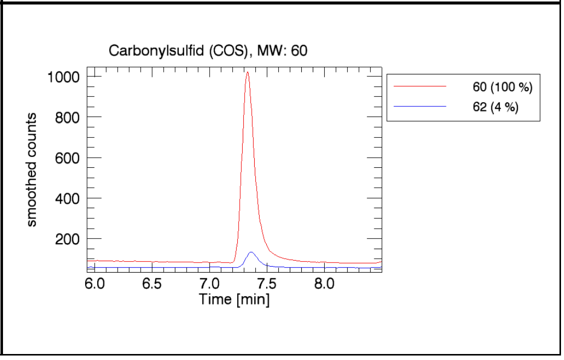

Figure set A.S.2. Identification: EI-Scan-MS.

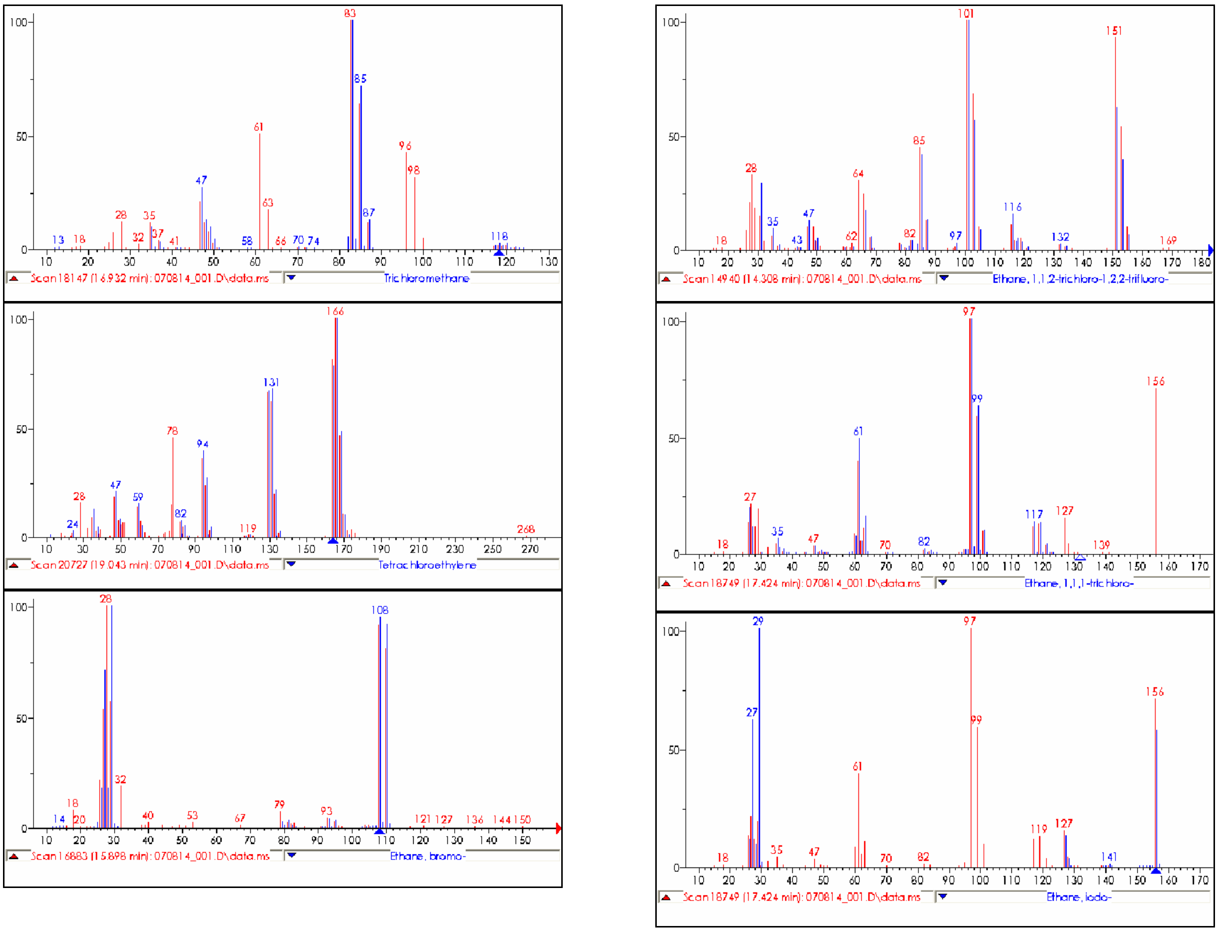

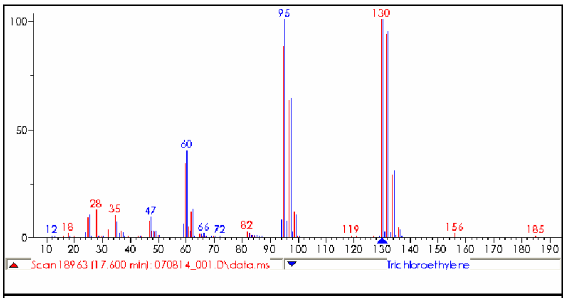
100
50
0
95
130
60
28
35
47
12 18
66 72
82
119
156
185
Scan 18963 (17.600 min): 070814_001.D\data.ms
Trichloroethylene

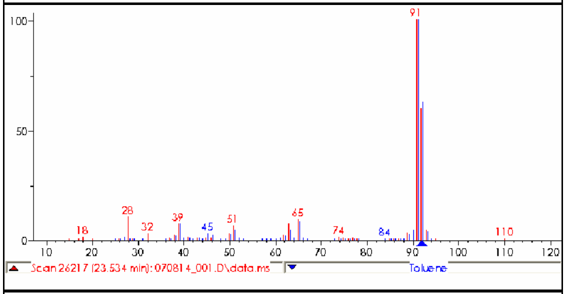
100
50
0
91
18
28
32
39
45
51
65
74
84
110
Scan 26217 (23.534 min): 070814_001.D\data.ms
Toluene

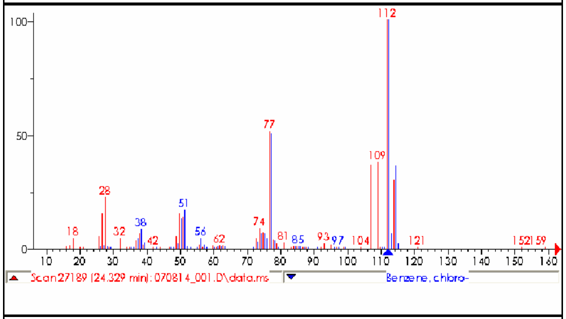
100
50
0
112
77
109
28
18
32
38
42
51
56
62
74
81 85
93 97
104
121
152 159
Scan 27189 (24.329 min): 070814_001.D\data.ms
Benzene, chloro-

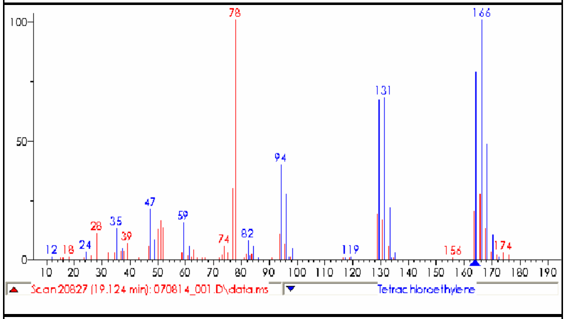
100
50
0
78
166
131
94
47
28
35
39
59
12 18 24
74
82
119
156
174
Scan 20827 (19.124 min): 070814_001.D\data.ms
Tetrachloroethylene

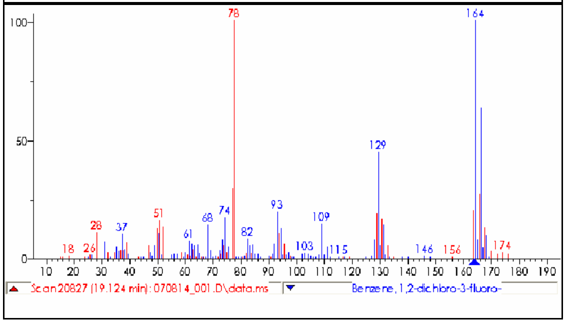
100
50
0
78
164
129
28
37
51
61
68
74
82
93
103
109
115
18 26
146 156
174
Scan 20827 (19.124 min): 070814_001.D\data.ms
Benzene, 1,2-dichloro-3-fluoro-

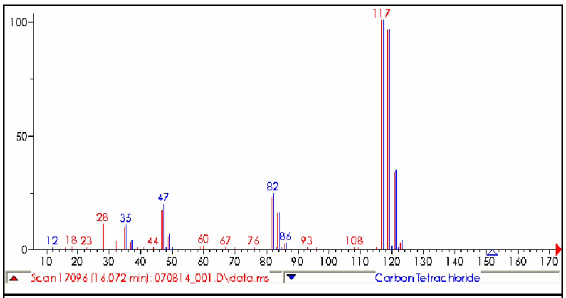
100
50
0
117
82
47
28
35
12 18 23
44
60 67 76
86 93
108
Scan 17096 (16.072 min): 070814_001.D\data.ms
Carbon Tetrachloride

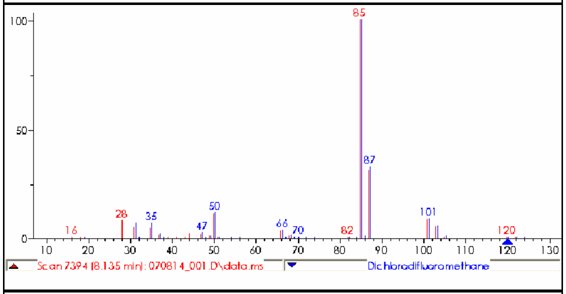
100
50
0
85
87
101
16
28
35
47
50
66 70
82
120
Scan 7394 (8.135 min): 070814_001.D\data.ms
Dichlorodifluoromethane

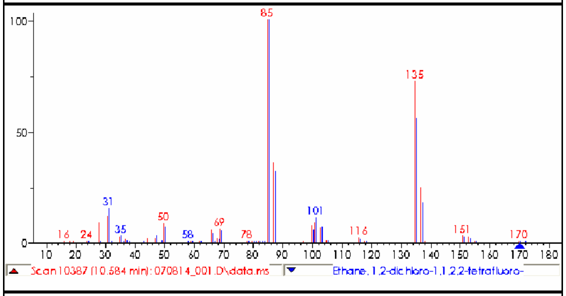
100
50
0
85
135
31
16 24
35
50
58
69
78
101
116
151
170
Scan 10387 (10.584 min): 070814_001.D\data.ms
Ethane, 1,2-dichloro-1,1,2,2-tetrafluoro-

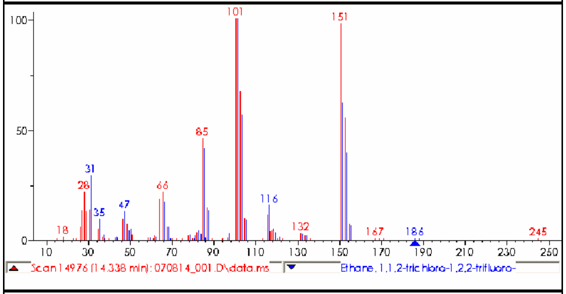
100
50
0
101
151
85
31
28
35
47
66
116
18
132
167
186
245
Scan 14976 (14.338 min): 070814_001.D\data.ms
Ethane, 1,1,2-trichloro-1,2,2-trifluoro-

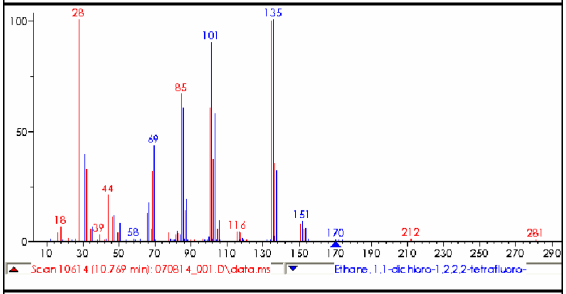
100
50
0
28
135
101
85
69
44
18
39
58
116
151
170
212
281
Scan 10614 (10.769 min): 070814_001.D\data.ms
Ethane, 1,1-dichloro-1,2,2,2-tetrafluoro-

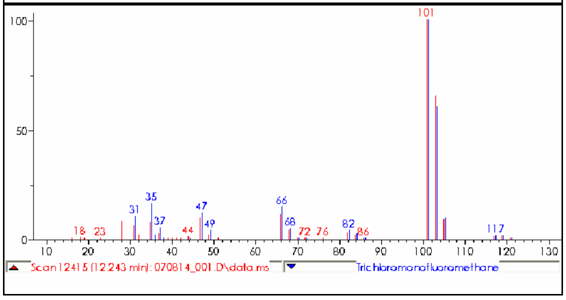
100
50
0
101
35
31
37
47
49
66
68
18 23
44
72 76
82
86
117
Scan 12415 (12.243 min): 070814_001.D\data.ms
Trichloromonofluoromethane

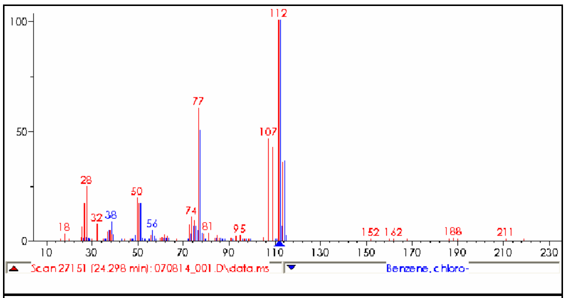
100
50
0
18
28
32
38
50
56
74
77
81
95
107
112
152 162
188
211
10 30 50 70 90 110 130 150 170 190 210 230
Scan 27151 (24.298 min): 070814_001.D\data.ms
Benzene, chloro-

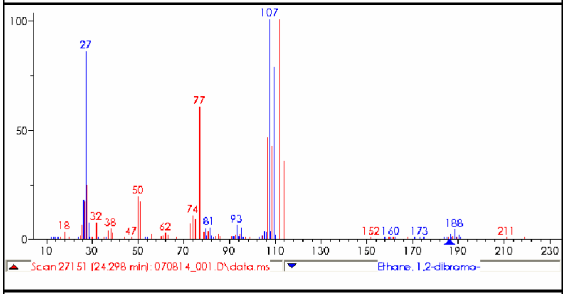
100
50
0
18
27
32
38
47
50
62
74
77
81
93
107
152 160
173
188
211
10 30 50 70 90 110 130 150 170 190 210 230
Scan 27151 (24.298 min): 070814_001.D\data.ms
Ethane, 1,2-dibromo-

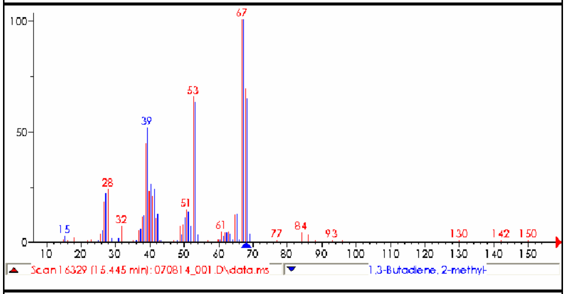
100
50
0
15
28
32
39
51
53
61
67
77
84
93
130
142
150
10 20 30 40 50 60 70 80 90 100 110 120 130 140 150
Scan 16329 (15.445 min): 070814_001.D\data.ms
1,3-Butadiene, 2-methyl-

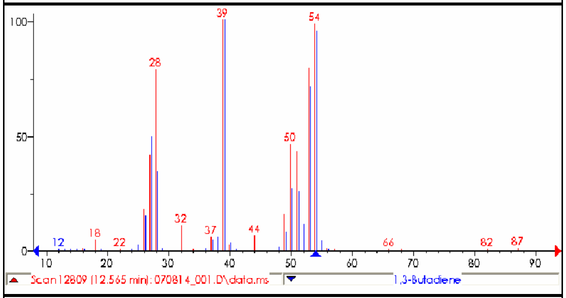
100
50
0
12
18
22
28
32
37
39
44
50
54
66
82
87
10 20 30 40 50 60 70 80 90
Scan 12809 (12.565 min): 070814_001.D\data.ms
1,3-Butadiene

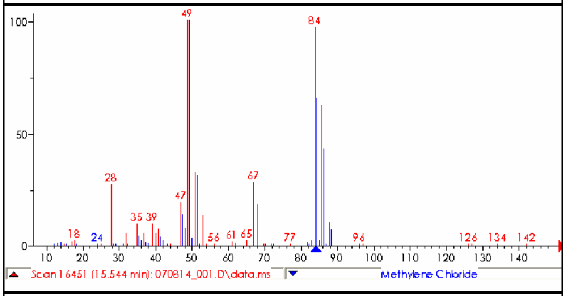
100
50
0
18
24
28
35 39
47
49
56
61 65
67
77
84
96
126
134
142
10 20 30 40 50 60 70 80 90 100 110 120 130 140
Scan 16451 (15.544 min): 070814_001.D\data.ms
Methylene Chloride

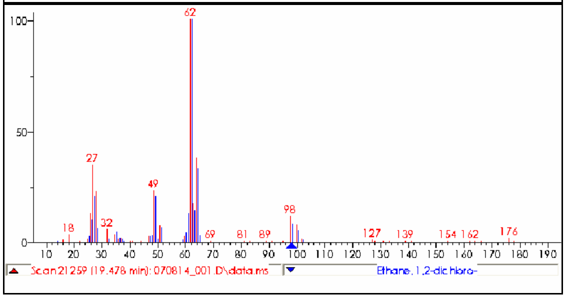
100
50
0
18
27
32
49
62
69
81
89
98
127
139
154 162
176
10 20 30 40 50 60 70 80 90 100 110 120 130 140 150 160 170 180 190
Scan 21259 (19.478 min): 070814_001.D\data.ms
Ethane, 1,2-dichloro-

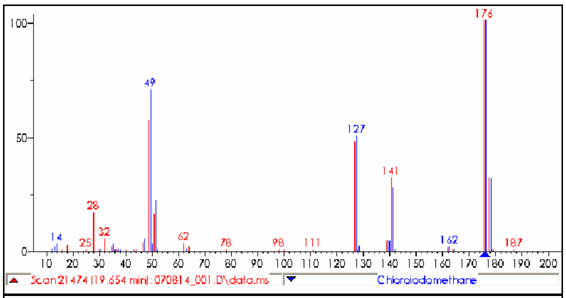
100
50
0
14
25
28
32
49
62
78
98
111
127
141
162
176
187
10 20 30 40 50 60 70 80 90 100 110 120 130 140 150 160 170 180 190 200
Scan 21474 (19.654 min): 070814_001.D\data.ms
Chloroiodomethane

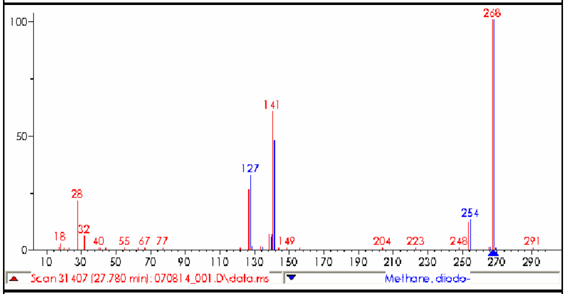
100
50
0
18
28
32
40
55
67
77
127
141
149
204
223
248
254
268
291
10 30 50 70 90 110 130 150 170 190 210 230 250 270 290
Scan 31407 (27.780 min): 070814_001.D\data.ms
Methane, diiodo-

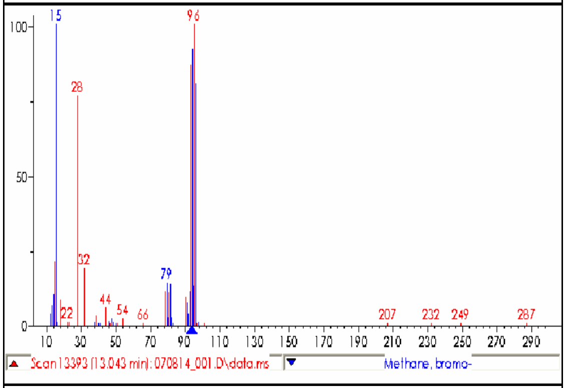
100
50
0
15
22
28
32
44
54
66
79
96
207
232
249
287
10 30 50 70 90 110 130 150 170 190 210 230 250 270 290
Scan 13393 (13.043 min): 070814_001.D\data.ms
Methane, bromo-

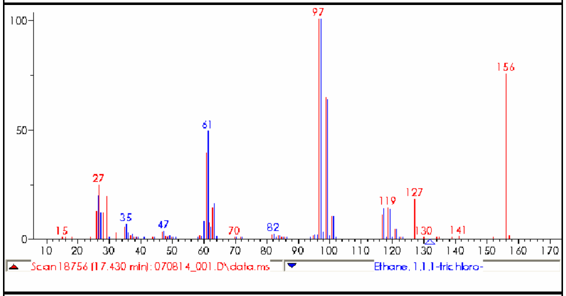
100
50
0
15
27
35
47
61
70
82
97
119
127
130
141
156
10 20 30 40 50 60 70 80 90 100 110 120 130 140 150 160 170
Scan 18756 (17.430 min): 070814_001.D\data.ms
Ethane, 1,1,1-trichloro-

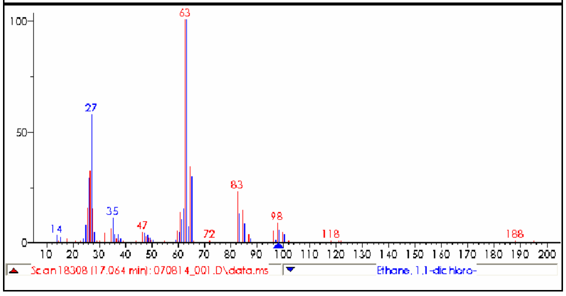
100
50
0
14
27
35
47
63
72
83
98
118
188
10 20 30 40 50 60 70 80 90 100 110 120 130 140 150 160 170 180 190 200
Scan 18308 (17.064 min): 070814_001.D\data.ms
Ethane, 1,1-dichloro-

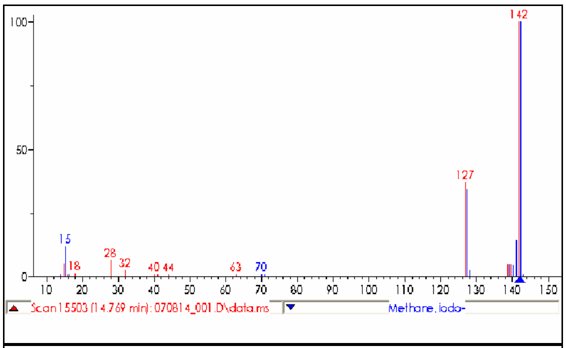

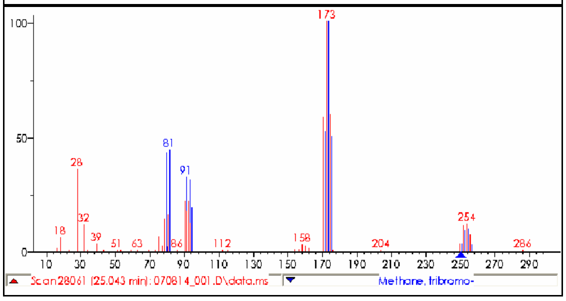

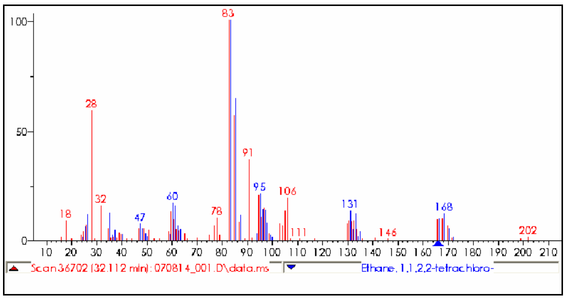

Figure set A.S.3. Identification: NICI-SIM-MS.

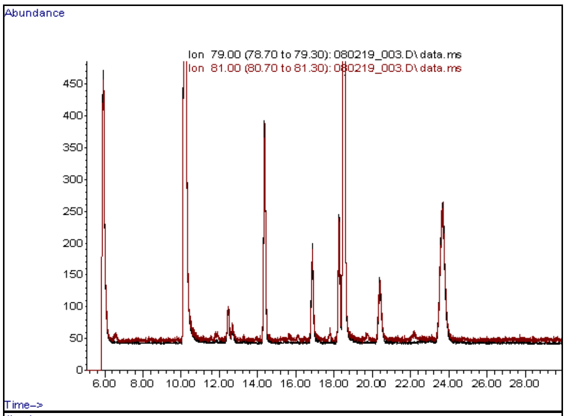

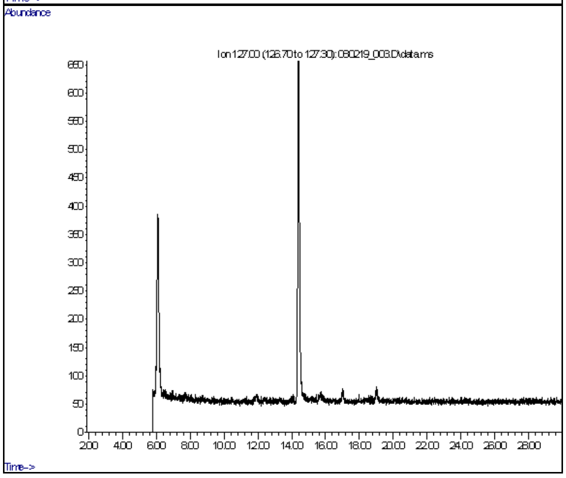

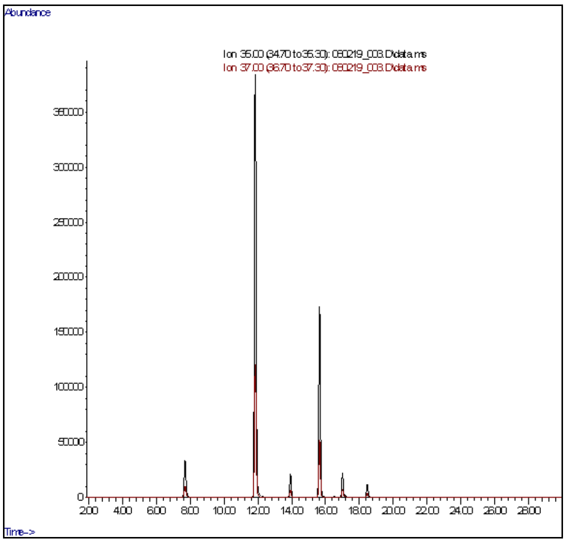

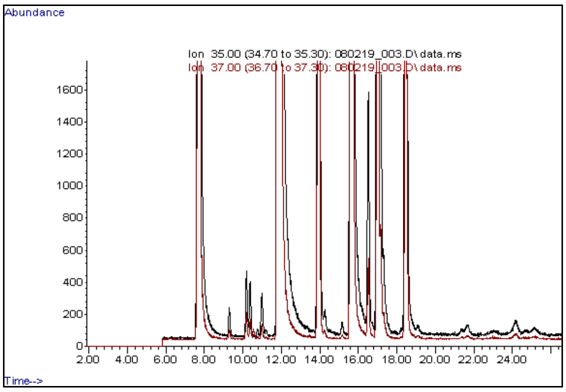

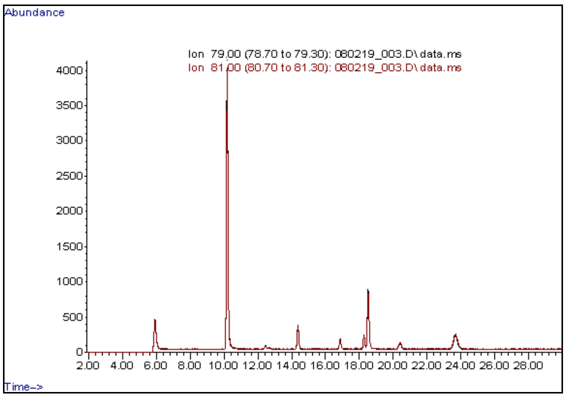

Figure set A.S.4. Identification confirmation: EI-SIM-MS.

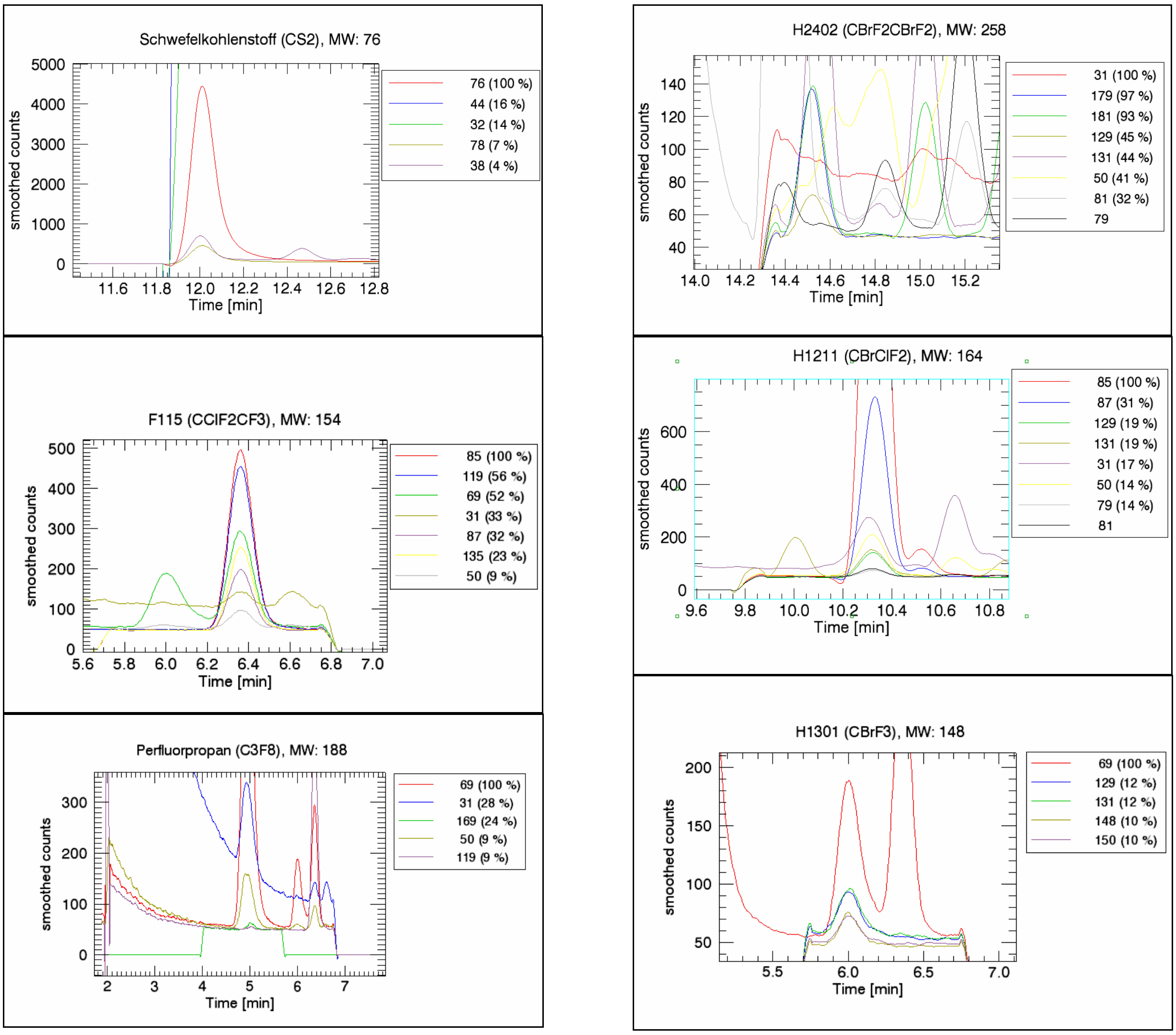
Schwefelkohlenstoff (CS2), MW: 76

H2402 (CBrF2CBrF2), MW: 258

F115 (CClF2CF3), MW: 154

H1211 (CBrClF2), MW: 164

Perfluorpropan (C3F8), MW: 188

H1301 (CBrF3), MW: 148

Methylenbromid (CH2Br2), MW: 172

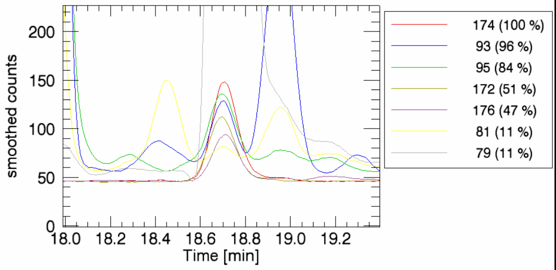

HFC134a (CH2FCF3), MW: 102

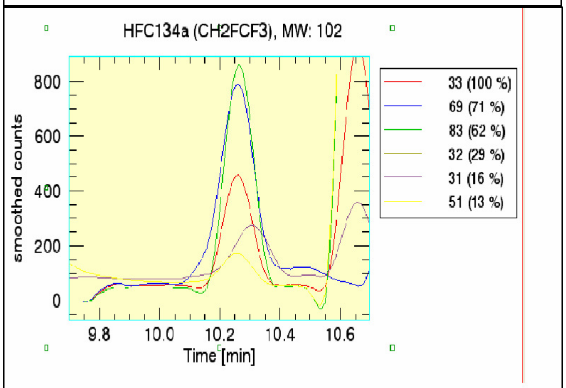

F142b (CH3CClF2), MW: 100

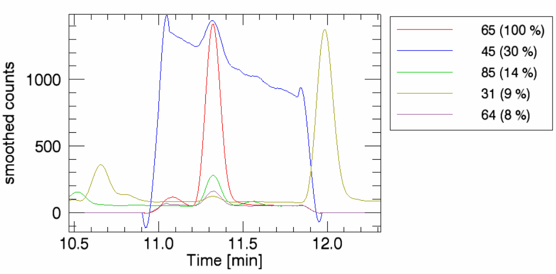

F141b (CH3CCl2F), MW: 116

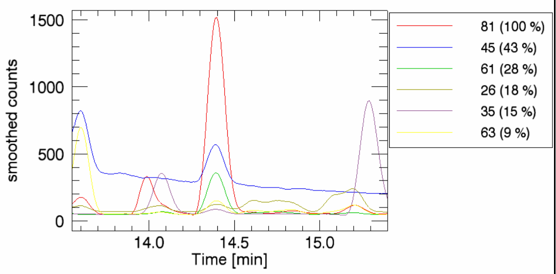

F124a (CHF2CF2Cl), MW: 136

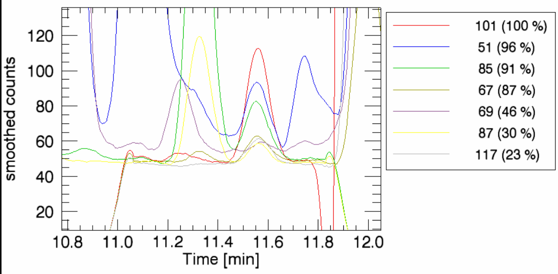

HFC125 (CHF2CF3), MW: 120

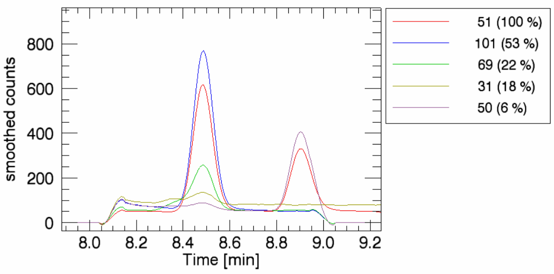

HFC23 (CHF3), MW: 70

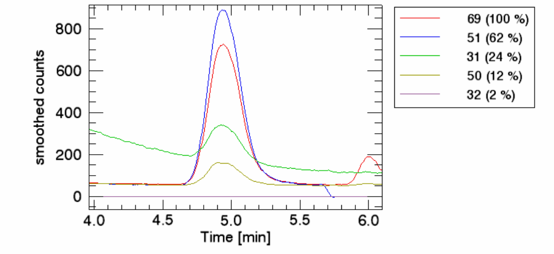

F124 (CHClFCF3), MW: 136

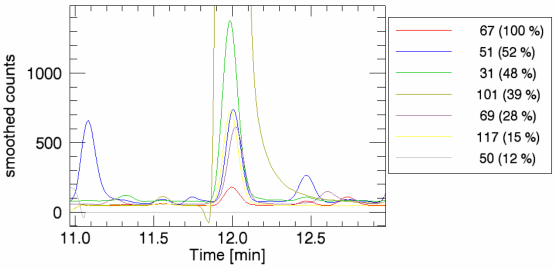

Figure set A.S.5. Integration method comparison for peak heights and areas of 12 substances as retrieved from three pressure series.

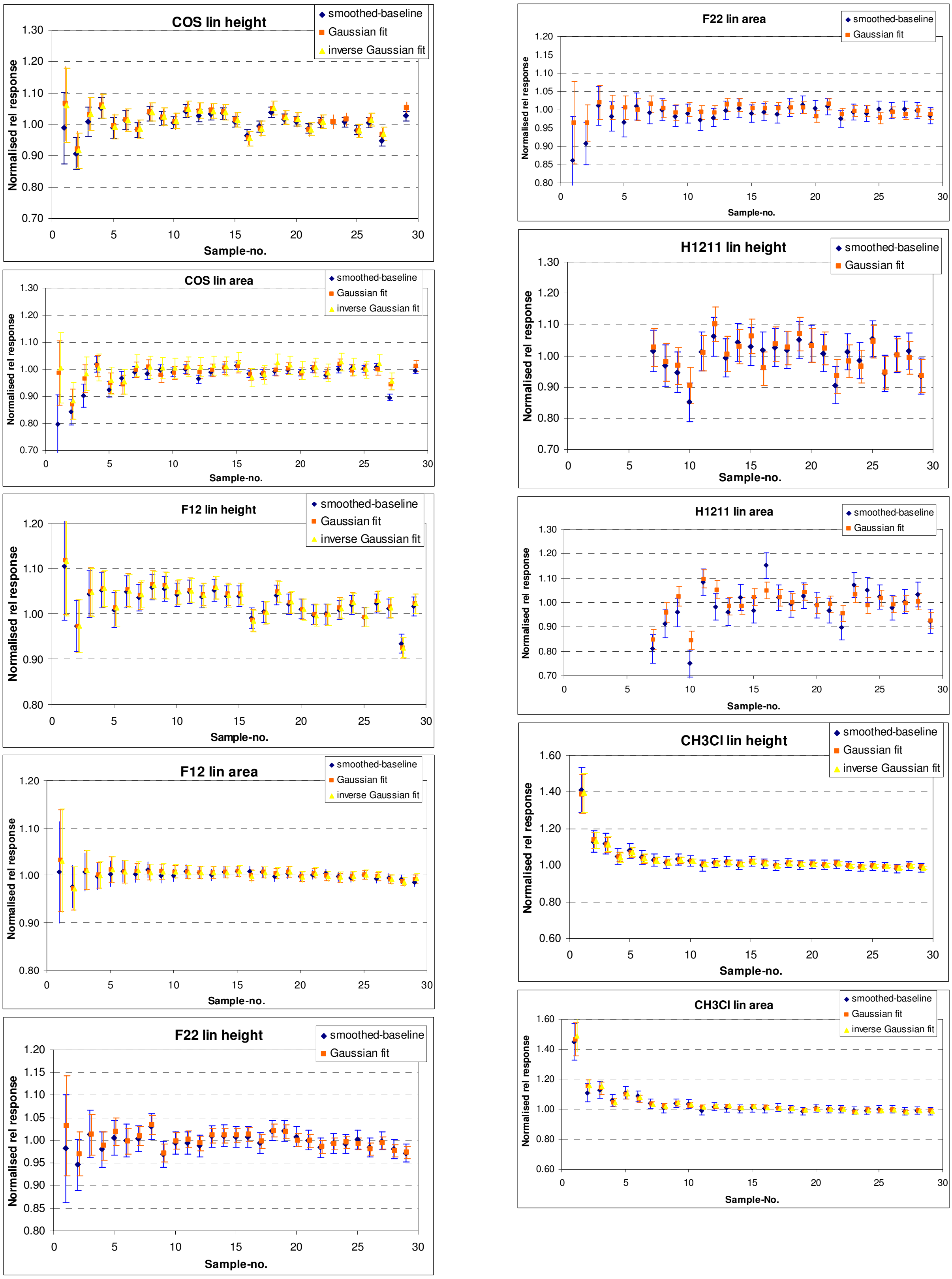

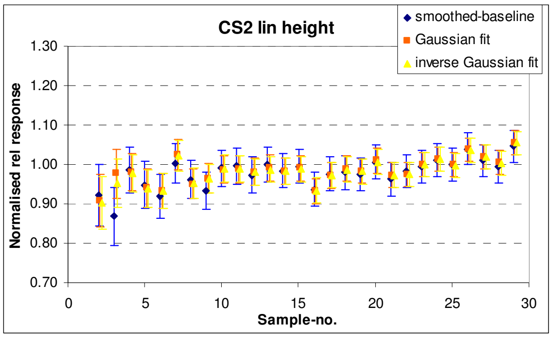
CS2 lin height
smoothed-baseline
Gaussian fit
inverse Gaussian fit
Normalised rel response
1.30
1.20
1.10
1.00
0.90
0.80
0.70
0
5
10
15
20
25
30
Sample-no.

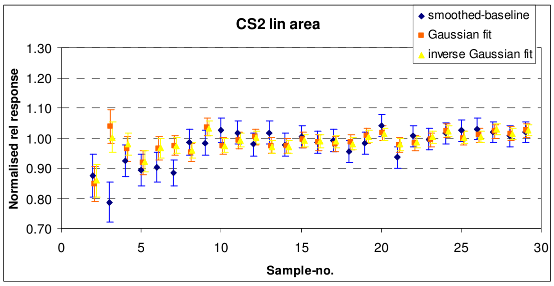
CS2 lin area
smoothed-baseline
Gaussian fit
inverse Gaussian fit
Normalised rel response
1.30
1.20
1.10
1.00
0.90
0.80
0.70
0
5
10
15
20
25
30
Sample-no.

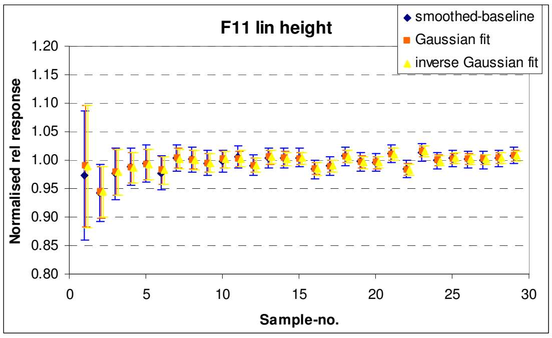
F11 lin height
smoothed-baseline
Gaussian fit
inverse Gaussian fit
Normalised rel response
1.20
1.15
1.10
1.05
1.00
0.95
0.90
0.85
0.80
0
5
10
15
20
25
30
Sample-no.

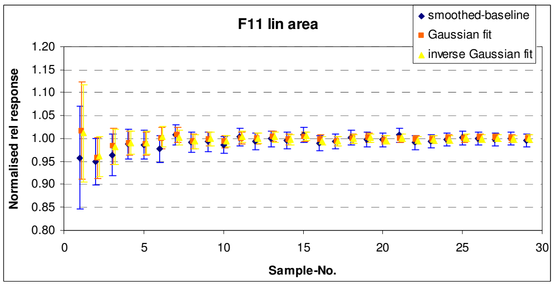
F11 lin area
smoothed-baseline
Gaussian fit
inverse Gaussian fit
Normalised rel response
1.20
1.15
1.10
1.05
1.00
0.95
0.90
0.85
0.80
0
5
10
15
20
25
30
Sample-No.

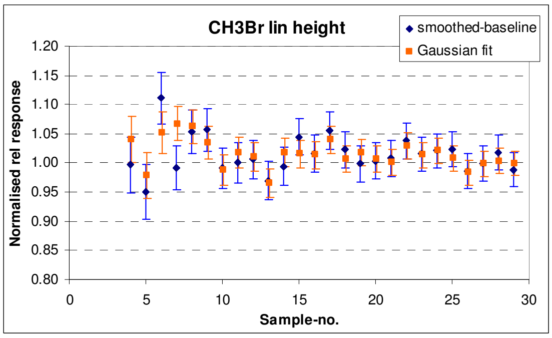
CH3Br lin height
smoothed-baseline
Gaussian fit
Normalised rel response
1.20
1.15
1.10
1.05
1.00
0.95
0.90
0.85
0.80
0
5
10
15
20
25
30
Sample-no.

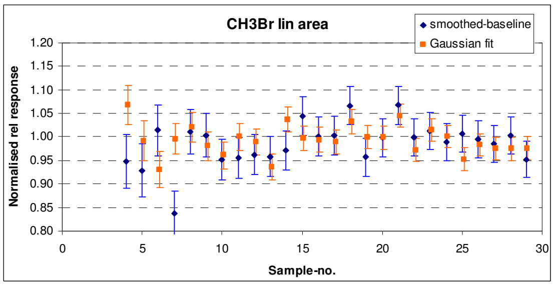
CH3Br lin area
smoothed-baseline
Gaussian fit
Normalised rel response
1.20
1.15
1.10
1.05
1.00
0.95
0.90
0.85
0.80
0
5
10
15
20
25
30
Sample-no.

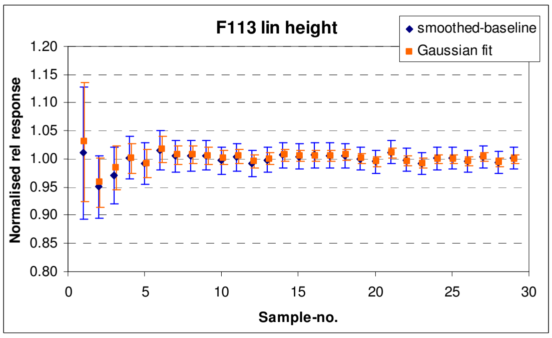
F113 lin height
smoothed-baseline
Gaussian fit
Normalised rel response
1.20
1.15
1.10
1.05
1.00
0.95
0.90
0.85
0.80
0
5
10
15
20
25
30
Sample-no.

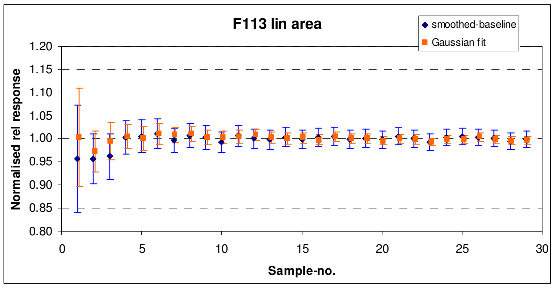
F113 lin area
smoothed-baseline
Gaussian fit
Normalised rel response
1.20
1.15
1.10
1.05
1.00
0.95
0.90
0.85
0.80
0
5
10
15
20
25
30
Sample-no.

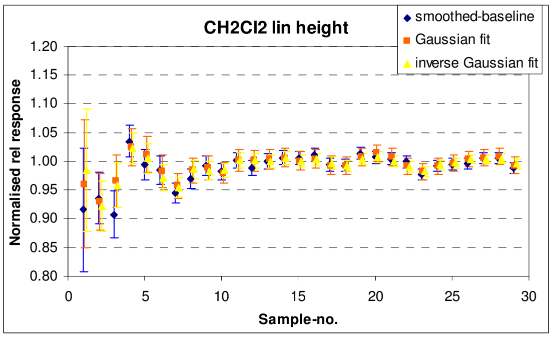
CH2Cl2 lin height
smoothed-baseline
Gaussian fit
inverse Gaussian fit
Normalised rel response
1.20
1.15
1.10
1.05
1.00
0.95
0.90
0.85
0.80
0
5
10
15
20
25
30
Sample-no.

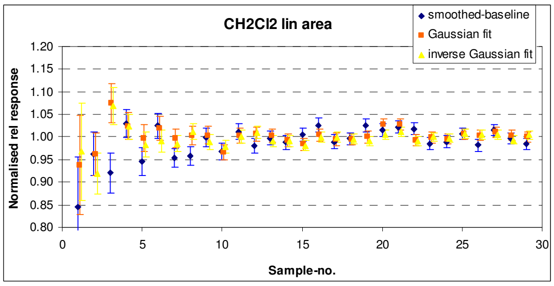
CH2Cl2 lin area
smoothed-baseline
Gaussian fit
inverse Gaussian fit
Normalised rel response
1.20
1.15
1.10
1.05
1.00
0.95
0.90
0.85
0.80
0
5
10
15
20
25
30
Sample-no.

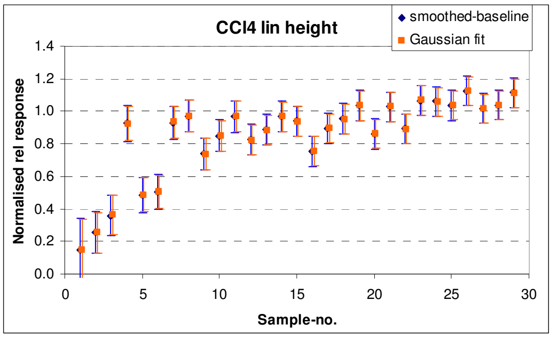

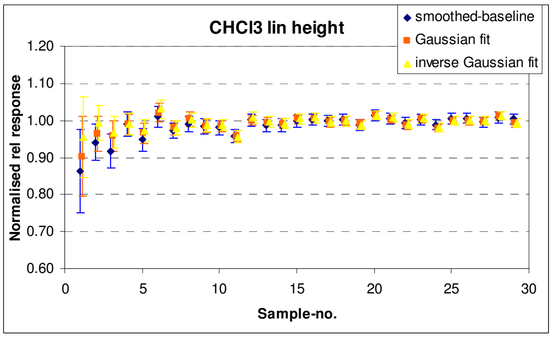

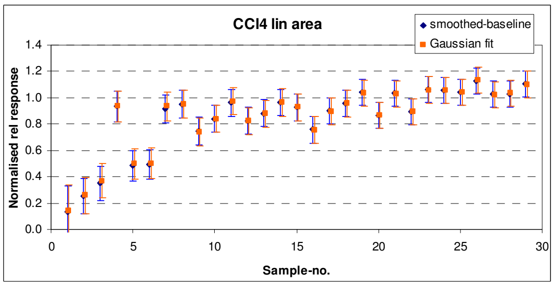

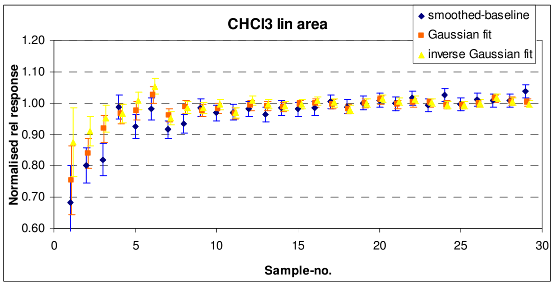

Figure set A.S.6. Linearity diagrams for remaining target substances.

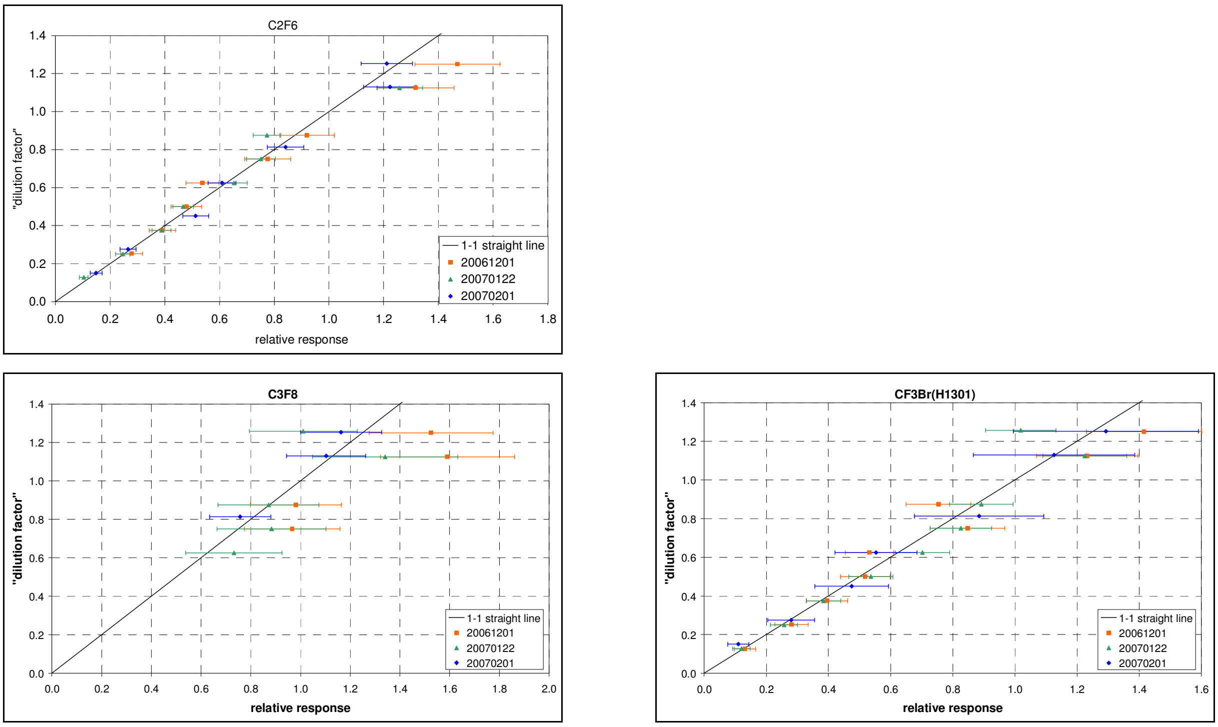

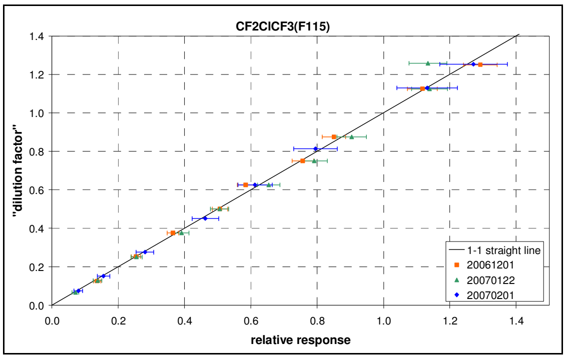
CF2ClCF3(F115)
"dilution factor"
relative response
0.0
0.2
0.4
0.6
0.8
1.0
1.2
1.4
1-1 straight line
20061201
20070122
20070201

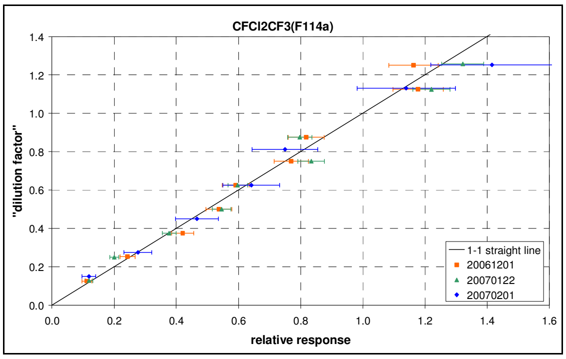
CFCl2CF3(F114a)
"dilution factor"
relative response
0.0
0.2
0.4
0.6
0.8
1.0
1.2
1.4
1.6
1-1 straight line
20061201
20070122
20070201

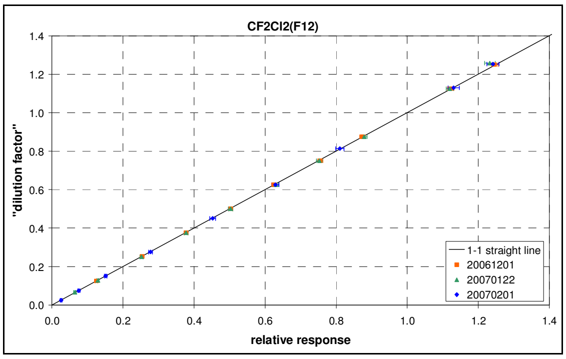
CF2Cl2(F12)
"dilution factor"
relative response
0.0
0.2
0.4
0.6
0.8
1.0
1.2
1.4
1-1 straight line
20061201
20070122
20070201

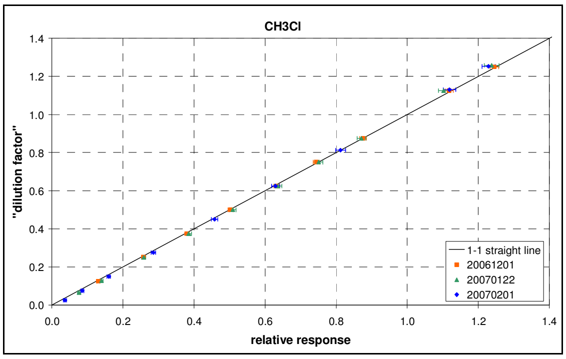
CH3Cl
"dilution factor"
relative response
0.0
0.2
0.4
0.6
0.8
1.0
1.2
1.4
1-1 straight line
20061201
20070122
20070201

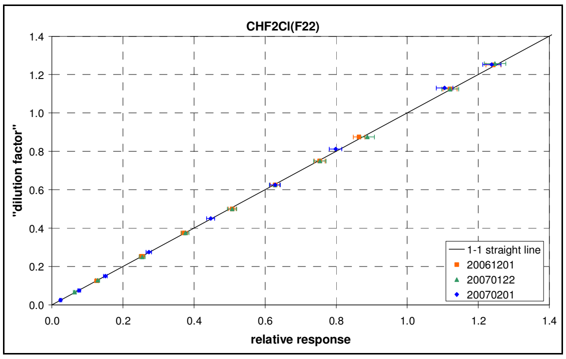
CHF2Cl(F22)
"dilution factor"
relative response
0.0
0.2
0.4
0.6
0.8
1.0
1.2
1.4
1-1 straight line
20061201
20070122
20070201

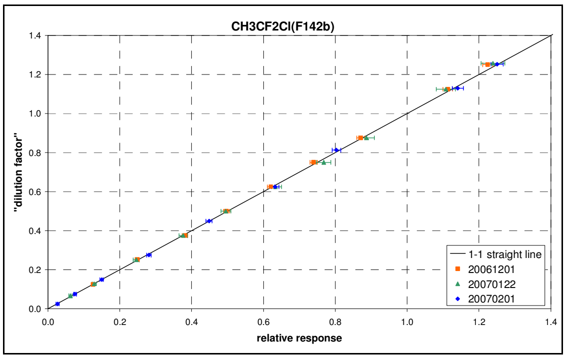
CH3CF2Cl(F142b)
"dilution factor"
relative response
0.0
0.2
0.4
0.6
0.8
1.0
1.2
1.4
1-1 straight line
20061201
20070122
20070201

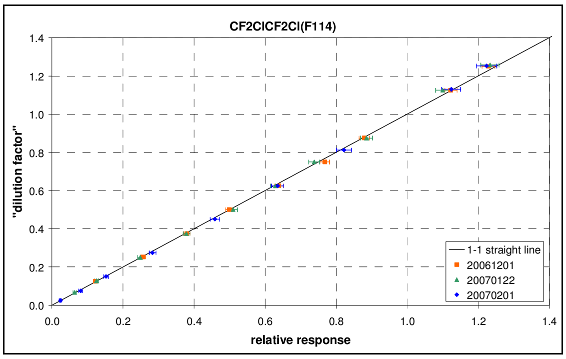
CF2ClCF2Cl(F114)
"dilution factor"
relative response
0.0
0.2
0.4
0.6
0.8
1.0
1.2
1.4
1-1 straight line
20061201
20070122
20070201

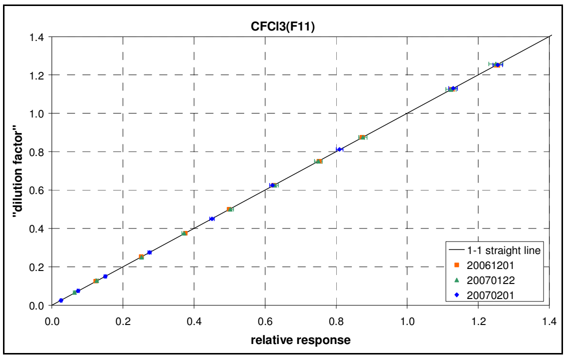
CFCl3(F11)
"dilution factor"
relative response
0.0
0.2
0.4
0.6
0.8
1.0
1.2
1.4
1-1 straight line
20061201
20070122
20070201

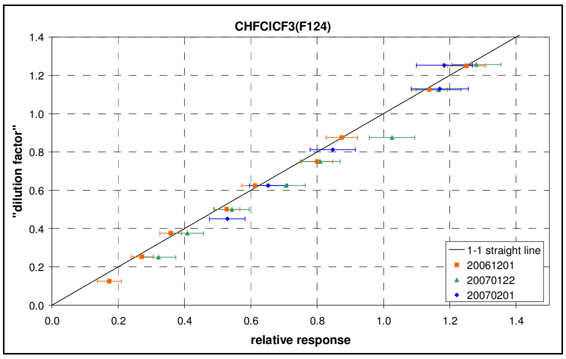
CHFClCF3(F124)
"dilution factor"
relative response
0.0
0.2
0.4
0.6
0.8
1.0
1.2
1.4
1-1 straight line
20061201
20070122
20070201

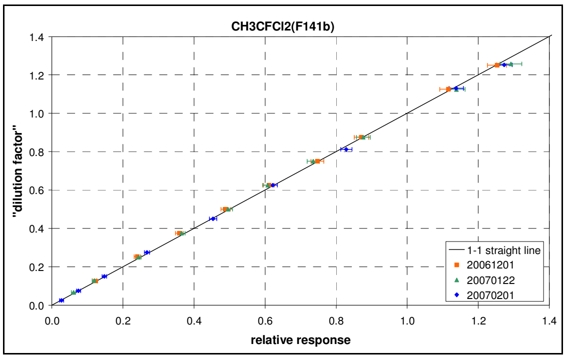
CH3CFCl2(F141b)
"dilution factor"
relative response
0.0
0.2
0.4
0.6
0.8
1.0
1.2
1.4
1-1 straight line
20061201
20070122
20070201

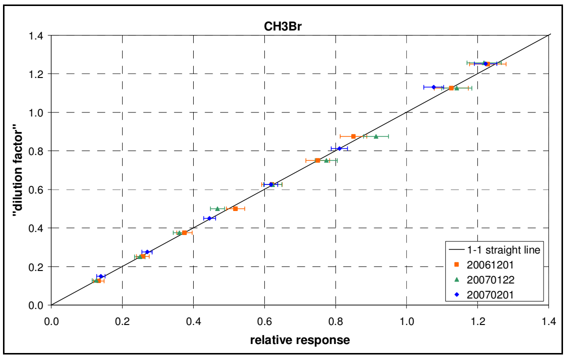
CH3Br
"dilution factor"
relative response
0.0
0.2
0.4
0.6
0.8
1.0
1.2
1.4
1-1 straight line
20061201
20070122
20070201

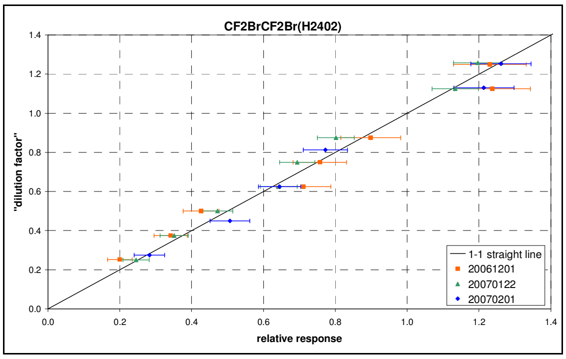
CF2BrCF2Br(H2402)
"dilution factor"
relative response
0.0
0.2
0.4
0.6
0.8
1.0
1.2
1.4
1-1 straight line
20061201
20070122
20070201

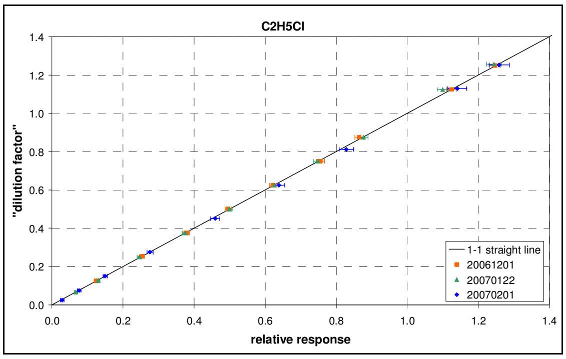
C2H5Cl
"dilution factor"
relative response
0.0
0.2
0.4
0.6
0.8
1.0
1.2
1.4
1-1 straight line
20061201
20070122
20070201

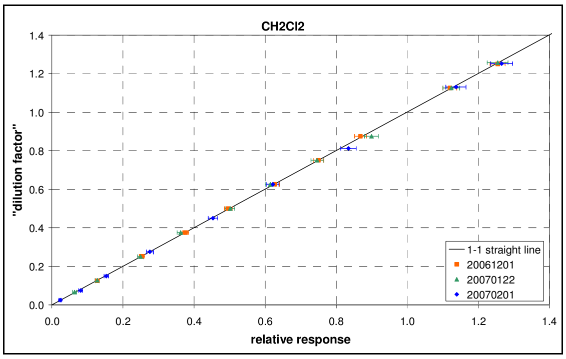
CH2Cl2
"dilution factor"
relative response
0.0
0.2
0.4
0.6
0.8
1.0
1.2
1.4
1-1 straight line
20061201
20070122
20070201

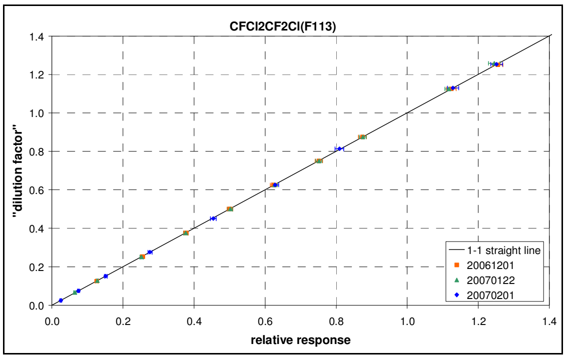
CFCl2CF2Cl(F113)
"dilution factor"
relative response
0.0
0.2
0.4
0.6
0.8
1.0
1.2
1.4
1-1 straight line
20061201
20070122
20070201

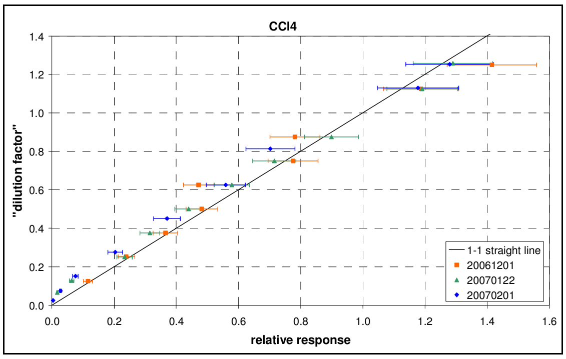
CCl4
"dilution factor"
relative response
0.0
0.2
0.4
0.6
0.8
1.0
1.2
1.4
1.6
1-1 straight line
20061201
20070122
20070201

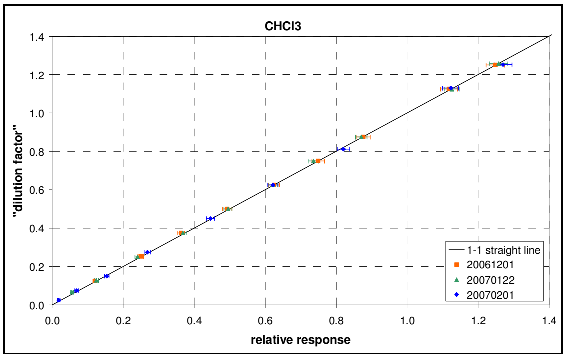

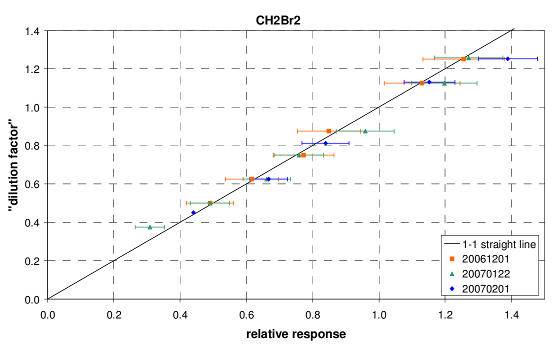

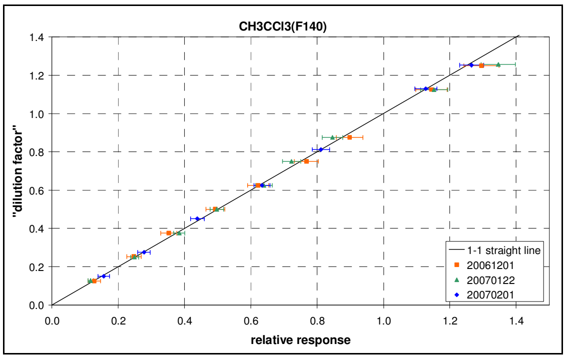

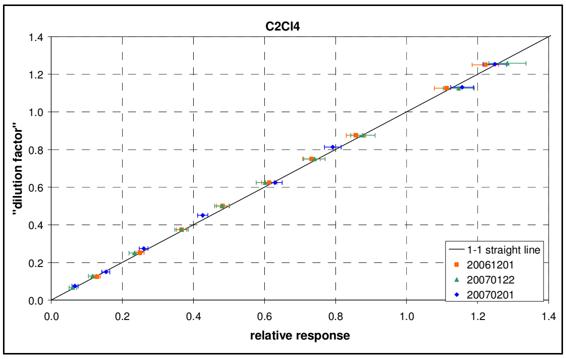

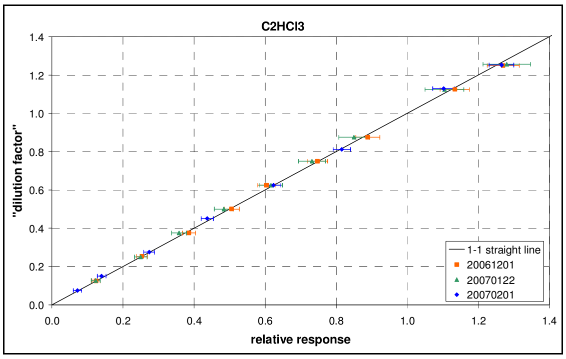

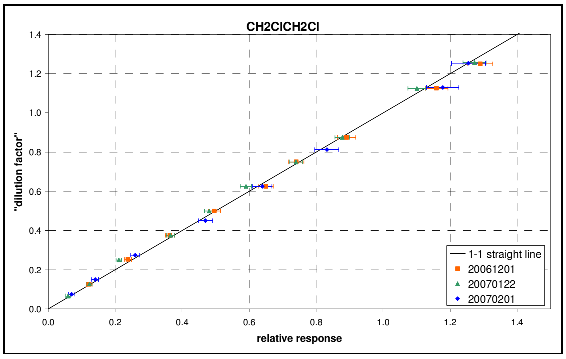

Figure set A.S.7. Comparison of mixing ratios of one stratospheric balloon flight (C1) as derived from different ECD nonlinearity corrections with corresponding MS results.

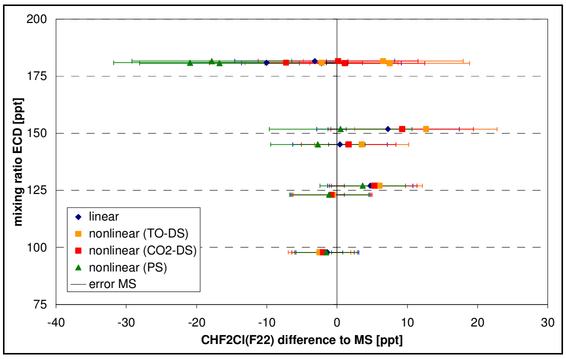

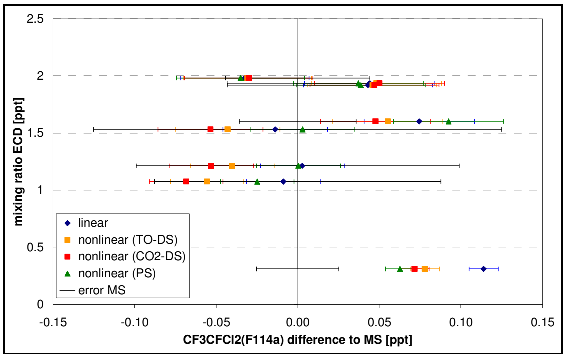

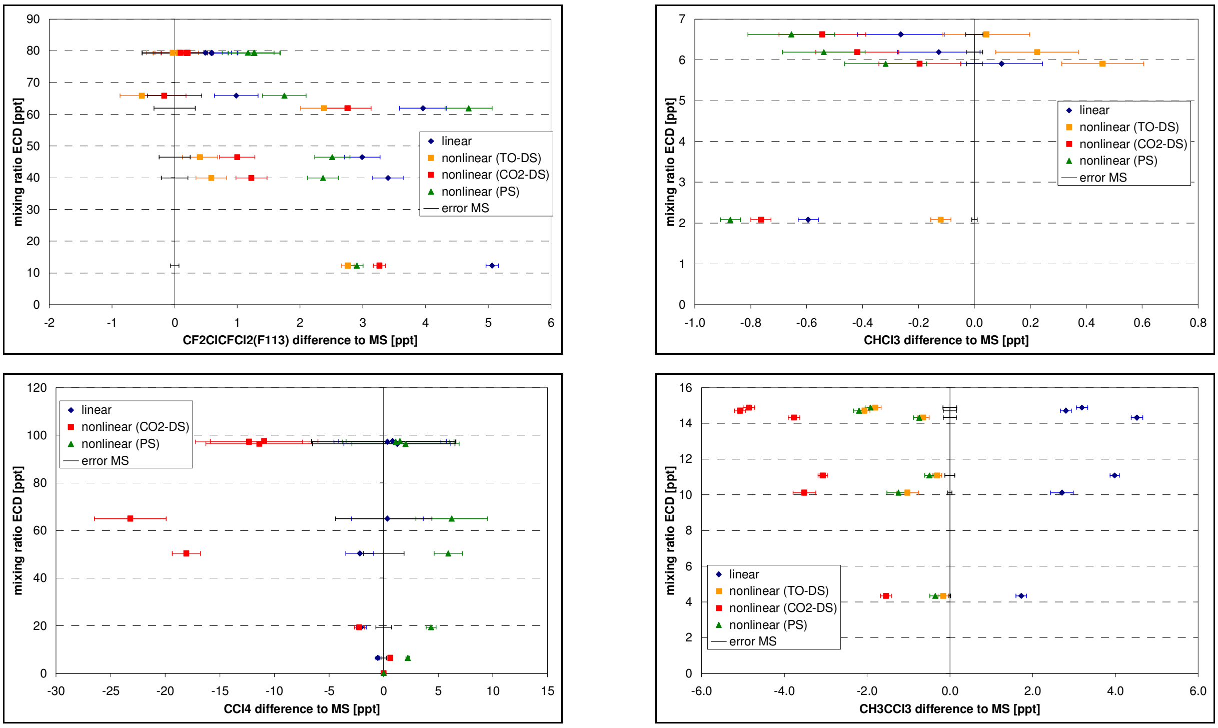

Figure set A.S.8. Internal calibration standard comparison. Relative responses of 4 standards against the ALM-39767 standard over a period of 25 months for target substances.

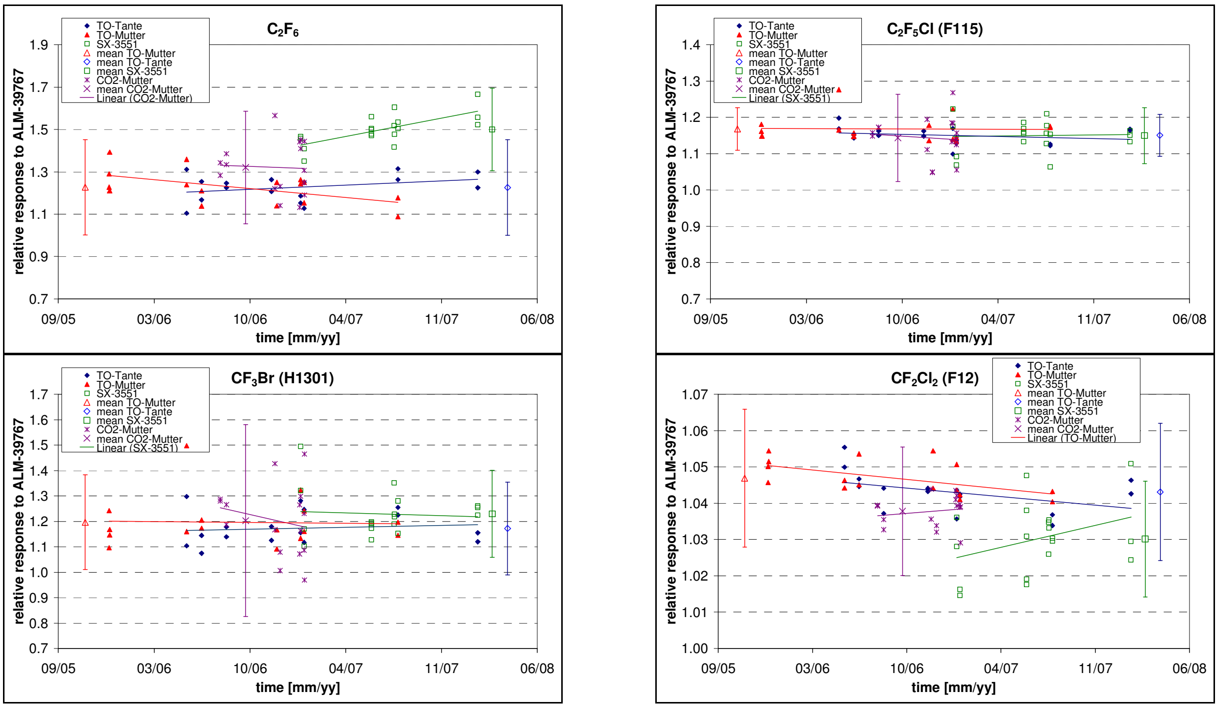

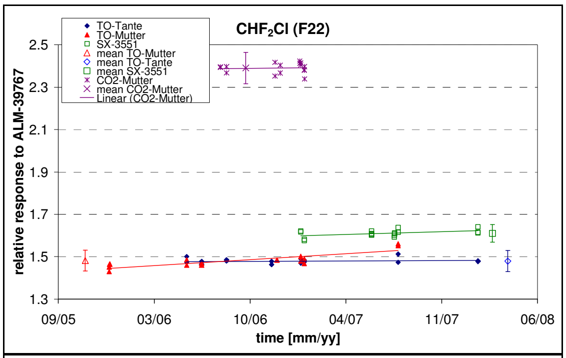
CHF$_2$Cl (F22)
TO-Tante
TO-Mutter
SX-3551
mean TO-Mutter
mean TO-Tante
mean SX-3551
CO2-Mutter
mean CO2-Mutter
Linear (CO2-Mutter)
relative response to ALM-39767
2.5
2.3
2.1
1.9
1.7
1.5
1.3
09/05
03/06
10/06
04/07
11/07
06/08
time [mm/yy]

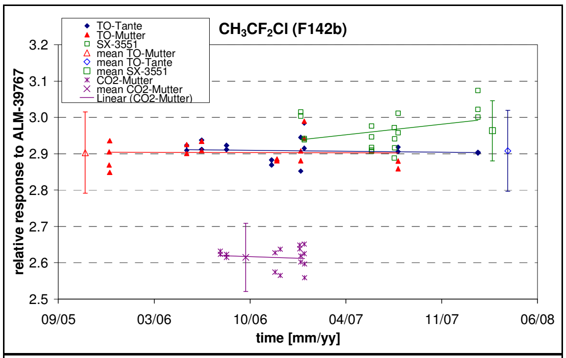
CH$_3$CF$_2$Cl (F142b)
TO-Tante
TO-Mutter
SX-3551
mean TO-Mutter
mean TO-Tante
mean SX-3551
CO2-Mutter
mean CO2-Mutter
Linear (CO2-Mutter)
relative response to ALM-39767
3.2
3.1
3.0
2.9
2.8
2.7
2.6
2.5
09/05
03/06
10/06
04/07
11/07
06/08
time [mm/yy]

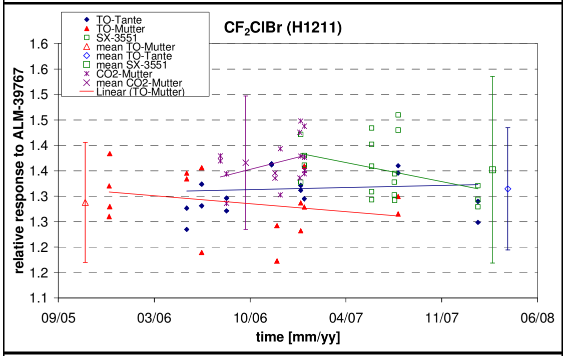
CF$_2$ClBr (H1211)
TO-Tante
TO-Mutter
SX-3551
mean TO-Mutter
mean TO-Tante
mean SX-3551
CO2-Mutter
mean CO2-Mutter
Linear (TO-Mutter)
relative response to ALM-39767
1.6
1.6
1.5
1.5
1.4
1.4
1.3
1.3
1.2
1.2
1.1
09/05
03/06
10/06
04/07
11/07
06/08
time [mm/yy]

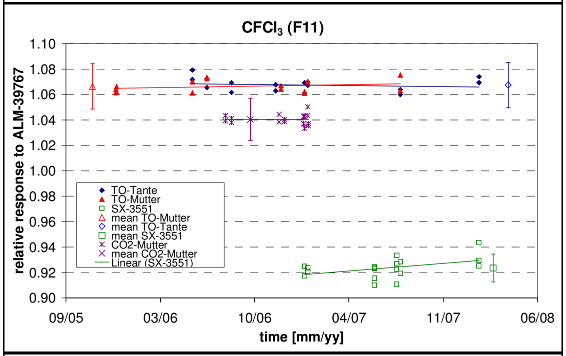
CFCl$_3$ (F11)
TO-Tante
TO-Mutter
SX-3551
mean TO-Mutter
mean TO-Tante
mean SX-3551
CO2-Mutter
mean CO2-Mutter
Linear (SX-3551)
relative response to ALM-39767
1.10
1.08
1.06
1.04
1.02
1.00
0.98
0.96
0.94
0.92
0.90
09/05
03/06
10/06
04/07
11/07
06/08
time [mm/yy]

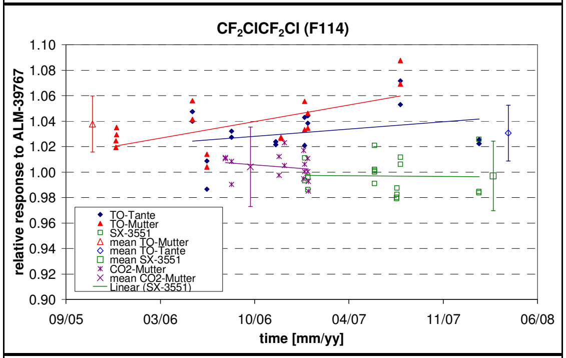
CF$_2$ClCF$_2$Cl (F114)
TO-Tante
TO-Mutter
SX-3551
mean TO-Mutter
mean TO-Tante
mean SX-3551
CO2-Mutter
mean CO2-Mutter
Linear (SX-3551)
relative response to ALM-39767
1.10
1.08
1.06
1.04
1.02
1.00
0.98
0.96
0.94
0.92
0.90
09/05
03/06
10/06
04/07
11/07
06/08
time [mm/yy]

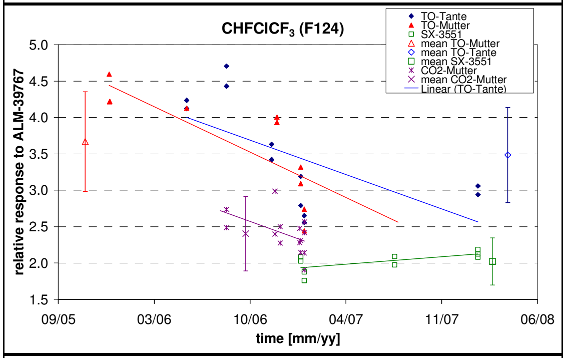
CHFClCF$_3$ (F124)
TO-Tante
TO-Mutter
SX-3551
mean TO-Mutter
mean TO-Tante
mean SX-3551
CO2-Mutter
mean CO2-Mutter
Linear (TO-Tante)
relative response to ALM-39767
5.0
4.5
4.0
3.5
3.0
2.5
2.0
1.5
09/05
03/06
10/06
04/07
11/07
06/08
time [mm/yy]

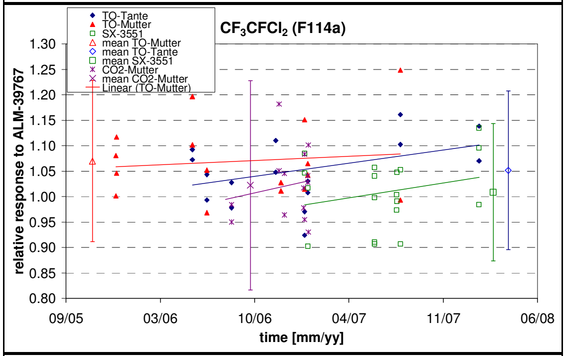
CF$_3$CFCl$_2$ (F114a)
TO-Tante
TO-Mutter
SX-3551
mean TO-Mutter
mean TO-Tante
mean SX-3551
CO2-Mutter
mean CO2-Mutter
Linear (TO-Mutter)
relative response to ALM-39767
1.30
1.25
1.20
1.15
1.10
1.05
1.00
0.95
0.90
0.85
0.80
09/05
03/06
10/06
04/07
11/07
06/08
time [mm/yy]

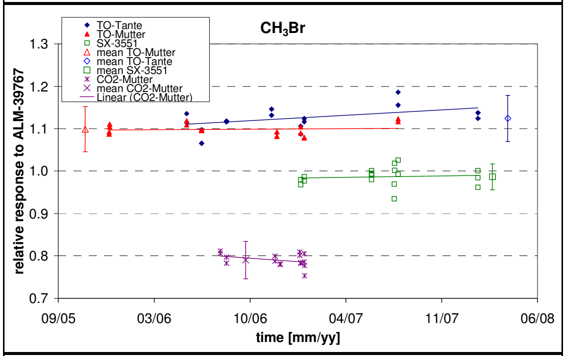
CH$_3$Br
TO-Tante
TO-Mutter
SX-3551
mean TO-Mutter
mean TO-Tante
mean SX-3551
CO2-Mutter
mean CO2-Mutter
Linear (CO2-Mutter)
relative response to ALM-39767
1.3
1.2
1.1
1.0
0.9
0.8
0.7
09/05
03/06
10/06
04/07
11/07
06/08
time [mm/yy]

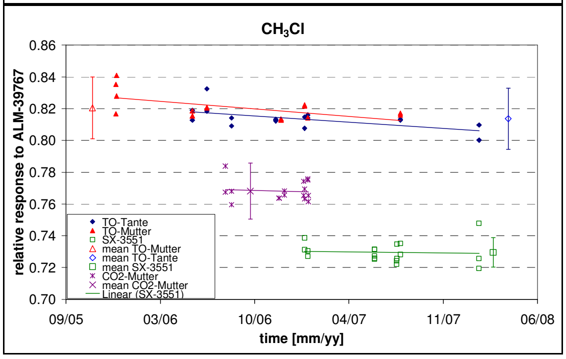
CH$_3$Cl
TO-Tante
TO-Mutter
SX-3551
mean TO-Mutter
mean TO-Tante
mean SX-3551
CO2-Mutter
mean CO2-Mutter
Linear (SX-3551)
relative response to ALM-39767
0.86
0.84
0.82
0.80
0.78
0.76
0.74
0.72
0.70
09/05
03/06
10/06
04/07
11/07
06/08
time [mm/yy]

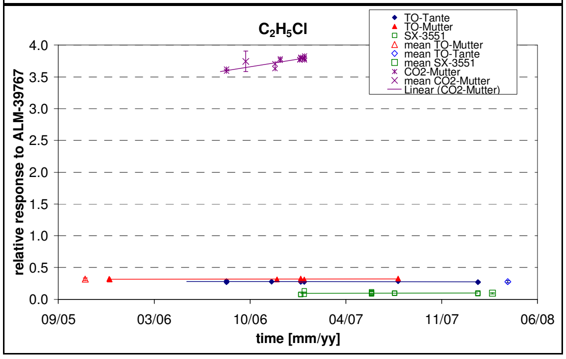
C$_2$H$_5$Cl
TO-Tante
TO-Mutter
SX-3551
mean TO-Mutter
mean TO-Tante
mean SX-3551
CO2-Mutter
mean CO2-Mutter
Linear (CO2-Mutter)
relative response to ALM-39767
4.0
3.5
3.0
2.5
2.0
1.5
1.0
0.5
0.0
09/05
03/06
10/06
04/07
11/07
06/08
time [mm/yy]

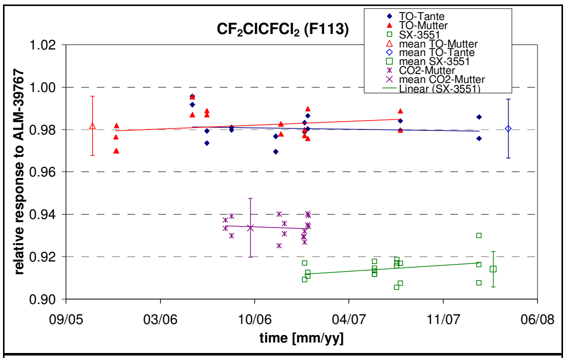
CF$_2$ClCFCl$_2$ (F113)
relative response to ALM-39767
1.02
1.00
0.98
0.96
0.94
0.92
0.90
09/05
03/06
10/06
04/07
11/07
06/08
time [mm/yy]
TO-Tante
TO-Mutter
SX-3551
mean TO-Mutter
mean TO-Tante
mean SX-3551
CO2-Mutter
mean CO2-Mutter
Linear (SX-3551)

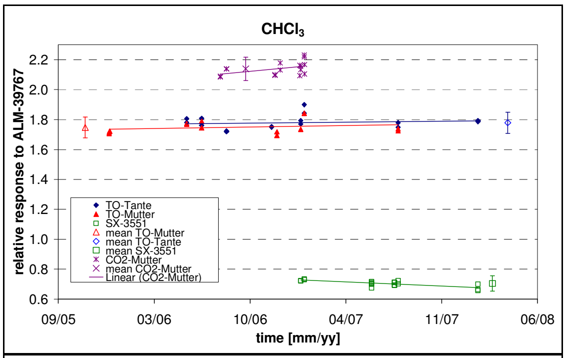
CHCl$_3$
relative response to ALM-39767
2.2
2.0
1.8
1.6
1.4
1.2
1.0
0.8
0.6
09/05
03/06
10/06
04/07
11/07
06/08
time [mm/yy]
TO-Tante
TO-Mutter
SX-3551
mean TO-Mutter
mean TO-Tante
mean SX-3551
CO2-Mutter
mean CO2-Mutter
Linear (CO2-Mutter)

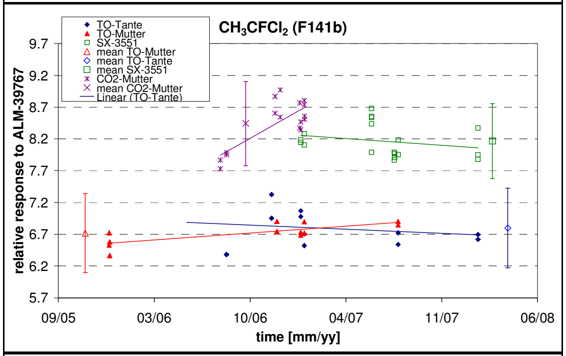
CH$_3$CFCl$_2$ (F141b)
relative response to ALM-39767
9.7
9.2
8.7
8.2
7.7
7.2
6.7
6.2
5.7
09/05
03/06
10/06
04/07
11/07
06/08
time [mm/yy]
TO-Tante
TO-Mutter
SX-3551
mean TO-Mutter
mean TO-Tante
mean SX-3551
CO2-Mutter
mean CO2-Mutter
Linear (TO-Tante)

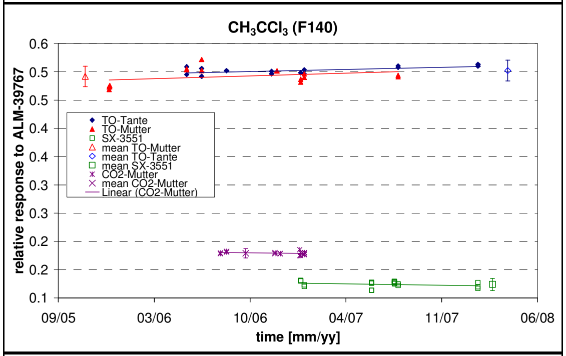
CH$_3$CCl$_3$ (F140)
relative response to ALM-39767
0.6
0.5
0.5
0.4
0.4
0.3
0.3
0.2
0.2
0.1
09/05
03/06
10/06
04/07
11/07
06/08
time [mm/yy]
TO-Tante
TO-Mutter
SX-3551
mean TO-Mutter
mean TO-Tante
mean SX-3551
CO2-Mutter
mean CO2-Mutter
Linear (CO2-Mutter)

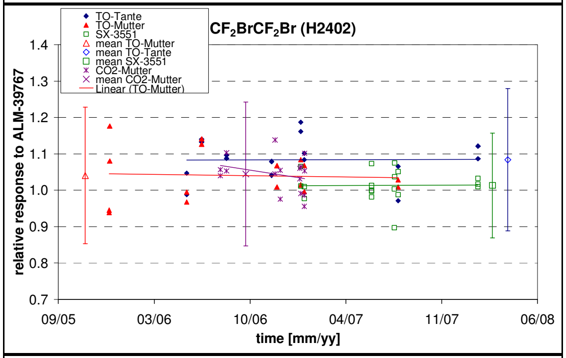
CF$_2$BrCF$_2$Br (H2402)
relative response to ALM-39767
1.4
1.3
1.2
1.1
1.0
0.9
0.8
0.7
09/05
03/06
10/06
04/07
11/07
06/08
time [mm/yy]
TO-Tante
TO-Mutter
SX-3551
mean TO-Mutter
mean TO-Tante
mean SX-3551
CO2-Mutter
mean CO2-Mutter
Linear (TO-Mutter)

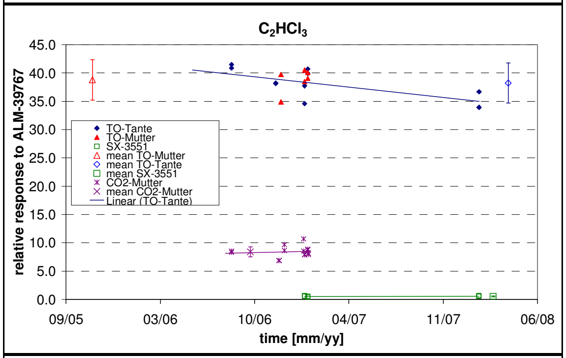
C$_2$HCl$_3$
relative response to ALM-39767
45.0
40.0
35.0
30.0
25.0
20.0
15.0
10.0
5.0
0.0
09/05
03/06
10/06
04/07
11/07
06/08
time [mm/yy]
TO-Tante
TO-Mutter
SX-3551
mean TO-Mutter
mean TO-Tante
mean SX-3551
CO2-Mutter
mean CO2-Mutter
Linear (TO-Tante)

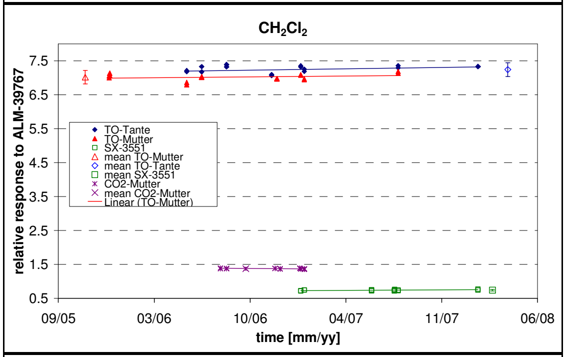
CH$_2$Cl$_2$
relative response to ALM-39767
7.5
6.5
5.5
4.5
3.5
2.5
1.5
0.5
09/05
03/06
10/06
04/07
11/07
06/08
time [mm/yy]
TO-Tante
TO-Mutter
SX-3551
mean TO-Mutter
mean TO-Tante
mean SX-3551
CO2-Mutter
mean CO2-Mutter
Linear (TO-Mutter)

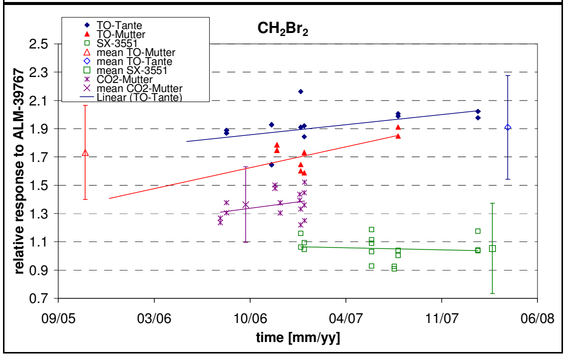
CH$_2$Br$_2$
relative response to ALM-39767
2.5
2.3
2.1
1.9
1.7
1.5
1.3
1.1
0.9
0.7
09/05
03/06
10/06
04/07
11/07
06/08
time [mm/yy]
TO-Tante
TO-Mutter
SX-3551
mean TO-Mutter
mean TO-Tante
mean SX-3551
CO2-Mutter
mean CO2-Mutter
Linear (TO-Tante)

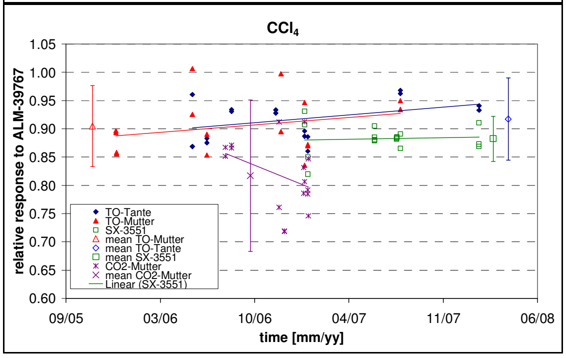
CCl$_4$
relative response to ALM-39767
1.05
1.00
0.95
0.90
0.85
0.80
0.75
0.70
0.65
0.60
09/05
03/06
10/06
04/07
11/07
06/08
time [mm/yy]
TO-Tante
TO-Mutter
SX-3551
mean TO-Mutter
mean TO-Tante
mean SX-3551
CO2-Mutter
mean CO2-Mutter
Linear (SX-3551)

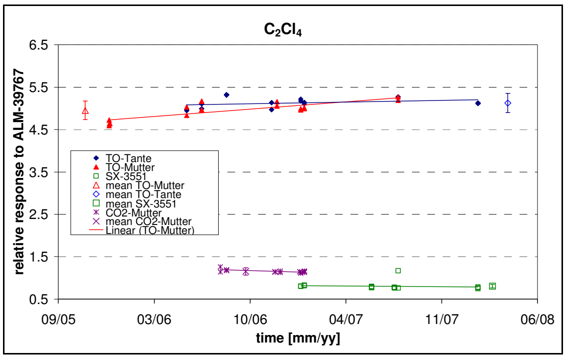

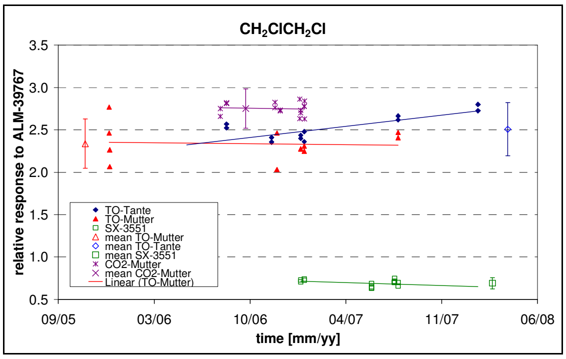

Figure set A.S.9. Fractional release factors of long-lived halocarbons in tropical and mid-latitudes compared to mid- and high-latitude correlation functions derived by Newman et al. (2006).

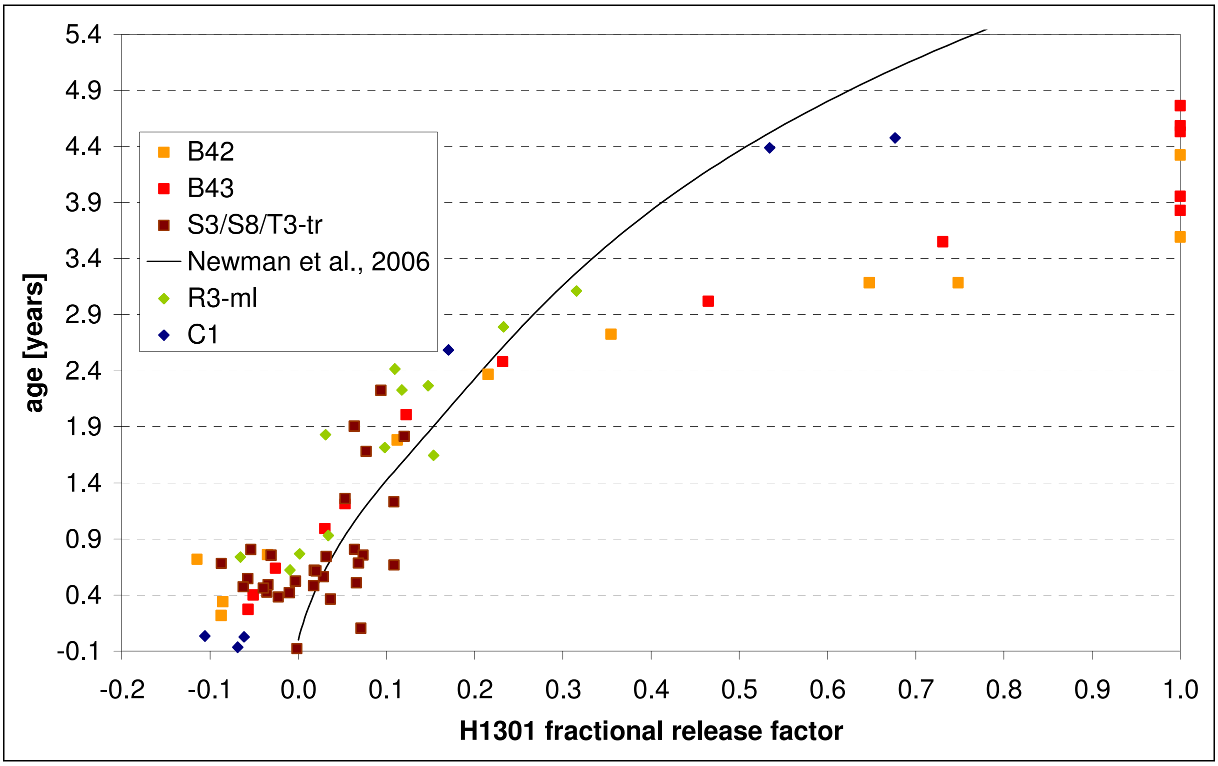

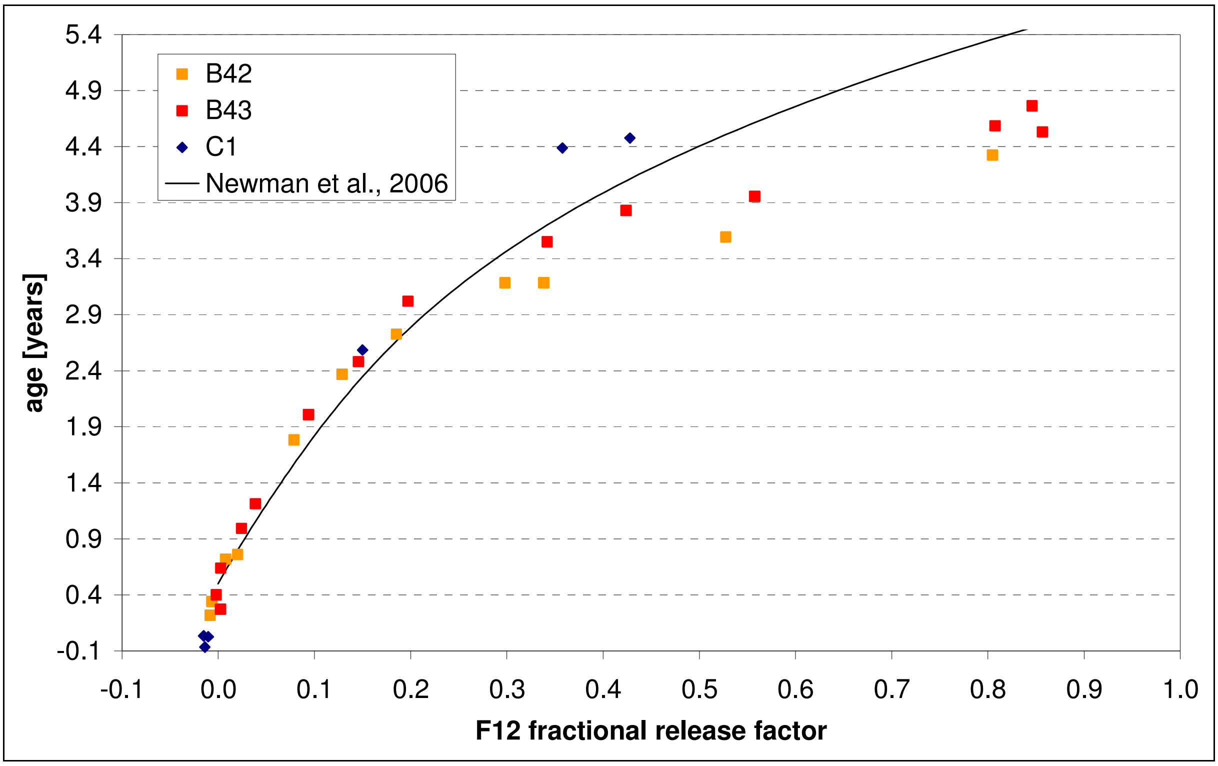
B42
B43
C1
Newman et al., 2006
age [years]
5.4
4.9
4.4
3.9
3.4
2.9
2.4
1.9
1.4
0.9
0.4
-0.1
-0.1
0.0
0.1
0.2
0.3
0.4
0.5
0.6
0.7
0.8
0.9
1.0
F12 fractional release factor

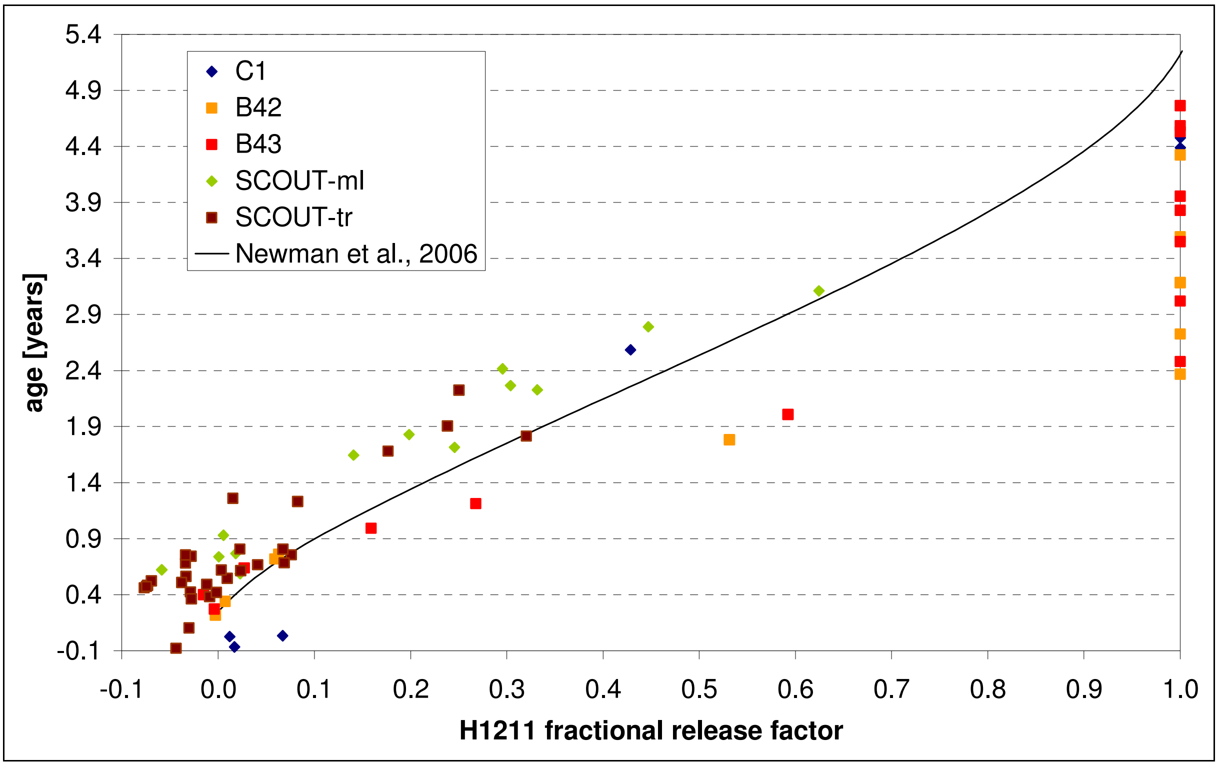
C1
B42
B43
SCOUT-ml
SCOUT-tr
Newman et al., 2006
age [years]
5.4
4.9
4.4
3.9
3.4
2.9
2.4
1.9
1.4
0.9
0.4
-0.1
-0.1
0.0
0.1
0.2
0.3
0.4
0.5
0.6
0.7
0.8
0.9
1.0
H1211 fractional release factor

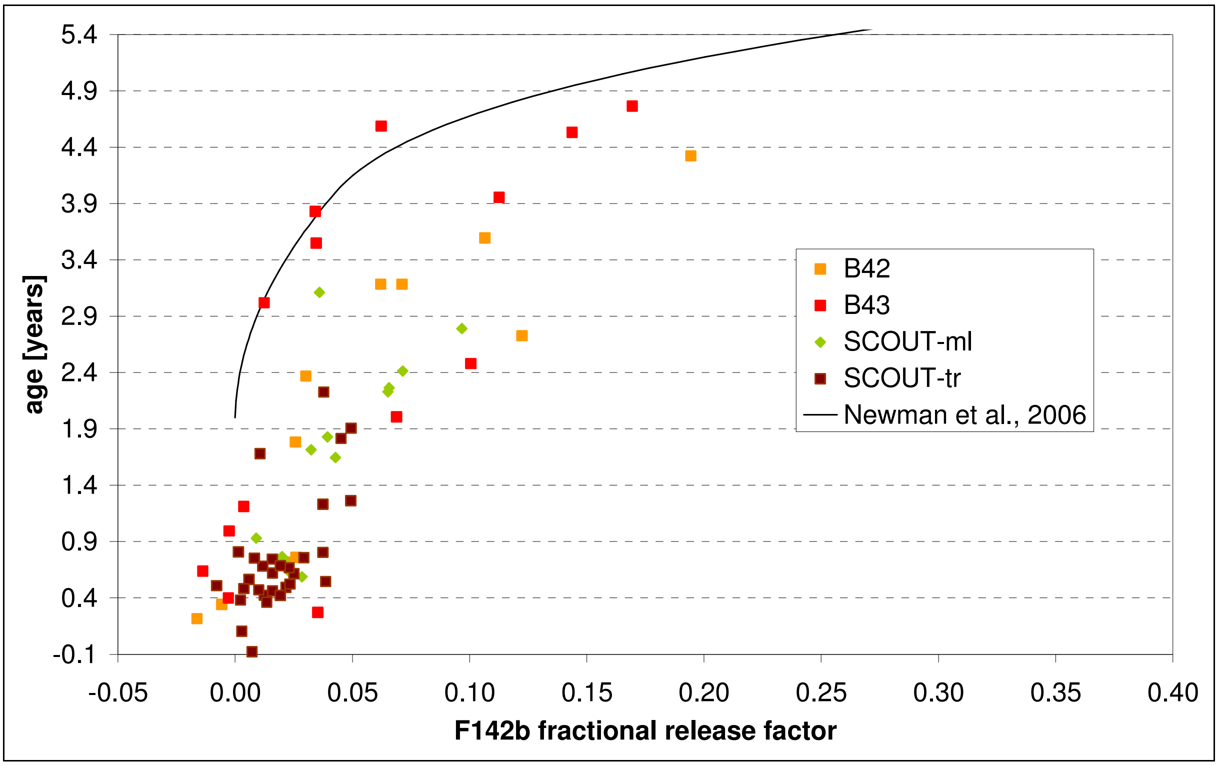
age [years]
5.4
4.9
4.4
3.9
3.4
2.9
2.4
1.9
1.4
0.9
0.4
-0.1
-0.05
0.00
0.05
0.10
0.15
0.20
0.25
0.30
0.35
0.40
F142b fractional release factor
B42
B43
SCOUT-ml
SCOUT-tr
Newman et al., 2006

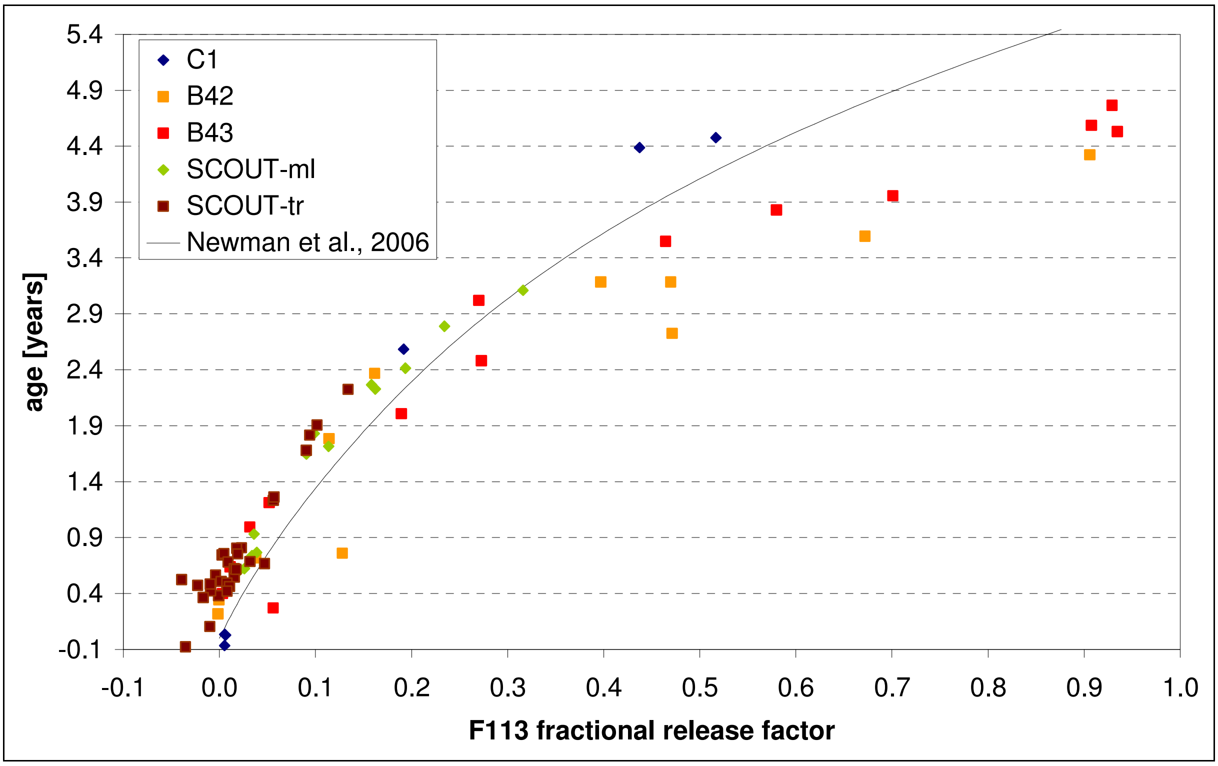
age [years]
5.4
4.9
4.4
3.9
3.4
2.9
2.4
1.9
1.4
0.9
0.4
-0.1
-0.1
0.0
0.1
0.2
0.3
0.4
0.5
0.6
0.7
0.8
0.9
1.0
F113 fractional release factor
C1
B42
B43
SCOUT-ml
SCOUT-tr
Newman et al., 2006

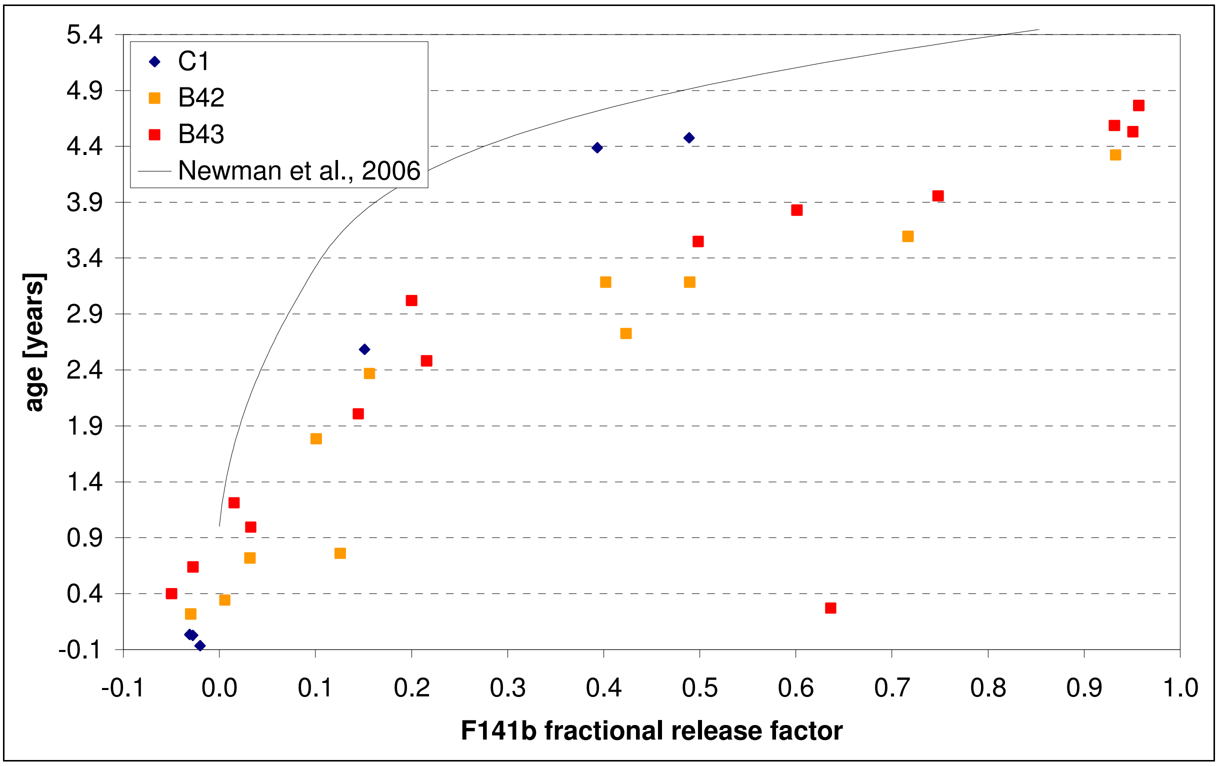
age [years]
5.4
4.9
4.4
3.9
3.4
2.9
2.4
1.9
1.4
0.9
0.4
-0.1
-0.1
0.0
0.1
0.2
0.3
0.4
0.5
0.6
0.7
0.8
0.9
1.0
F141b fractional release factor
C1
B42
B43
Newman et al., 2006

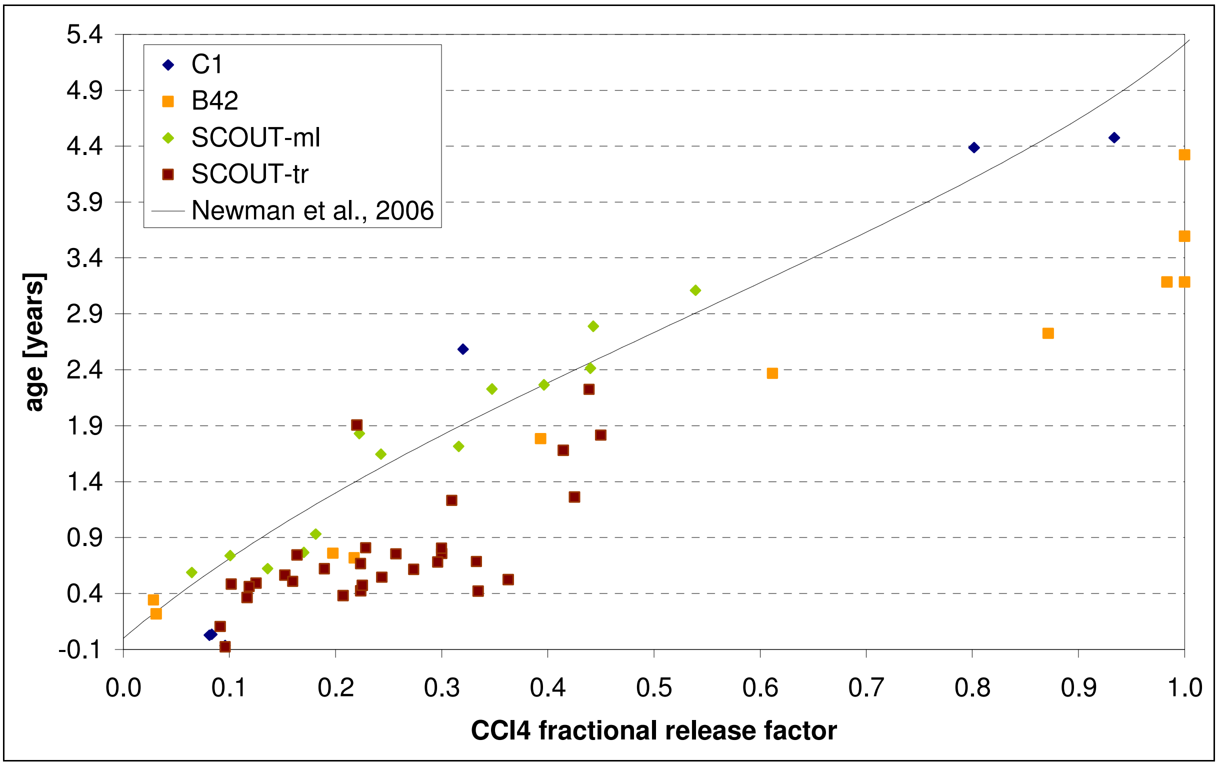
age [years]
5.4
4.9
4.4
3.9
3.4
2.9
2.4
1.9
1.4
0.9
0.4
-0.1
0.0
0.1
0.2
0.3
0.4
0.5
0.6
0.7
0.8
0.9
1.0
CCl4 fractional release factor
C1
B42
SCOUT-ml
SCOUT-tr
Newman et al., 2006

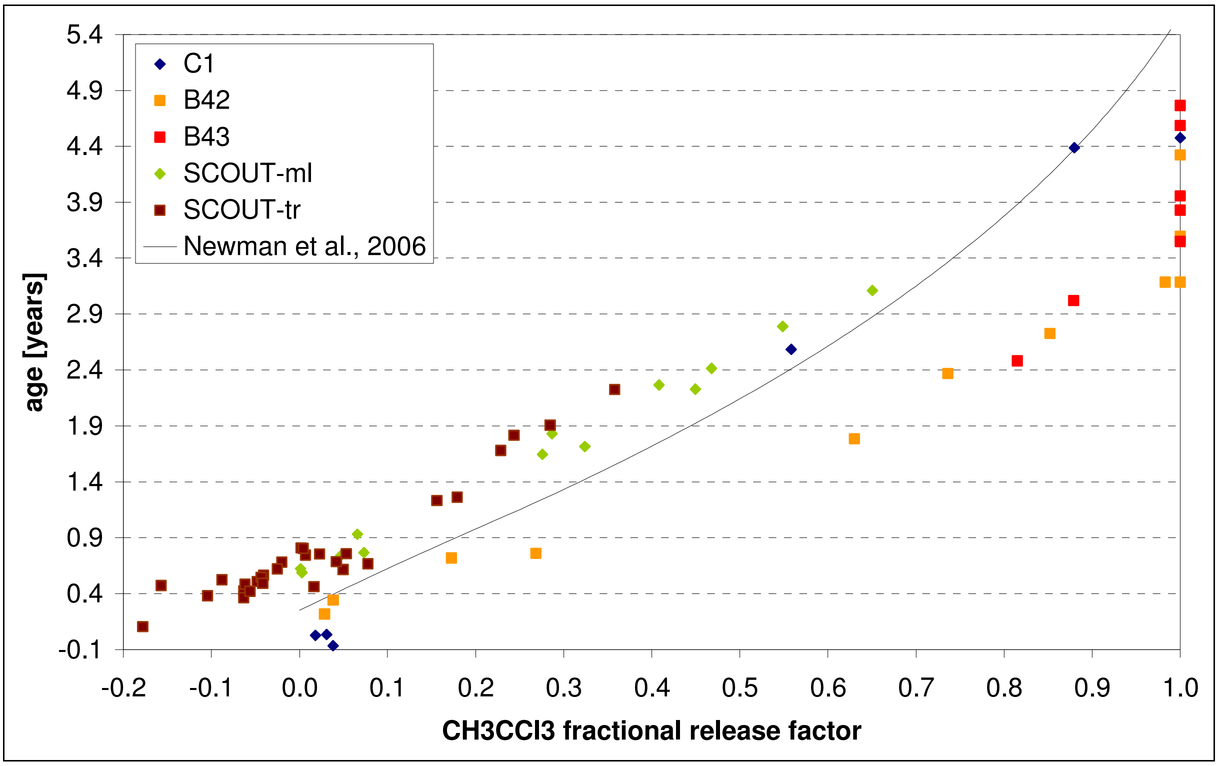
C1
B42
B43
SCOUT-ml
SCOUT-tr
Newman et al., 2006
age [years]
5.4
4.9
4.4
3.9
3.4
2.9
2.4
1.9
1.4
0.9
0.4
-0.1
-0.2
-0.1
0.0
0.1
0.2
0.3
0.4
0.5
0.6
0.7
0.8
0.9
1.0
CH3CCl3 fractional release factor

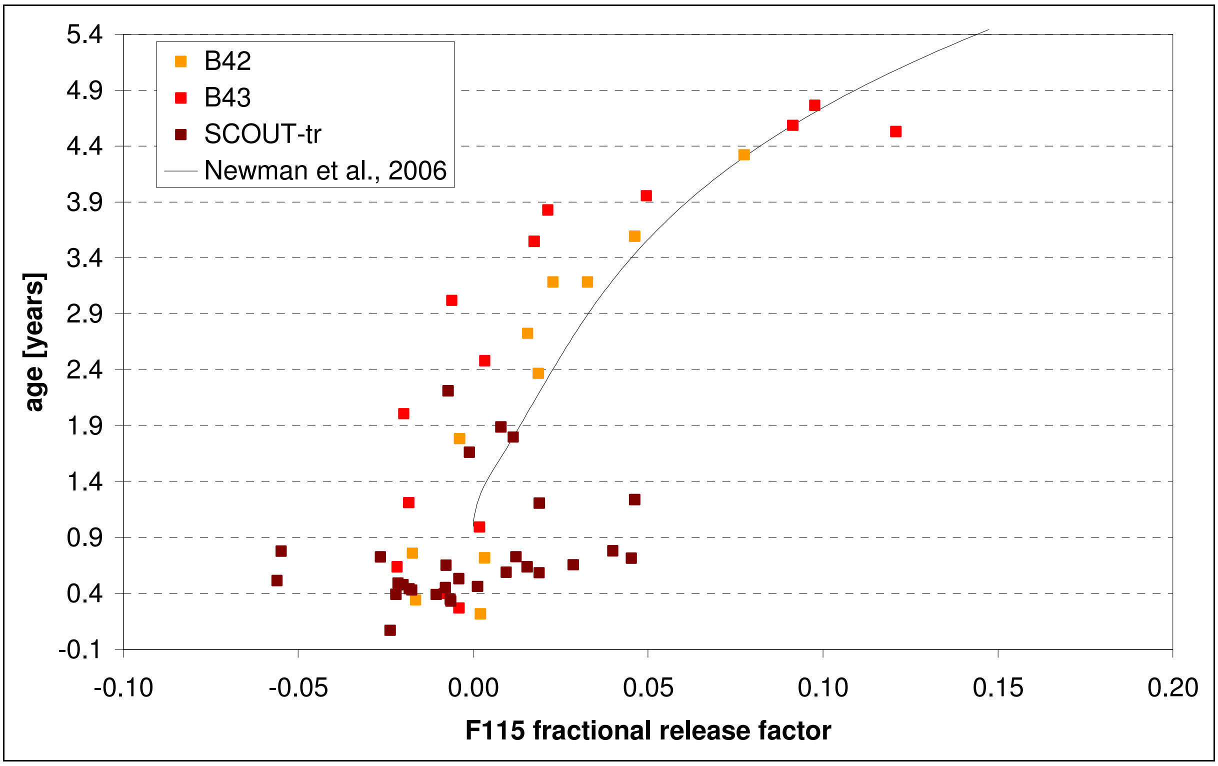
B42
B43
SCOUT-tr
Newman et al., 2006
age [years]
5.4
4.9
4.4
3.9
3.4
2.9
2.4
1.9
1.4
0.9
0.4
-0.1
-0.10
-0.05
0.00
0.05
0.10
0.15
0.20
F115 fractional release factor

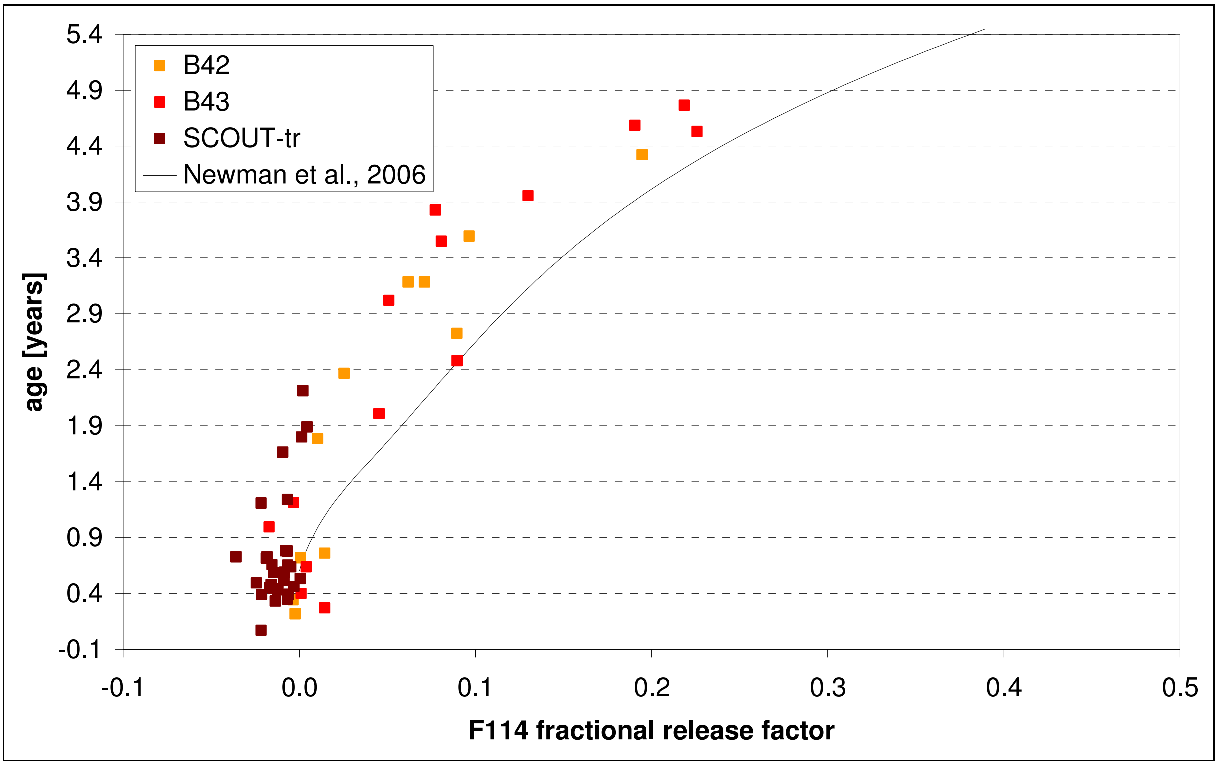
B42
B43
SCOUT-tr
Newman et al., 2006
age [years]
5.4
4.9
4.4
3.9
3.4
2.9
2.4
1.9
1.4
0.9
0.4
-0.1
-0.1
0.0
0.1
0.2
0.3
0.4
0.5
F114 fractional release factor

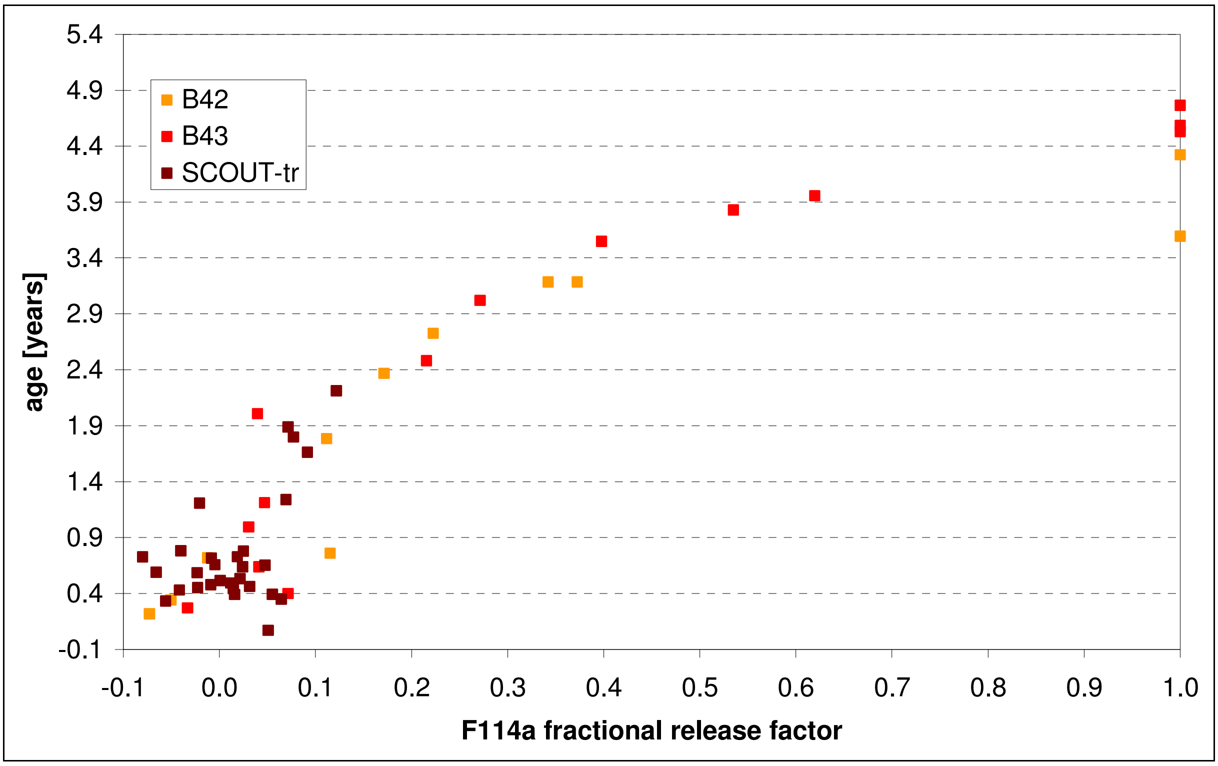
B42
B43
SCOUT-tr
age [years]
5.4
4.9
4.4
3.9
3.4
2.9
2.4
1.9
1.4
0.9
0.4
-0.1
-0.1
0.0
0.1
0.2
0.3
0.4
0.5
0.6
0.7
0.8
0.9
1.0
F114a fractional release factor

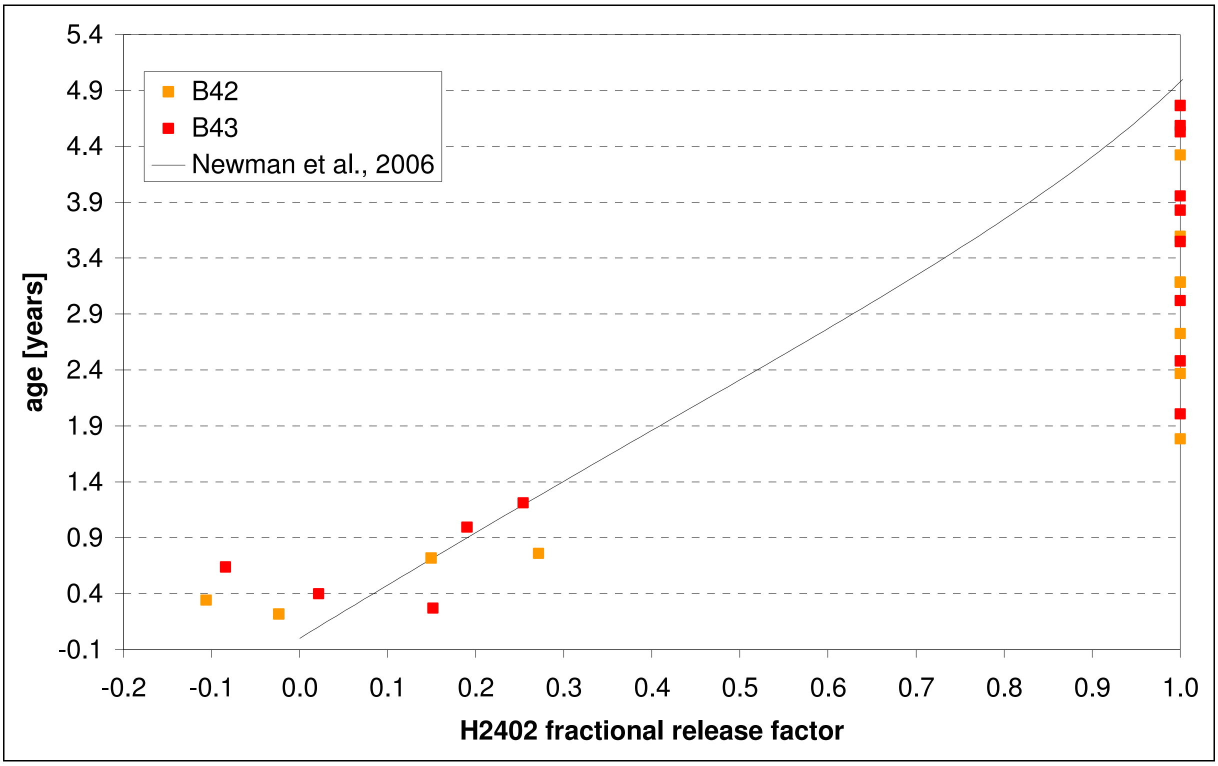
B42
B43
Newman et al., 2006
age [years]
5.4
4.9
4.4
3.9
3.4
2.9
2.4
1.9
1.4
0.9
0.4
-0.1
-0.2
-0.1
0.0
0.1
0.2
0.3
0.4
0.5
0.6
0.7
0.8
0.9
1.0
H2402 fractional release factor

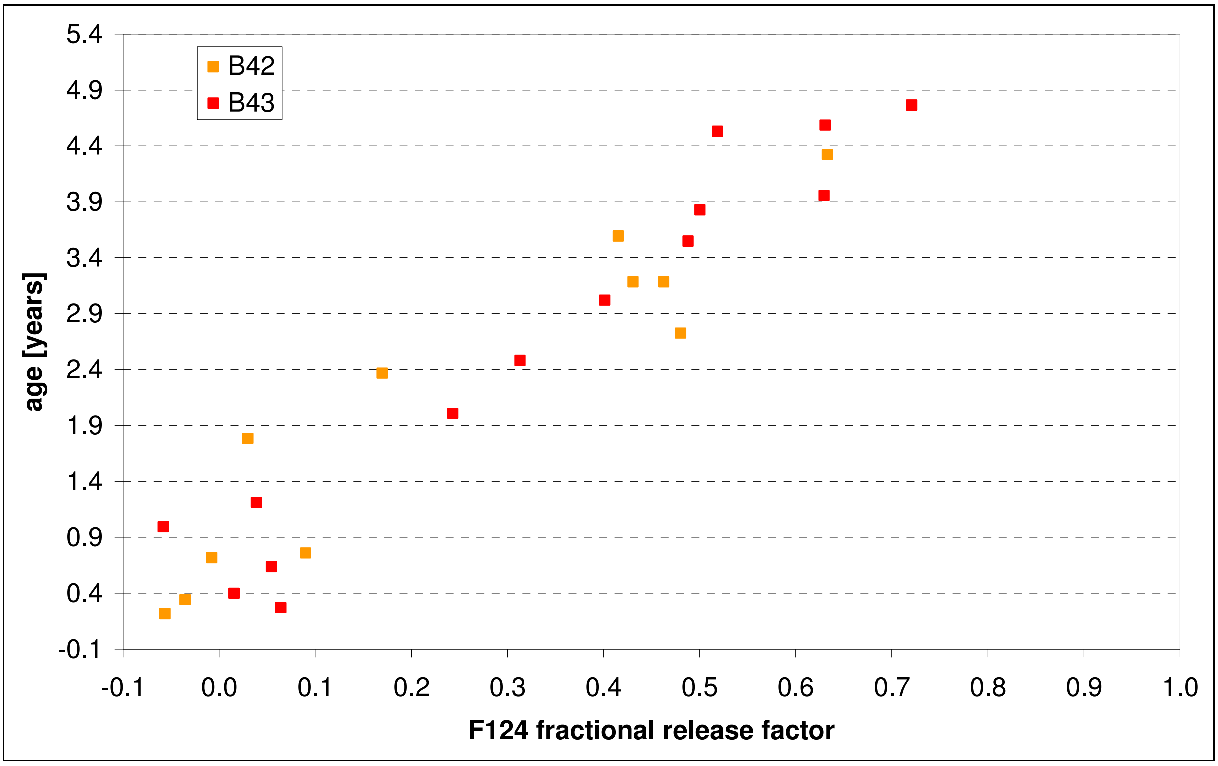
B42
B43
age [years]
5.4
4.9
4.4
3.9
3.4
2.9
2.4
1.9
1.4
0.9
0.4
-0.1
-0.1
0.0
0.1
0.2
0.3
0.4
0.5
0.6
0.7
0.8
0.9
1.0
F124 fractional release factor

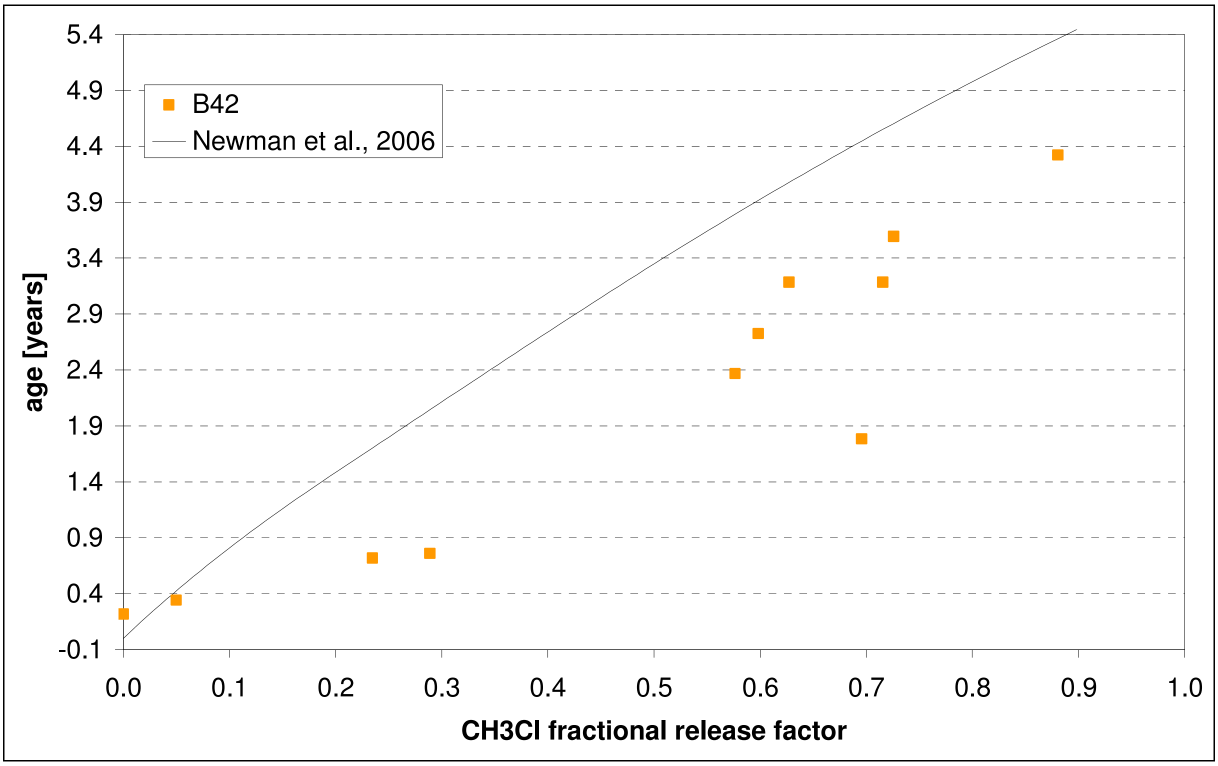
5.4
4.9
4.4
3.9
3.4
2.9
2.4
1.9
1.4
0.9
0.4
-0.1
age [years]
B42
Newman et al., 2006
0.0
0.1
0.2
0.3
0.4
0.5
0.6
0.7
0.8
0.9
1.0
CH3Cl fractional release factor

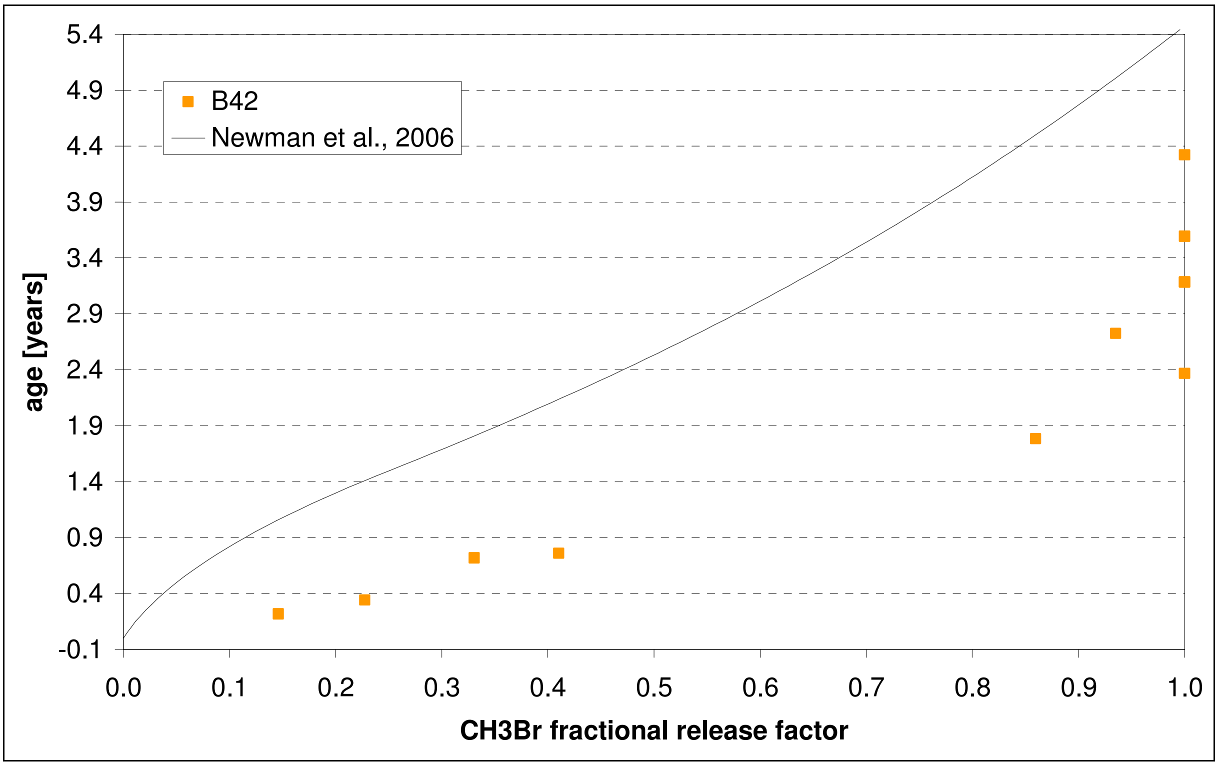
5.4
4.9
4.4
3.9
3.4
2.9
2.4
1.9
1.4
0.9
0.4
-0.1
age [years]
B42
Newman et al., 2006
0.0
0.1
0.2
0.3
0.4
0.5
0.6
0.7
0.8
0.9
1.0
CH3Br fractional release factor